



PHD

Novel Methodologies for the Catalytic Synthesis of Amides

Sanz Sharley, Daniel

Award date:
2019

Awarding institution:
University of Bath

[Link to publication](#)

Alternative formats

If you require this document in an alternative format, please contact:
openaccess@bath.ac.uk

General rights

Copyright and moral rights for the publications made accessible in the public portal are retained by the authors and/or other copyright owners and it is a condition of accessing publications that users recognise and abide by the legal requirements associated with these rights.

- Users may download and print one copy of any publication from the public portal for the purpose of private study or research.
- You may not further distribute the material or use it for any profit-making activity or commercial gain
- You may freely distribute the URL identifying the publication in the public portal ?

Take down policy

If you believe that this document breaches copyright please contact us providing details, and we will remove access to the work immediately and investigate your claim.



Citation for published version:

Sanz Sharley, D 2019, 'Novel Methodologies for the Catalytic Synthesis of Amides'.

Publication date:
2019

[Link to publication](#)

University of Bath

General rights

Copyright and moral rights for the publications made accessible in the public portal are retained by the authors and/or other copyright owners and it is a condition of accessing publications that users recognise and abide by the legal requirements associated with these rights.

Take down policy

If you believe that this document breaches copyright please contact us providing details, and we will remove access to the work immediately and investigate your claim.

Novel Methodologies for the Catalytic Synthesis of Amides

Daniel Domenec Sanz Sharley

A thesis submitted for the degree of Doctor of Philosophy

University of Bath
Department of Chemistry
July 2019

Copyright Notice

Attention is drawn to the fact that copyright of this thesis rests with its author. A copy of this thesis has been supplied on the condition that anyone who consults it is understood to recognise that its copyright rests with its author and they must not copy it or use material from it except as permitted by law or with the consent of the author. This thesis may be made available for consultation within the University Library and may be photocopied or lent to other libraries for the purposes of consultation.

Candidate's signature.....*D. S. Sharkey*.....

Restrictions on Use and Licensing

Access to this thesis in print or electronically is restricted until.....

Signed on behalf of the Doctoral College.....

Declaration of any Previous Submission of the Work

The material presented here for examination for the award of a higher degree by research has not been incorporated into a submission for another degree.

Candidate's signature.....*D. S. Sharkey*.....

Declaration of Authorship

I am the author of this thesis, and the work described herein was carried out by myself personally, with the exception of chapter 5 where 5% of the work was carried out by other researchers.

Candidate's signature.....*D. S. Sharkey*.....

Contents

<i>Acknowledgements</i>	<i>iv</i>
<i>Abbreviations</i>	<i>v</i>
<i>Abstract</i>	<i>ix</i>
1. Introduction	1
1.1. Introduction to Amides	1
1.2. Synthesis of Amides	3
1.2.1. Direct Couplings	3
1.2.2. Use of Coupling Reagents	5
1.2.3. Catalytic Methods	11
1.2.3.1 Amides from Carboxylic Acids	11
1.2.3.2 Amides from Esters	19
1.2.3.3 Primary Amides from Nitriles	26
1.2.3.4 Primary Amides from Aldehydes and Aldoximes	36
1.3. Summary	50
2. Results and Discussion I – Amides from Esters	51
2.1. Aims and Objectives	52
2.2. Initial Investigations	52
2.3. <i>N</i> -Acetylation of Amines: Optimisation	54
2.3.1. Primary Amines	54
2.3.2. Secondary Amines	57
2.3.3. Aniline Derivatives	61
2.4. <i>N</i> -Acetylation of Amines: Amine Substrate Scope	64
2.4.1. Primary Amines	65
2.4.2. Secondary Amines	67
2.4.3. Aniline Derivatives	68
2.5. <i>N</i> -Acylation of Amines: Optimisation and Ester Substrate Scope	69
2.6. Mechanistic Investigations	73
2.6.1. Use of 3-Phenylpropionic Acid as the Catalyst	73
2.6.2. Use of ¹³ C-Labelled Acetic Acid	75
2.6.3. Plausible Reaction Mechanism	78
2.7. Conclusions	79
3. Results and Discussion II – Amides from Nitriles	81

3.1. Previous Work in the Group	82
3.2. Initial Aims and Objectives	82
3.3. Initial Work	83
3.4. New Aims and Objectives	88
3.5. Optimisation	88
3.6. Substrate Scope	101
3.6.1. Successful Substrates	101
3.6.2. Less Successful Substrates	104
3.6.3. Pharmaceutical Applicability and Large Scale Reaction	107
3.7. Formation of Secondary Amides	108
3.8. Mechanistic Investigations	109
3.9. Conclusions	111
4. Results and Discussion III – Amides from Aldoximes	113
4.1. Previous Work in the Group	114
4.2. Aims and Objectives	115
4.3. Optimisation	115
4.4. Substrate Scope	130
4.4.1. Successful Substrates	130
4.4.2. Less Successful Substrates	132
4.5. Reaction Mechanism	134
4.6. Conclusions	135
5. Results and Discussion IV – Amides from Aldehydes	137
5.1. Aims and Objectives	138
5.2. Optimisation	138
5.3. Substrate Scope	150
5.4. Reaction Mechanism	152
5.5. Conclusions	153
6. Experimental	155
6.1. Materials and Methods	156
6.2. Chapter 2 Experimental Methods and Compound Characterisation	157
6.3. Chapter 3 Experimental Methods and Compound Characterisation	184
6.4. Chapter 4 Experimental Methods and Compound Characterisation	208
6.5. Chapter 5 Experimental Methods and Compound Characterisation	226

Acknowledgements

First and foremost, I would like to thank Professor Jonathan Williams for giving me the opportunity to carry out my PhD research under his supervision. I am extremely grateful for his guidance, advice and ideas throughout my PhD. In addition, I wish to thank Professor Christ Frost for his support towards the end of my time in Bath. I would also like to acknowledge the EPSRC for funding my research.

In addition, I would like to thank the members of the Williams group I was fortunate enough to work with. In particular, I'm extremely grateful to Dr Patricia Marcé (Patri), whose endless support throughout my PhD has been invaluable. Thank you for always being there to answer my questions; your help and advice has had a great impact on my work. I also owe special thanks to Dr Caroline Jones for the excellent supervision I received during my Masters year. Without your guidance and the knowledge you passed on to me I wouldn't have been so well prepared for my PhD. In addition, I would also like to acknowledge my final year Masters student, Dmitry Gorbachev, who contributed to the work presented in Chapter 5.

I also wish to thank all of the Bull and James group members who made my time in the office and lab a thoroughly enjoyable experience. In particular, I would like to thank Jordan Gardiner (Gordi), Dr Liam Stephens (Lima), Dr Adam Sedgwick and Dr Bill Cunningham for all of the good times I shared with you, including our trip to Thailand. Gordi, thank you for the daily Monster and flapjack trips to the shop, as well as all of the support you have kindly given me since we started our PhDs together – cheers mate!

I would like to express my appreciation to all my friends and family who have been there for me during my time in Bath. I would especially like to thank my mum Jane and her partner Ian who have encouraged and supported me throughout the last few years. Finally, I wish to extend my heartfelt gratitude to a very important person who has been there for every step of my PhD journey. Tasha, I cannot thank you enough for your constant love, support and weekend visits to Bath, to name just a few things. None of it will ever be forgotten.

Abbreviations

Å	Ångstrom
°C	Degrees celsius
ν	Infrared absorption
μL	Microlitre(s)
δ	NMR chemical shift
$[\alpha]_{\text{D}}$	Optical rotation
acac	Acetylacetonate
anh.	Anhydrous
Ar	Aryl
BEMP	2- <i>tert</i> -Butylimino-2-diethylamino-1,3-dimethylperhydro-1,3,2-diazaphosphorine
Bipy	2,2'-Bipyridine
Boc	<i>tert</i> -Butyloxycarbonyl
BOMI	Benzotriazol-1-yloxy- <i>N,N</i> -dimethylmethaniminium hexachloroantimonate
BOP	(Benzotriazol-1-yloxy)tris(dimethylamino)phosphonium hexafluorophosphate
br	Broad
Bu	Butyl
BuOAc	Butyl acetate
CHCl_3	Chloroform
cod	1,5-Cyclooctadiene
Cp	Cyclopentadienyl
Cy	Cyclohexyl
DBU	1,8-Diazabicyclo[5.4.0]undec-7-ene
DCC	<i>N,N'</i> -Dicyclohexylcarbodiimide

DCM	Dichloromethane
DFT	Density Functional Theory
DIC	<i>N,N'</i> -Diisopropylcarbodiimide
DMSO	Dimethyl sulfoxide
dppe	1,2-Bis(diphenylphosphino)ethane
dppf	1,1'-Ferrocenediyl-bis(diphenylphosphine)
EDCI	1-Ethyl-3-(3-dimethylaminopropyl)carbodiimide
<i>ee</i>	Enantiomeric excess
equiv.	Equivalent(s)
ESI-TOF	Electrospray ionisation – time of flight
Et	Ethyl
EtOAc	Ethyl acetate
EtOH	Ethanol
G	Gram(s)
Gly	Glycine
H	Hour(s)
HATU	1-[Bis(dimethylamino)methylene]-1 <i>H</i> -1,2,3-triazolo[4,5- <i>b</i>]pyridinium 3-oxid hexafluorophosphate
HMPA	Hexamethylphosphoramide
HOAt	1-Hydroxy-7-azabenzotriazole
HOBt	Hydroxybenzotriazole
HPLC	High pressure liquid chromatography
HRMS-ESI	High resolution mass spectrometry – electrospray ionisation
Hz	Hertz
IPA	Isopropyl alcohol
<i>i</i> Pr	Isopropyl
IR	Infrared

<i>J</i>	Coupling constant
<i>m</i>	<i>meta</i>
M	Molar
Me	Methyl
MeCN	Acetonitrile
MeOH	Methanol
mg	Milligram(s)
MHz	Megahertz
min	Minute(s)
mL	Millilitre(s)
mmol	Millimole(s)
mol	Mole(s)
mp	Melting point
MS	Molecular sieves
NAD	Nicotinamide adenine dinucleotide
NBD	Norbornadiene
NHC	<i>N</i> -Heterocyclic carbene
nm	Nanometre(s)
NMP	<i>N</i> -Methyl-2-pyrrolidone
NMR	Nuclear Magnetic Resonance
NP	Nanoparticle(s)
Nuc	Nucleophile
<i>o</i>	<i>ortho</i>
OAc	Acetate
OTf	Triflate
OTs	Tosylate

Oxyma	Ethyl cyanohydroxyiminoacetate
<i>p</i>	<i>para</i>
PEG	Polyethylene glycol
Ph	Phenyl
pK _a	Logarithmic acid dissociation constant
ppm	Parts per million
PVP	Polyvinylpyrrolidone
PyBOP	(Benzotriazol-1-yloxy)tripyrrolidinophosphonium hexafluorophosphate
R	Generic group
rt	Room temperature
S _N Ar	Nucleophilic aromatic substitution
TAME	<i>tert</i> -Amyl methyl ether
^t Bu	<i>tert</i> -Butyl
Temp.	Temperature
TEMPO	(2,2,6,6-Tetramethylpiperidin-1-yl)oxyl
Terpy	Terpyridine
TFE	Trifluoroethanol
THF	Tetrahydrofuran
TLC	Thin Layer Chromatography
TON	Turnover number
UV	Ultraviolet

Abstract

The amide bond is one of the most important functionalities in both industrial and medicinal chemistry. Traditional amidation methods involve the use of coupling reagents; however the production of stoichiometric by-products resulted in the ACS's Green Chemistry Institute Pharmaceutical Roundtable highlighting the need for catalytic and waste-free syntheses of amides in 2005.

This thesis details research concerning the development of novel catalytic protocols for the synthesis of amides from a variety of different starting materials. These methods have been fully optimised and the substrate scope for each approach has been explored. Mechanistic studies have also been performed to elucidate plausible reaction pathways.

In Chapter 1, following an introduction to amides, a discussion on their synthesis is detailed. This section covers the direct uncatalysed coupling of carboxylic acids and amines, the use of coupling reagents and catalytic methods. Metal/non-metal and homogeneous/heterogeneous catalysts for the preparation of amides from a variety of different starting materials are presented.

The Results and Discussion section begins with a report detailing a cheap and simple method for the acylation of amines using catalytic acetic acid and esters as the acyl source. The *N*-acetylation of amines formed the initial focus of the investigations, however it was also shown the methodology could be successfully applied to synthesise higher amides as well.

Chapter 3 details work on a selective and relatively mild protocol for the hydration of organonitriles in water. Low loadings of a commercially available palladium catalyst and a cheap ligand afford primary amide products in high yields in the absence of hydration-promoting additives such as oximes and hydroxylamines.

In Chapter 4, a low temperature method for the efficient rearrangement of aldoximes into primary amides is presented. The protocol successfully converts aldoximes into primary amides using cheap and simple reagents, namely a copper catalyst and sodium salt, without the need for nitriles to accelerate the process.

Chapter 5 builds on the work outlined in the previous chapter to enable the conversion of aldehydes into primary amides in a one-pot reaction at low temperature.

1. Introduction

1.1. Introduction to Amides

The amide bond is one of the most important functionalities in both industrial and medicinal chemistry; essential to both the pesticide and polymer industries, for example, and present in more than 25% of pharmaceuticals (Figure 1.1). The large number of amide-containing drug molecules is due to the significance and prevalence of the functionality in biologically important compounds, for example peptides and proteins.¹

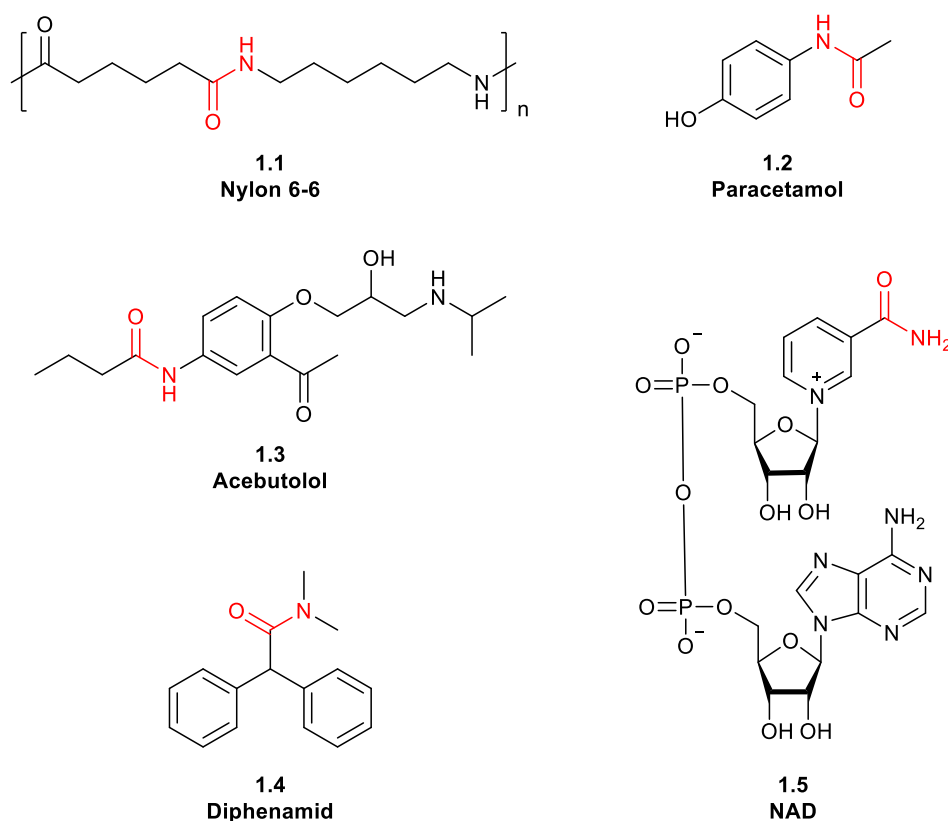
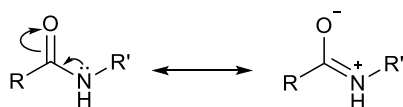


Figure 1.1. Polymers (1.1), pharmaceuticals (1.2 and 1.3), agrochemicals (1.4) and biological molecules (1.5) containing amide bonds.

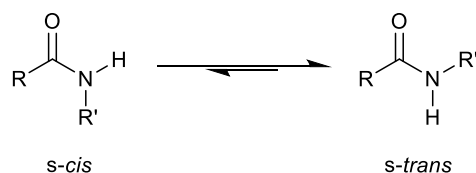
Amides have several notable characteristics, including their ability to form hydrogen bonds; a result of the presence of a hydrogen bond acceptor (the carbonyl oxygen) and hydrogen bond donor (the NH group) within the functionality.^{2,3} The formation of hydrogen bonds is vital to the stability of the two protein secondary structures – α -helices and β -sheets – as well as protein-ligand recognition.⁴

In addition, the delocalisation of electron density over the amide bond confers both stability and a partial double bond character (Scheme 1.1). As a result of this resonance, the N-C-O fragment is coplanar whilst there is also limited free rotation about the bond. These two characteristics account for several properties of polypeptide chains – which consist of α -amino acids linked by covalent amide bonds – and contribute to their secondary structure.⁵



Scheme 1.1. The resonance forms of amides.

In addition, the small degree of rotation about the amide bond allows both the *s-cis* and *s-trans* conformations to be adopted, although *s-trans* is favoured over *s-cis* due to steric effects (Scheme 1.2). This flexibility is thought to be essential for the function of proteins.⁵



Scheme 1.2. The two different configurations of amides.

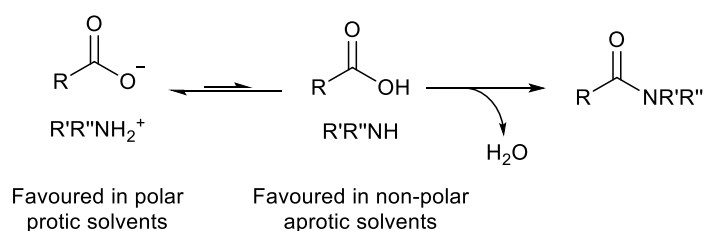
Despite the significance and prevalence of amides in both industrial and medicinal chemistry, traditional methods for their formation are less than ideal. Major concerns include the need for high temperatures, limited substrate scopes and the generation of stoichiometric by-products.¹ As a result, the last decade has seen the emergence of a range of catalytic methods for the formation of amides in order to circumvent these problems. The development of both metal and non-metal catalysts has allowed amides to be accessed from a variety of starting materials, including carboxylic acids, amides, aldehydes, nitriles, esters, aldoximes and alcohols.^{6,7} It is hoped that these modern approaches can provide a recyclable, low cost and environmentally benign route to industrially and medically relevant amides.

1.2. Synthesis of Amides

The literature includes a variety of different amidation protocols; ranging from traditional direct couplings and the use of stoichiometric activating agents to more novel catalytic methods. This section firstly outlines the direct coupling of both carboxylic acids and acid chlorides with amines, followed by a discussion on the use of coupling reagents in amide bond formation. Finally, the catalytic synthesis of amides from carboxylic acids, esters, nitriles, aldoximes and aldehydes is presented.

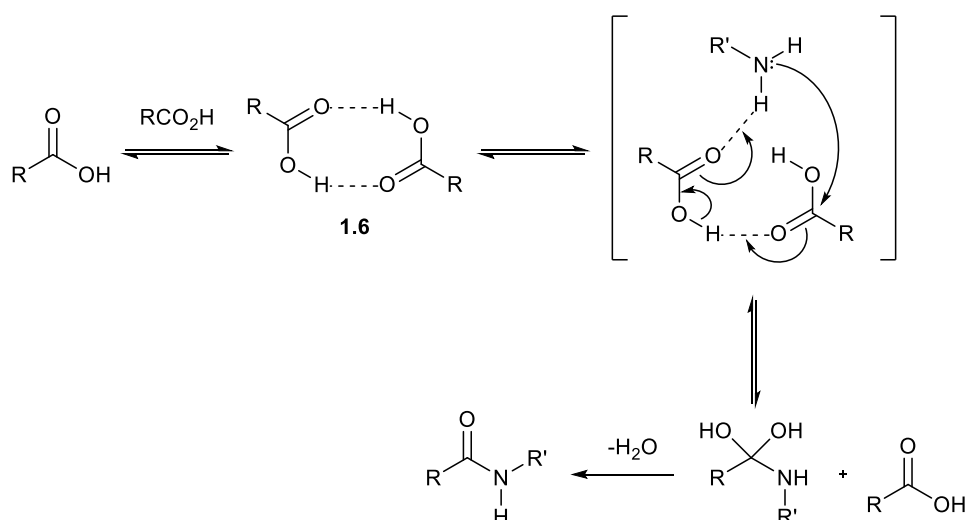
1.2.1. Direct Couplings

One of the most attractive methods for the formation of amides is the direct coupling of carboxylic acids and amines, involving the release of one equivalent of water (Scheme 1.3). Although this condensation reaction is relatively atom efficient, problems arise from the competing acid-base reaction which can occur; leading to the formation of an unreactive ammonium-carboxylate salt.¹ In order to overcome the energy barrier of this salt, high temperatures of 180 °C must be used.⁸ However, sensitive functional groups are incompatible with these forcing conditions and therefore this direct coupling strategy has limited scope.⁹



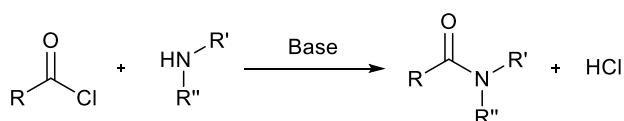
Scheme 1.3. Direct coupling of a carboxylic acid and an amine in a condensation reaction.

The reaction mechanism for the direct coupling of carboxylic acids and amines in non-polar aprotic media was investigated by Whiting *et al.* in 2011.¹⁰ They revealed limited formation of the unreactive salt in this type of solvent system and, based on DFT calculations and additional experiments, proposed a reaction mechanism which proceeds through the dimeric carboxylic acid species **1.6** (Scheme 1.4).



Scheme 1.4. Proposed mechanism for direct amidation by Whiting *et al.*

The direct coupling of acid chlorides and amines has also been a well-researched area. The Schotten-Baumann reaction, dating back to 1883, involves the synthesis of an amide from an amine and an acid chloride (Scheme 1.5).^{11,12} However, hydrochloric acid is also generated as a by-product and therefore base (for example Hünig's base) must be added in order to neutralise the solution and prevent the formation of the inactive ammonium salt. An alternative procedure involves a two-phase system involving water and an immiscible organic solvent. The acid chloride and amine react in the organic phase, whilst the HCl by-product moves to the aqueous layer where it is neutralised by the base.^{11,12}

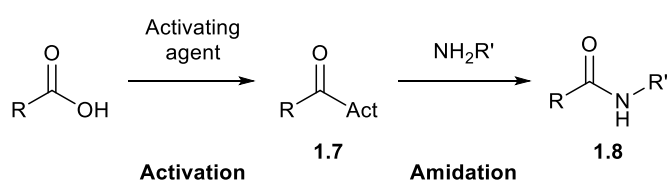


Scheme 1.5. The Schotten-Baumann reaction.

The Schotten-Baumann protocol is used to synthesise Nonivamide (also known as pelargonic acid vanillylamide or PAVA), a food additive which adds pungency to flavourings, seasonings and spices. This reaction was also employed during the Fischer peptide synthesis in 1903, in which α -chloro acid chlorides were condensed with amino acid esters.¹³ This was followed by hydrolysis of the ester and then conversion of the resultant acid into an acid chloride. Subsequent coupling of the new acid chloride to a second amino acid ester extended the chain, before the process was repeated. Reaction with ammonia converted the terminal chloride into an amino group.

1.2.2. Use of Coupling Reagents

As detailed, the direct coupling of a carboxylic acid and an amine, either in solution or solid phase, results in the formation of the unreactive ammonium-carboxylate salt.¹ Therefore, in order to prevent salt formation a variety of methods have been developed involving two consecutive steps – activation of the carboxylic acid into **1.7** using so-called coupling reagents and then subsequent amidation into **1.8** (Scheme 1.6). Depending on the coupling reagent used, these two steps can either be performed separately or as a one-pot reaction. Activation of the carboxylic acid usually involves conversion into a more reactive functional group, such as an acid chloride, acid anhydride, acyl azide or active ester.¹⁴



Scheme 1.6. Activation of a carboxylic acid and subsequent amidation.

One of the most popular classes of coupling reagent for the production of amides is the carbodiimides, such as DCC (**1.9**), DIC (**1.10**) and EDCI (**1.11**);¹⁵ the former first used in 1955 by Sheehan (Figure 1.2).¹⁶ Whereas DCC and DIC are only soluble in organic solutions, EDCI is a water-soluble carbodiimide, typically obtained as the hydrochloride salt.¹⁵

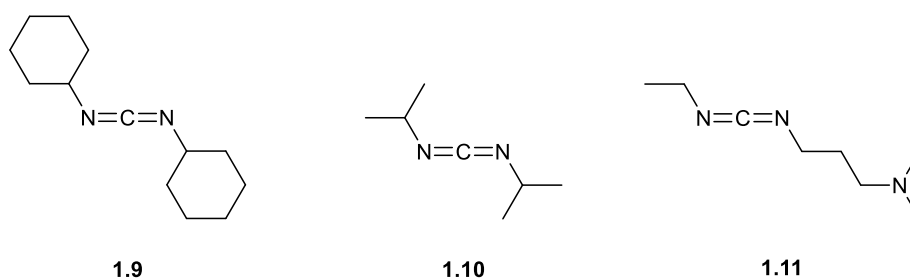
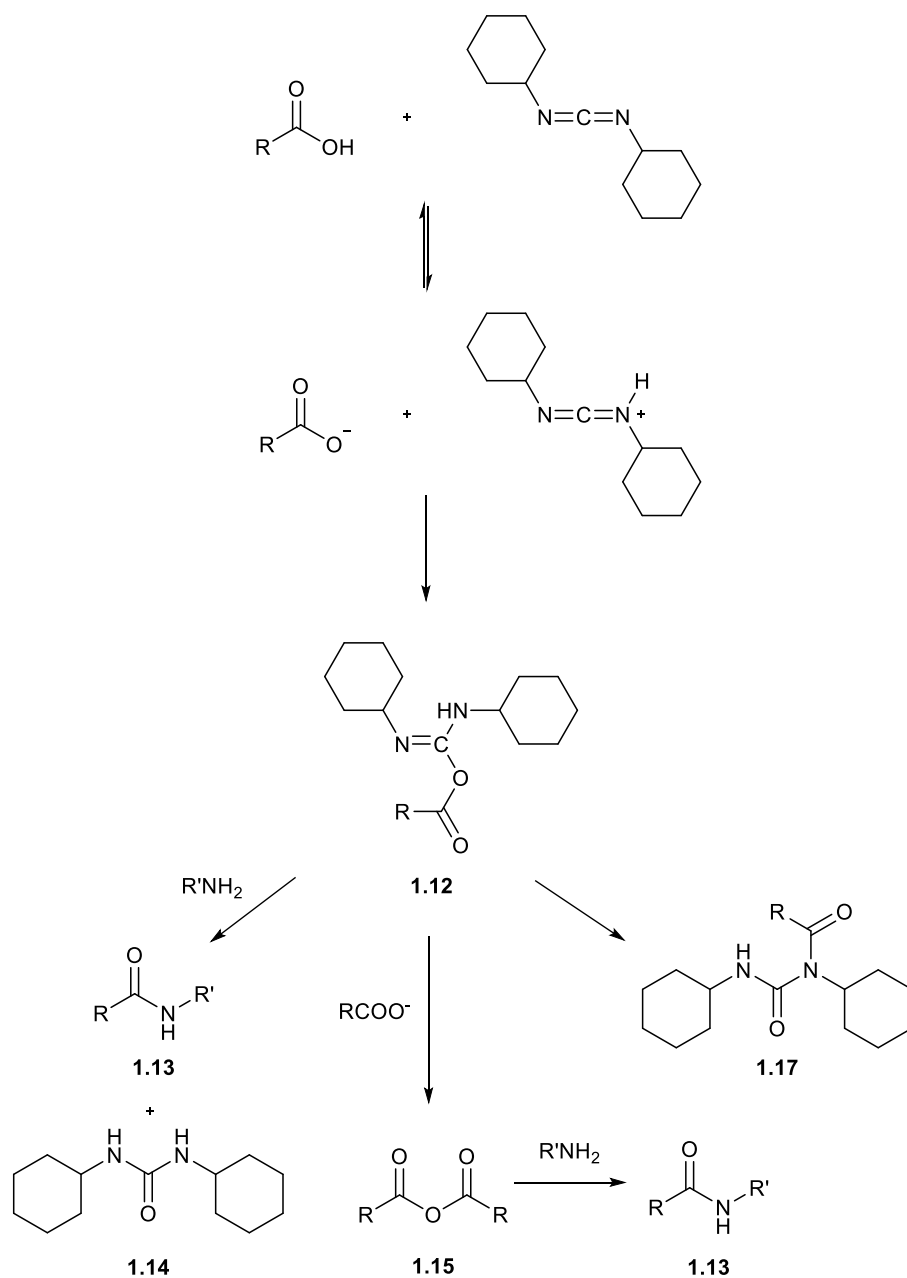


Figure 1.2. Common carbodiimide coupling reagents.

The DCC coupling mechanism firstly involves nucleophilic attack of the carboxylic acid on the carbodiimide to yield *O*-acylurea intermediate **1.12** (Scheme 1.7). Three different possible pathways then follow; two leading to the desired product and a third route resulting in the production of an unwanted side product. The most direct pathway to desired amide product **1.13** involves nucleophilic attack on the carbonyl group of **1.12** by the amine. As well as the amide, dicyclohexylurea (**1.14**) is also generated (the driving force of the reaction) and must

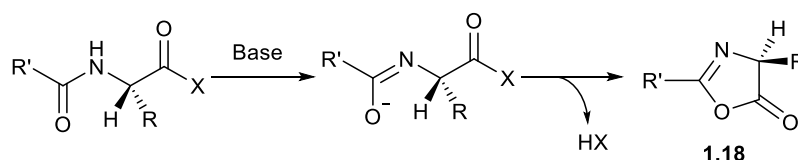
be removed by filtration as it is insoluble in most solvents. Due to this, DCC is rarely used in solid phase synthesis.

In addition, another pathway exists in which anhydride **1.15** is formed after nucleophilic attack by another equivalent of acid on **1.12**, before reaction with the amine yields desired amide **1.13**. However, a third pathway also operates which reduces the efficiency of the DCC coupling method. Intermediate **1.12** is partially unstable and therefore intramolecular acyl migration can occur resulting in unreactive *N*-acylurea **1.17**.



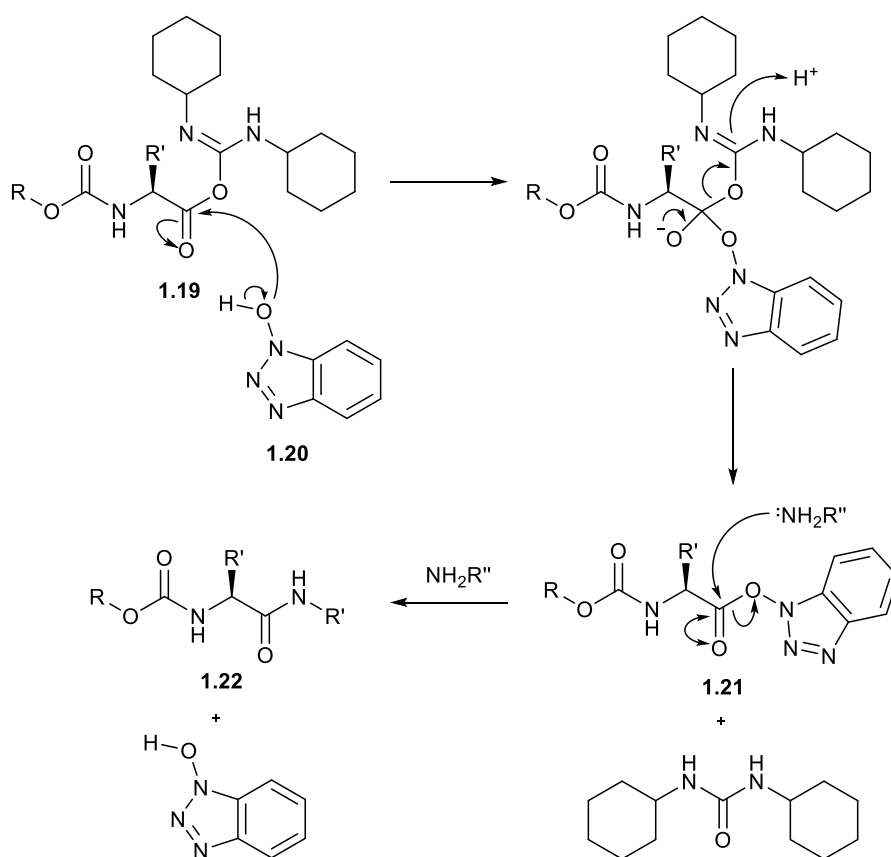
Scheme 1.7. Coupling of an amine and a carboxylic acid using DCC.

Further to this, the presence of basic conditions can result in *O*-acylurea derivatives undergoing oxazolone formation (**1.18**) and subsequently, epimerisation or racemisation (peptide and amino acid couplings respectively) (Scheme 1.8). The electronic nature of the group bound to the α -position of the amide bond has an effect on the level of epimerisation/racemisation; higher levels are observed with electron-withdrawing moieties, such as peptide fragments, present.¹⁷



Scheme 1.8. Oxazolone formation under basic conditions.

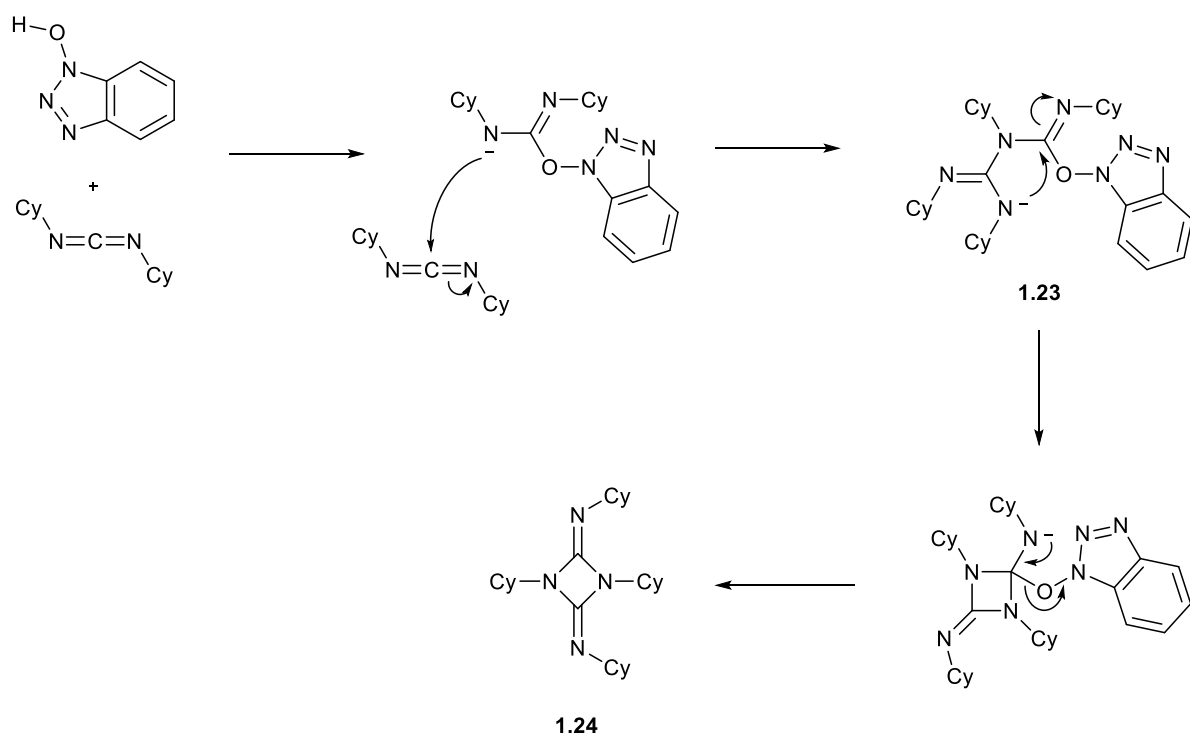
In order to increase yields and minimise the formation of *N*-acylureas and epimers, the first additive, hydroxybenzotriazole (HOBt), was developed.¹⁸ The presence of HOBt (**1.20**) results in the generation of OBt-ester **1.21**, which is less inclined to form oxazolones, following reaction with *O*-acylurea **1.19** (Scheme 1.9). Nucleophilic attack by HOBt on *O*-acylurea **1.19** occurs much faster than the competing acyl transfer, resulting in reduced levels of the *N*-acylurea side product.¹⁹ Reaction of the amine with OBt-ester **1.21** then follows, affording desired product **1.22** whilst also regenerating HOBt.



Scheme 1.9. Mechanism of carboxylic acid activation by DCC and HOBT.

Following the development of HOBT, a similar additive, 1-hydroxy-7-azabenzotriazole (HOAt), was introduced by Carpino in 1994.²⁰ This new additive displayed increased efficiency compared to HOBT, exemplified by the DCC activated coupling of two valine-based residues. Epimerisation levels were reduced to 15% with HOAt compared to 42% when HOBT was used. Carpino subsequently investigated a variety of HOAt isomers and revealed that the most efficient was the 7-isomer,²¹ whilst Ven den Nest and colleagues detailed the use of Cu(II) complexes in combination with both HOAt and HOBT to lower epimerisation levels.²² However, although much work has been undertaken, the explosive properties of these additives have rendered their application limited.²³

However, use of HOBT as an additive in combination with carbodiimides such as DCC can lead to the formation of by-products. For example, cyclisation of intermediate **1.23**, formed from HOBT and two equivalents of DCC, leads to the formation of diazetidine **1.24** (Scheme 1.10).²⁴



Scheme 1.10. Formation of a diazotidine side product when using HOBT in combination with DCC.

Subsequent studies led to the development of 1*H*-benzotriazole-derived onium salts and an improved activation system.^{19,25} These coupling reagents can be categorised into aminium, phosphonium and immonium salts, for example, HATU (**1.25**), PyBOP (**1.26**) and BOMI (**1.27**) respectively (Figure 1.3).

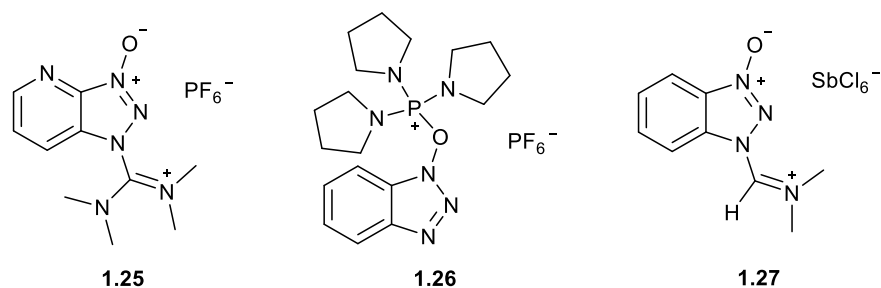
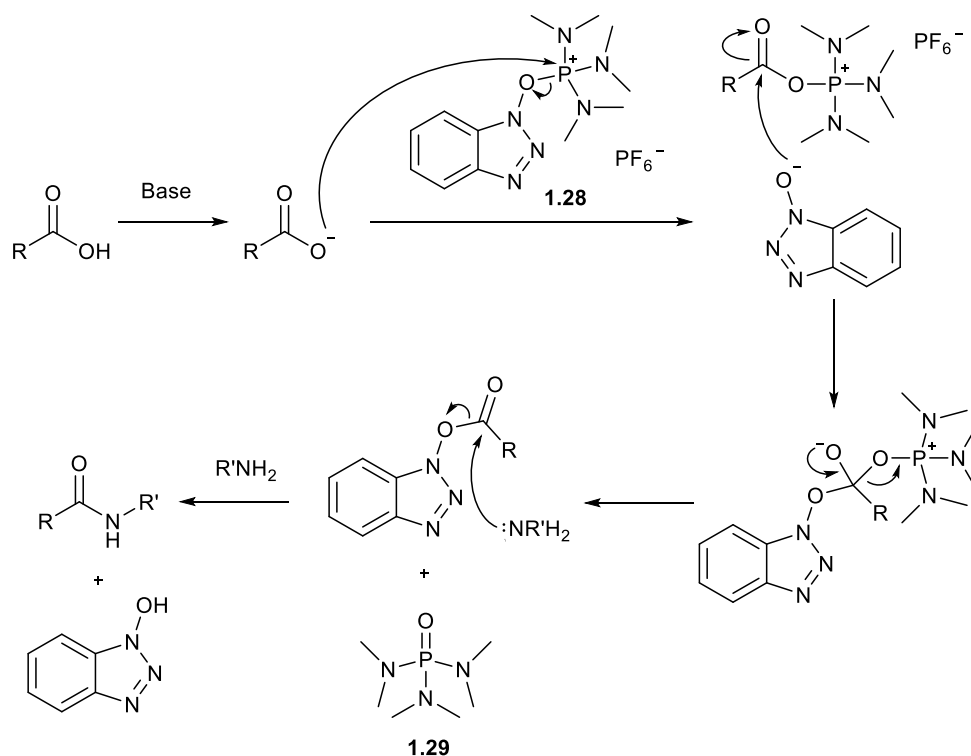


Figure 1.3. Examples of aminium, phosphonium and immonium salts respectively.

Aminium salts suffer from the unwanted formation of guanidinium by-products, a result of nucleophilic attack of the amine on the salt.²⁶ However, HOXt-based phosphonium salts do not undergo such side reactions and are therefore often preferred. The first phosphonium salt, BOP (**1.28**), was introduced in 1975 by Castro and its mechanism of action is illustrated in Scheme 1.11.²⁷ The emergence of BOP soon led to the second generation derivative PyBOP

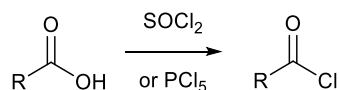
which, unlike its predecessor, does not lead to the production of the known carcinogen HMPA (**1.29**).²⁸



Scheme 1.11. Mechanism of amide formation using BOP.

The toxicity of some of these HOBT/HOAt-based salts, such as BOP, and side reactions caused by use of the aminium derivatives exemplify the issues associated with this class of coupling reagent. As a result, despite extensive investigations into the carbodiimide/additive coupling method, limitations still remain.

Another class of coupling reagent which can be used to activate carboxylic acids are the acid halide generating reagents. After activation, the acid halide can then be directly coupled to the amine as discussed in Section 1.2.1. Acid chlorides can be synthesised from carboxylic acids using a variety of reagents, including thionyl chloride and a wide range of phosphorous reagents.¹⁹ For example, the first dipeptide synthesis (Gly-Gly) in 1901 involved synthesis of the acid chloride from the carboxylic acid using thionyl chloride or phosphorous pentachloride (Scheme 1.12).²⁹



Scheme 1.12. Formation of an acid chloride from a carboxylic acid.

Further acid halide-generating reagents have been developed, including reagents that result in the production of acid fluorides (Figure 1.4). The direct coupling of amines and acid fluorides is often advantageous as, unlike acid chlorides, racemisation under basic conditions is not observed.³⁰

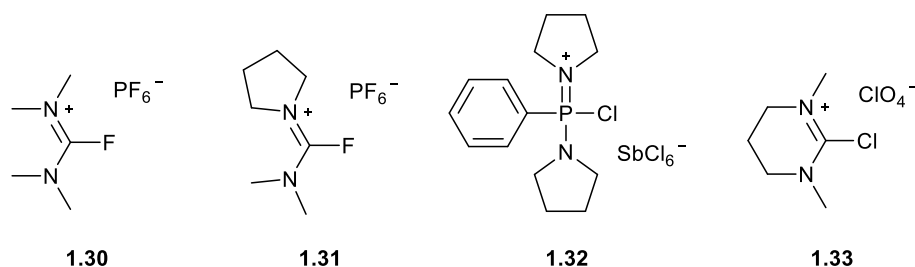


Figure 1.4. Coupling reagents used to generate acid fluorides (**1.30** and **1.31**) and acid chlorides (**1.32** and **1.33**).

As detailed, many coupling reagents have been developed in order to couple unactivated carboxylic acids and amines. These protocols generally afford good yields whilst employing mild reaction conditions. However, in addition to the occurrence of side reactions and increased levels of epimerisation, the main drawback of the coupling reagent-based method concerns the production of stoichiometric amounts of waste. This reduces the efficiency of the reaction, whilst the practical work is made more laborious as further purification steps are required to remove the by-products. As a result of these limitations, a catalytic waste-free synthesis of amides was highlighted as a key area of research by the ACS's Green Chemistry Institute Pharmaceutical Roundtable in 2005.³¹

1.2.3. Catalytic Methods

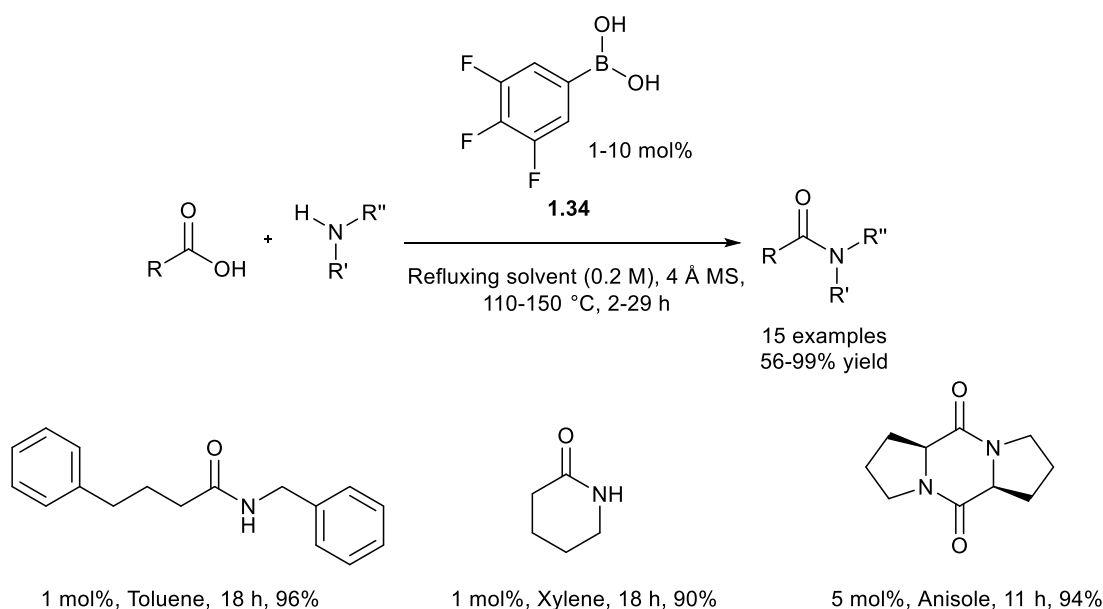
1.2.3.1. Amides from Carboxylic Acids

As detailed, the condensation of amines and carboxylic acids is highly desirable; however, the issues associated with traditional coupling reagent-mediated protocols have resulted in the need for more efficient methods. Therefore, the last decade has seen the emergence of a variety of both non-metal and metal catalysts to promote the formation of amides from carboxylic acids.^{1,7}

Boron-Based Catalysts

Many of the non-metal catalysts that have been developed are based on boron complexes, for example boronic acids and related compounds such as boric acids and esters. These compounds often tolerate a wide variety of functionalities.¹ As a result, their use as catalysts has been explored in recent years, although boron-based compounds have long been employed as stoichiometric reagents in amidation reactions since the 1960's.³²

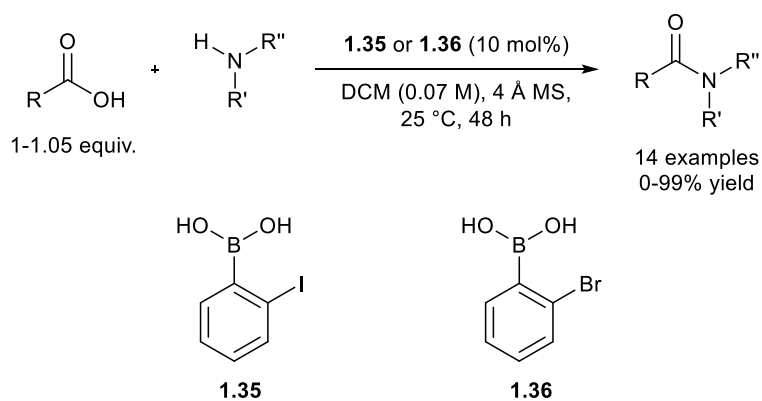
The first boron-based catalytic procedure was developed by Yamamoto in 1996; the group illustrated that electron-deficient boronic acids display high catalytic activity.³³ In particular, 1-10 mol% 3,4,5-trifluorobenzeneboronic acid (**1.34**) was found to efficiently transform both aromatic and aliphatic substrates into a wide range of secondary and tertiary amides in refluxing solvents (110-150 °C) such as toluene, mesitylene, anisole and xylene (Scheme 1.13). Catalyst **1.34** is unstable towards hydrolysis and therefore molecular sieves were employed to remove the water from the reaction.



Scheme 1.13. Selected examples of 3,4,5-trifluorobenzeneboronic acid-catalysed amide formation.

In addition, other notable boron-based catalysts include the *ortho*-haloarylboronic acids **1.35** and **1.36** reported by Hall and colleagues in 2008.³⁴ Low catalyst loadings of 10 mol% catalysed the formation of a variety of secondary and tertiary amides in chloroform at room temperature after 48 hours in the presence of molecular sieves (Scheme 1.14). Pleasingly, the group found that only low levels of racemisation (< 5%) were observed when

enantiomerically pure acids and amines were employed, a result of the mild conditions associated with the protocol. Further investigations revealed the presence of an unsubstituted *ortho* position was vital for efficient catalysis, with *o,o*-disubstituted haloarylboronic acids displaying much lower levels of catalytic activity. Meanwhile, subsequent studies showed an increase in catalytic activity could be achieved if an electron-donating methoxy group was added *para* to the iodo substituent.³⁵



Scheme 1.14. *ortho*-Haloarylboronic acids used as catalysts in amidation reactions.

Another study by Whiting and colleagues in 2008 employed chiral boronic acid catalyst **1.37** in order to synthesise enantiopure amides from racemic amines and carboxylic acids (Figure 1.5).³⁶ However, the method resulted in poor yields and low enantiomeric excesses. For example, a yield of 21% was obtained for the reaction of α -methylbenzylamine with benzoic acid in fluorobenzene, whilst the enantioselectivity was also relatively low (41%).

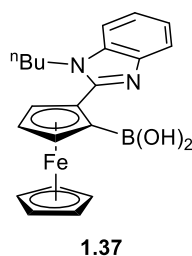
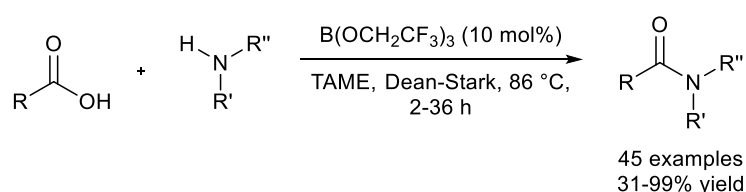


Figure 1.5. Chiral boronic catalyst prepared by Whiting *et al.*

More recently, a simple, commercially available borate ester catalyst has been shown to successfully promote the coupling of carboxylic acids and amines.³⁷ Screening a range of borate reagents in the model reaction of benzoic acid with benzylamine in *tert*-amyl methyl ether (TAME) revealed $\text{B}(\text{OCH}_2\text{CF}_3)_3$ to be the most efficient catalyst for the amidation

reaction. The protocol converted a remarkable range of carboxylic acids and amines into amides using 10 mol% catalyst and Dean-Stark apparatus for water removal (Scheme 1.15). The method also boasts an efficient purification process, with Amberlite and Amberlyst scavenger resins removing unreacted acid and amine as well as boron-containing impurities. Finally, the group also extended their work to enable the coupling of unprotected amino acids and amines, in addition to the synthesis of multiple pharmaceutically relevant targets and functionalised heterocycles.

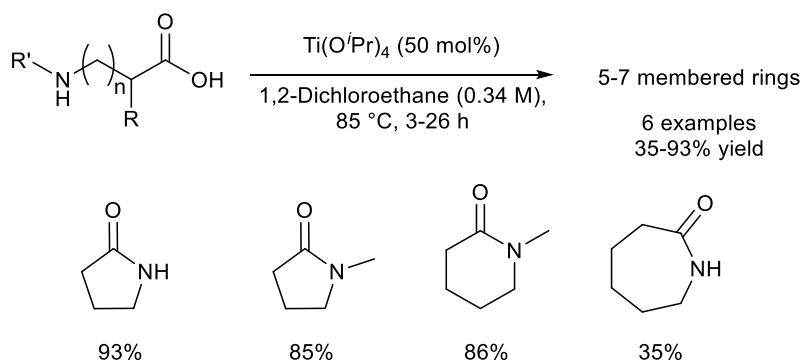


Scheme 1.15. Borate ester-catalysed coupling of carboxylic acids and amines.

Boron-based compounds have potential as catalysts for the coupling of amines and carboxylic acids; however, their use is limited by the high reaction temperatures often required and the need to remove water from the reaction. Although methods employing lower temperatures have been reported, such as that by Hall and colleagues, these require considerably longer reaction times in order to achieve efficient conversion.

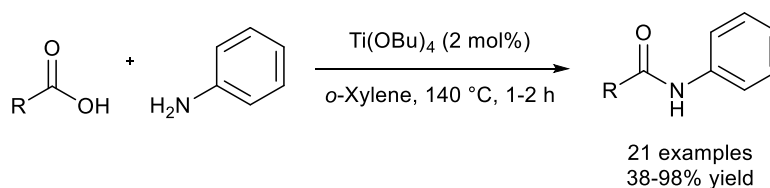
Metal Catalysts

In addition to boron-based catalysts, a variety of studies have also reported the use of metal complexes as catalysts for the condensation of amines and carboxylic acids. Many of these catalysts are based on oxophilic early transition metals such as titanium and zirconium. For example, an early report detailed the use of 0.6-1 mol% Ti(IV), Zr(IV) and Ta(IV) in the coupling of amines and long chain fatty acids at 120-200 °C.³⁸ Meanwhile, a later study reported the lactamisation of a selection of amino acids, employing $\text{Ti}(\text{O}^i\text{Pr})_4$ as the catalyst in refluxing DCM (Scheme 1.16).³⁹ Catalyst loadings of 50 mol% afforded a wide variety of lactams in yields ranging from 35-93%. Disappointingly, the methodology could not be applied to the formation of linear amides, whilst lower yields were observed when reduced catalyst loadings were employed.



Scheme 1.16. Lactamisation reaction using 50 mol% $\text{Ti(O}^i\text{Pr)}_4$ catalyst, including selected examples.

Other studies have since detailed efficient intermolecular coupling methods, for example a report by Shteinberg *et al.* in 1988.⁴⁰ They screened a variety of metal complexes, including Ti(OBu)_4 , TiCl_4 , SnCl_4 , Bu_2SnO and $\text{BF}_3 \cdot \text{OEt}_2$, and revealed Ti(OBu)_4 to be the most efficient catalyst for the coupling of benzoic acid and aniline in refluxing *ortho*-xylene. Employing the model reaction conditions, the group showed catalyst loadings of only 2 mol% were able to efficiently transform 21 different carboxylic acids into the corresponding amide products after reaction with aniline for 1-2 hours (Scheme 1.17). The couplings afforded yields between 38-98%, with only a minimal contribution (0-5%) from the background reaction.

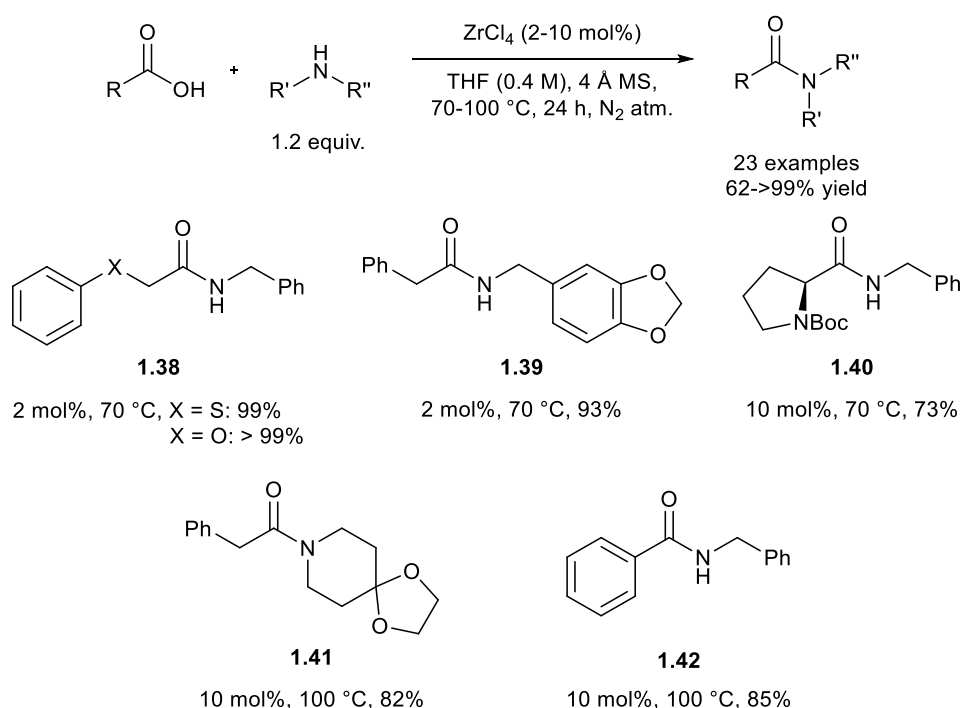


Scheme 1.17. Ti(OBu)_4 -catalysed amidation of aniline and carboxylic acids.

Further studies by the group revealed hydrolysis of the butoxide ligands by water results in a more active catalyst form,⁴¹ whilst the reaction was also more efficient in non-polar aprotic solvents as expected.⁴² Other investigations showed the presence of substituents on the aniline and benzoic acid had a large effect on the efficiency of the reaction; electron-donating groups on the aniline generally resulted in higher conversions, although hydroxyl groups led to reduced conversions as a result of coordination to the metal centre.⁴³

Two more recent studies published in 2012 investigated the use of zirconium-based catalysts for the coupling of amines and carboxylic acids.^{9,44} The first of these, by Adolfsson *et al.*,

showed that in the presence of 4 Å molecular sieves, $Zr(O^tBu)_4$, $Zr(OEt)_4$ and $ZrCl_4$ catalysed the coupling of phenylacetic acid and benzylamine at 70 °C in a variety of different solvents.⁹ The study showed $ZrCl_4$ to be the most effective catalyst for the model amidation reaction, with catalyst loadings as low as 2 mol% affording excellent yields. The group also found that couplings performed in ethereal solvents, such as THF, were the most efficient. The methodology was applied to the synthesis of 23 different secondary and tertiary amides, employing 2-10 mol% $ZrCl_4$ catalyst loading (Scheme 1.18).

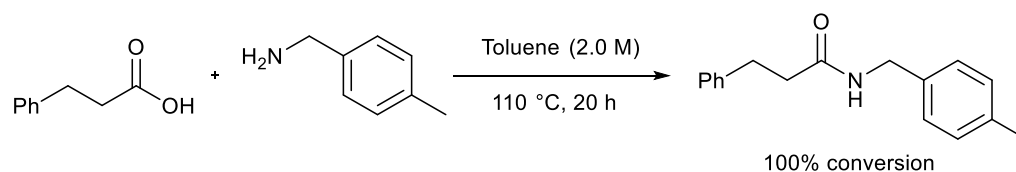


Scheme 1.18. $ZrCl_4$ -catalysed amidation protocol developed by Adolfsson *et al.* with selected products.

In most of the amidation reactions an excess of the amine was found to give improved yields (Scheme 1.18). The methodology was shown to tolerate a wide range of functionalities including (thio)ethers (**1.38**) and acetals (**1.39**). Furthermore, enantiomerically pure amines underwent amidation with retention of stereochemistry (**1.40**). In order to achieve desirable yields, more unreactive substrates, for example secondary amines (**1.41**) and aromatic acids (**1.42**), required higher temperatures of 100 °C and increased catalyst loadings.

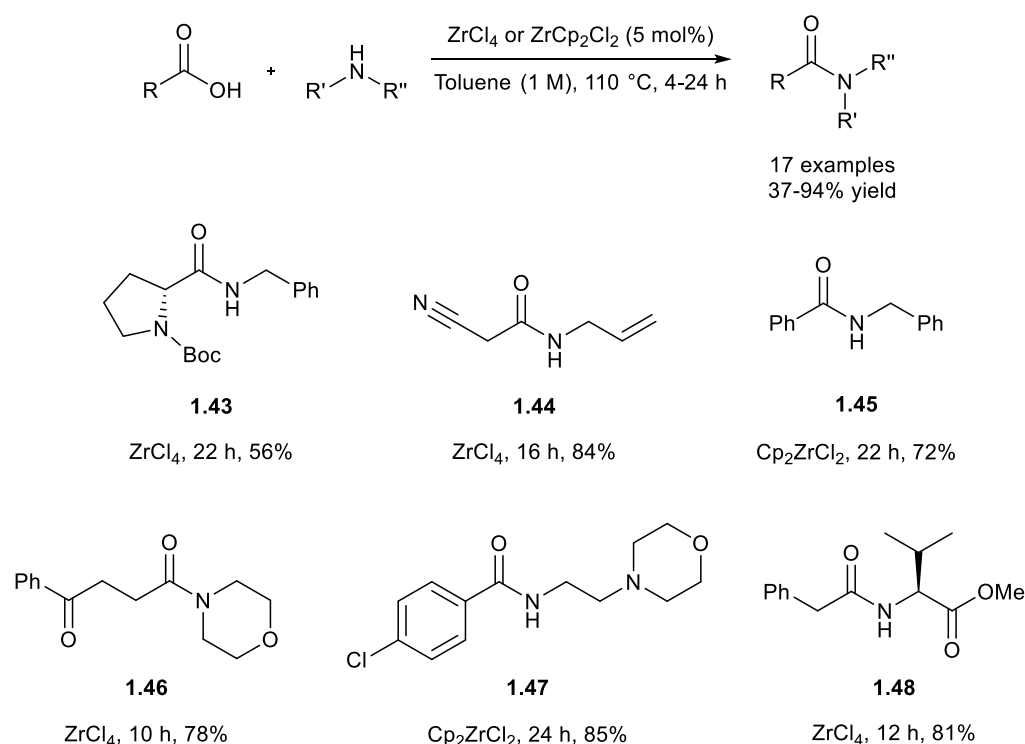
A similar study was performed by Williams *et al.* in which zirconocene dichloride (Cp_2ZrCl_2) was used as a catalyst for the amidation of a variety of amine and carboxylic acid substrates.⁴⁴ However, before investigating a catalytic approach the group explored the direct coupling of

3-phenylpropionic acid and 4-methylbenzylamine in a variety of solvents. Non-polar solvents, which disfavour ammonium-carboxylate salt formation, resulted in increased conversion into the desired amide product. Toluene was found to be a particularly good solvent for this direct coupling, affording 100% conversion for the model reaction (Scheme 1.19).



Scheme 1.19. The direct uncatalysed coupling of 3-phenylpropionic acid and 4-methylbenzylamine.

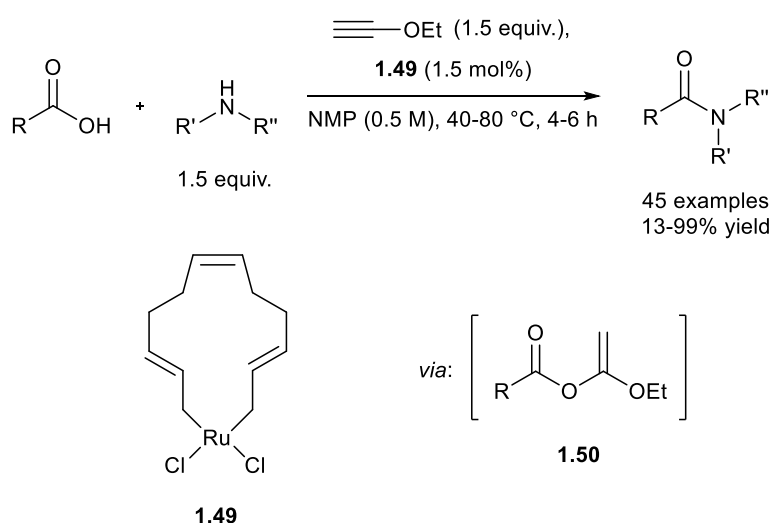
Subsequently, the catalytic ability of a range of metal complexes, including CuBr, ZrCl₄, Ni(NO₃)₂, FeCl₂, Cp₂ZrCl₂ and TiCl₄, was then investigated. Using the same model reaction, the group found the zirconium-based complexes to be the most efficient catalysts after 4 hours; as little as 5 mol% Cp₂ZrCl₂ was required to achieve quantitative conversion. Meanwhile, use of ZrCl₄ resulted in 83% conversion, compared with 20% for the background reaction. As a result, Cp₂ZrCl₂ and ZrCl₄ were employed as catalysts (5 mol%) for the coupling of a wide variety of amine and carboxylic acid substrates (Scheme 1.20).



Scheme 1.20. Zirconium-catalysed coupling of carboxylic acids and amines as developed by Williams *et al.* with selected examples.

Similarly to the study performed by Adolfsson *et al.*,⁹ the methodology tolerated a wide range of functional groups; ketones (**1.46**), alkenes (**1.44**), esters (**1.48**), nitriles (**1.44**), heterocycles (**1.43**, **1.46** and **1.47**) and protecting groups such as Boc (**1.43**) were all unaffected by the relatively mild reaction conditions (Scheme 1.20). In addition to this, no racemisation of chiral product **1.48** was observed. However, reactions involving aniline were less efficient – both with and without a catalyst – due to delocalisation of the nitrogen’s lone pair into the aromatic ring. Reduced reactivity was also observed for amine couplings with benzoic acid, although use of Cp₂ZrCl₂ resulted in 72% yield (83% conversion) into **1.45**. To test the synthetic utility of the protocol the group successfully synthesised a selection of pharmaceuticals, including moclobemide (**1.47**).

A further protocol has been published by Gooßen *et al.* based on ruthenium catalyst **1.49** and simple alkynes as coupling reagents.⁴⁵ Both acetylene and ethoxyacetylene effectively activated the carboxylic acid in the reaction, although the ethoxy derivative was favoured due to the generation of ethyl acetate as opposed to highly reactive acetaldehyde. An extremely vast range of amide products were efficiently synthesised in *N*-methyl-2-pyrrolidone at 40-80 °C using 1.5 equivalents of the alkyne and just 1.5 mol% of ruthenium catalyst **1.49** (Scheme 1.21). The reaction proceeds *via* enol ester intermediate **1.50** which is formed by ruthenium-catalysed addition of the carboxylic acid to the alkyne.



Scheme 1.21. Ruthenium-catalysed coupling of amines and carboxylic acids using alkynes as activators.

Meanwhile, although the coupling of carboxylic acids and amines is attractive, it is often useful to be able to access amides from other sources. As a result, other studies have

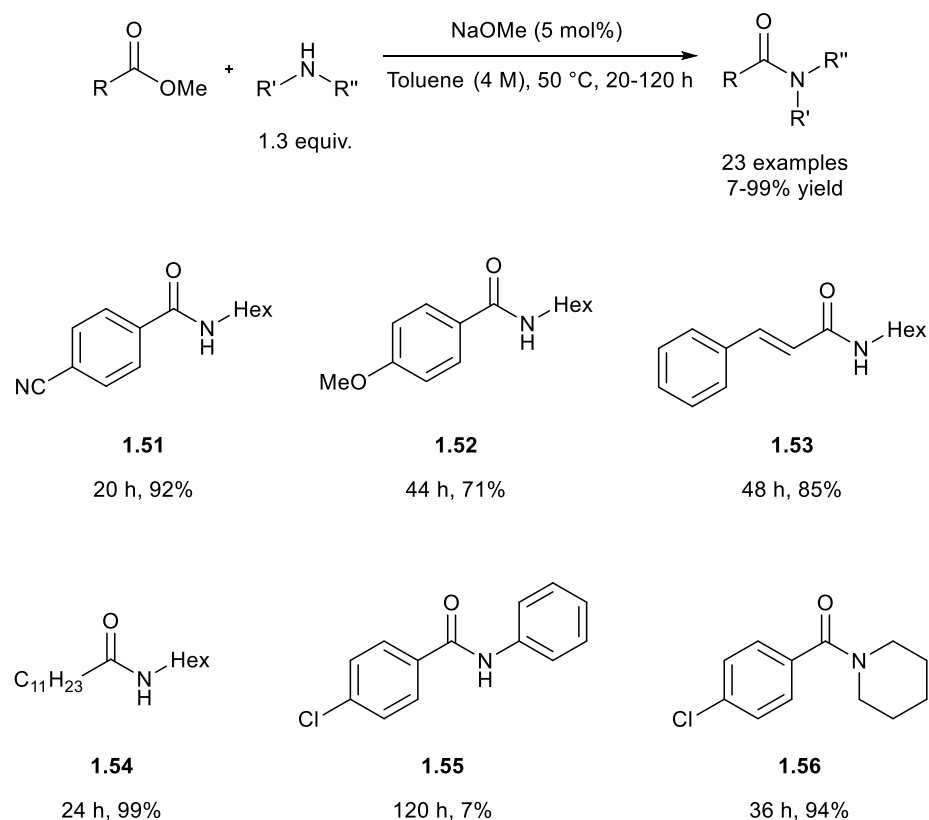
investigated the use of catalysts, including metal complexes, for the formation of amides from a wide range of other starting materials such as aldehydes,^{46,47} nitriles,⁴⁸⁻⁵⁰ oximes,⁵¹⁻⁵⁴ alcohols,⁵⁵⁻⁵⁸ amides⁵⁹⁻⁷¹ and esters.⁷²⁻⁷⁴

1.2.3.2. Amides from Esters

In addition to the use of carboxylic acids as starting materials for amidation reactions, significant attention has been given to the catalytic coupling of esters and amines. The ester functionality contains a superior leaving group compared with carboxylic acids and therefore the coupling reaction is less challenging.

Following the development of a number of stoichiometric approaches for the formation of amides from esters,^{75,76} more recent studies have focussed on investigating the use of catalysts for the transformation. A number of catalytic systems have since been developed, for example InI_3 ,⁷² $\text{Sb}(\text{OEt})_3$ ^{76,77} and $\text{Zr}(\text{O}^t\text{Bu})_4\text{-HOAt}$ ⁷⁴ have all been found to be efficient inorganic catalysts, whilst organic compounds such as *N*-heterocyclic carbene (NHC),⁷⁸ triazabicyclo[4.4.0]dec-5-ene,⁷⁹ DBU⁸⁰ and 1,2,4-triazole-DBU⁸¹ have also been shown to successfully catalyse the formation of amides from esters. However, these approaches often display a poor substrate scope, whilst the catalytic coupling of chiral α -amino esters was not investigated.

A report by Ohshima *et al.* looked to address these issues by attempting to develop an improved catalyst; several salts of both group 1 (Li, Na, K) and group 2 elements (Mg, Ca) were firstly screened, along with zinc-containing compounds.⁸² The group found NaOMe to be the most efficient catalyst, with a loading of 5 mol% in toluene at 50 °C generally affording good to excellent yields (Scheme 1.22). Anhydrous conditions were also very important for achieving efficient transformation, as any water present in the reaction led to saponification of the ester which ultimately halted the amidation process.

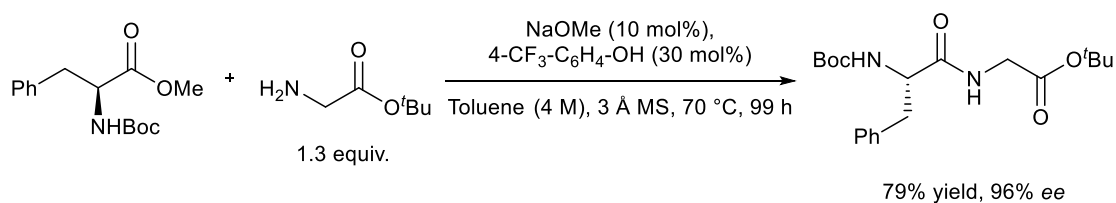


Scheme 1.22. NaOMe-catalysed formation of amides from esters, including selected examples.

Excellent yields were obtained using electron deficient methyl benzoates (**1.51**), whereas substrates with electron-donating substituents on the aromatic ring required longer reaction times and resulted in decreased yields (**1.52**). Pleasingly, α,β -unsaturated esters could be transformed into their amide products without the formation of side products, such as those from competing 1,4-addition reactions (**1.53**). Alkanoates (**1.54**) and lactones were also tolerated by the methodology, however anilines were found to be poor substrates under the reaction conditions (**1.55**). Tertiary amides could also be successfully generated from their corresponding amine/ester starting materials (**1.56**).

Furthermore, Ohshima *et al.* then applied the methodology to peptide coupling reactions. To prevent epimerisation under basic conditions, acidic alcohols were used as additives to increase the acidity of the reaction mixture. Although this resulted in a decreased yield, it considerably increased the enantiomeric excess of the reaction from 2% to <99%. Following the screening of various different acidic alcohols in combination with NaOMe, the group found 30 mol% 4-trifluoromethylphenol and 10 mol% of the catalyst gave the best results.

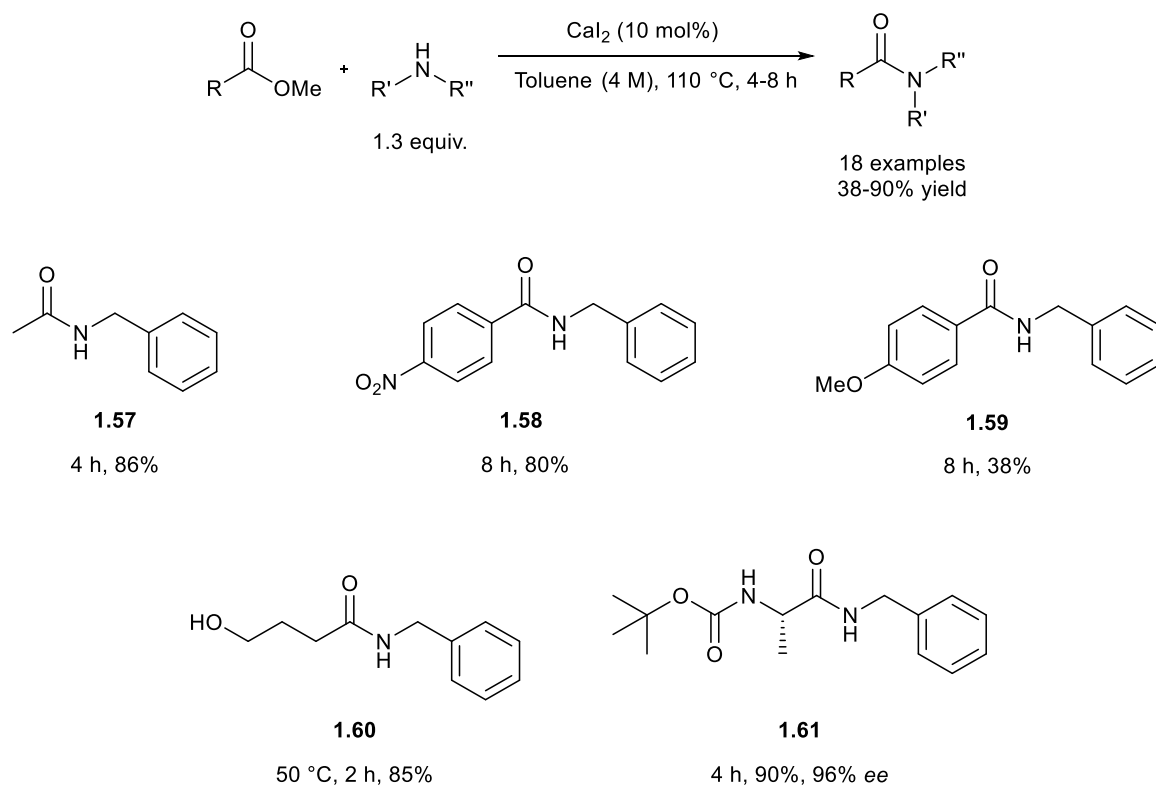
These conditions were successfully applied to the coupling of Boc-Phe-OMe and H-Gly-O^tBu (Scheme 1.23).



Scheme 1.23. NaOMe-catalysed peptide coupling of Boc-Phe-OMe and H-Gly-O^tBu.

In 2015, a similar study by Mecinović *et al.* reported the use of CaI₂ to promote the formation of amides.⁸³ Whereas calcium alkoxides and calcium carbonates were found to have poor catalytic activity by Ohshima *et al.*, Mecinović and colleagues revealed the iodine-based calcium salt efficiently catalysed the direct amidation reaction. The screening of alkali metals and alkaline earth metals also revealed MgI₂, CaBr₂, Ca(OTf)₂, SrI₂ and BaI₂ to be efficient catalysts (> 85% conversion) for the model coupling of methyl butyrate and benzylamine. Meanwhile, water-containing CaI₂ catalysts (CaI₂·xH₂O, x = 4-6) resulted in equally good conversions; illustrating that the progress of the reaction is not effected by the presence of water.

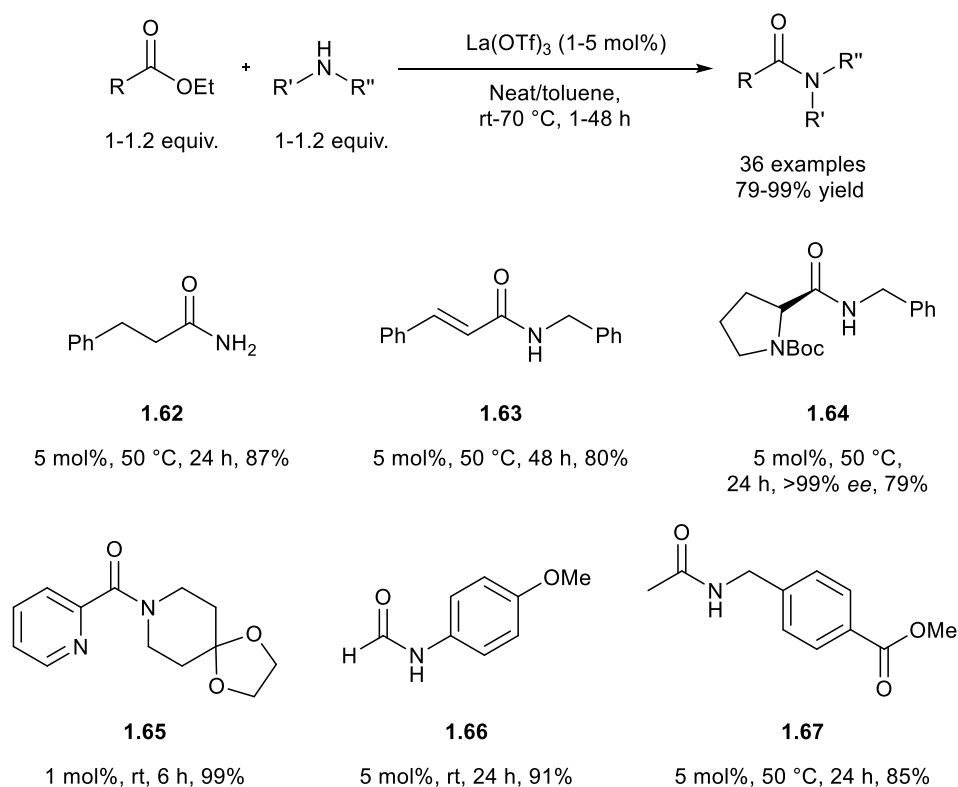
The group subsequently employed the optimal conditions, 10 mol% CaI₂ in toluene at 110 °C for 4 hours, to synthesise a wide variety of amides (Scheme 1.24). Aliphatic methyl and ethyl esters (**1.57**) were transformed in excellent yields, whilst the coupling of *para*-substituted methyl benzoates with amines gave a range of yields depending on the electronic nature of the *para*-substituent. Electron-withdrawing functionalities, such as nitro groups, afforded good yields (**1.58**) whereas the presence of an electron-donating group resulted in poor conversion (**1.59**). The conditions allowed the ring opening of cyclic γ -butyrolactone to afford the desired product after just 2 hours (**1.60**).



Scheme 1.24. CaI_2 -catalysed formation of amides from esters, including selected examples.

In addition, Boc protecting groups were unaffected by the mild conditions and enantiopure substrates reacted with retention of stereochemistry (**1.61**, 96% *ee*). However, secondary amines were unsuitable substrates for the CaI_2 -catalysed methodology with no conversion into the desired products observed. The group however did show that the reaction conditions were highly chemoselective for carboxylic esters; carboxylic acids and amides afforded considerably lower conversions. In comparison, Cp_2ZrCl_2 -mediated amidation is able to transform all three derivatives into the amide product.^{44,84,85}

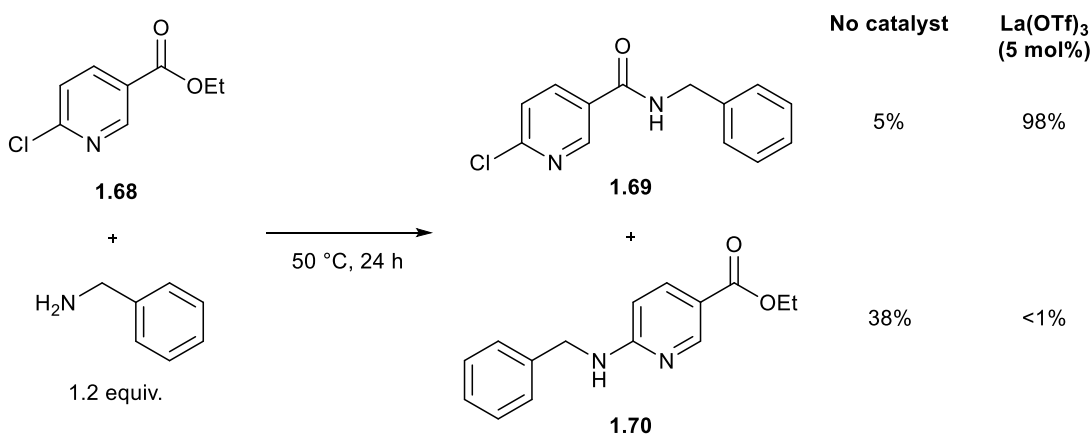
A further study performed by Morimoto in 2014 reported the use of the rare earth metal complex $\text{La}(\text{OTf})_3$ as an efficient catalyst for promoting the formation of amides under mild conditions.⁸⁶ The group had previously investigated the cleavage of amide bonds⁸⁷ and they proposed that acidic complexes would catalyse the direct amidation reaction. A catalyst loading of 5 mol% was applied to a wide range of amine and ester substrates to furnish a selection of amides at rt-70 °C in 1-48 hours (Scheme 1.25).



Scheme 1.25. La(OTf)₃-catalysed formation of amides from esters, including selected examples.

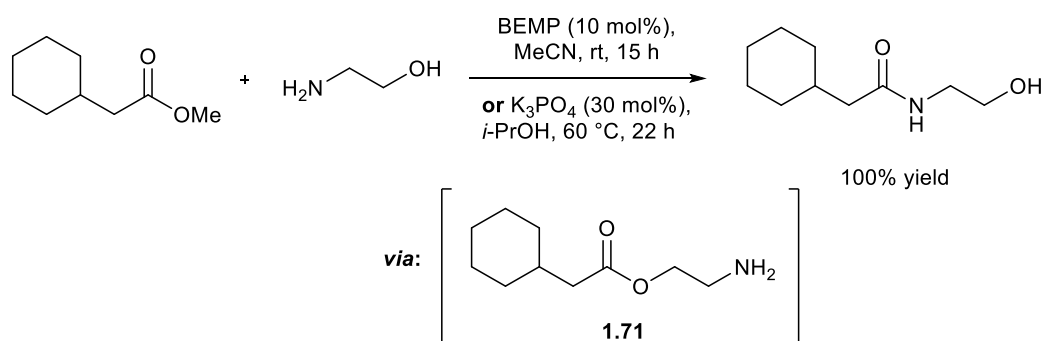
The methodology was suitable for the formation of primary amides such as **1.62**; performed using saturated NH₃ solution in EtOH. Meanwhile, a variety of functional groups, including iodo, cyano, phosphonate, carbamate, amide and α,β -unsaturated esters (**1.63**) were well tolerated by the reaction conditions. In addition, amide **1.64** was formed with retention of stereochemistry and no deprotection of the Boc group. Unlike with the CaI₂-mediated approach detailed previously, a variety of tertiary amides could be synthesised from secondary amines, including the 2-pyridinecarboxamide derivative **1.65**. The methodology also allowed the formation of both formamides (**1.66**) and acetamides (**1.67**) in excellent yields.

The catalyst control of chemoselectivity was also investigated; the group performed the reactions with and without the catalyst present and observed the ratios of products in each case. For example, in the absence of the catalyst, ester **1.68** reacted in a S_NAr manner with benzylamine to afford ester **1.70** as the major product (Scheme 1.26). However, when 5 mol% of La(OTf)₃ is present the amidation reaction is preferred and amide **1.69** is generated instead.



Scheme 1.26. Example of catalyst control of chemoselectivity.

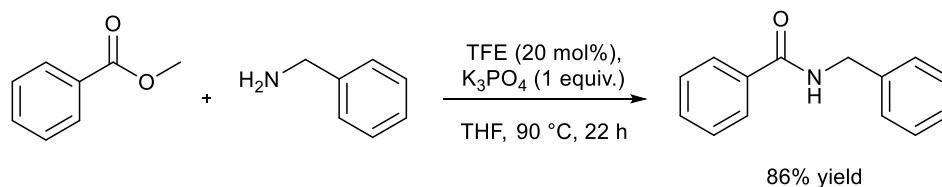
However, the use of rare earth metals for the conversion of unactivated esters to amides is not ideal from a sustainability perspective. Jamieson and colleagues have since attempted to confront this issue. Earlier studies by the group showed that organobases, such as 2-*tert*-butylimino-2-diethylamino-1,3-dimethylperhydro-1,3,2-diazaphosphorine (BEMP) and K_3PO_4 , were able to efficiently catalyse the coupling of unactivated esters and amino alcohols (Scheme 1.27).^{88,89} The group revealed the mechanism proceeds through ester intermediate **1.71**, before intramolecular rearrangement to the more thermodynamically stable amide occurs to give the desired product.⁹⁰ As a result, for a successful transformation, amines containing an alcohol moiety must be employed.



Scheme 1.27. BEMP- or K_3PO_4 -catalysed amidation of esters.

In order to extend the substrate scope, the group investigated whether alcohol-derived additives could be used to generate an active ester *in situ*, followed by reaction with the amine to afford the desired product.⁹¹ A variety of additives, including HOAt, oxyma, *N*-hydroxysuccinamide, hexafluoroisopropanol and 2,2,2-trifluoroethanol (TFE), were added in

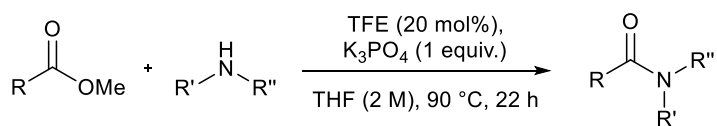
stoichiometric amounts to the model reaction of methyl benzoate and benzylamine. The group showed that TFE in combination with K_3PO_4 gave efficient conversion into the amide product in THF (Scheme 1.28). Notably, employing either TFE or the base in isolation resulted in minimal conversion, illustrating the need for them to be used in combination.



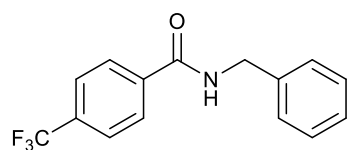
In the presence of just K_3PO_4 or TFE: < 2% conversion

Scheme 1.28. Trifluoroethanol-mediated catalytic amidation of unactivated esters.

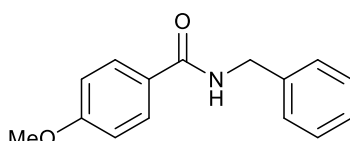
Examination of the ester substrate scope revealed aryl electron-deficient groups were well tolerated by the methodology (**1.72**, Scheme 1.29), whereas the presence of electron-rich moieties resulted in less efficient conversion (**1.73**). Amidation reactions involving aliphatic esters could also be achieved, although **1.74** underwent significant racemisation (6% *ee*), thus highlighting a potential limitation of this protocol. Heterocyclic motifs proved to be compatible with the methodology (**1.75-1.77**), whilst secondary amines were also efficiently transformed into their tertiary amide products in good yield. These include **1.76** as well as the Ampakine Farampator (**1.77**).



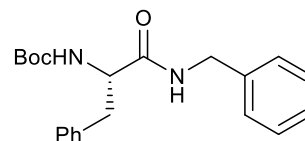
22 examples
41-95% yield



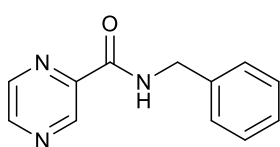
1.72
95%



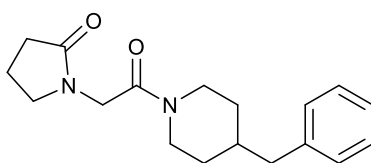
1.73
41%



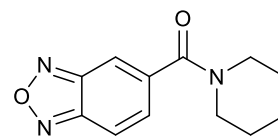
1.74
6% ee, 42%



1.75
64%



1.76
63%

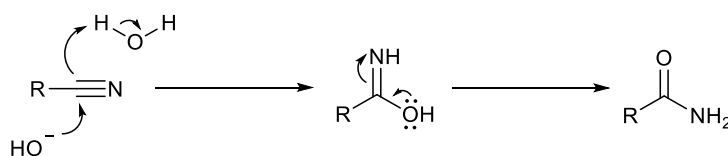


1.77
60%

Scheme 1.29. TFE-catalysed formation of amides from esters, including selected examples.

1.2.3.3. Primary Amides from Nitriles

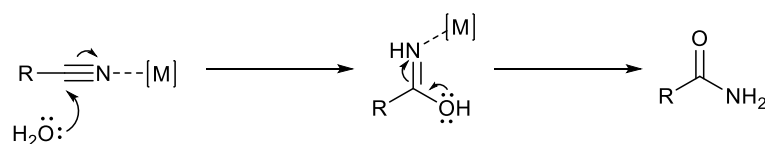
One of the most attractive methods for the preparation of primary amides, in both industry and academia, is the hydration of nitriles.⁹²⁻⁹⁷ Early methods focussed on employing strong acids and bases to access the desired amide product from the nitrile (Scheme 1.30).⁹⁸ However, these approaches suffer several drawbacks, including the formation of carboxylic acids through over-hydrolysis of the amide, low functional group tolerance and extensive formation of salts after neutralisation.^{14,98-100}



Scheme 1.30. Base-catalysed hydration of nitriles.

As a result, widespread research has been performed to establish more mild and efficient methods for the hydration of nitriles into primary amides. The generally accepted mechanism for the metal-catalysed hydration of nitriles in water under neutral conditions is outlined in Scheme 1.31. Coordination of the nitrile to the metal centre increases the electrophilicity of

the nitrile carbon, thus increasing its susceptibility to nucleophiles. Nucleophilic attack by water then affords an iminolate species which rearranges to yield the desired amide.



Scheme 1.31. Metal-catalysed hydration of nitriles in water.

In 2009, Nolan *et al.* detailed the first nitrile hydration catalysed by gold (Figure 1.6).⁵⁰ Employing a [(NHC)Au^I] complex, aromatic, heteroaromatic and aliphatic nitriles were efficiently transformed into their corresponding nitriles in only 2 hours at 140 °C.

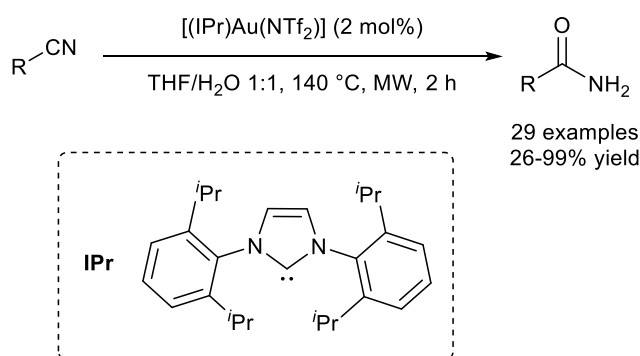
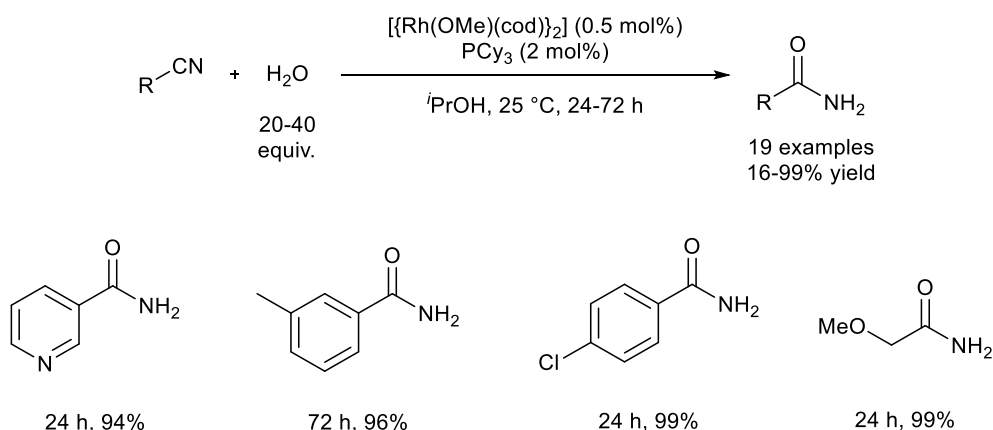


Figure 1.6. Gold-catalysed hydration of nitriles developed by Nolan *et al.*

Around the same time, Saito and colleagues published a ground-breaking report in which a Rh^I complex was used to hydrate nitriles at low temperature.¹⁰¹ Although transition metal complexes had previously been employed under ambient conditions,^{102,103} this was the first approach that successfully converted nitriles into primary amides at room temperature without requiring a base. The active Rh^I complex was firstly prepared by reacting PCy₃ (2 mol%) with commercially available [{Rh(OMe)(cod)}₂] (0.5 mol%) in anhydrous THF for 15 minutes at 25 °C. The catalyst was able to transform an extensive range of nitriles into their corresponding primary amide products at 25 °C in 24-72 hours (Scheme 1.32).



Scheme 1.32. Rh^I-catalysed hydration of nitriles under ambient conditions.

Homogeneous ruthenium catalysis has also been a popular area of research. The Cadierno group have been particularly active in this field, developing a wide variety of hydrophilic ruthenium complexes which are able to selectively hydrate nitriles in refluxing water under neutral conditions.¹⁰⁴⁻¹¹¹ Specifically, arene-ruthenium(II) (**1.78-1.80**) and bis(allyl)-ruthenium(IV) (**1.81** and **1.82**) complexes containing phosphine ligands have been a key area of interest (Figure 1.7).

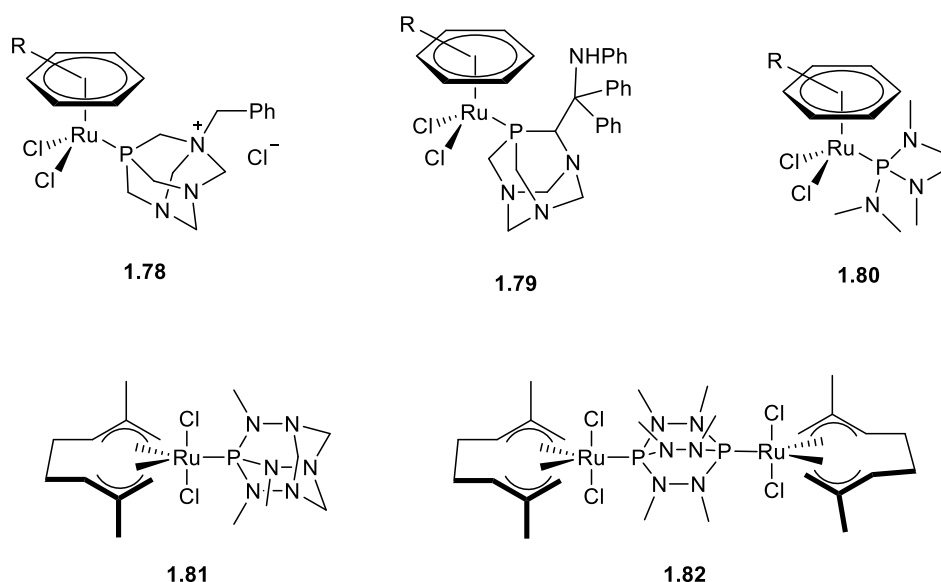
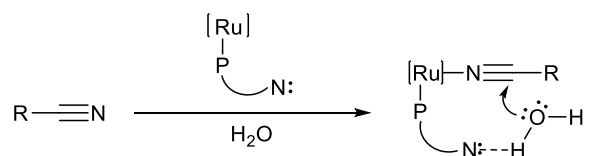


Figure 1.7. Arene-ruthenium(II) (**1.78-1.80**) and bis(allyl)-ruthenium(IV) (**1.81** and **1.82**) complexes developed by the Cadierno group for the catalytic hydration of nitriles in water under neutral conditions.

The efficiency of these catalysts is attributed to the hydrophilic phosphine ligands present in the metal complexes.^{106,108,112-115} As well as increasing the solubility of the catalysts in water, the phosphine ligands also promote the key nucleophilic addition step in the reaction. The

phosphine ligands contain Lewis basic atoms which are able to hydrogen-bond to water molecules, thereby activating them towards nucleophilic attack on the coordinated nitrile species (Scheme 1.33). These complexes are therefore examples of ‘bifunctional catalysts’, whereby the metal centre functions as a Lewis acid and the ligand as a Lewis base.^{116,117}



Scheme 1.33. The activating effect of phosphine ligands on water molecules during the hydration of nitriles.

Following these earlier protocols, the group later reported *N*-protonated thiazolyl-phosphine salts to be effective ligands in the ruthenium-catalysed selective hydration of nitriles.¹¹⁰ In particular, **1.83**, containing the tris(5-(2-aminothiazolyl))phosphine trihydrochloride salt, proved to be a superior catalyst for the reaction compared to the bis- and mono- derivatives (Figure 1.8). The authors concluded that the trend in reactivity was a result of the increased number of hydrogen acceptors (S and NH₂) as more thiazolium units are added to the complex.

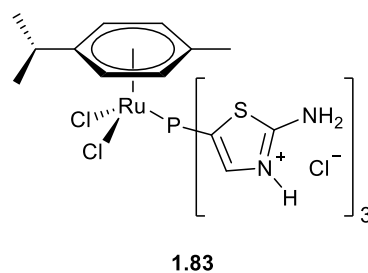
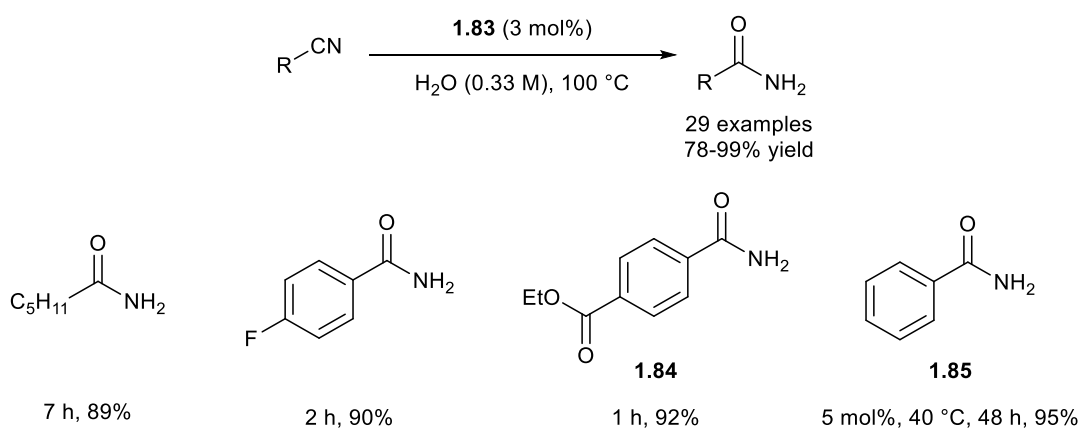


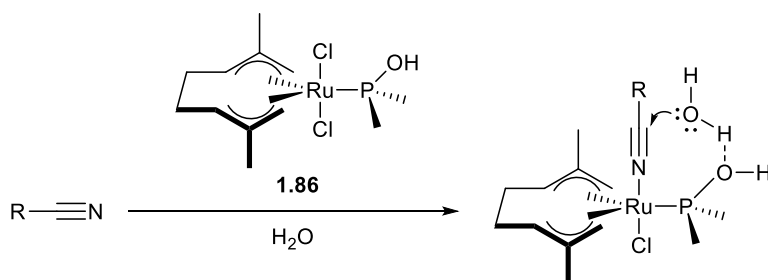
Figure 1.8. Water-soluble ruthenium complex containing a thiazolium-based phosphine ligand.

Employing just 3 mol% of **1.83** in water at 100 °C, a vast array of primary amides were isolated in excellent yield after purification by recrystallisation (Scheme 1.34). Specifically, ester-containing nitriles were tolerated by the methodology, with no over-hydrolysis into the carboxylic acid observed (**1.84**). In addition, the group demonstrated that by using a slightly higher catalyst loading and increased reaction times, the reaction could be efficiently performed at just 40 °C (**1.85**).



Scheme 1.34. Synthesis of primary amides from nitriles using **1.83**.

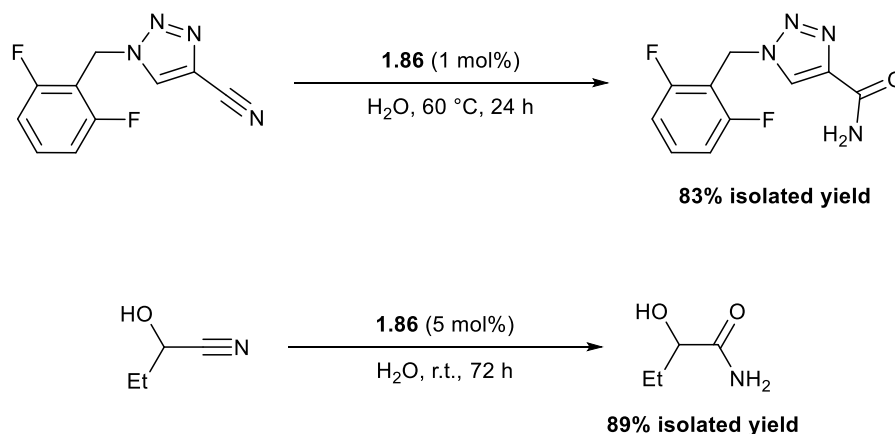
Cadierno *et al.* proceeded to develop a milder method for the hydration of nitriles in water compared with those already reported by the group.¹¹¹ Whereas the previous ruthenium-catalysed protocols had employed refluxing conditions, this new approach afforded primary amides from nitriles in water at just 60 °C. Once again a phosphine ligand was responsible for increasing the nucleophilicity of the water molecules in the reaction (Scheme 1.35). In addition, following crystallisation of the amide product at room temperature or 0 °C, the group showed that the aqueous phase containing **1.86** could be recycled and reused up to six times without any loss of activity.



Scheme 1.35. Coordination and activation of the nitrile species.

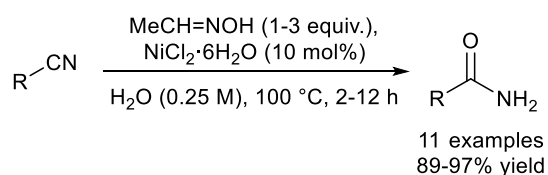
As well as affording aliphatic, aromatic and heteroaromatic nitriles in good to excellent yield, the synthetic utility of the protocol was also demonstrated (Scheme 1.36). Firstly, the antiepileptic drug rufinamide (Inovelon®) was isolated in 83% yield using 1 mol% **1.86**. Secondly, the approach was able to successfully hydrate the notoriously challenging cyanohydrins. These substrates decompose in aqueous media into the corresponding carbonyl compounds and HCN, a by-product which inhibits the majority of previous nitrile hydration catalysts. In contrast, ruthenium complex **1.86** is more tolerant to these reaction

conditions, especially when the reaction is performed at room temperature to minimise degradation of the substrate (Scheme 1.36).



Scheme 1.36. Synthetic utility of **1.86**: synthesis of an antiepileptic drug and the hydration of cyanohydrins.

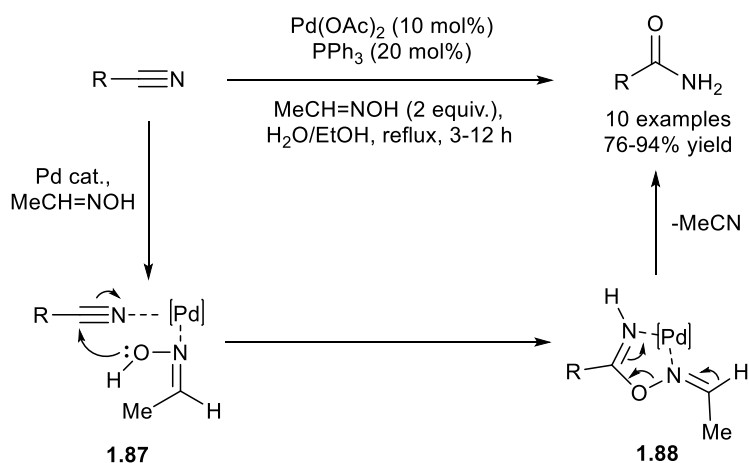
Other methods for the hydration of nitriles have focussed on employing aldoximes in the reaction. For example, Lu *et al.* reported the use of commercially available acetaldoxime (1-3 equivalents) in combination with simple and inexpensive transition metal catalysts, such as nickel, zinc, cobalt and manganese salts, for the hydration of nitriles in water at reflux.¹¹⁸ Among these salts, NiCl₂·6H₂O (10 mol%) showed the highest catalytic activity, transforming a range of nitriles into their corresponding primary amides in 2-12 hours (Scheme 1.37).



Scheme 1.37. Hydration of nitriles using acetaldoxime and nickel(II) chloride hexahydrate.

The authors proposed the reaction proceeded through a similar mechanism to that previously reported in the literature by Chang/Lee and Kim.¹¹⁹⁻¹²¹ Kim and colleagues had detailed an efficient palladium-catalysed hydration of nitriles, employing Pd(OAc)₂ (10 mol%), PPh₃ (20 mol%) and acetaldoxime (2 equivalents) in a H₂O/EtOH solvent medium (Scheme 1.38). The group postulated that the palladium metal coordinates to the nitrile and aldoxime *via* the nitrogen atoms of the two molecules (**1.87**). The oxygen of the aldoxime is then delivered to

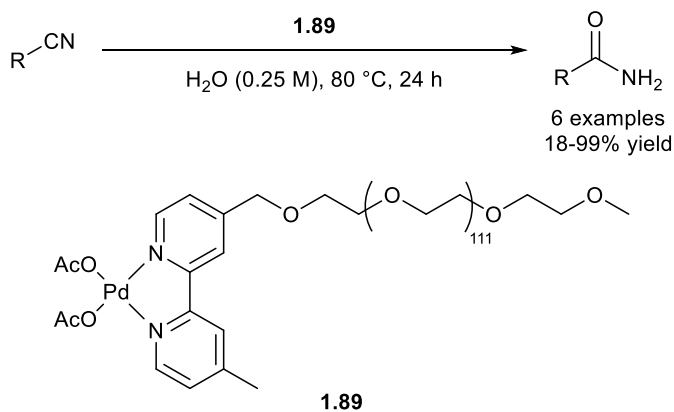
the electrophilic carbon of the nitrile to form intermediate **1.88**, which then rearranges to liberate the desired primary amide product and acetonitrile as a by-product.



Scheme 1.38. Palladium-catalysed nitrile hydration with acetaldoxime.

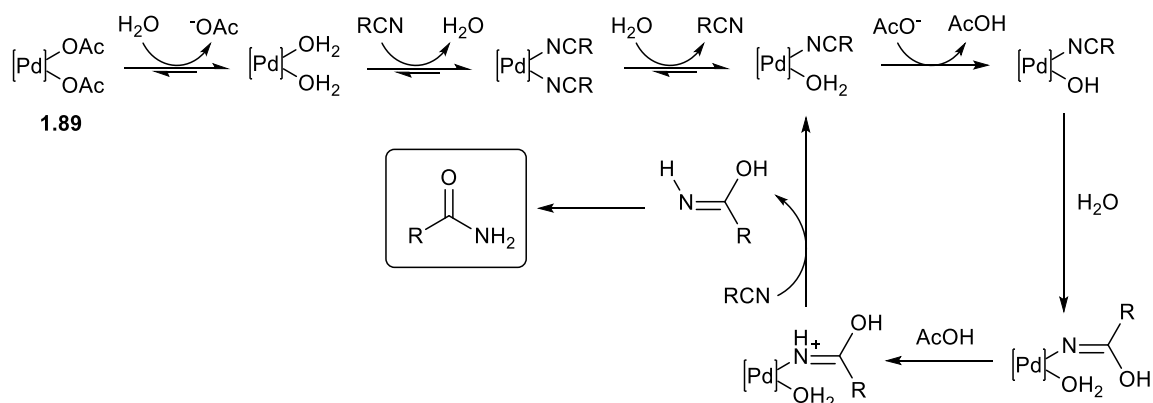
Palladium-catalysed homogeneous protocols for nitrile hydration which operate without aldoxime additives have also been reported. These systems date back to 1972 when Goetz and Mador detailed the hydration of acetonitrile using sodium chloropalladate and 2,2'-bipyridine (bipy) under alkaline conditions.¹²² Following this, a number of palladium complexes have been reported for the transformation, including $\text{PdCl}(\text{OH})(\text{bipy})(\text{H}_2\text{O})$,¹²³ $[\text{Pd}(\text{H}_2\text{O})_4][\text{ClO}_4]_2$,¹²⁴ *cis*- $[\text{Pd}(\text{en})(\text{H}_2\text{O})_2][\text{ClO}_4]_2$ ¹²⁴ and *cis*- $[\text{Pd}(\text{dtod})(\text{H}_2\text{O})_2][\text{ClO}_4]_2$.¹²⁵

More recently, Oberhauser *et al.* published literature investigating the catalytic performance of commercially available $\text{Pd}(\text{OAc})_2$ in water.¹²⁶ In order to solubilise the catalyst, $\text{Pd}(\text{OAc})_2$ was stabilised with a poly(ethyleneglycol) (PEG) functionalised bipy ligand (Scheme 1.39). Palladium complex **1.89** was able to hydrate nitriles at 80 °C in 24 hours; however, the method exhibited a very limited substrate scope.



Scheme 1.39. Catalytic hydration of nitriles in water using a stabilised Pd(OAc)₂ complex.

The group subsequently proceeded to investigate the reaction mechanism using *operando* ¹H NMR spectroscopy (bipy hydrogens as the diagnostic signals) with D₂O as the solvent. In order to determine the effect of the acetate anion on the reaction mechanism, the same studies were also performed on a bipy-stabilised Pd(OTs)₂-catalysed reaction as well. Comparison between the reactions employing **1.89** and the 'OTs' complex indicated the acetate anion has a negligible effect on the efficiency of the process. A reaction mechanism consistent with all of the ¹H NMR data was then proposed; starting with activation of catalyst **1.89** upon displacement of the acetate anions with water molecules (Scheme 1.40).



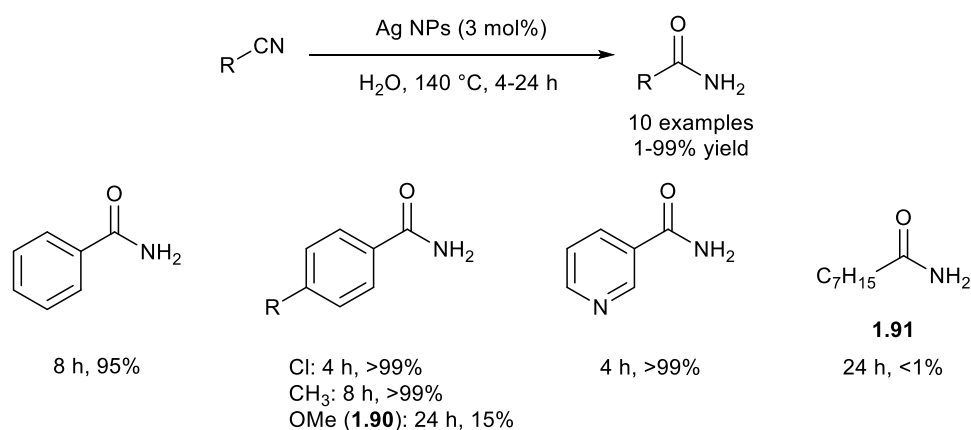
Scheme 1.40. Proposed catalytic cycle for the hydration of nitriles using **1.89** as a catalyst.

The group compared the efficiency of **1.89** to the catalytic performance of modified palladium nanoparticles (NPs). These NPs were also stabilised with the PEG functionalised bipy ligand and partially covered by chemisorbed oxygen atoms. Comparison of the normalised turnover number (TON) values for this system with the homogeneous protocol revealed that the palladium NP-based catalyst exhibited significantly increased catalytic

activity. However, following the first catalytic run, the palladium NPs became deactivated due to the formation of a hydroxide-water layer on their surface.

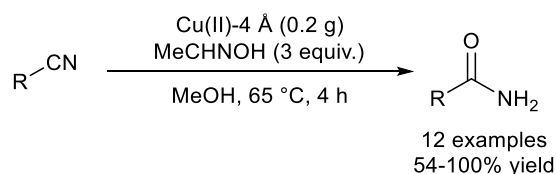
The use of NPs in the hydration of nitriles to primary amides has also been exploited by other groups. Further palladium NP-catalysed protocols have been reported,^{127,128} as well as NP-based approaches employing transition metals such as Ni,¹²⁹ Pt,¹²⁷ Au,¹³⁰ Ru,^{131,132} Mo¹³³ and Ag (the most prevalent).¹³⁴⁻¹³⁶ In 2015, Yonezawa and colleagues reported the selective hydration of nitriles to amides using water-dispersible silver nanoparticles, which are stabilised by silver-carbon covalent bonds between the metal and benzoic acid molecules.¹³⁴ This arrangement results in a hydrophobic layer between the hydrophilic layer and the Ag surface, thereby increasing the concentration of substrate molecules near the particle surface.

Owing to the stabilisation described, this system showed increased catalytic activity compared to previous Ag NP-based methods, for example PVP-stabilised Ag NPs.¹³⁴ Employing 3 mol% Ag NPs, a number of aromatic nitriles were converted into their corresponding primary amides at 140 °C in 4-24 hours (Scheme 1.41). Notably however, the strongly electron-donating methoxy substrate (**1.90**) was transformed in low conversion (15%), therefore illustrating the effect electron donation has on the catalytic performance of Ag NPs. Similarly to previous Ag NP studies, aliphatic nitriles exhibited significantly decreased reactivity (**1.91**).



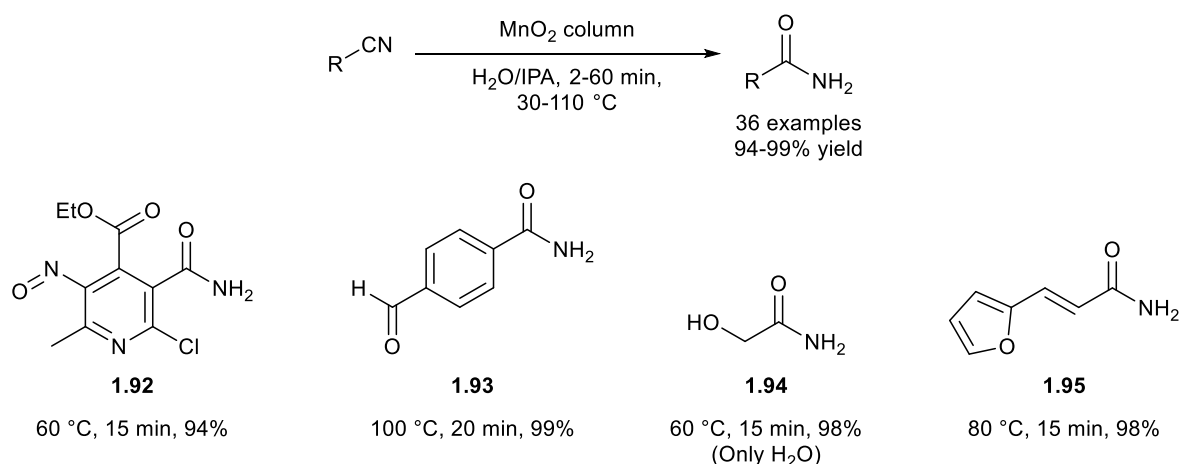
Scheme 1.41. Silver NP-catalysed hydration of nitriles to amides developed by Yonezawa *et al.*

A range of other heterogeneous catalysts have also been developed for the preparation of primary amides from nitriles.^{130,137,138} Copper(II) supported on 4 Å molecular sieves, prepared *via* impregnation of the molecular sieves with copper salt, has been reported as an effective and recyclable catalyst for the transformation (Scheme 1.42).¹³⁸ In contrast, when palladium(II) and palladium(0) were used as the metal, the reaction proceeded with decreased efficiency.



Scheme 1.42. Cu(II)-4 Å-catalysed hydration of nitriles into primary amides.

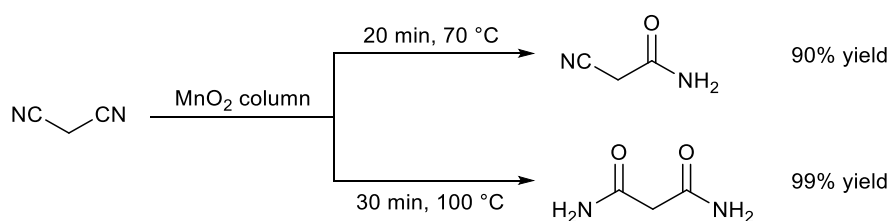
In 2014, Ley *et al.* detailed a mild and sustainable flow process for the hydration of nitriles using a column containing commercially available manganese dioxide (MnO_2).¹³⁹ After an aqueous solution of the nitrile has been passed through the heterogeneous catalyst, the output is concentrated to afford the amide product without any further purification steps. The protocol displayed a remarkable level of chemical tolerance – substrates containing esters (**1.92**), aldehydes (**1.93**), hydroxyls (**1.94**) and alkenes (**1.95**) were all efficiently transformed into the corresponding primary amides in excellent yields (Scheme 1.43).



Scheme 1.43. Flow hydration of nitriles and selected functional groups tolerated.

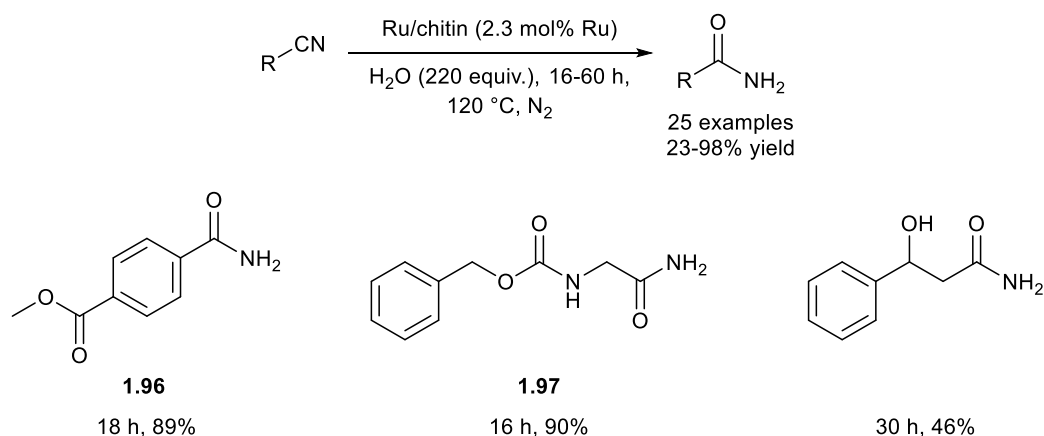
In addition, acrylonitrile was hydrated to acrylamide without polymerisation, therefore illustrating the mildness of the protocol. The authors also showed that dinitriles could be

partially or fully hydrated by simply changing the temperature of the reaction and the time spent in the MnO₂ column (Scheme 1.44).



Scheme 1.44. Flow hydration of dinitriles.

A further heterogeneous protocol tolerating an impressively wide range of functional groups was published in 2015 by Naka, Saito and Wheatley.¹⁴⁰ A chitin-supported ruthenium catalyst, prepared by impregnating commercially available chitin with ruthenium(III) chloride (aqueous) and then reducing the product with sodium borohydride, successfully hydrated nitriles in 16-60 hours at 120 °C (Scheme 1.45). Notably, ester (**1.96**) and carbamate (**1.97**) functionalities, which are base- and redox- sensitive respectively, were tolerated by the methodology.

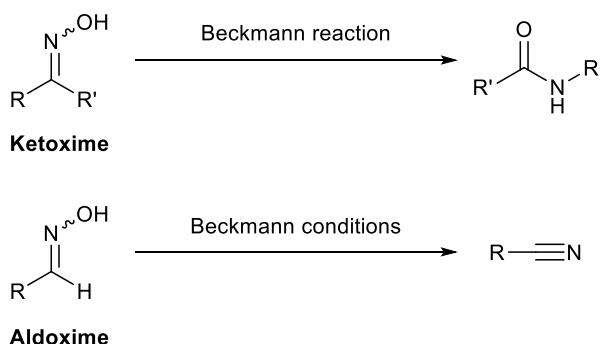


Scheme 1.45. Ru/chitin-catalysed hydration of nitriles.

1.2.3.4. Primary Amides from Aldehydes and Aldoximes

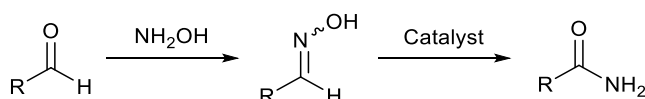
Another well-documented approach for forming amides is the rearrangement of oximes. Specifically, the Beckmann rearrangement of ketoximes is a popular method for the preparation of secondary amides. In contrast, when aldoximes are exposed to classical

Beckmann conditions, the corresponding nitriles are formed instead of primary amides (Scheme 1.46).



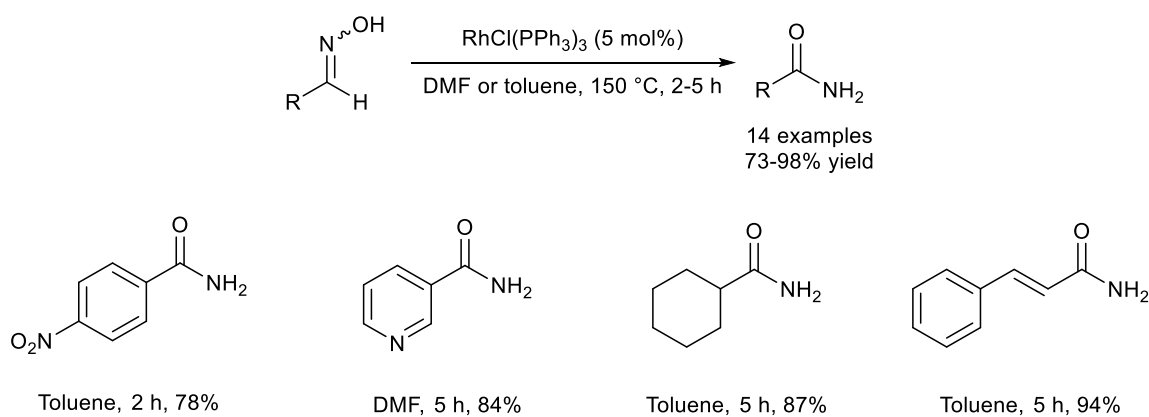
Scheme 1.46. Reaction of ketoximes and aldoximes under Beckmann conditions.

However, a multitude of metal complexes have since been reported which catalyse efficient transformation of aldoximes into their corresponding primary amides. In addition, methods have also been developed for the direct conversion of aldehydes (and alcohols) into primary amides (Scheme 1.47). Reaction of the aldehyde with hydroxylamine generates the aldoxime *in situ* before the rearrangement occurs.



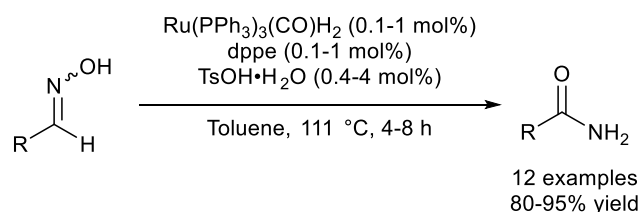
Scheme 1.47. Rearrangement of aldoximes into primary amides starting from an aldehyde.

In 2001 and 2002, Sharghi and co-workers detailed a number of reports in which stoichiometric amounts of ZnO,¹⁴¹ Al₂O₃/CH₃SO₃H¹⁴² and wet Al₂O₃/MeSO₂Cl¹⁴³ were employed for the rearrangement of aldoximes into primary amides, starting from either the aldehyde or aldoxime. Shortly after, the first catalytic protocol for the transformation was published by Chang *et al.*¹⁴⁴ The group detailed a highly selective and efficient method for the rearrangement of aldoximes into primary amides using Wilkinson's catalyst, RhCl(PPh₃)₃, at 150 °C. The protocol, which is performed under essentially neutral conditions, is able to convert a range of aldoximes into the corresponding primary amides in 2-5 hours using 5 mol% of the rhodium catalyst (Scheme 1.48). Lower catalyst loadings of 0.5-1 mol% could also be employed if the reaction was left for a longer period of time (8-12 hours).



Scheme 1.48. Aldoxime rearrangement catalysed by Wilkinson's catalyst, $\text{RhCl}(\text{PPh}_3)_3$.

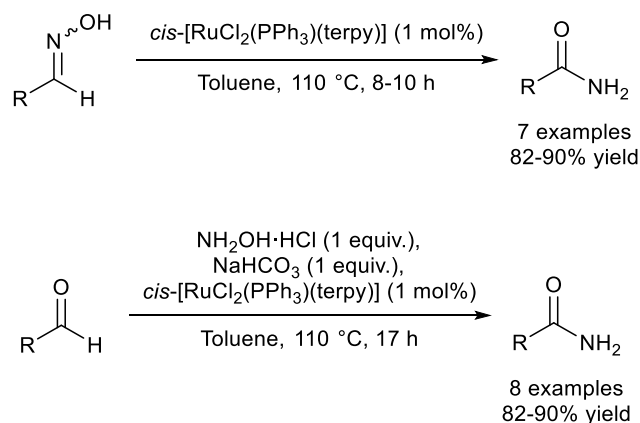
In 2007, the first ruthenium-based procedure was reported by the Williams group.¹⁴⁵ A combination of $\text{Ru}(\text{PPh}_3)_3(\text{CO})\text{H}_2$ (0.1-1 mol%), dppe and TsOH (in a 1:1:4 ratio) successfully converted aliphatic, aromatic and heteroaromatic aldoximes into their corresponding primary amides in toluene under reflux conditions (Scheme 1.49).



Scheme 1.49. Ruthenium-catalysed aldoxime rearrangement developed by Williams *et al.*

Since this initial report, many groups have focused their research on the conversion of both aldehydes and aldoximes into primary amides using ruthenium catalysts. In 2009, Crabtree detailed the use of *cis*- $[\text{RuCl}_2(\text{PPh}_3)(\text{terpy})]$ for the rearrangement reaction.¹⁴⁶ In contrast to the Williams group's protocol, the method didn't require any chelating phosphines or additives. Employing 1 mol% of the ruthenium catalyst in toluene at 110 °C aliphatic and aromatic substrates, including both *E*- and *Z*-isomers, were converted into their corresponding primary amide products (Scheme 1.50).

In addition, the group also adapted their protocol in order to convert aldehydes into primary amides in a one-pot process using a 1:1:1 mixture of aldehyde, hydroxylamine hydrochloride and NaHCO_3 (Scheme 1.50).¹⁴⁶ The presence of the base in the reaction is important as without it, the HCl produced during the aldoxime-forming step catalyses over-hydrolysis of the amides into the carboxylic acids.



Scheme 1.50. *cis*-[RuCl₂(PPh₃)(terpy)]-catalysed formation of primary amides from aldoximes and aldehydes.

Following Crabtree's report, a number of other protocols have been developed based on octahedral ruthenium(II) complexes containing polydentate O-, N- and/or S-donor ligands.¹⁴⁷⁻¹⁵² These complexes, displayed in Figure 1.9, are able to catalyse the transformation of aldoximes and/or aldehydes into their corresponding primary amides using 0.5-1 mol% catalyst loading in refluxing toluene or acetonitrile.

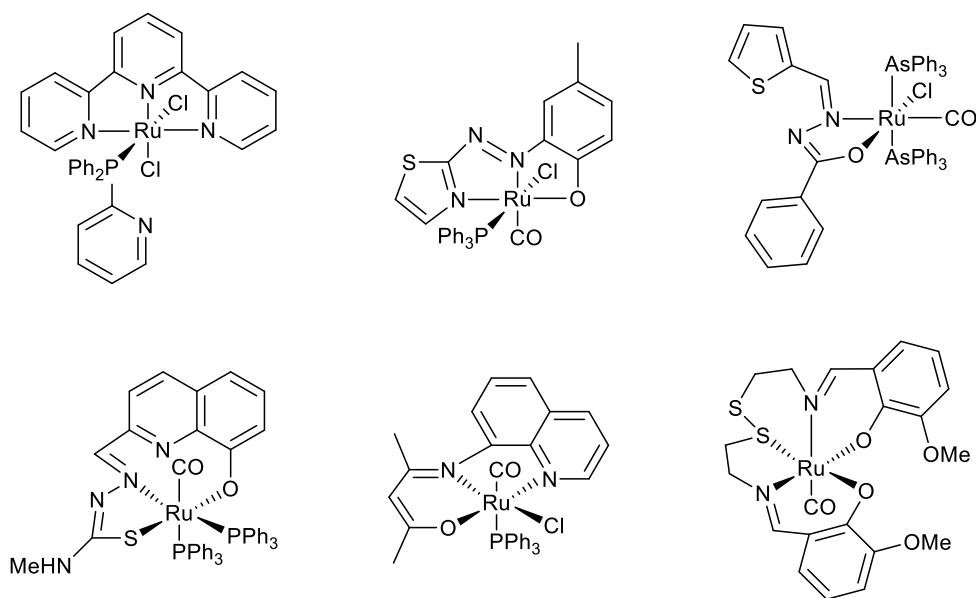


Figure 1.9. Examples of octahedral ruthenium complexes containing O-, N- and/or S-ligands for the transformation of aldoximes and/or aldehydes into primary amides.

In addition, ruthenium complexes containing arene ligands have also been shown to catalyse these transformations. As well as their work on nitrile hydration reactions, Cadierno and colleagues have also published important research on the rearrangement of aldoximes,

including protocols involving phosphine-containing arene-ruthenium(II) complexes (Figure 1.10).^{110,153,154}

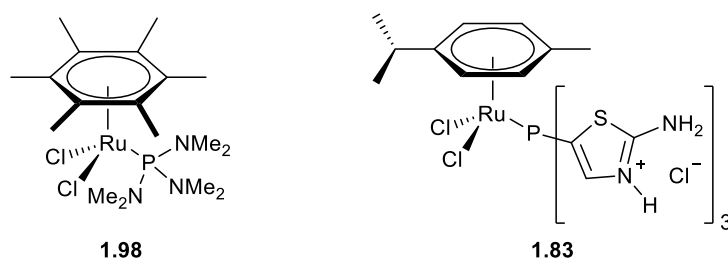
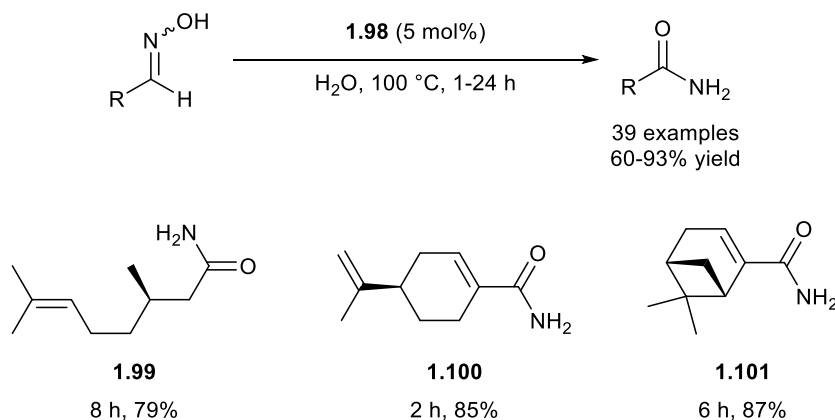


Figure 1.10. Arene-ruthenium(II) complexes employed in aldoxime rearrangement reactions.

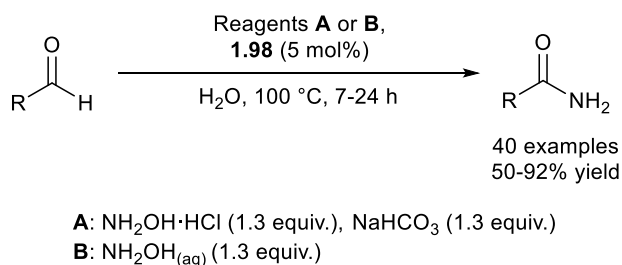
Arene-ruthenium complex **1.98** (5 mol%), which contains the commercially available and inexpensive tris(dimethylamino)phosphine ligand, efficiently rearranged a wide array of aldoximes at 100 °C in water (Scheme 1.51).¹⁵³ Aliphatic, aromatic, heteroaromatic and α,β -unsaturated aldoximes were all tolerated by the methodology, as were a broad spectrum of functional groups, including halide, nitro, hydroxyl, thioether and amino moieties. Significantly, the authors demonstrated the methodology could also be applied to optically active aldoximes, with minimal loss of stereochemistry (**1.99-1.101**).



Scheme 1.51. Rearrangement of aldoximes, including optically active substrates, employing **1.98** as the catalyst.

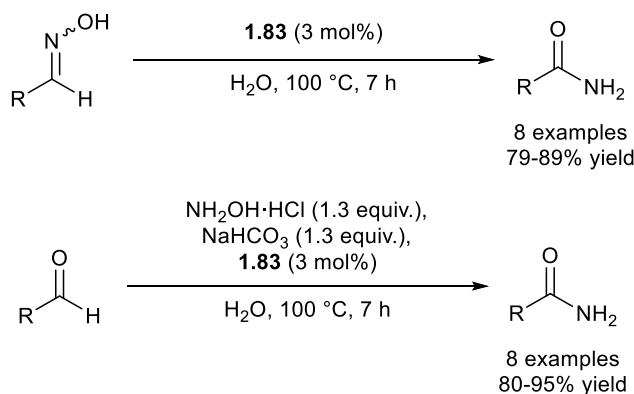
A follow-up report by the group demonstrated the use of **1.98** for the direct conversion of aldehydes into primary amides, *via in situ* formation of aldoximes, in a one-pot procedure (Scheme 1.52).¹⁵⁴ Employing double the amount of hydroxylamine hydrochloride and NaHCO_3 allowed the conversion of benzenedicarboxaldehydes into benzenediamides under the same conditions. In addition, the authors also adapted the methodology to develop a greener procedure in which commercially available hydroxylamine solution was used as the

hydroxylamine source instead. This avoids the use of a base in the reaction and therefore reduces the generation of waste.



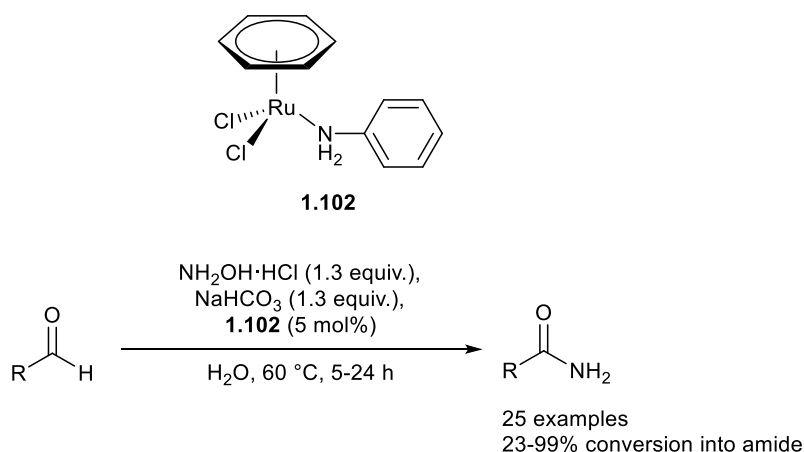
Scheme 1.52. One-pot synthesis of primary amides from aldehydes catalysed by **1.98**, using different sources of hydroxylamine.

The Cadierno research group also showed that complex **1.83** (Figure 1.10), which had also been successful in catalysing nitrile hydration reactions, was able to transform aldoximes and aldehydes into primary amides (Scheme 1.53).¹¹⁰ A wide range of aliphatic, aromatic, heteroaromatic and α,β -unsaturated primary amides were synthesised using just 3 mol% of ruthenium catalyst **1.83** in both protocols.



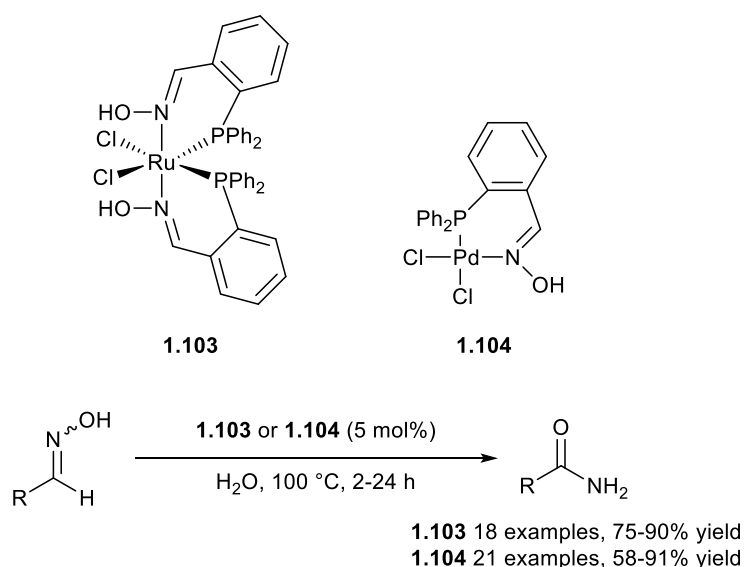
Scheme 1.53. Conversion of aldoximes and aldehydes into primary amides using ruthenium catalyst **1.83**.

In addition, Singh *et al.* have developed a highly active phosphine-free ruthenium catalyst, with a similar structure to **1.98**, containing a readily available aniline ligand (Scheme 1.54).¹⁵⁵ The excellent catalytic ability of the complex allowed the direct conversion of aldehydes into primary amides at a remarkably lower temperature (60 °C) compared with those reported previously (100-110 °C).



Scheme 1.54. Phosphine-free arene-ruthenium(II)-catalysed synthesis of primary amides from aldehydes in a one-pot reaction.

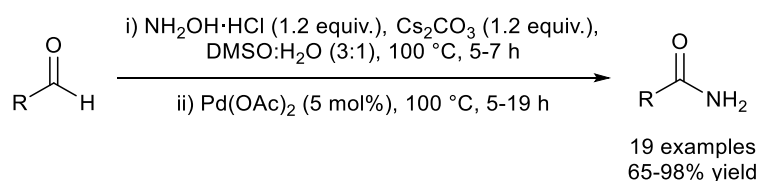
More recently, other non-arene ruthenium catalysts have been developed, including those based on bis(allyl)-ruthenium(IV) complexes.¹⁵⁶ In addition, the first ruthenium complexes containing phosphino-oxime ligands (**1.103**) were found to be active in the catalytic rearrangement of aldoximes.¹⁵⁷ Similar complexes based on palladium (**1.104**) were also able to catalyse the transformation (Scheme 1.55).¹⁵⁸ In both cases primary amides were synthesised from aldoximes using 5 mol% catalyst in water at 100 °C.



Scheme 1.55. Ruthenium and palladium complexes containing phosphino-oxime ligands in the catalytic rearrangement of aldoximes.

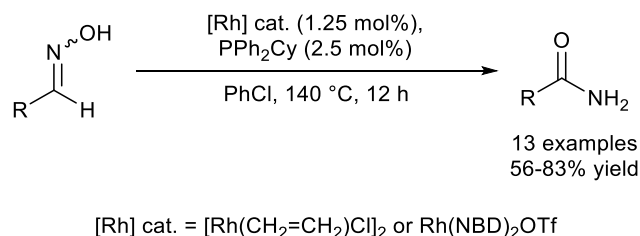
Other palladium-based protocols for the rearrangement reaction have also been reported.¹⁵⁹ Punniyamurthy *et al.* developed a simple and effective method for the one-pot conversion of aldehydes into primary amides in aqueous dimethyl sulfoxide at 100 °C (Scheme 1.56).⁵³ In

contrast to the other methods, the aldoxime was generated first before the metal catalyst was added to form the primary amide.



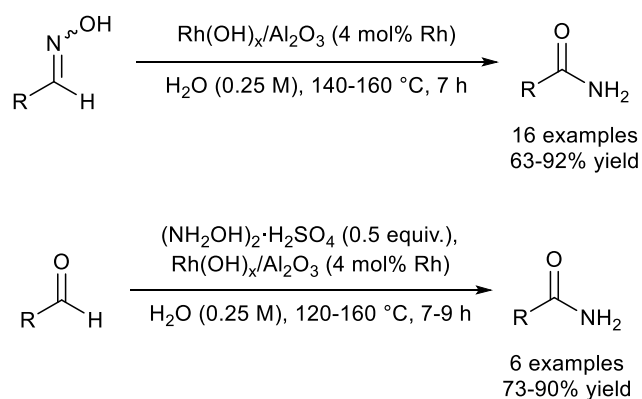
Scheme 1.56. Palladium-catalysed conversion of aldehydes into primary amides.

Methods employing rhodium as the catalytic metal have also been established. Very recently, Xu and Liu showed that low catalyst loadings of two rhodium complexes, $[\text{Rh}(\text{CH}_2=\text{CH}_2)\text{Cl}]_2$ and $\text{Rh}(\text{NBD})_2\text{OTf}$, could be employed in combination with the phosphine ligand PPh_2Cy in the rearrangement of aromatic and heteroaromatic aldoximes (Scheme 1.57).¹⁶⁰



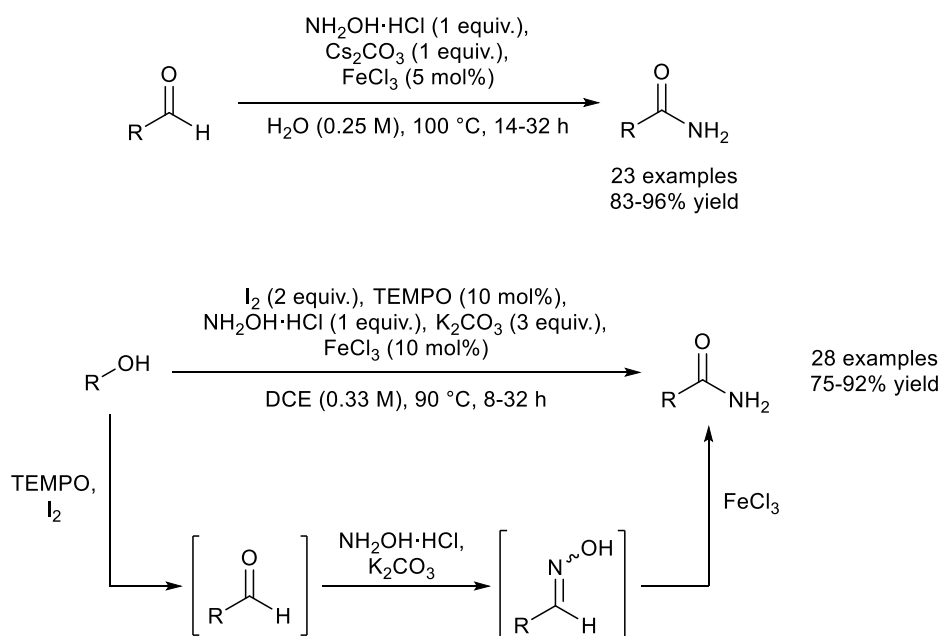
Scheme 1.57. Rearrangement of aldoximes catalysed by homogenous rhodium catalysts.

The much less studied area of heterogeneous catalysis has also yielded protocols based on rhodium.¹⁶¹⁻¹⁶⁴ In fact, the first heterogeneous system developed for the conversion of aldoximes into primary amides employed supported rhodium hydroxide ($\text{Rh}(\text{OH})_x/\text{Al}_2\text{O}_3$) in water at high temperatures (Scheme 1.58).^{165,166} A variety of aldoximes were tolerated by the methodology, including aliphatic, aromatic, heteroaromatic and α,β -unsaturated substrates. The catalyst could also be easily recovered and then reused with minimal loss of its catalytic ability. In addition, the method was applied to the one-pot synthesis of primary amides from aldehydes, with $(\text{NH}_2\text{OH})_2\cdot\text{H}_2\text{SO}_4$ used as the hydroxylamine source (Scheme 1.58).



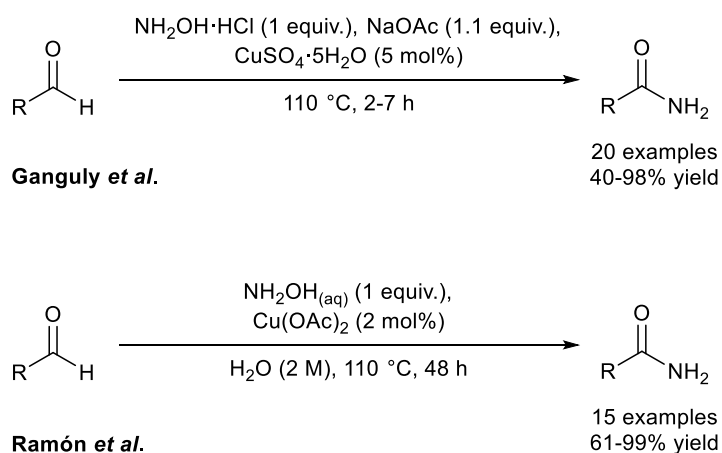
Scheme 1.58. One-pot synthesis of primary amides from aldoximes and aldehydes using $\text{Rh(OH)}_x/\text{Al}_2\text{O}_3$.

Other groups have explored the use of cheaper metals for the rearrangement reaction. A simple, efficient and inexpensive method for the direct synthesis of primary amides from aldehydes using commercially available FeCl_3 was detailed by Chakraborty and co-workers in 2011 (Scheme 1.59).¹⁶⁷ The importance of employing water as the solvent was also illustrated as use of anhydrous organic media resulted in the synthesis of the corresponding nitrile instead. In addition, no racemisation was observed when chiral substrates were subjected to the methodology. The authors also revealed that the catalytic system could directly convert alcohols into primary amides when combined with an Iodine-TEMPO oxidant (Scheme 1.59).¹⁶⁸ This is similar to a previous method developed by Williams *et al.* in which an iridium catalyst transformed alcohols into primary amides in a one-pot process *via in situ* formation of the aldehyde and aldoxime.¹⁶⁹



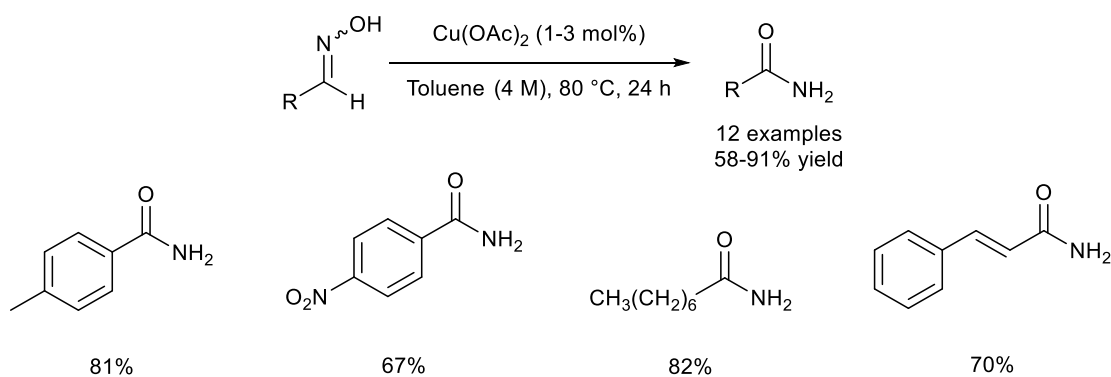
Scheme 1.59. One-pot synthesis of primary amides from aldehydes and alcohols employing catalytic FeCl_3 , as developed by Chakraborty *et al.*

In 2012 two studies reported the use of commercially available copper salts for the conversion of aldehydes into primary amides *via in situ* aldoxime formation at 110 °C (Scheme 1.60).^{170,171} Ganguly *et al.* showed copper(II) sulphate pentahydrate could be employed under neat conditions,¹⁷⁰ whilst copper(II) acetate was also shown to be a suitable catalyst for the transformation in water by Ramón *et al.*¹⁷¹ Remarkably, the copper(II) acetate catalyst could be recovered and reused up to 10 times without losing its catalytic activity.



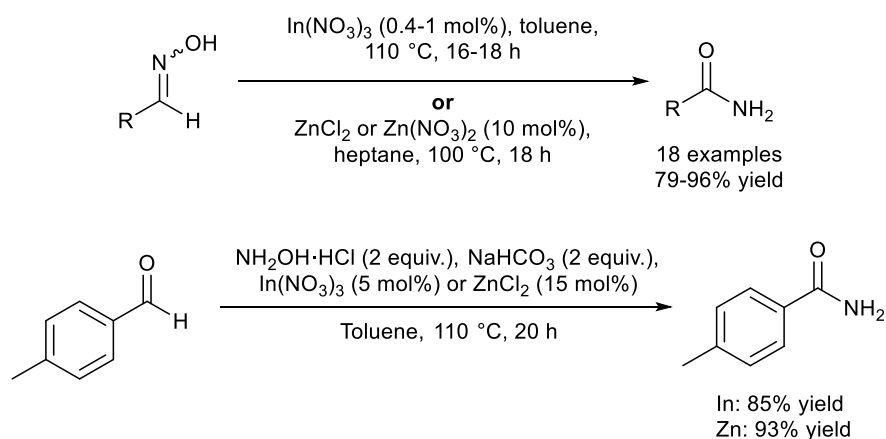
Scheme 1.60. Copper-catalysed direct synthesis of primary amides from aldehydes.

These reports followed a study by Williams and co-workers which showed 1-3 mol% of $\text{Cu}(\text{OAc})_2$ in toluene was able to transform a broad array of aldoximes into their corresponding primary amide products at 80 °C in 24 hours (Scheme 1.61).¹⁷² The group also demonstrated that the rearrangement reactions could be performed using microwave irradiation in only 2 hours at 80 °C, whilst a heterogeneous system consisting of CuO/ZnO (10% wt) on activated carbon was also shown to be an efficient catalyst.¹⁷²



Scheme 1.61. $\text{Cu}(\text{OAc})_2$ -catalysed rearrangement of aldoximes developed by Williams *et al.* with selected products.

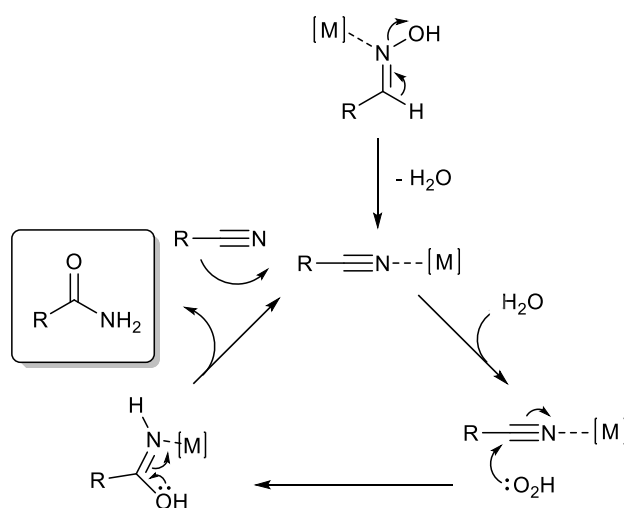
The Williams group detailed a further low-cost method for the rearrangement reaction. The authors found that indium and zinc salts promoted the conversion of their model substrate butyraldoxime into butyramide in excellent yield, with $\text{In}(\text{NO}_3)_3$ (0.4-1 mol%), $\text{Zn}(\text{NO}_3)_2$ (10 mol%) and ZnCl_2 (10 mol%) proving the most efficient catalysts (Scheme 1.62).¹⁷³ The group subsequently demonstrated their methodology could also be extended to convert aldehydes into primary amides (Scheme 1.62).



Scheme 1.62. Low-cost conversion of aldoximes and aldehydes into primary amides catalysed by zinc and indium salts.

Mechanistic Investigations

In addition to the novel methodologies invented by the group, Williams *et al.* also investigated the mechanism of the metal-catalysed aldoxime rearrangement reaction.⁵¹ Originally, it was thought that the reaction proceeded *via* a dehydration/rehydration process in which the metal promotes both steps (Scheme 1.63, Mechanism A). Firstly, a nitrile intermediate is formed through dehydration of the starting aldoxime, before nucleophilic attack by water and a subsequent rearrangement step affords the final primary amide product.

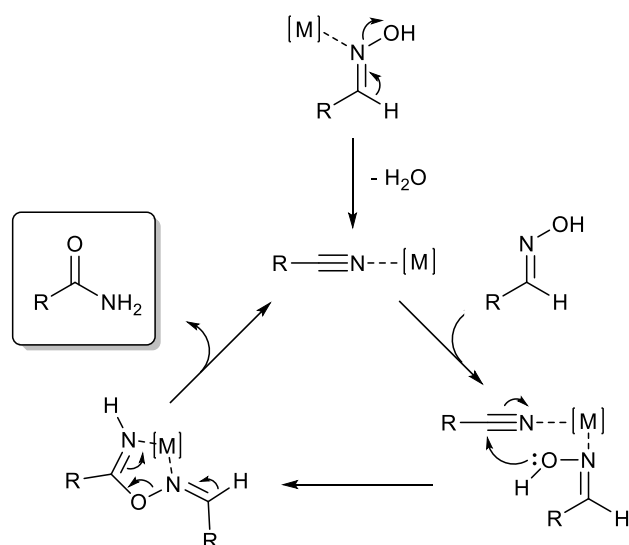


Scheme 1.63. Original proposed mechanism (A) involving a dehydration/rehydration process.

In support of this mechanistic proposal, studies have observed the formation of nitriles during the rearrangement reaction.^{144,145,174} In addition, a range of metal complexes have been shown to catalyse the dehydration (aldoxime to nitrile) and rehydration (nitrile to primary amide) steps when both of the reactions are performed separately.^{159, 175-180}

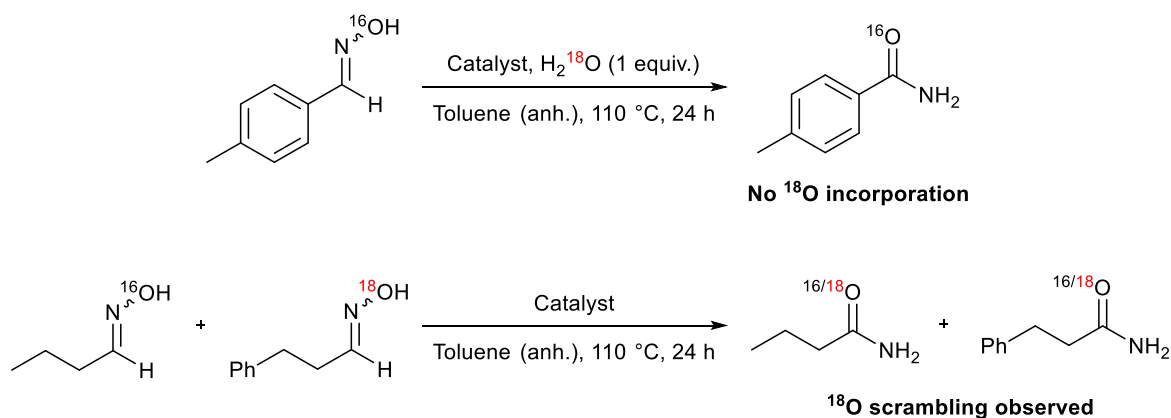
However, Williams and co-workers presented evidence suggesting the metal-mediated aldoxime rearrangement reaction did not proceed *via* mechanism A. Firstly, many of the complexes used to catalyse the rearrangement reaction were shown to be inactive in the hydration of a nitrile with water. In addition, the authors also noted that aldoximes were converted into primary amides in completely anhydrous conditions. These inconsistencies resulted in the proposal of a second mechanism (B) in which, following the initial dehydration step, another molecule of aldoxime attacks the metal-coordinated nitrile to generate a 5-

membered cyclic intermediate (Scheme 1.64). Rearrangement of this cyclic intermediate affords another metal-coordinated nitrile and the desired primary amide product.



Scheme 1.64. Second proposed mechanism (B) in which another molecule of aldoxime acts as the nucleophile.

This alternative mechanism, which had also been suggested by Noltes¹⁸¹ and Chang,^{119,182} was supported by two studies employing ¹⁸O-labelled reagents and a variety of metal catalysts (Scheme 1.65). Firstly, use of one equivalent of H₂¹⁸O in the reaction afforded the unlabelled primary amide as the product; therefore illustrating water does not act as the nucleophile. In addition, when the rearrangement of ¹⁸O-labelled 3-phenylpropanaloxime was performed in the presence of an equivalent of unlabelled butyraldoxime, scrambling of the ¹⁸O label was observed between the two different amide products. This supports a pathway in which the coordinated nitrile is attacked by a second molecule of aldoxime.

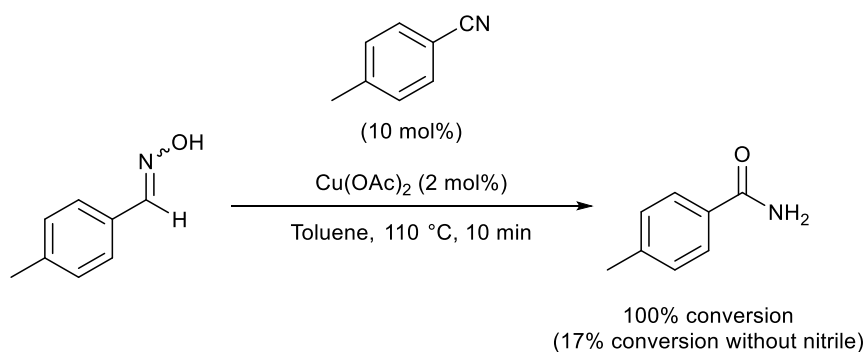


Catalyst = RhCl(PPh₃)₃, Ru(PPh₃)₃(CO)H₂, Pd(OAc)₂, In(NO₃)₃, ZnCl₂ and Cu(OAc)₂.

Scheme 1.65. ¹⁸O-Labelled experiments performed by Williams *et al.* supporting proposed mechanism B.

In addition, Williams *et al.* also followed the conversion of 4-methylbenzaloxime into 4-methylbenzamide over time. This revealed that the initial rate of reaction is comparatively slow and that dehydration of the starting aldoxime into the nitrile is the rate determining step. Using the knowledge of both the rate determining step of the reaction and the newly proposed reaction mechanism, the group hypothesised that the rate of reaction could be increased by adding a nitrile additive to the rearrangement process.

As hoped, the group revealed a positive correlation between the mol% of nitrile additive and the conversion of aldoxime into primary amide. However, for every mol% of nitrile added to the reaction, an equal amount of amide product derived from this nitrile was formed, reducing conversion into the desired amide product by the same amount. However, the group illustrated that if the 'same' nitrile was added to the oxime rearrangement then quantitative conversion into the desired amide product could be achieved (Scheme 1.66). A similar study investigating the effect of nitrile additives on the rearrangement process using a rhodium complex, Rh(cod)(IMes)Cl, was also reported by Chang and colleagues.¹⁸²



Scheme 1.66. Rearrangement of 4-methylbenzaloxime in the presence of 4-methylbenzonitrile.

1.3. Summary

The direct coupling of amines and unactivated carboxylic acids, involving the release of one equivalent of water, is one of the most attractive methods for the preparation of amides due to its high atom efficiency. However, high temperatures are required to overcome the energy barrier created by the formation of the ammonium-carboxylate salt.

In order to circumvent this problem, a wide variety of coupling reagents were developed. These reagents activate the carboxylic acid, which then couples with the amine to generate the desired amide product. However, although these protocols generally afford good yields under mild conditions, the use of coupling reagents results in the production of a stoichiometric amount of waste. This reduces the atom economy of the reaction, whilst also adding further purification steps to remove the by-products.

As a result of these limitations, a catalytic waste-free synthesis of amides was highlighted as a key area of research by the ACS's Green Chemistry Institute Pharmaceutical Roundtable in 2005. The development of catalytic amide syntheses has eliminated the need for stoichiometric coupling reagents and also allowed the formation of amides from a wide range of other starting materials, including esters, nitriles, aldoximes and aldehydes. Despite the advances in catalytic amide formation, research continues in order to find cheaper and more sustainable catalysts for the reactions, as well as methods which tolerate the broadest number of substrates.

Results and Discussion I

Amides from Esters

“Acetic acid as a catalyst for the *N*-acylation of amines using esters as the acyl source”

D. D. Sanz Sharley and J. M. J. Williams, *Chem. Commun.*, 2017, **53**, 2020.

2. Results and Discussion I – Amides from Esters

2.1. Aims and Objectives

Traditional methods used to synthesise acetamides usually involve the use of activated acylating agents, such as acetic anhydride and acetyl chloride.¹⁸³⁻¹⁸⁹ Although these reagents are cheap, their toxicity and hygroscopic nature make them less than ideal acyl sources. The bases traditionally used, namely pyridine-based compounds,¹⁹⁰ are also toxic and harmful to humans and the environment. In addition, many procedures employ metal catalysts,¹⁹¹⁻²⁰⁰ both heterogeneous and homogeneous, which can be expensive and add further purification steps.

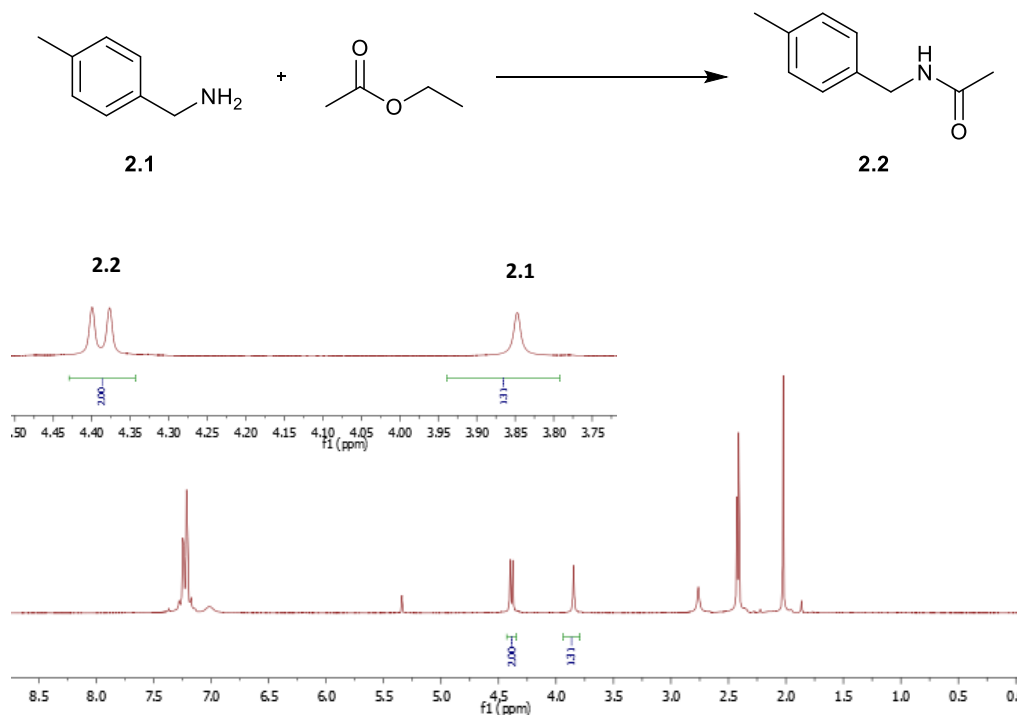
As a result, the aim of this work was to develop a novel non-metal catalysed protocol for the acetylation of amines using a less activated acylating agent – in this case ethyl acetate – to go alongside previous work in the area. The lower reactivity of ethyl acetate makes it a more desirable acylating agent compared with acid chlorides and acid anhydrides. It was hoped that acetic acid could be used as an effective catalyst for the transformation as it is cheap and readily available, whilst any reaction with the amine would still produce the desired product. After fully exploring the acetylation reaction, the methodology could then be applied to other esters to form higher amides.

2.2. Initial Investigations

Early work focussed on the suitability of acetic acid as a catalyst for the *N*-acetylation of amines. As reported previously, it is well known that in polar solvents salt formation usually occurs upon mixing of amines and acids, thus disfavours the amidation reaction.¹ However, other studies, such as that by Brahmachari and co-workers,²⁰¹ have shown that the presence of acetic acid in amidation reactions does not inhibit the formation of amides from amines. This is likely due to the relatively moderate pK_a value of acetic acid (12.6 in DMSO at 25 °C) compared with stronger acids such as H_2SO_4 .²⁰² It was thought that, as a result of the lower acidity of acetic acid, the protonation/deprotonation equilibrium would be shifted in favour of the free amine, thus allowing transfer of the acyl group.

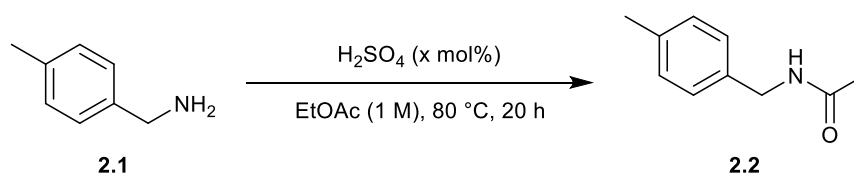
With this theory in mind, we decided to explore the effect of different acids on the acetylation of our model substrate, 4-methylbenzylamine (**2.1**), using ethyl acetate as the acyl

source. Percentage conversion into product **2.2** was determined by analysis of the relative integrals of the benzyl protons in the starting material (3.85 ppm, singlet) and product (4.39 ppm, doublet) in the crude ^1H NMR spectra (Scheme 2.1).



Scheme 2.1. An example of the ^1H NMR spectrum used to determine percentage conversion into acetamide **2.2**, showing benzyl protons in the starting material (**2.1**) and product (**2.2**).

Use of one equivalent of sulfuric acid in refluxing ethyl acetate resulted in no conversion into acetamide **2.2** after 20 hours; presumably due to protonation of the amine nitrogen (Table 2.1, entry 1). Notably, even a small catalytic amount of sulfuric acid led to minimal conversion, thus illustrating the ineffectiveness of strong acids as catalysts in this reaction (Table 2.1, entry 2).

Table 2.1. Effect of sulfuric acid on the acetylation of 4-methylbenzylamine.

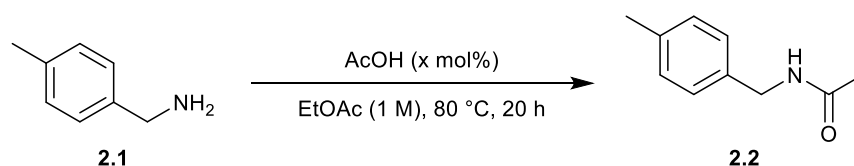
Entry	H ₂ SO ₄ (mol%)	Conversion into 2.2 (%)
1	100	0
2	5	6

Reactions were performed on a 1 mmol scale. Conversions determined by analysis of the ¹H NMR spectra of the crude reaction mixtures.

2.3. N-Acetylation of Amines: Optimisation

2.3.1. Primary Amines

With a strong acid catalyst yielding poor conversions, it was then decided to investigate whether weaker acids would provide a more efficient alternative. Initial experiments showed that, under the same reaction conditions employed in the sulfuric acid studies, quantitative conversion of the model substrate into acetamide product **2.2** could be achieved using a stoichiometric amount of acetic acid (Table 2.2, entry 6). Pleasingly, analysis of the crude ¹H NMR spectra revealed that catalyst loadings as low as 10 mol% afforded the acetamide product in quantitative conversion (Table 2.2, entry 3-5), compared with only traces for the background reaction (Table 2.2, entry 1). However, when the catalyst loading was lowered to 5 mol% the conversion dropped fractionally (Table 2.2, entry 2).

Table 2.2. Optimisation of the AcOH catalyst loading for the acetylation of 4-methylbenzylamine.

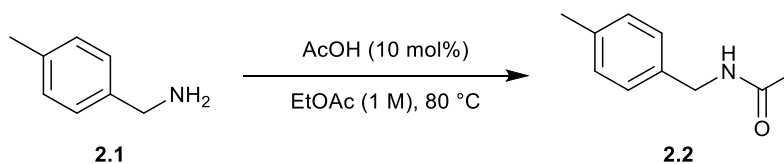
Entry	AcOH (mol%)	Conversion into 2.2 (%)
1	-	Traces
2	5	98
3	10	100

4	20	100
5	50	100
6	100	100

Reactions were performed on a 1 mmol scale. Conversions determined by analysis of the ^1H NMR spectra of the crude reaction mixtures.

Using the optimum catalyst loading of 10 mol%, it was decided to investigate the effect of reaction time on the overall progress of the model reaction. Analysis of the crude ^1H NMR spectra showed that a decrease in the reaction time from 20 hours to 16 hours led to a reduction in the conversion from 100% to 96% (Table 2.3, entries 1 and 2). Conversions into acetamide **2.2** then dropped off further as the reaction time was lowered from 16 hours to 8 hours (Table 2.3, entries 3 and 4).

Table 2.3. Optimisation of the reaction time for the acetylation of 4-methylbenzylamine.

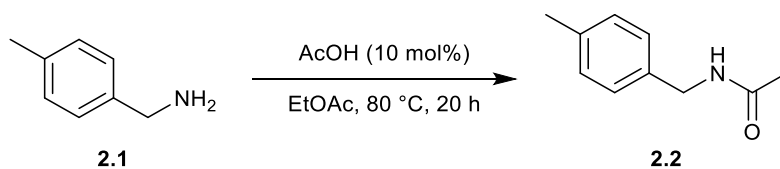


Entry	Time (h)	Conversion into 2.2 (%)
1	20	100
2	16	96
3	12	95
4	8	85

Reactions were performed on a 1 mmol scale. Conversions determined by analysis of the ^1H NMR spectra of the crude reaction mixtures.

Further screening experiments showed that both an increase and decrease in the reaction concentration from 1 M to 2 M and 0.5 M respectively also resulted in quantitative conversion into acetamide **2.2** (Table 2.4, entries 1-3). As the solvent is also the acylating agent in the reaction, a higher concentration, and thus less equivalents of ethyl acetate, was thought to be more desirable. However, when the concentration was increased beyond 2 M, analysis of the crude ^1H NMR spectra showed a reduction in the reaction conversion (Table 2.4, entry 4).

Table 2.4. Optimisation of the solvent concentration for the acetylation of 4-methylbenzylamine.

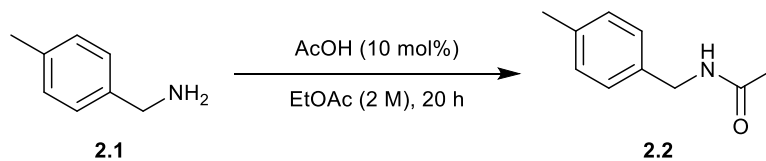


Entry	EtOAc (mL)	Conversion into 2.2 (%)
1	2	100
2	1	100
3	0.5	100
4	0.25	90

Reactions were performed on a 1 mmol scale. Conversions determined by analysis of the ^1H NMR spectra of the crude reaction mixtures.

A screen of reaction temperatures was then performed (Table 2.5). Unfortunately, analysis of the crude ^1H NMR spectra revealed that reaction temperatures lower than 80 °C resulted in considerably decreased conversions; temperatures of 40 and 60 °C afforded conversions of 10 and 53% respectively (Table 2.5, entries 2 and 3). This therefore confirmed the need for refluxing conditions in order to achieve efficient transformation into acetamide **2.2**.

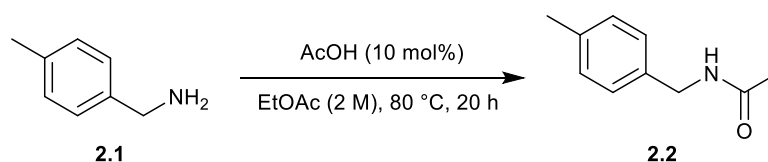
Table 2.5. Optimisation of the reaction temperature for the acetylation of 4-methylbenzylamine.



Entry	Temperature (°C)	Conversion into 2.2 (%)
1	80	100
2	60	53
3	40	10

Reactions were performed on a 1 mmol scale. Conversions determined by analysis of the ^1H NMR spectra of the crude reaction mixtures.

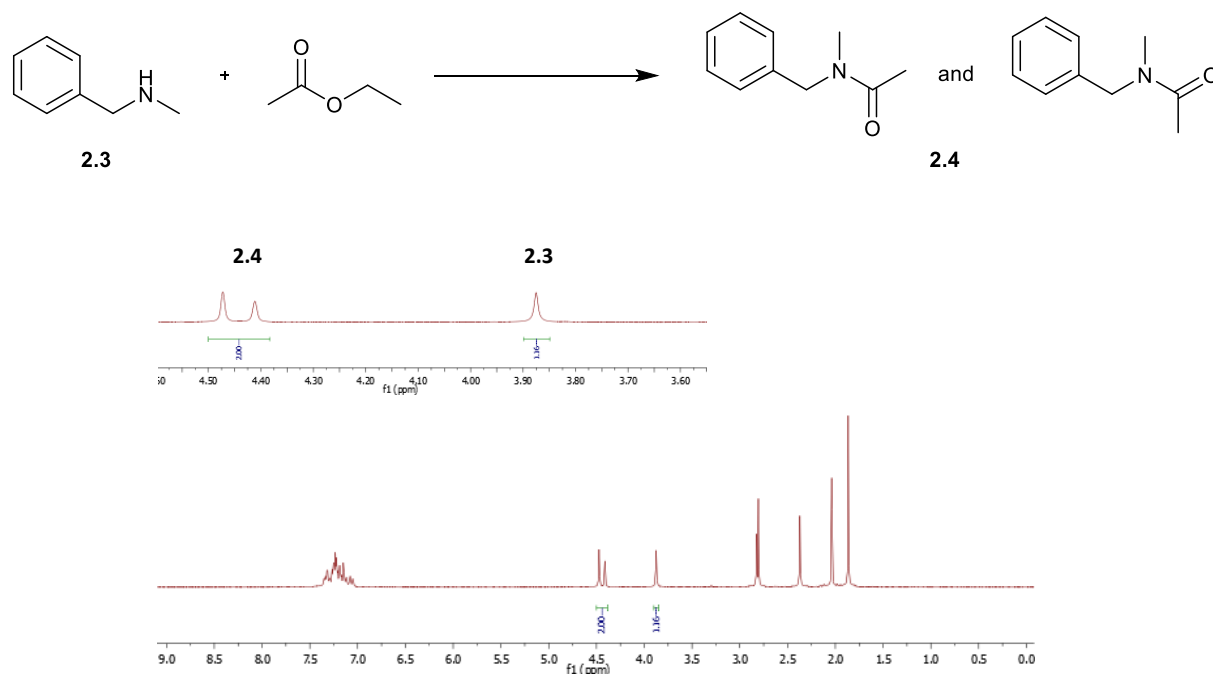
These optimisation studies generated reaction conditions A, in which 4-methylbenzylamine (**2.1**) could be transformed into acetamide **2.2** using 10 mol% acetic acid and ethyl acetate as the acyl source/solvent at 80 °C in 20 hours (Scheme 2.2).



Scheme 2.2. Final optimised reaction conditions for the transformation of primary amine **2.1** into acetamide **2.2** (reaction conditions A).

2.3.2. Secondary Amines

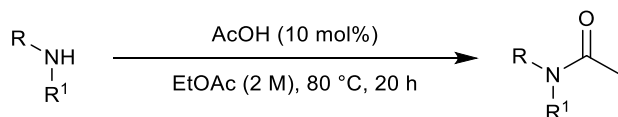
Following optimisation of the reaction conditions for the model primary amine substrate, secondary amines were then explored. A model reaction system of *N*-benzylmethylamine and ethyl acetate was selected for the reaction screening due to ease of spectral determination of conversion into the desired product. Product **2.4** is observed as two rotamers in its ^1H and ^{13}C NMR spectra as rotation around the N-C(O) bond occurs slower than the NMR timescale. Percentage conversion into product **2.4** was determined by analysis of the relative integrals of the benzyl protons in the starting material (3.88 ppm, singlet) and the product (4.41 and 4.47 ppm, major and minor rotamers, singlets) in the crude ^1H NMR spectra (Scheme 2.3).

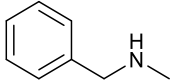
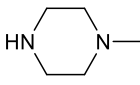
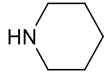


Scheme 2.3. An example of the ^1H NMR spectrum used to determine percentage conversion into acetamide **2.4**, showing benzyl protons in the starting material (**2.3**) and product (**2.4**).

Based on previous findings in the group we postulated that harsher reaction conditions would be required to acetylate secondary amines.⁵⁶ To investigate this claim, our secondary amine model substrate was subjected to reaction conditions A, and as expected analysis of the crude ¹H NMR spectrum revealed poor conversion into the acetamide product (Table 2.6, entry 1).

Table 2.6. Conversion of secondary amines into their acetamide products under reaction conditions A.



Entry	Secondary amine	Conversion (%)
1		15
2		19
3		13

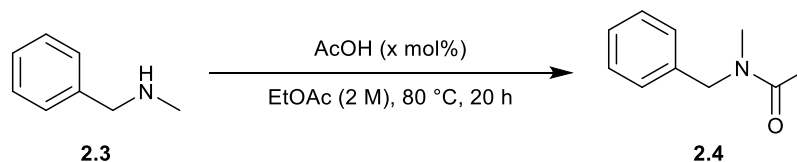
Reactions were performed on a 1 mmol scale. Conversions determined by analysis of the ¹H NMR spectra of the crude reaction mixtures.

To confirm this result was representative of other secondary amines, reaction conditions A were employed on 1-methylpiperazine and piperidine (Table 2.6, entries 2 and 3). Low conversions of 19% and 13%, respectively, into the corresponding acetamide products were achieved, thus illustrating the need for more forcing reaction conditions.

Employing the same reaction conditions that were developed for primary amines, the catalyst loading was firstly increased to 50 mol%; however poor conversion into acetamide **2.4** was observed after analysis of the ¹H NMR spectra (Table 2.7, entry 1). It was then thought a further increase in the amount of acetic acid would perhaps drive the reaction towards completion. Unfortunately, use of stoichiometric acetic acid only resulted in a slight increase in the conversion from 31 to 45%, whilst a further increase in acid led to the conversion

decreasing to 31% (Table 2.7, entries 2 and 3). The latter result is likely due to protonation of the nitrogen's lone pair by the large excess of acid present in the reaction, thus preventing nucleophilic attack on the ethyl acetate.

Table 2.7. Optimisation of the catalyst loading for the acetylation of *N*-benzylmethylamine, using EtOAc as the solvent.

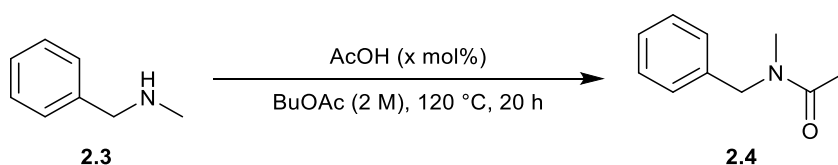


Entry	AcOH (equiv.)	Conversion into 2.4 (%)
1	0.5	32
2	1	45
3	2.5	31

Reactions were performed on a 1 mmol scale. Conversions determined by analysis of the ^1H NMR spectra of the crude reaction mixtures.

With increased catalyst loadings failing to drive the reaction towards completion, it was decided that higher reaction temperatures would be investigated. In order to do this a higher-boiling acetate ester would need to be used as the solvent. Butyl acetate (BuOAc) was chosen due to its cheap cost and common use as a solvent. Using our model substrate, a new catalyst loading screen was performed in butyl acetate (2 M) at 120 °C for 20 hours. Analysis of the crude ^1H NMR spectra showed that even low catalyst loadings of 10 mol% resulted in a considerable increase in the conversion into acetamide **2.4** compared with the results obtained using ethyl acetate as the solvent at 80 °C (Table 2.8, entry 2; Table 2.6, entry 1). This is in contrast to the background reaction which only yielded traces of desired acetamide **2.4** (Table 2.8, entry 1). Pleasingly, quantitative conversion was obtained when using both a stoichiometric amount of acetic acid and a catalyst loading of 50 mol% (Table 2.8, entries 4 and 5).

Table 2.8. Optimisation of the catalyst loading for the acetylation of *N*-benzylmethylamine, using BuOAc as the solvent.



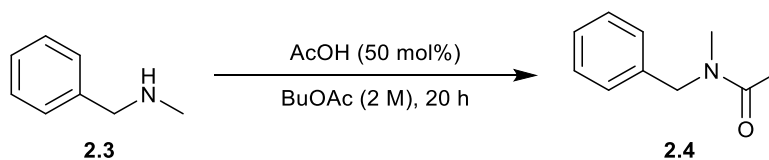
Entry	AcOH (mol%)	Conversion into 2.4 (%)
1	-	Traces
2	10	76
3	25	94
4	50	100
5	100	100

Reactions were performed on a 1 mmol scale. Conversions determined by analysis of the ^1H NMR spectra of the crude reaction mixtures.

Finally, we decided to explore whether the increased conversions observed were a result of the higher temperature used or the change in acylating agent. We predicted that the longer alkyl chain in butyl acetate, compared with ethyl acetate, was unlikely to have a significant effect on the efficiency of the reaction, and that it was the higher temperature that resulted in quantitative conversion into acetamide **2.4**. This was confirmed by an investigation in which the model substrate was subjected to 50 mol% acetic acid at 80 °C in butyl acetate. This resulted in 44% conversion into the desired product (Table 2.9, entry 1), only marginally higher than the 32% conversion obtained when ethyl acetate was employed as the acylating agent (Table 2.7, entry 1).

Moreover, we found that even a slight decrease in the reaction temperature from 120 °C to 110 °C, using butyl acetate as the acylating agent, led to a reduction in the efficiency of the transformation (Table 2.9, entry 2); thus proving 120 °C to be the optimal reaction temperature under this set of conditions (Table 2.9, entry 3).

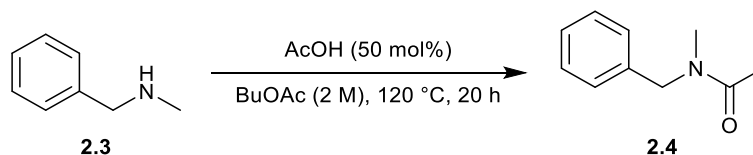
Table 2.9. Optimisation of the reaction temperature for the acetylation of *N*-benzylmethylamine.



Entry	Temperature (°C)	Conversion into 2.4 (%)
1	80	44
2	110	96
3	120	100

Reactions were performed on a 1 mmol scale. Conversions determined by analysis of the ^1H NMR spectra of the crude reaction mixtures.

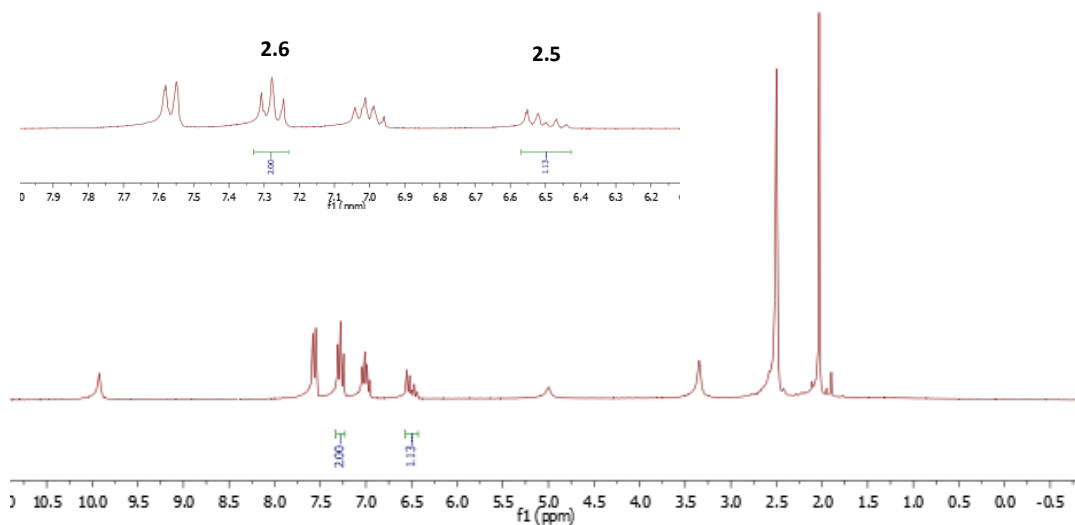
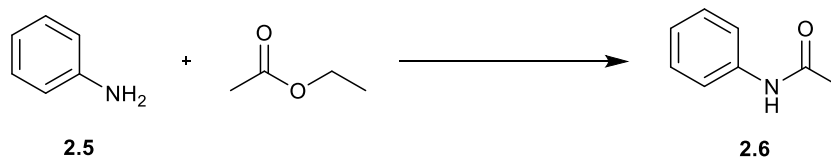
The final optimised secondary amine reaction conditions (reaction conditions *B*) were able to transform *N*-benzylmethylamine (**2.3**) into acetamide **2.4** using 50 mol% acetic acid and butyl acetate as the acyl source/solvent at 120 °C in 20 hours (Scheme 2.4).



Scheme 2.4. Final optimised reaction conditions for the transformation of secondary amine **2.3** into acetamide **2.4** (reaction conditions *B*).

2.3.3. Aniline Derivatives

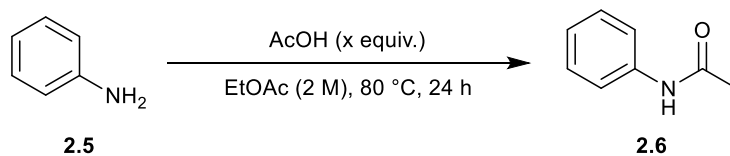
Although the intention was to primarily focus on the *N*-acetylation of primary and secondary amines, we also decided to investigate whether aniline derivatives could be transformed using our methodology. Percentage conversion into product **2.6** was determined by analysis of the relative integrals of the aromatic protons in the starting material (6.50-6.66 ppm, 3H, multiplet) and product (7.28 ppm, 2H, triplet) in the crude ^1H NMR spectra (Scheme 2.5).



Scheme 2.5. An example of the ¹H NMR spectrum used to determine percentage conversion into acetamide **2.6**, showing aromatic protons in the starting material (**2.5**) and product (**2.6**).

Similarly to the case of secondary amines, limited conversion into acetamide **2.6** was achieved using ethyl acetate as the acylating agent; with a maximum conversion of 58% observed when using 2.5 equivalents of acetic acid (Table 2.10). The background reaction revealed no conversion into acetamide **2.6** (Table 2.10, entry 1).

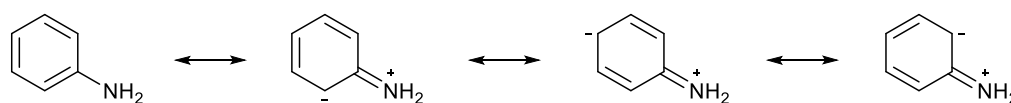
Table 2.10. Optimisation of the catalyst loading for the acetylation of aniline derivatives.



Entry	AcOH (equiv.)	Conversion into 2.6 (%)
1	-	0
2	0.5	16
3	1	37
4	2.5	58

Reactions were performed on a 1 mmol scale. Conversions determined by analysis of the ¹H NMR spectra of the crude reaction mixtures.

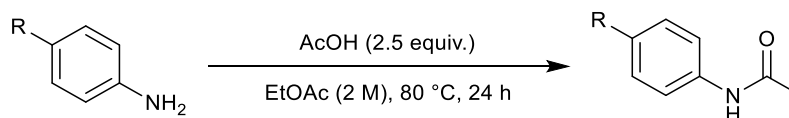
The low reactivity exhibited by aniline can be attributed to its reduced nucleophilicity; a result of electron delocalisation of the nitrogen's lone pair into the aromatic ring (Scheme 2.6).



Scheme 2.6. Electron delocalisation in aniline.

Applying these conditions to *para*-anilinic substrates resulted in varying degrees of conversion into their corresponding acetamide products (Table 2.11). Analysis of the crude ^1H NMR spectra showed that 4-chloroaniline afforded the lowest conversion of 41% (Table 2.11, entry 1), presumably a result of the chlorine's electron withdrawing nature, whilst the bulky ^tBu derivative gave 72% conversion into the acetamide product (Table 2.11, entry 2).

Table 2.11. Reaction of *para*-anilinic substrates with ethyl acetate in the presence of acetic acid.

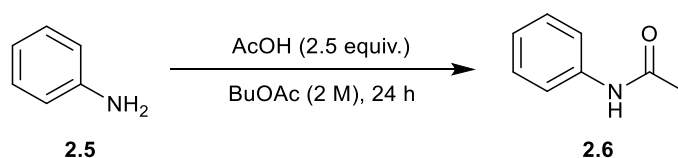


Entry	R	Conversion (%)
1	Cl	41
2	^tBu	72

Reactions were performed on a 1 mmol scale. Conversions determined by analysis of the ^1H NMR spectra of the crude reaction mixtures.

As with our secondary amine investigations, use of the higher-boiling solvent butyl acetate in the aniline model reaction resulted in near-quantitative conversion (Table 2.12). The study showed that reactions differing only in the acetate ester present afford near identical conversions, as expected (Table 2.10, entry 4; Table 2.12, entry 1). However, analysis of the crude ^1H NMR spectrum revealed an increase in temperature to 110 °C, using butyl acetate, results in near quantitative conversion into acetamide product **2.6** (Table 2.12, entry 3). Interestingly, beyond this temperature the conversions appear to decrease (Table 2.12, entries 4 and 5).

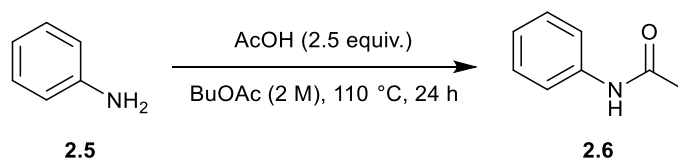
Table 2.12. Optimisation of the reaction temperature for the acetylation of aniline derivatives.



Entry	Temperature (°C)	Conversion into 2.6 (%)
1	80	60
2	100	86
3	110	>99
4	120	96
5	130	93

Reactions were performed on a 1 mmol scale. Conversions determined by analysis of the ^1H NMR spectra of the crude reaction mixtures.

The final reaction conditions (reaction conditions C) transformed aniline (2.5) into acetamide 2.6 using 2.5 equivalents of acetic acid and butyl acetate as the acyl source/solvent at 110 °C in 24 hours (Scheme 2.7).



Scheme 2.7. Final optimised reaction conditions for the transformation of aniline (2.5) into acetamide 2.6 (reaction conditions C).

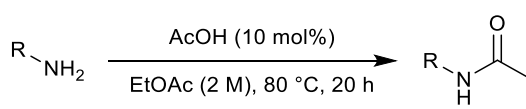
2.4. N-Acetylation: Amine Substrate Scope

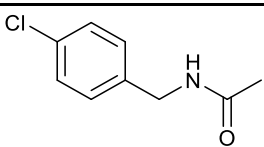
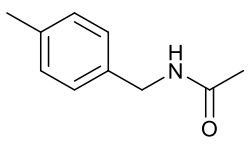
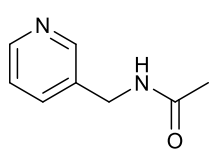
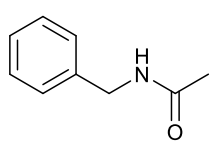
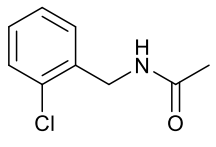
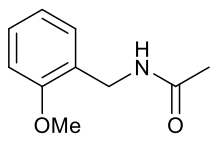
It was hoped that reaction conditions A-C would allow the transformation of a wide variety of primary amines, secondary amines and aniline derivatives into their corresponding acetamide products. An aqueous base wash using NaHCO_3 was firstly attempted in order to purify the products, however this afforded low yields as many of the products were partially soluble in the water layer. Therefore, in all cases where yields were obtained, purification involved a facile column chromatography procedure using DCM/MeOH as the eluent.

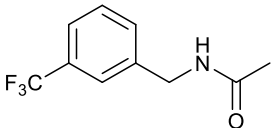
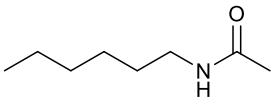
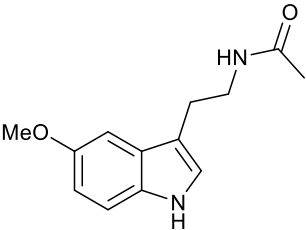
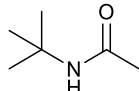
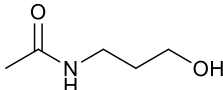
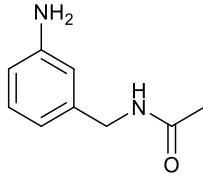
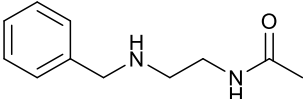
2.4.1. Primary Amines

Reaction conditions A were applied to a range of primary amines and encouragingly, good to excellent yields were achieved in most cases (Table 2.13). Varying the substituent on the arene ring of benzylamine had little to no effect on the efficiency of the reaction. Halogens (Table 2.13, entries 1 and 5), methoxy groups (Table 2.13, entry 6) and trifluoromethyl groups (Table 2.13, entry 7) were all tolerated by the methodology. Moreover, changing the chlorine ring position from *para* to *ortho* resulted in comparable conversion (Table 2.13, entries 1 and 5). In addition, reaction conditions A were shown to tolerate heteroaromatic groups, such as the pyridine moiety found in **2.8** (Table 2.13, entry 3).

Table 2.13. Primary amine substrate scope using reaction conditions A.



Entry	Product	Conversion (%)	Yield (%)	
1		2.7	100	93
2		2.2	100	97
3		2.8	96	90
4		2.9	100	92
5		2.10	96	95
6		2.11	100	93

7		2.12	100	97
8		2.13	100	96
9		2.14	78	70
10		2.15	31	-
11		2.16	99	89
12		2.17	97	94
13		2.18	100	90

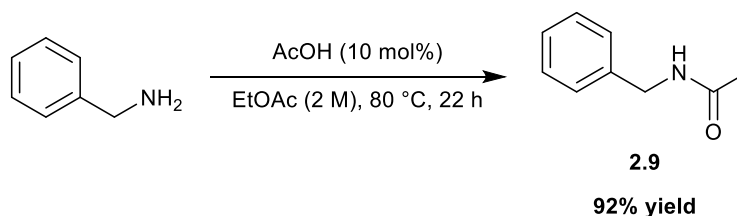
Reactions were performed on a 2 mmol scale. Percentage conversions were determined by analysis of the crude ^1H NMR spectra.

As well as the benzylamine-based starting materials employed, other classes of primary amine could also be successfully subjected to reaction conditions A. For instance, the methodology is able to transform long alkyl chain amines, such as hexylamine, into their corresponding acetamide products in excellent yields (Table 2.13, entry 8).

To test the pharmaceutical applicability of the methodology, we decided to synthesise the hormone and sleep disorder drug, melatonin (**2.14**), from 5-methoxytryptamine. To our delight, we were able to apply reaction conditions A and isolate the target molecule in good yield (Table 2.13, entry 9). However, *tert*-butylamine showed poor conversion into **2.15** under reaction conditions A; likely due to steric hinderance (Table 2.13, entry 10).

Furthermore, the chemoselectivity of the methodology was investigated by applying the protocol to bifunctional amines (Table 2.13, entries 11-13). The methodology is able to selectively acetylate amino groups over alcohols; negligible *O*-acetylation was observed when 3-amino-1-propanol was subjected to the reaction conditions to afford **2.16** (Table 2.13, entry 11). In addition, when both an aromatic and benzyl amine are present in a substrate, the latter is selectively acetylated (Table 2.13, entry 12). Finally, the protocol is also able to distinguish between primary and secondary amines, operating only on the first functionality; for example, when *N*-benzylethylenediamine was employed only acetamide **2.18** was obtained (Table 2.13, entry 13).

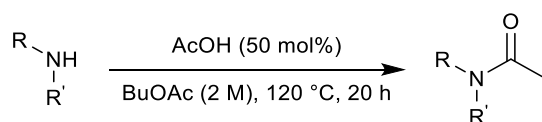
The scalability of the reaction was also assessed by performing the *N*-acetylation of benzylamine on a 67 mmol scale. Quantitative conversion into **2.9** was achieved after 22 hours and the product isolated in 92% yield (9.2 g) after purification (Scheme 2.8).



Scheme 2.8. Scaled-up *N*-acetylation of benzylamine (67 mmol scale).

2.4.2. Secondary Amines

The substrate scope for secondary amines was subsequently explored (Table 2.14). A selection of secondary amines was subjected to reaction conditions *B* to afford tertiary acetamides in excellent conversions, before purification by column chromatography using DCM/MeOH as the elution system.

Table 2.14. Secondary amine substrate scope using reaction conditions *B*.

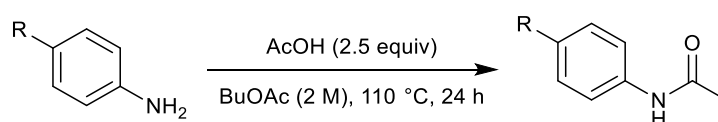
Entry	Product	Conversion (%)	Yield (%)
1	 2.19	88	78
2	 2.4	100	91
3	 2.20	100	92

Reactions were performed on a 2 mmol scale. Percentage conversions were determined by analysis of the crude ¹H NMR spectra.

Reaction conditions *B* revealed alkenes are unaffected by the methodology (Table 2.14, entry 3). Analysis of the crude ¹H NMR spectrum of acetamide **2.20** showed no presence of by-products in the reaction mixture. This was further confirmed by mass spectrometry and ¹³C NMR spectroscopy.

2.4.3. Aniline Derivatives

Finally, the substrate scope for aniline derivatives was partially investigated. As well as the synthesis of **2.6** in excellent yield, we also illustrated that substrates containing a methoxy substituent *para* to the aniline moiety could be transformed into the acetamide product (**2.21**) in comparable yield using reaction conditions *C* (Table 2.15).

Table 2.15. Aniline derivative substrate scope using reaction conditions C.

Entry	Product	Conversion (%)	Yield (%)	
1		2.6	100	92
2		2.21	100	88

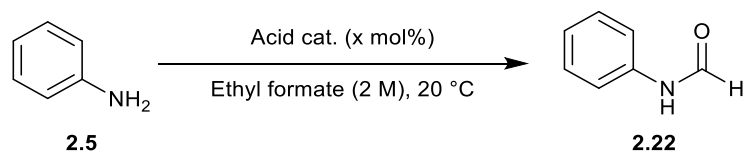
Reactions were performed on a 2 mmol scale. Percentage conversions were determined by analysis of the crude ^1H NMR spectra.

2.5. N-Acylation of Amines: Optimisation and Ester Substrate Scope

Following investigations into the *N*-acetylation of amines, we subsequently decided to explore the substrate scope of the ester component in the reaction. Previous literature describes the use of ethyl formate as a formylating agent, often in the presence of formic acid.²⁰³⁻²⁰⁵ However, these reactions usually require increased temperatures ranging from 60 to 90 °C,^{204,205} although one report details the formylation of a primary alkyl amine at room temperature.²⁰³ With this in mind, we decided to explore whether less reactive anilinic substrates, namely aniline and *p*-anisidine, could undergo formylation at room temperature in the presence of catalytic formic acid.

Preliminary experiments were conducted using aniline as the model substrate and ethyl formate as the formyl donor. Percentage conversion into product **2.22** was determined by analysis of the relative integrals of the aromatic protons in the starting material (6.50-6.66 ppm, 3H, multiplet) and product (7.26-7.37 ppm, 2H, major and minor rotamers, multiplet) in the crude ^1H NMR spectra. Analysis of the ^1H NMR spectra revealed that in the presence of no acidic catalyst only 36% conversion into formamide **2.22** was observed at 20 °C in 20 hours (Table 2.16, entry 1). In comparison, very high conversions could be achieved with as low as 10 mol% formic acid catalyst present; whilst use of 50 mol% formic acid drove the reaction to quantitative conversion (Table 2.16, entries 2-4).

Table 2.16. Optimisation of the catalyst loading and reaction time for the formylation of aniline derivatives.



Entry	Acid	Acid (mol%)	Time (h)	Conversion into 2.22 (%)
1	-	-	20	36
2	Formic acid	10	20	94
3	Formic acid	20	20	97
4	Formic acid	50	20	100
5	Acetic acid	50	20	100
6	Formic acid	50	16	100
7	Acetic acid	50	16	100

Reactions were performed on a 1 mmol scale. Conversions determined by analysis of the ^1H NMR spectra of the crude reaction mixtures.

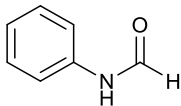
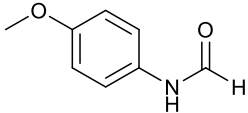
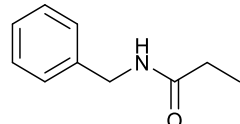
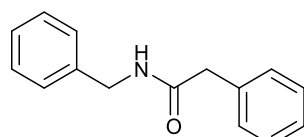
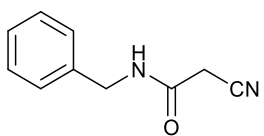
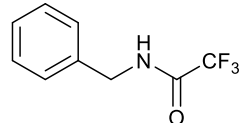
Notably, the use of acetic acid instead of formic acid also resulted in quantitative conversion with no acetamide product generated in the reaction (Table 2.16, entry 5). The absence of an acetamide side-product is presumably due to the increased reactivity of ethyl formate compared with acetic acid. Quantitative conversion using either formic acid or acetic acid was also achieved in 16 hours (Table 2.16, entries 6 and 7). Pleasingly, both **2.22** and **2.23** were isolated in excellent yield using both formic acid and acetic acid as the catalyst (Table 2.17, entries 1 and 2).

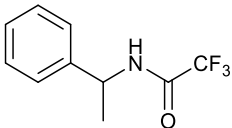
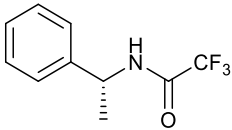
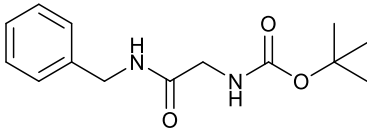
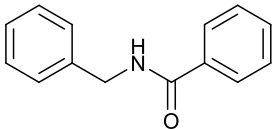
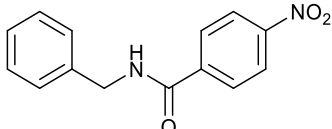
In addition, a number of other methyl and ethyl esters were reacted with benzylamine or 1-phenylethylamine to afford a range of secondary amides. Ethyl propionate and related substrates were successfully transformed into their corresponding amide products using 2 equivalents of the ester and 10 mol% of acetic acid (Table 2.17, entries 3-6). Notably, product **2.26** illustrates that the methodology is tolerant to nitriles.

Remarkably, the transformation of ethyl trifluoroacetate into **2.27-2.29** was achieved at room temperature (25 °C) with no acid catalyst present (Table 2.17, entries 7 and 8). Pleasingly, the reaction of ethyl trifluoroacetate with (*R*)-(+)- α -methylbenzylamine to afford **2.29** proceeded with retention of stereochemistry, as determined by chiral HPLC analysis (Table 2.17, entry 8).

The measured specific rotation of +138 (*c* 1.0 in CHCl₃) was consistent with literature values ($[\alpha]_D^{25}$ +137 (*c* 1.0 in CHCl₃)).²⁰⁶ In addition, the methodology was shown to tolerate amino acid esters (Table 2.17, entry 9). Amide **2.30** was afforded in excellent yield, with no deprotection of the Boc protecting group by the acetic acid catalyst.

Table 2.17. Ester component substrate scope.

Entry	Product	Conversion into desired amide (%)	Conversion into acetamide (%)	Yield (%)	
1		2.22	100	0	94 ^a
2		2.23	100	0	92 ^a
3		2.24	>99	Traces	92 ^b
4		2.25	>99	Traces	93 ^b
5		2.26	>99	Traces	94 ^b
6		2.27	100	0	100 ^{c,d}

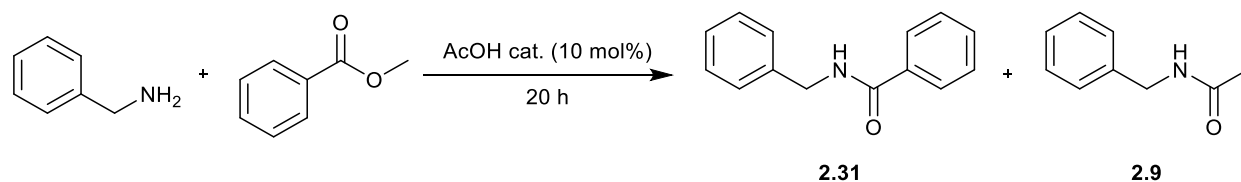
7		2.28	100	0	100 ^c
8		2.29	100	0	100 ^c >99% ee ^e
9		2.30	100	0	97 ^{d,f}
10		2.31	32 ^g	6	-
11		2.32	72	13	60 ^g

Reactions were performed on a 2 mmol scale (using the appropriate amine). Percentage conversions were determined by analysis of the crude ¹H NMR spectra. ^a Reaction conditions: ethyl formate (2 M), AcOH or formic acid (50 mol%), 20 °C, 16 h. ^b Reaction conditions: ethyl ester (2 equiv.), AcOH (10 mol%), 110 °C, 20 h. ^c Reaction conditions: ethyl trifluoroacetate (1 equiv.), no catalyst, 25 °C, 20 h. ^d Can also be performed in toluene (2 M). ^e As determined by chiral HPLC analysis. ^f Reaction conditions: Boc-Gly-OMe (1 equiv.), AcOH (10 mol%), 110 °C, 20 h. ^g Reaction conditions: methyl benzoate or methyl 4-nitrobenzoate (1 equiv.), AcOH (10 mol%), 150 °C, 20 h.

However, methyl benzoate proved relatively unreactive under the reaction conditions (neat and in toluene), likely as a result of electron donation from the aromatic ring into the C=O π* orbital, thus making the carbonyl less electrophilic (Table 2.18). Although a greater total conversion from the starting materials was achieved, an increase in the catalyst loading resulted in a higher proportion of the acetamide side-product being formed (Table 2.18, entry 2). Meanwhile, an increase in temperature to 150 °C resulted in only 32% conversion into desired amide product **2.31** (Table 2.18, entry 3; Table 2.17, entry 10), whilst use of excess ester inhibited the reaction further (Table 2.18, entry 4). However, methyl 4-nitro benzoate, a

more reactive benzoate ester, was successfully converted into **2.32** in 72% conversion at 150 °C (Table 2.17, entry 11).

Table 2.18. Reaction of methyl benzoate with benzylamine using AcOH as the catalyst.



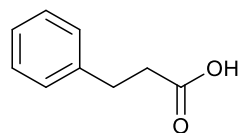
Entry	Temperature (°C)	Equivalents of Ester	Conversion into 2.31 (%)	Conversion into 2.9 (%)	Total Conversion (%)
1	110	1	23 (6)	5 (3)	28 (9)
2 ^a	110	1	17 (7)	21 (13)	38 (20)
3	150	1	32	6	38
4	150	3	18	2	20

Reactions were performed on a 1 mmol scale. Percentage conversions were determined by analysis of the crude ¹H NMR spectra. Numbers in brackets represent conversions when the reaction was performed in toluene (2 M). ^a Reaction performed using 50 mol% AcOH.

2.6. Mechanistic Investigations

2.6.1. Use of 3-Phenylpropionic Acid as the Catalyst

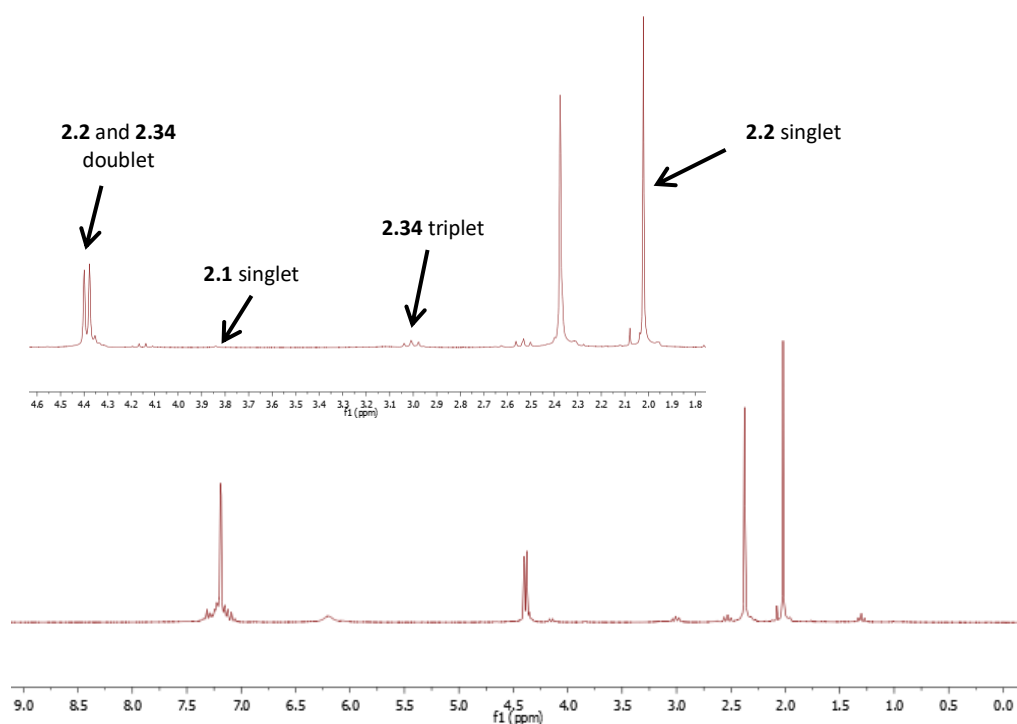
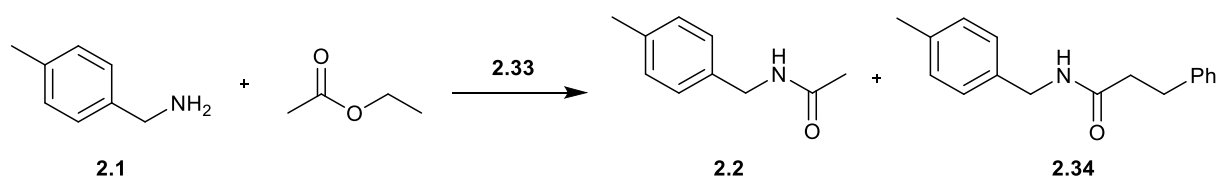
The origin of the acetyl group which is subsequently transferred to the amine was firstly explored. It was thought that this group could have originated from either the ethyl acetate or acetic acid. Experiments were conducted using 4-methylbenzylamine in which the acetic acid was replaced with a different organic acid. 3-Phenylpropionic acid was chosen for two reasons (Figure 2.1). Firstly, a structurally similar organic acid was required to ensure that the acid was performing the same role as acetic acid in the reaction. Secondly, use of 3-phenylpropionic acid enabled facile spectral determination of conversion into the two amide products, as the amide derived from this acid was easily distinguishable from the amide derived from acetic acid. Determining the ratio of amide products enabled us to elucidate whether transfer of the acyl group from the ester or the acid was favoured during the reaction.



2.33

Figure 2.1. Structure of 3-phenylpropionic acid.

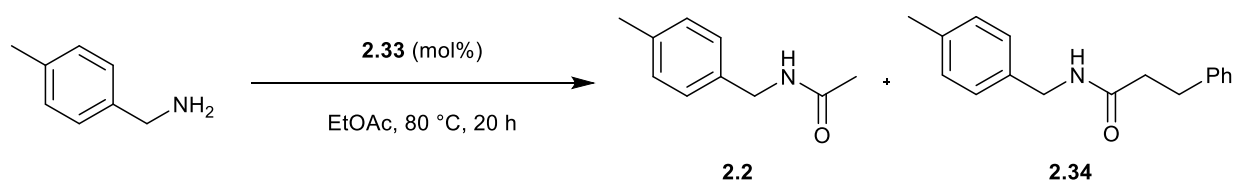
Following an aqueous basic work-up to remove the excess acid, percentage conversion into **2.2** and **2.34** was determined by analysis of the relative integrals of the benzyl protons in the starting material (3.85 ppm, singlet) and products (4.39 ppm, doublet) in the crude ^1H NMR spectra (Scheme 2.9). Product ratios were also calculated from the crude ^1H NMR spectra by comparison of the peaks at 3.00 ppm (**2.34**, 2H, triplet) and 2.02 ppm (**2.2**, 3H, singlet).



Scheme 2.9. ^1H NMR spectrum showing the signals used to calculate percentage conversions and product ratios after reaction of **2.1** with ethyl acetate in the presence of acid **2.33**.

Using ethyl acetate (1 M) as the solvent and a stoichiometric amount of 3-phenylpropionic acid, analysis of the crude ^1H NMR spectra showed that the majority of the resulting mixture contained acetamide product **2.2**, with only a small proportion of **2.34** present (Table 2.19, entry 1). As the amount of acid used in the reaction decreased, the product ratio (**2.2** : **2.34**), as expected, shifted towards quantitative conversion into **2.2** (Table 2.19, entries 2-5). In addition, a reduction in the amount of ethyl acetate employed resulted in a decrease in the **2.2** : **2.34** ratio (Table 2.19, entries 6-8). Meanwhile, use of an equimolar amount of amine, acid and ester gave acetamide **2.2** as the major product (Table 2.19, entry 8). These results suggest that the acetyl moiety largely originates from the acetate ester and not the acetic acid.

Table 2.19. Investigations into acetyl group transfer using 3-phenylpropionic acid as the catalyst.



Entry	2.33 (mol%)	EtOAc (mL)	Conversion into 2.2 and 2.34 (%)	2.2 : 2.34
1	100	1	100	95 : 5
2	50	1	100	96 : 4
3	20	1	100	97 : 3
4	10	1	100	98 : 2
5	5	1	97	99 : 1
6	100	0.5	100	93 : 7
7	100	0.25	97	91 : 9
8	100	0.098	62	84 : 16

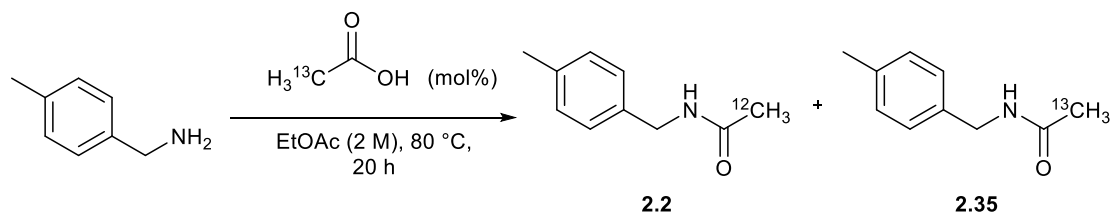
Reactions were performed on a 1 mmol scale. Percentage conversions and product ratios were determined by analysis of the crude ^1H NMR spectra.

2.6.2. Use of ^{13}C -Labelled Acetic Acid

Further investigations were subsequently undertaken using ^{13}C -methyl-labelled acetic acid (acetic acid-2- ^{13}C , 99%) as the catalyst. This enabled us to confirm whether the acetyl group had been transferred from the ethyl acetate or acetic acid. If the acetyl group had been transferred from the acetic acid catalyst then the amide product would contain the ^{13}C label.

Two experiments were performed in which the model substrate, 4-methylbenzylamine, was reacted with catalyst loadings of 10 mol% and 50 mol% to give a mixture of products **2.2** and **2.35**. A further experiment was performed in which unlabelled acetic acid was employed. Two methods of analysis were then used to determine percentage incorporation of the acid catalyst into the product (Table 2.20).

Table 2.20. Investigations into catalyst incorporation using ^{13}C -labelled AcOH.



Entry	AcOH (mol%)	^{13}C Incorporation (%) ^a	^{13}C Incorporation (%) ^b
1	10 ^c	0	0
2	10 ^d	0.5	0.5
3	50 ^d	3.0	3.0

Reactions were performed on a 1 mmol scale. ^a Percentage incorporation calculated using the ^1H NMR spectra; ^b Percentage incorporation calculated using the crude ^{13}C NMR spectra; ^c Unlabelled AcOH employed; ^d Labelled AcOH-2- ^{13}C employed.

Firstly, quantitative ^{13}C NMR experiments allowed direct integration of the signals in the three spectra relative to the arene methyl signals (Figure 2.2). If the product was fully labelled it was expected that the acetyl signal in the ^{13}C NMR spectrum would integrate to 99% of the arene methyl signal (as the labelled acetic acid was 99% ^{13}C). Analysis of the ^{13}C NMR spectra showed minimal incorporation of acetic acid into the final product, with use of 10 mol% and 50 mol% acetic acid giving 0.5% and 3.0% incorporation respectively (Table 2.20, entries 2 and 3). As expected, employing unlabelled acetic acid resulted in no incorporation (Table 2.20, entry 1).

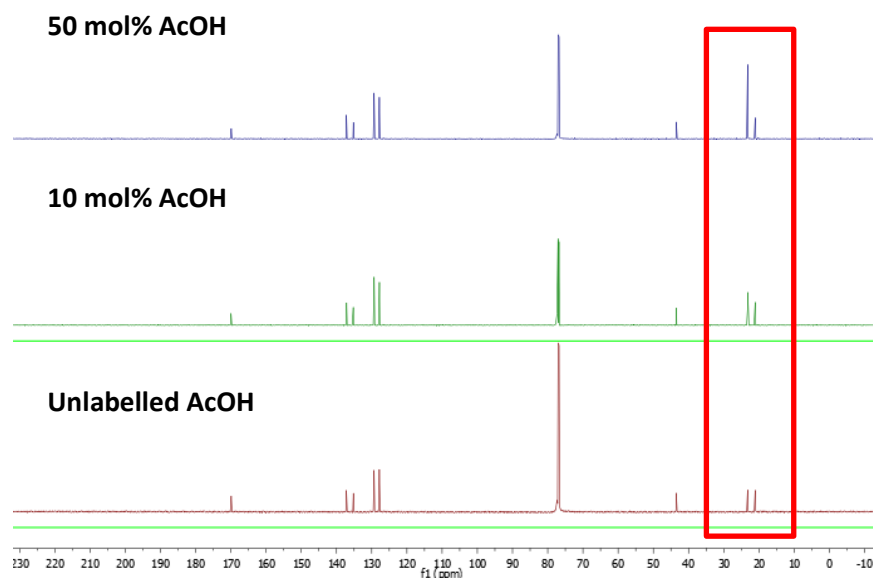


Figure 2.2. ^1H NMR stacked spectra of the ^{13}C -labelled studies showing the relative intensities of the arene methyl group and the acetyl group.

These results were further confirmed through analysis of the acetyl group satellites in the crude ^1H NMR spectra for each experiment, relative to the arene methyl group satellites observed in the spectra (Table 2.20, Figure 2.3). These two pairs of satellites are a result of the CH_3 protons coupling to the ^{13}C isotope present in the adjacent carbon. The satellites of both the arene methyl group and the acetyl group were integrated in all three ^1H NMR spectra and percentage incorporation values calculated based on 100% incorporation giving an overall satellite integral of 3 (1.5 for each satellite peak).

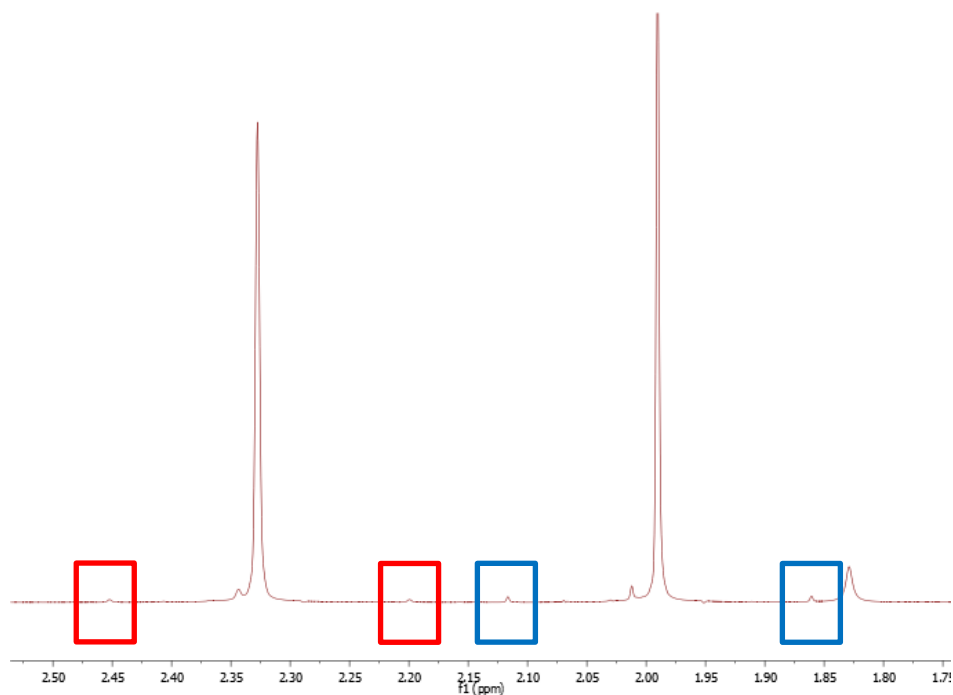


Figure 2.3. Crude ^1H NMR spectra showing the arene methyl group satellites (red) and the acetyl group satellites (blue) used to calculate the percentage incorporation.

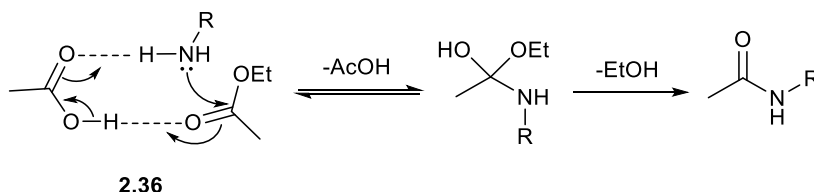
2.6.3. Plausible Reaction Mechanism

It is believed that the role of the acid catalyst is not simply that of a proton transfer reagent. As detailed previously, when H_2SO_4 was used as the acid catalyst, little to no conversion was observed following analysis of the crude ^1H NMR spectra. This was presumably due to formation of the $\text{HSO}_4^-/\text{RNH}_3^+$ or $\text{HSO}_4^-/\text{R}'\text{R}''\text{NH}_2^+$ salt. However, RNH_3^+ and $\text{R}'\text{R}''\text{NH}_2^+$ are stronger acids than acetic acid when comparing pK_a values of these species in dimethylsulfoxide (Table 2.21);^{202,207} a more similar solvent to ethyl acetate than water (both non-protic). Therefore, if the reaction mechanism solely involved proton transfer, a higher conversion would be expected with the protonated amine present compared with acetic acid.

Table 2.21. pK_a values of selected acids in DMSO.^{202,207}

Entry	Acid	pK_a in DMSO
1	AcOH	12.6
2	BnNH_3^+	10.2
3	BuNH_3^+	11.1
4	PhNH_3^+	3.8
5	Et_3NH^+	9.0

However, as detailed, this is not the case, leading us to believe that the reaction mechanism proceeds through a transition state involving acetic acid rather than just a proton (**2.36**), similar to that proposed by Whiting *et al.* in 2011 (Scheme 1.4 and Scheme 2.10).¹⁰ Further mechanistic studies are to be performed in the future.



Scheme 2.10. Plausible mechanism for the *N*-acetylation of amines using acetic acid as a catalyst and ethyl acetate as the acyl source.

2.7. Conclusions

In conclusion, we have identified acetic acid as an effective catalyst for the *N*-acetylation of a variety of amines using either ethyl acetate or butyl acetate as the acyl source. The methodology has been shown to transform primary and secondary amines into their acetamide products in excellent yields at 80 °C and 120 °C, respectively. A broad range of functional groups were tolerated under the reaction conditions, whilst the chemoselectivity of the protocol was also investigated – primary amines were selectively acetylated over alcohols, aromatic amines and secondary amines. In addition to illustrating the scalability of the reaction, the synthetic utility of the approach was also highlighted through the synthesis of the hormone and sleep disorder drug, melatonin.

The methodology was then successfully applied to other esters, including electron deficient benzoates and amino acid esters, in order to form higher amides. In addition, formamides were synthesised at 20 °C whilst enantiomerically pure substrates were transformed with retention of stereochemistry. Finally, mechanistic studies were performed, involving the use of ¹³C-labelled acetic acid, and a plausible reaction mechanism was given which is consistent with the data.

Results and Discussion II

Amides from Nitriles

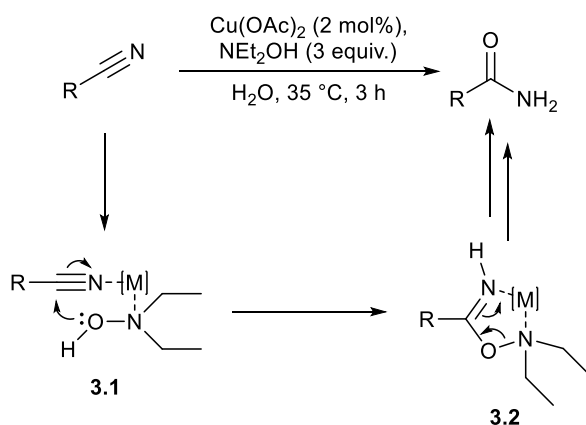
“A selective hydration of nitriles catalysed by a Pd(OAc)₂-based system in water”

D. D. Sanz Sharley and J. M. J. Williams, *Tetrahedron Lett.*, 2017, **58**, 4090.

3. Results and Discussion II – Amides from Nitriles

3.1. Previous Work in the Group

The use of aldoximes, particularly acetaldoxime, to hydrate nitriles has been explored by a number of groups.¹¹⁸⁻¹²¹ However, the need for at least stoichiometric amounts of the oxime and the risk of a competing hydration reaction involving the liberated nitrile, unless the equivalent oxime is used, is less than ideal. Other research has focussed on employing more simple oxygen sources such as hydroxylamines.^{92,208} Recent studies in the Williams group have shown that *N,N*-diethylhydroxylamine in combination with catalytic $\text{Cu}(\text{OAc})_2$ can transform a wide variety of nitriles into their corresponding primary amide products (Scheme 3.1).⁹²



Scheme 3.1. Hydroxylamine-promoted hydration of nitriles developed by Williams *et al.*

This transformation proceeds through a similar mechanism to the acetaldoxime-promoted reaction; the nitrogen of the hydroxylamine coordinates to the metal, allowing the oxygen to be delivered to the coordinated nitrile (**3.1**). Rearrangement of immolate species **3.2** affords the desired amide product. However, although the methodology employs a low temperature and short reaction time, three equivalents of the hydroxylamine are required for efficient hydration of the nitrile.

3.2. Initial Aims and Objectives

The aim of this project was to develop a catalytic method for the hydration of nitriles based on the aldoxime/hydroxylamine work discussed in Sections 1.2.3.3 and 3.1. In a similar manner, an appropriate additive would bind to the metal (which is also coordinated to the nitrile) and deliver its oxygen in an intramolecular process to the electrophilic carbon of the

nitrile (Figure 3.1). Alternatively, the ligand of a commercially available metal complex could potentially perform the same process.

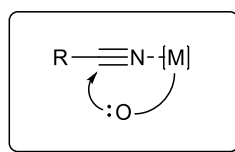
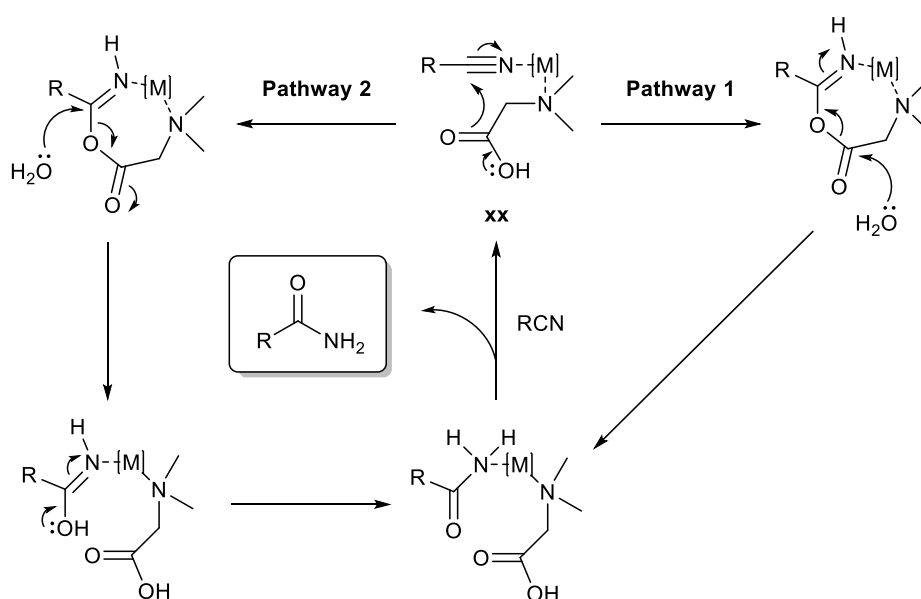


Figure 3.1. Generic intramolecular oxygen delivery to the nitrile.

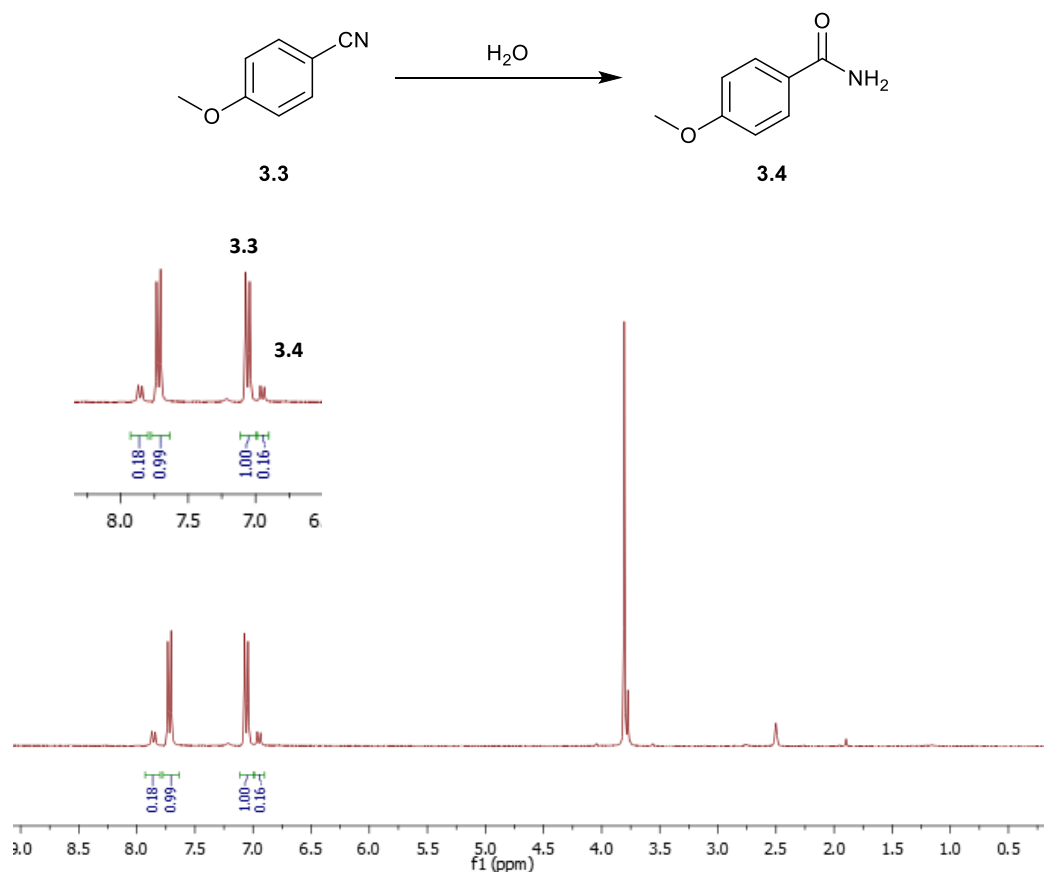
Attack by water, through two possible pathways, would then afford the amide product and recycle the additive/ligand. A representative example of this proposed mechanism is illustrated in Scheme 3.2, employing *N,N*-dimethylglycine as the additive.



Scheme 3.2. Representative example of the proposed catalytic hydration methodology, employing *N,N*-dimethylglycine as the additive.

3.3. Initial Work

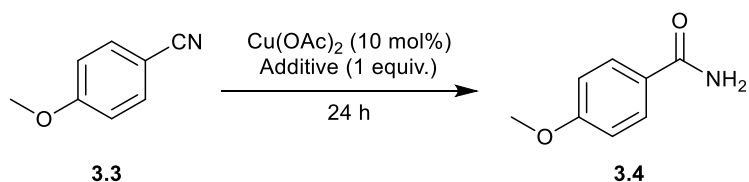
For the optimisation process we used the same model substrate, 4-methoxybenzonitrile (**3.3**), as had been previously employed during the group's previous nitrile hydration work. Percentage conversion into product **3.4** was determined by analysis of the relative integrals of the peaks corresponding to the aromatic protons in product **3.4** (6.95 ppm and 7.86 ppm, doublets) and starting material **3.3** (7.06 ppm and 7.72 ppm, doublets) in the crude ^1H NMR spectra (Scheme 3.3).

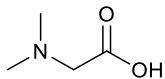
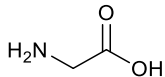
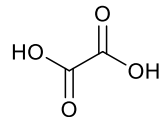
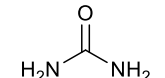
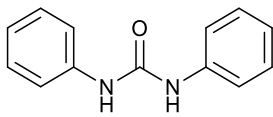
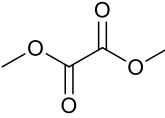
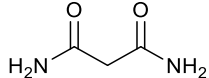
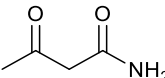
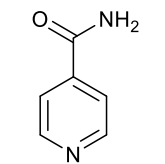
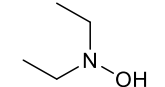


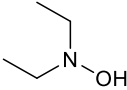
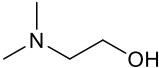
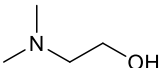
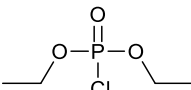
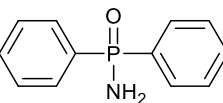
Scheme 3.3. An example of the ^1H NMR spectrum used to determine percentage conversion into **3.4**, showing aromatic protons in the starting material (**3.3**) and product (**3.4**).

Due to the success achieved in the group's previous nitrile hydration work, $\text{Cu}(\text{OAc})_2$ was used as the catalyst for the additive screening reactions. The reactions were performed under two sets of conditions; in toluene with 4 equivalents of water (reaction conditions **A**) and in a 1:1 toluene:water solvent mixture (reaction conditions **B**). Stoichiometric amounts of each additive were firstly used to determine which compound, if any, could promote the hydration reaction (Table 3.1). A number of phosphates, organophosphates and phosphinamides were also subjected to the reaction conditions as these compounds have precedence for accelerating oxime rearrangements, as illustrated by previous work in the group.²⁰⁹

Table 3.1. Additive screen for the nitrile hydration reaction.



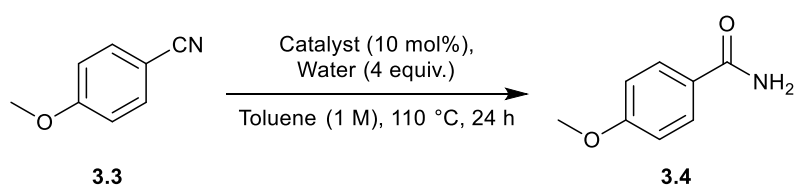
Entry	Additive	Reaction conditions A: Conversion into 3.4 (%) ^a	Reaction conditions B: Conversion into 3.4 (%) ^b
1	No catalyst or additive	9	Traces
2	No additive	Traces	Traces
3		Traces	Traces
4		Traces	Traces
5		12	Traces
6		Traces	Traces
7		Traces	Traces
8		9	Traces
9		Traces	Traces
10		Traces	Traces
11		Traces	Traces
12		100	100

13		20 ^c	-
14		3	6
15		Traces ^c	-
16		13	11
17		Traces	Traces
18	KH ₂ PO ₄	Traces	Traces
19	K ₂ HPO ₄	Traces	Traces

Reactions were performed on a 1 mmol scale. Conversions determined by analysis of the ¹H NMR spectra of the crude reaction mixtures. ^a Reaction conditions **A**: In toluene (1 M) with 4 equivalents of H₂O at 110 °C. ^b Reaction conditions **B**: In 1:1 toluene:H₂O solvent mixture at 100 °C. ^c Reaction performed using 20 mol% of the additive.

Unfortunately, analysis of the crude ¹H NMR spectra revealed that all of the novel additives employed were unsuccessful in promoting the reaction. In comparison, the use of *N,N*-diethylhydroxylamine afforded quantitative conversion as expected (Table 3.1, entry 12). In contrast to the other reactions, the addition of *N,N*-diethylhydroxylamine to the reaction mixture prompted a rapid colour change from green/blue to orange/brown. Meanwhile, it is interesting to note that when the reaction was performed with *N,N*-dimethylethanolamine, a hydroxylamine with carbons between the two functional groups, very limited formation of primary amide **3.4** was observed (Table 3.1, entry 14). This therefore highlights the importance of the OH and NR₂ groups being adjacent to each other for efficient transformation to be achieved.

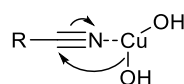
Following this, a number of first row metal oxalate and metal acetate complexes were screened under reaction conditions **A** (Table 3.2). In a similar mechanism to that shown in Scheme 3.2, it was hoped that the oxalate/acetate ligand would deliver its oxygen to the nitrile, before being recycled following attack by water. However, ¹H NMR analysis showed all of the metal complexes gave similarly low conversions, thus illustrating the inefficiency of this approach.

Table 3.2. Metal oxalate and metal acetate complex screen.

Entry	Catalyst	Conversion into 3.4 (%)
1	No catalyst	4
2	Copper(II) oxalate hemihydrate	5
3	Iron(II) oxalate dihydrate	4
4	Cobalt(II) oxalate dihydrate	4
5	Nickel(II) oxalate dihydrate	4
6	Copper(II) acetate	4
7	Copper(II) acetate	7 ^a
8	Cobalt(II) acetate tetrahydrate	5
9	Nickel(II) acetate tetrahydrate	4
10	Iron(II) acetate	5
11	Zinc(II) acetate tetrahydrate	4

Reactions were performed on a 1 mmol scale. Conversions determined by analysis of the ¹H NMR spectra of the crude reaction mixtures. ^a 20 mol% oxalic acid added to the reaction.

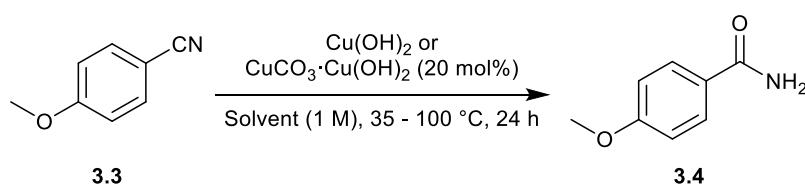
Finally, it was noticed Cazin *et al.* had developed a NaOH-catalysed system for the hydration of aromatic nitriles.⁹⁶ The group employed 10 mol% NaOH in a solvent system of EtOH/H₂O (7:3) and found quantitative conversion of their model substrate, benzonitrile, could be achieved in 17 hours. It was thought that the efficiency of this approach could be enhanced if copper hydroxide (Cu(OH)₂) was employed instead of NaOH. We hypothesised that coordination of copper to the nitrile would increase the reactivity of the substrate and make hydroxide addition more facile (Figure 3.2).

**Figure 3.2.** Proposed intramolecular mechanism for Cu(OH)₂-catalysed hydration.

Unfortunately however, use of Cu(OH)₂ in combination with the reaction conditions identified by Cazin *et al.* resulted in no reaction at 35–100 °C (Table 3.3, entry 1). Similarly disappointing

results were obtained with $\text{CuCO}_3 \cdot \text{Cu}(\text{OH})_2$ and when $\text{H}_2\text{O}:\text{dioxane}$ (1:1) was employed as the solvent system (Table 3.3, entries 2 and 3).

Table 3.3. Employing $\text{Cu}(\text{OH})_2$ and $\text{CuCO}_3 \cdot \text{Cu}(\text{OH})_2$ as catalysts in the hydration reaction.



Entry	Copper complex (20 mol%)	Solvent system	Conversion into 3.4 (%)
1	$\text{Cu}(\text{OH})_2$	$\text{EtOH}:\text{H}_2\text{O}$ (7:3)	0
2	$\text{Cu}(\text{OH})_2$	$\text{H}_2\text{O}:\text{dioxane}$ (1:1)	0
3	$\text{CuCO}_3 \cdot \text{Cu}(\text{OH})_2$	$\text{EtOH}:\text{H}_2\text{O}$ (7:3)	0

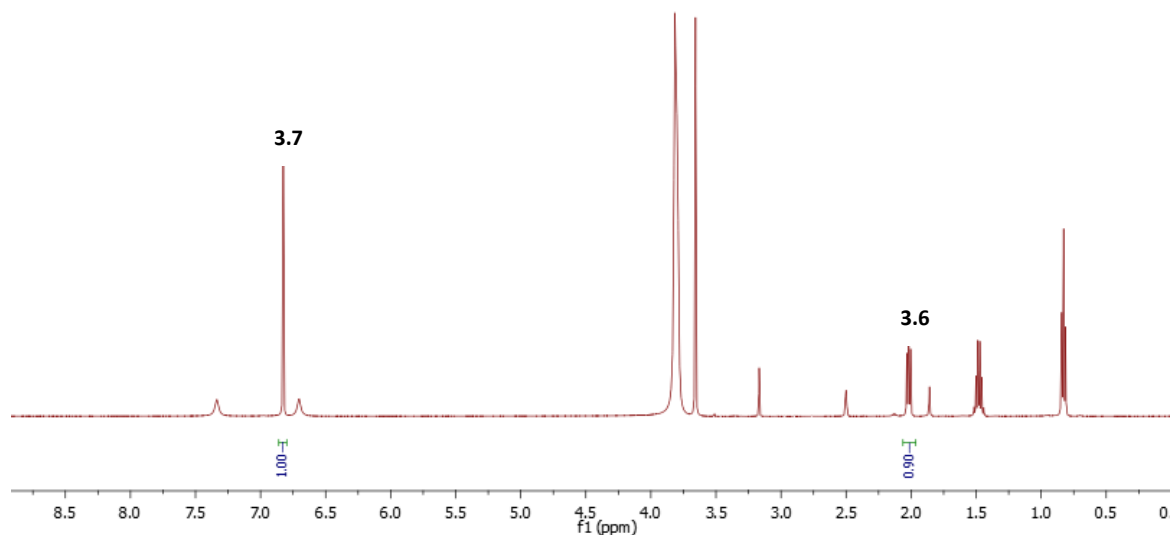
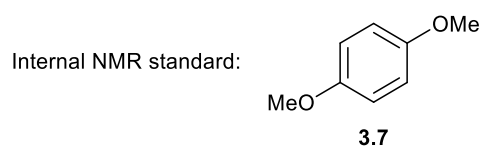
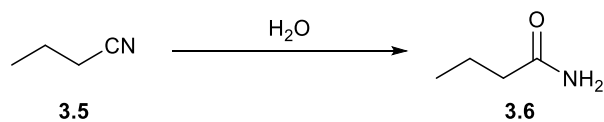
Reactions were performed on a 1 mmol scale. Conversions determined by analysis of the ^1H NMR spectra of the crude reaction mixtures. Reactions employing $\text{Cu}(\text{OH})_2$ were performed at temperatures of 35, 55, 80 and 100 °C. Reactions employing $\text{CuCO}_3 \cdot \text{Cu}(\text{OH})_2$ were performed at temperatures of 55 and 100 °C.

3.4. New Aims and Objectives

Due to the poor results obtained up until this point, we decided to alter the direction of the project and instead focus on finding the most efficient metal catalyst for the hydration of nitriles. This catalyst would be able to convert nitriles into their corresponding primary amide products without the need for stoichiometric quantities of a hydroxylamine/oxime-type additive.

3.5. Optimisation

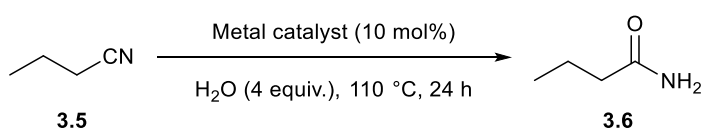
Initially, a wide range of commercially available metal complexes were screened using the hydration of butyronitrile (**3.5**) as the model reaction. Percentage conversion into product **3.6** was determined by analysis of the relative integrals of the peaks corresponding to the protons *alpha* to the amide group in product **3.6** (2.02 ppm, triplet) and the internal standard 1,4-dimethoxybenzene (**3.7**, 6.83 ppm, singlet) in the crude ^1H NMR spectra (Scheme 3.4). An internal NMR standard was necessary when measuring conversions due to the volatility of starting nitrile **3.5**.



Scheme 3.4. An example of the ^1H NMR spectrum used to determine percentage conversion into **3.6**.

Cheap first row metal catalysts – including metal chlorides, nitrates and triflates – were firstly explored followed by a selection of alkali and alkali earth metal complexes; however their use resulted in no conversion into primary amide **3.6** (Table 3.4, entries 1-11). Subsequently, a variety of second and third row transition metal chloride complexes were then investigated (Table 3.4, entries 16-20). We were pleased to find that some of these catalysts promoted the reaction, although the conversions achieved were very low.

Table 3.4. Metal catalyst screen.

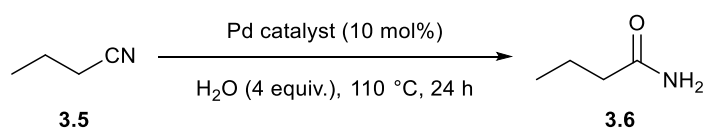


Entry	Catalyst	Conversion into 3.6 (%)
1	-	0
2	FeCl ₂	0
3	NiCl ₂	0

4	CoCl ₂	0
5	ZnCl ₂	0
6	FeCl ₃	0
7	Ni(NO ₃) ₂ ·6H ₂ O	0
8	Zn(NO ₃) ₂ ·6H ₂ O	0
9	Cu(OTf) ₂	0
10	FeBr ₂	0
11	Fe(BF ₄) ₂ ·6H ₂ O	0
12	InCl ₃	0
13	NaNO ₃	0
14	Mg(NO ₃) ₂ ·6H ₂ O	0
15	EuCl ₃ ·6H ₂ O	0
16	AgNO ₃	0
17 ^a	IrCl ₃ ·xH ₂ O	Traces
18 ^a	RuCl ₃ ·xH ₂ O	6
19 ^a	RhCl ₃ ·xH ₂ O	9
20	PdCl ₂	13

Reactions were performed on a 1 mmol scale. Conversions determined by analysis of the ¹H NMR spectra of the crude reaction mixtures using 1,4-dimethoxybenzene as an internal NMR standard. ^a 5 mol% catalyst employed.

Among these metal catalysts, use of PdCl₂ gave the highest conversion into primary amide **3.6** of 13% (Table 3.4, entry 20). As a result, we decided to explore the efficiency of other palladium complexes in the reaction. Upon inspection of the crude ¹H NMR spectra it was observed that similarly low conversions were achieved when employing PdCl₂-based metal complexes as the catalyst (Table 3.5, entries 2 and 3), whilst the Pd(acac)₂ complex afforded no primary amide product (Table 3.5, entry 4). Pleasingly however, use of Pd(OAc)₂ (73%) and Pd(NO₃)₂·xH₂O (55%) resulted in significantly increased conversions (Table 3.5, entries 5 and 6).

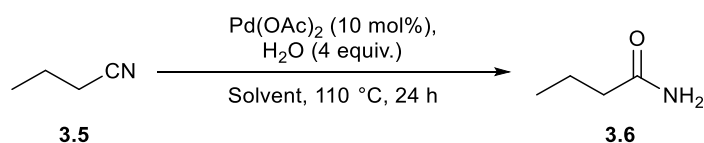
Table 3.5. Palladium catalyst screen.

Entry	Catalyst	Conversion into 3.6 (%)
1	PdCl ₂	13
2	PdCl ₂ (MeCN) ₂	15
3	PdCl ₂ (PhCN) ₂	7
4	Pd(acac) ₂	0
5	Pd(OAc) ₂	73
6	Pd(NO ₃) ₂ ·xH ₂ O	55

Reactions were performed on a 1 mmol scale. Conversions determined by analysis of the ¹H NMR spectra of the crude reaction mixtures using 1,4-dimethoxybenzene as an internal NMR standard..

The use of palladium-based catalysts for the hydration of nitriles has previously been explored. Among the heterogeneous examples,²¹⁰⁻²¹² palladium nanoparticles, in combination with other compounds such as metal oxides, have received a lot of attention.¹²⁶⁻¹²⁸ Other methods utilise homogeneous catalysts,^{122-124,213-215} including Pd(OAc)₂-based complexes.^{120,126} However, these methods require an additional Lewis acid co-catalyst²¹⁶ or complex co-ligands,¹²⁶ whilst other approaches also employing Pd(OAc)₂ only operate in the presence of an oxime (Scheme 1.38).^{120,217} As well as this, many protocols only exhibit a very limited substrate scope.¹²⁶ As a result, we felt that the hydration of nitriles using palladium catalysis was an area that required further investigation.

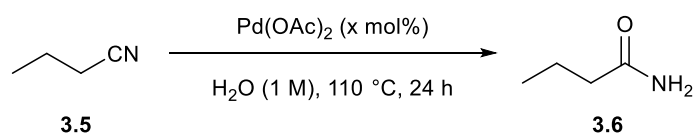
Analysis of the crude ¹H NMR spectrum showed that the use of water as a solvent (1 M), instead of only 4 equivalents, afforded a cleaner reaction and aided stirring (Table 3.6, entry 1). However, when the hydration of nitrile **3.5** was performed in organic solvents the efficiency of the reaction was reduced dramatically (Table 3.6, entries 2-9).

Table 3.6. Solvent screen.

Entry	Solvent	Conversion into 3.6 (%)
1	Water	74
2	Toluene	1
3	Ethanol	0
4	Acetonitrile	4
5	Heptane	4
6	Dioxane	15
7	Isopropyl alcohol	0
8	1,2-Dichloroethane	6
9	Ethyl acetate	4

Reactions were performed on a 1 mmol scale. Conversions determined by analysis of the ^1H NMR spectra of the crude reaction mixtures using 1,4-dimethoxybenzene as an internal NMR standard.

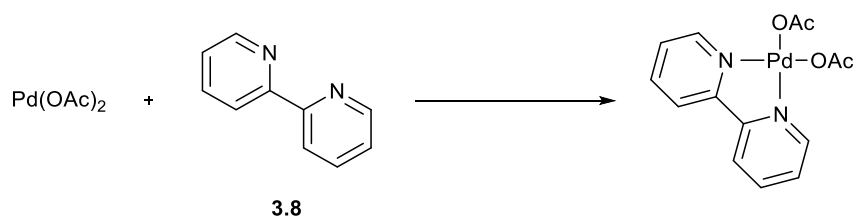
Subsequently, due to the cost of Pd(OAc)_2 it was necessary to reduce the catalyst loading; although doing so under the present reaction conditions resulted in decreased conversion into primary amide **3.6** (Table 3.7, entries 1-3). It was noticed, however, that a black precipitate was forming in these reactions at both 110 °C and 80 °C (Table 3.7, entries 2-5). This was likely due to decomposition of the catalyst to palladium black.

Table 3.7. Catalyst loading screen.

Entry	Pd(OAc)_2 loading (mol%)	Colour of reaction	Conversion into 3.6 (%)
1	-	Colourless	0
2	2	Black	27
3	5	Black	60
4 ^a	5	Black	45

Reactions were performed on a 1 mmol scale. Conversions determined by analysis of the ^1H NMR spectra of the crude reaction mixtures using 1,4-dimethoxybenzene as an internal NMR standard. ^a Reaction performed at 80 °C.

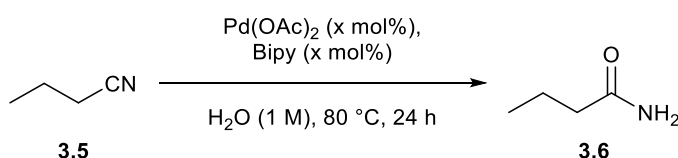
It was clear a coordinating ligand needed to be introduced into the reaction mixture in order to stabilise the catalyst, similar to previous studies. Oberhauser and co-workers showed $\text{Pd}(\text{OAc})_2$ could be solubilised in water using a poly(ethyleneglycol) monomethylether functionalised 2,2'-bipyridine (bipy) ligand.¹²⁶ Using this concept, we investigated whether a non-functionalised bipy unit (**3.8**) could perform the same role in our system (Scheme 3.5).



Scheme 3.5. Likely coordination of bipy to a $\text{Pd}(\text{OAc})_2$ metal centre.

Pleasingly, the cheap and readily available bipy ligand was able to solubilise the palladium catalyst *in situ* (Table 3.8). This solubilisation could be clearly observed as the reaction mixture turned yellow instead of black when bipy was present. Moreover, we were pleased to find that solubilisation of the $\text{Pd}(\text{OAc})_2$ catalyst increased the efficiency of the hydration reaction at 80 °C (Table 3.8, entries 3 and 5-7). Investigations into the ratio of bipy to $\text{Pd}(\text{OAc})_2$ revealed a 1:1 stoichiometry to be optimal; employing 5 mol% of each led to quantitative conversion (Table 3.8, entry 3). However, a decrease in reaction temperature to 60 °C led to reduced conversion into primary amide **3.6** compared with that achieved at 80 °C (Table 3.8, entry 4).

Table 3.8. $\text{Pd}(\text{OAc})_2$:bipy ratio screen.



Entry	$\text{Pd}(\text{OAc})_2$ loading (mol%)	Bipy loading (mol%)	$\text{Pd}(\text{OAc})_2$ solubilised?	Colour of reaction	Conversion into 3.6 (%)
1	-	-	-	Colourless	0
2	5	-	No	Black	45

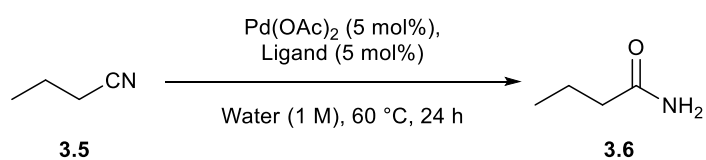
3	5	5	Yes	Light yellow	100
4 ^a	5	5	Yes	Light yellow	70
5	5	10	Yes	Light yellow	80
6	5	2	Partially	Dark yellow	87
7	2	2	Yes	Light yellow	90

Reactions were performed on a 1 mmol scale. Conversions determined by analysis of the ¹H NMR spectra of the crude reaction mixtures using 1,4-dimethoxybenzene as an internal NMR standard. ^a Reaction performed at 60 °C.

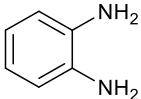
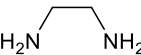
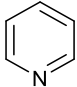
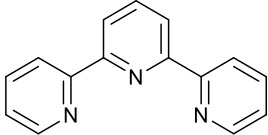
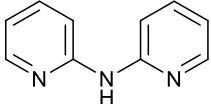
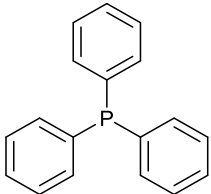
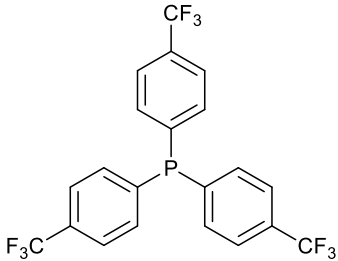
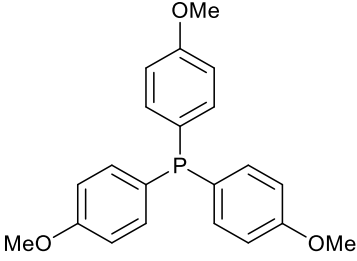
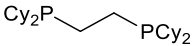
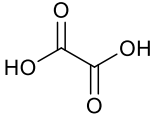
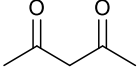
In an effort to reduce the reaction temperature, but still reach quantitative conversion, it was decided to investigate whether altering the electronic properties of the bipy moiety influenced the hydration reaction (Table 3.9). Analysis of the crude ¹H NMR spectra revealed that introducing electron donating (Table 3.9, entries 4 and 5) and electron withdrawing (Table 3.9, entries 6 and 7) groups to the 4-position of bipy made little difference to the efficiency of the reaction at 60 °C. It was also thought that higher conversions may be achievable if the active catalyst was preformed prior to the addition of the nitrile. Bipy and Pd(OAc)₂ were stirred in water for 5 minutes to produce a light yellow mixture, before the nitrile was introduced. Inspection of the crude ¹H NMR spectrum showed a slight increase in conversion (80%) compared with when the active catalyst wasn't preformed (Table 3.9, entries 2 and 3).

In addition, other bidentate nitrogen-based ligands, including phenanthrolines and ethylenediamine, were also investigated (Table 3.9, entries 8-14). Although some reactions afforded slightly higher conversions, the increase observed wasn't significant, whilst in some cases the ligand inhibited the hydration reaction. Similar results were also observed when mono and tridentate nitrogen-based ligands were employed in the reaction (Table 3.9, entries 15-17). Subsequently, a range of mono and bidentate phosphine additives were explored; however in all cases conversion into primary amide **3.6** was suppressed (Table 3.9, entries 18-22). Meanwhile, poor conversions were also achieved with common oxygen-based ligands (Table 3.9, entries 23 and 24).

Table 3.9. Ligand screen.



Entry	Ligand	Conversion into 3.6 (%)
1	-	30
2		70
3 ^a		80
4		74
5		77
6		76
7		79
8		78
9		83
10		3
11		33
12		3

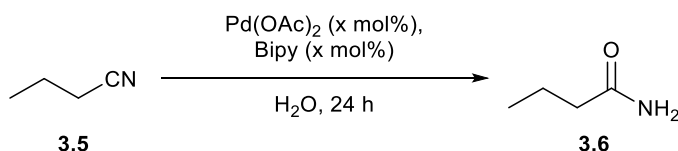
13		2
14		17
15		34
16		70
17		45
18		5
19		11
20		6
21	dppf	Traces
22		22
23		16
24	 + NaOH (5 mol%)	3

Reactions were performed on a 1 mmol scale. Conversions determined by analysis of the ^1H NMR spectra of the crude reaction mixtures using 1,4-dimethoxybenzene as an internal NMR standard. ^a Catalyst was preformed before the starting nitrile was added.

Although some of the other bidentate nitrogen-based ligands gave slightly higher conversions, it was decided that due to the ready availability and inexpensiveness of bipy we would continue our studies using this ligand in combination with $\text{Pd}(\text{OAc})_2$. An elevated temperature of 70 °C allowed higher conversions to be achieved and pleasingly, the reaction could be driven to quantitative conversion, with and without preformation of the catalyst, when increased water (0.5 M) was employed (Table 3.10, entries 3 and 4).

However, analysis of the crude ^1H NMR spectra revealed catalyst loadings lower than 5 mol% did not yield quantitative conversion (Table 3.10, entries 6-9). It should also be noted that preformation of the catalyst had no significant beneficial effect at this temperature (Table 3.10, entries 1-4 and 6-9). Meanwhile, employing increased amounts of water in the reaction at the lower temperature of 60 °C afforded decreased conversions compared with those achieved at 70 °C (Table 3.10, entries 10 and 11).

Table 3.10. Optimisation of the water concentration, temperature, catalyst loading and catalyst formation.

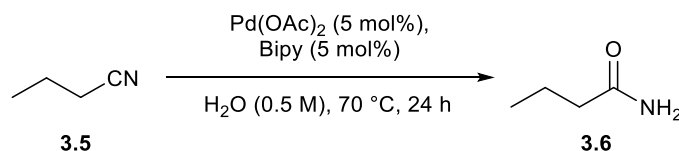


Entry	Water concentration (M)	$\text{Pd}(\text{OAc})_2$ and Bipy loading (mol%)	Catalyst preformed?	Temperature (°C)	Conversion into 3.6 (%)
1	1	5	No	70	95
2	1	5	Yes	70	94
3	0.5	5	No	70	100
4	0.5	5	Yes	70	100
5 ^a	0.5	5	-	70	37
6	0.5	3.5	No	70	94
7	0.5	3.5	Yes	70	95
8	0.5	2	No	70	71
9	0.5	2	Yes	70	74

10	0.5	5	No	60	81
11	0.5	5	Yes	60	85

Reactions were performed on a 1 mmol scale. Conversions determined by analysis of the ^1H NMR spectra of the crude reaction mixtures using 1,4-dimethoxybenzene as an internal NMR standard. ^o Reaction performed without bipy.

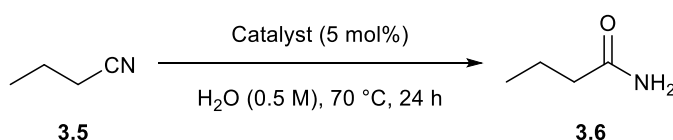
Scheme 3.6 details the fully optimised reaction conditions for the model substrate using a $\text{Pd}(\text{OAc})_2/\text{bipy}$ complex, which is formed *in situ*, as the catalyst.



Scheme 3.6. Model reaction conditions using $\text{Pd}(\text{OAc})_2/\text{bipy}$.

It was then investigated whether a cheaper catalyst could hydrate butyronitrile under these reaction conditions. Less expensive first row metal acetate complexes, namely $\text{Ni}(\text{OAc})_2 \cdot \text{H}_2\text{O}$ and $\text{Cu}(\text{OAc})_2$, were investigated; however analysis of the crude ^1H NMR spectra revealed no conversion into primary amide **3.6** either in the presence or absence of bipy at 70 °C (Table 3.11, entries 1-4). In addition, when the slightly cheaper palladium complex PdCl_2 was employed as the catalyst under our model reaction conditions, only 5% conversion into primary amide **3.6** was observed (Table 3.11, entry 5). Surprisingly, an increased conversion was achieved when PdCl_2 was used without bipy present in the reaction mixture (Table 3.11, entry 6).

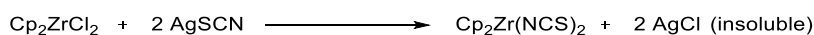
Table 3.11. Metal acetate and palladium chloride screen.



Entry	Catalyst	5 mol% Bipy present?	Conversion into 3.6 (%)
1	$\text{Ni}(\text{OAc})_2 \cdot 4\text{H}_2\text{O}$	Yes	0
2	$\text{Ni}(\text{OAc})_2 \cdot 4\text{H}_2\text{O}$	No	0
3	$\text{Cu}(\text{OAc})_2$	Yes	0
4	$\text{Cu}(\text{OAc})_2$	No	0
5	PdCl_2	Yes	5
6	PdCl_2	No	33

Reactions were performed on a 1 mmol scale. Conversions determined by analysis of the ^1H NMR spectra of the crude reaction mixtures using 1,4-dimethoxybenzene as an internal NMR standard.

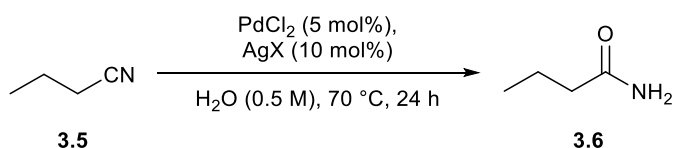
In previous work, the Williams group successfully used silver salts to generate a more active zirconium species *via* abstraction of chlorides from Cp₂ZrCl₂ (Scheme 3.7).²¹⁸ It was thought that this irreversible process, driven by precipitation of the highly insoluble silver chloride by-product as well as the high halophilicity of silver, could be used to potentially afford a more active palladium species.



Scheme 3.7. Generation of a more active zirconium species, *via* silver promoted halide abstraction, as developed by Williams *et al.*

A selection of four silver salts, containing anions with both low and high basicity, was investigated (Table 3.12). PdCl₂ (5 mol%) and the silver salt (10 mol%) were stirred in water for 30 minutes to preform the catalyst before the model nitrile was introduced and the reaction heated at 70 °C for 24 hours. In comparison to the background reaction without a silver salt present, the use of AgI and Ag(BPh)₄ was shown to inhibit catalytic activity. On the other hand, ¹H NMR analysis revealed that the addition of Ag(NO₃)₃ and Ag(CF₃COO) to the reaction resulted in an increase in conversion into primary amide **3.6**. However, despite this, none of the PdCl₂/Ag salt combinations rivalled the catalytic efficiency of Pd(OAc)₂/bipy.

Table 3.12. Silver salt screen.



Entry	Silver salt	Conversion into 3.6 (%)
1	-	33
2	Ag(NO ₃) ₃	56
3	AgI	9
4	Ag(CF ₃ COO)	54
5	Ag(BPh) ₄	16

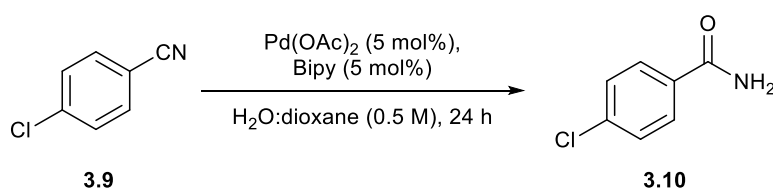
Reactions were performed on a 1 mmol scale. Conversions determined by analysis of the ¹H NMR spectra of the crude reaction mixtures using 1,4-dimethoxybenzene as an internal NMR standard.

With optimisation seemingly complete, we then started to apply the model reaction conditions, detailed in Scheme 3.6, to a range of nitriles. However, during preliminary

investigations into the substrate scope it was noticed that some substrates, particularly aromatic nitriles, were insoluble in water and therefore a co-solvent screen was required. Aromatic nitriles are soluble in alcohols and ethers; however, as Pd(OAc)₂ decomposes upon heating in the presence of alcohols, it was decided that ethers would be investigated as a potential co-solvent.²¹⁹

4-Chlorobenzonitrile (**3.9**) was chosen as the model substrate and experiments were conducted using the reaction conditions outlined in Scheme 3.6, except with either THF or dioxane as a co-solvent. We found that, in contrast to the dioxane-based reactions, when THF was employed as the co-solvent two distinct layers formed. As a result, we decided that dioxane was the most suitable co-solvent and were pleased to find that a 7:3 ratio of H₂O:dioxane afforded quantitative conversion into primary amide **3.10** (Table 3.13, entry 4). This therefore gave a second solvent system (**B**) to go alongside our original reaction medium of just water (**A**). It was also confirmed that when using solvent system **B**, bipy was still required in order to achieve efficient hydration (Table 3.13, entry 5), whilst lower temperatures resulted in decreased conversions (Table 3.13, entry 6).

Table 3.13. Dioxane co-solvent screen.



Entry	H ₂ O:Dioxane	Temperature (°C)	Conversion into 3.10 (%)
1	10:0	70	76
2	9:1	70	87
3	8:2	70	99
4	7:3	70	100
5 ^a	7:3	70	9
6	7:3	60	97

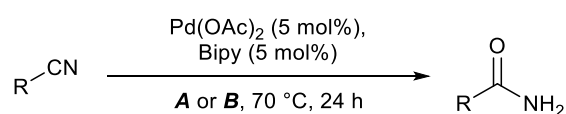
Reactions were performed on a 1 mmol scale. Conversions determined by analysis of the ¹H NMR spectra of the crude reaction mixtures using 1,4-dimethoxybenzene as an internal NMR standard. ^a Reaction performed without bipy.

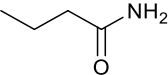
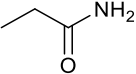
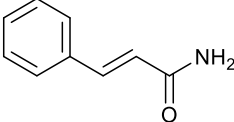
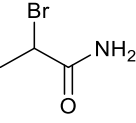
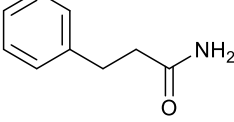
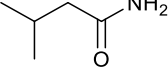
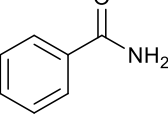
3.6. Substrate Scope

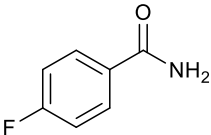
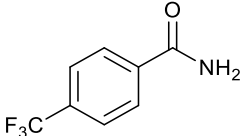
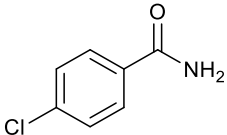
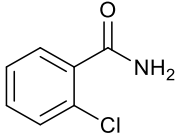
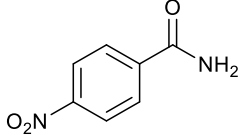
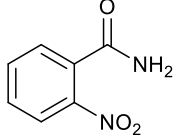
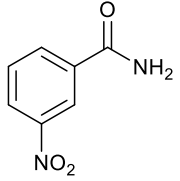
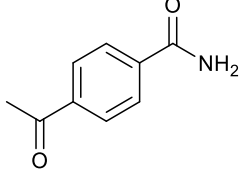
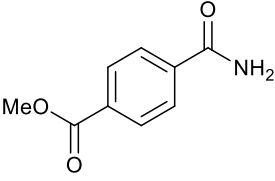
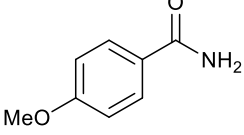
3.6.1. Successful Substrates

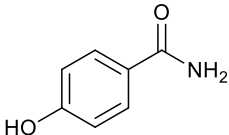
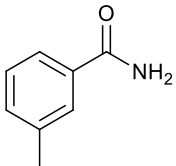
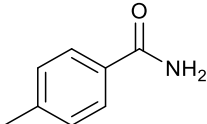
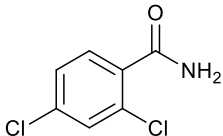
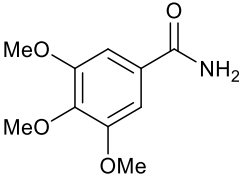
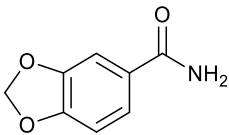
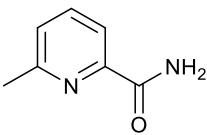
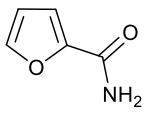
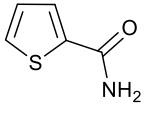
A comprehensive substrate scope was subsequently performed, employing solvent system **A** for substrates that were soluble in water and solvent system **B** for those that proved insoluble (Table 3.14). Two distinct purification procedures then afforded the final amide products in yields close to the percentage conversion. Reactions which had gone to completion or that contained a volatile nitrile were purified using a silica plug to remove the catalyst, whereas for more challenging purifications silica column chromatography was employed (eluting with DCM/MeOH).

Table 3.14. Scope of the hydration of nitriles.



Entry	Product	A: Conversion (%)	B: Conversion (%)	
1		3.6	100 (97)	-
2		3.11	91 (88)	-
3		3.12	77	96 (93)
4		3.13	87 (85)	-
5		3.14	97 (91)	-
6		3.15	80 (75)	-
7		3.16	100 (97)	-

8		3.17	91 (90)	-
9		3.18	96 (95)	-
10		3.10	76 (71)	100 (98)
11		3.19	41	73 (71)
12		3.20	76	100 (98)
13		3.21	86	100 (98)
14		3.22	84	100 (98)
15		3.23	100 (98)	100
16		3.24	80	100 (95)
17		3.4	80 (76)	83

18		3.25	93 (85)	94
19		3.26	82 (77)	-
20		3.27	69	100 (95)
21		3.28	47	88 (84)
22		3.29	19	100 (96)
23		3.30	97 (93)	97
24		3.31	80	88 (84)
25		3.32	100 (96)	-
26		3.33	100 (98)	-

Reactions were performed on a 1 mmol scale. Conversions determined by analysis of the ^1H NMR spectra of the crude reaction mixtures using 1,4-dimethoxybenzene as an internal NMR standard, where necessary. Isolated yields are shown in parentheses. Solvent system **A**: H_2O (0.5 M). Solvent system **B**: H_2O /dioxane (7:3, 0.5 M).

Aliphatic nitriles were transformed into their corresponding primary amide products in excellent yield, including the vinylic amide **3.12** (Table 3.14, entries 1-6). Pleasingly, primary amide **3.13** was afforded in excellent yield with no by-products observed from palladium insertion into the C-Br bond (Table 3.14, entry 4).

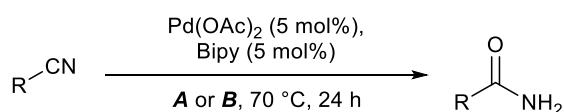
Electron-withdrawing substituents in the *ortho*, *meta* and *para* positions of benzonitrile were also well tolerated by the reaction conditions, including acetyl (**3.23**), ester (**3.24**), nitro (**3.20-3.22**), halogenic (**3.10**, **3.17** and **3.19**) and trifluoromethyl (**3.18**) groups (Table 3.14, entries 8-16). Benzonitrile substrates containing electron-donating groups in the *meta* and *para* positions, such as methoxy (**3.4**), hydroxyl (**3.25**) and methyl (**3.26** and **3.27**) moieties, were also converted into their primary amide products in good to excellent yield (Table 3.14, entries 17-20).

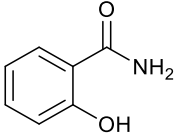
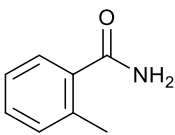
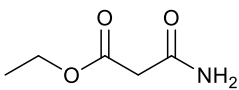
In addition, we were pleased to observe high conversions when di- (**3.28**) and tri-substituted (**3.29**) benzonitriles were subjected to the methodology, with a substantial increase in efficiency observed when employing solvent system **B** instead of solvent system **A** (Table 3.14, entries 21 and 22). The heteroaromatic amide products **3.31**, **3.32** and **3.33** were also synthesised in excellent yield from their corresponding nitriles (Table 3.14, entries 24-26).

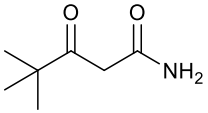
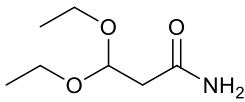
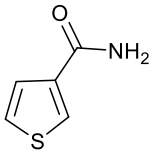
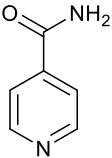
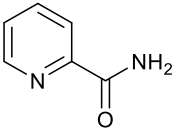
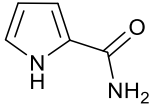
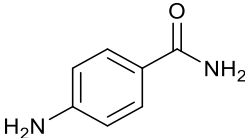
3.6.2. Less Successful Substrates

However, although a large variety of nitriles were successfully converted into their primary amide products under reaction conditions **A** and **B**, some substrates proved less successful (Table 3.15).

Table 3.15. Less successful substrates in the hydration of nitriles.



Entry	Product	A: Conversion (%)	B: Conversion (%)	
1		3.34	9	22
2		3.35	26	47
3		3.36	48	49

4		3.37	7	8
5		3.38	32	-
6		3.39	43	-
7		3.40	22	23
8		3.41	11	11
9		3.42	0	0
10		3.43	-	20

Reactions were performed on a 1 mmol scale. Conversions determined by analysis of the ^1H NMR spectra of the crude reaction mixtures using 1,4-dimethoxybenzene as an internal NMR standard, where necessary. Solvent system **A**: H_2O (0.5 M). Solvent system **B**: H_2O /dioxane (7:3, 0.5 M).

For example, electron-donating substituents, such as hydroxyl (**3.34**) and methyl (**3.35**) groups, in the *ortho* position of benzonitrile were poorly tolerated by both sets of reaction conditions (Table 3.15, entries 1 and 2).

Furthermore, amides **3.36**, **3.37** and **3.38** were also afforded in decreased conversions (Table 3.15, entries 3-5). These three products contain an oxygen δ to the amide oxygen and in the cases of **3.36** and **3.37** it belongs to a carbonyl group. We hypothesised that this configuration was the reason for the poor conversions observed. It was noticed that coordination of these products to palladium formed a similar structure to $\text{Pd}(\text{acac})_2$ (**3.44**). This similarity is shown in Figure 3.3, in which amide **3.37** is used as an example to form complex **3.45**. As detailed during our initial palladium complex screen, the use of $\text{Pd}(\text{acac})_2$ as the catalyst yielded no

amide product, compared to the 73% conversion observed for Pd(OAc)₂ (Table 3.5). Therefore, we postulated the following:

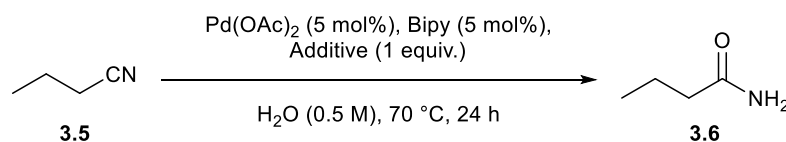
1. Small amounts of **3.36**, **3.37** and **3.38** formed at the beginning of the reaction.
2. These products then coordinated to the palladium catalyst.
3. This consequently inhibited the hydration reaction thereafter, in a similar manner to Pd(acac)₂.



Figure 3.3. Structures of Pd(acac)₂ (**3.44**) and the proposed palladium-**3.37** complex (**3.45**).

Although a variety of heteroaromatic nitriles were efficiently hydrated (Table 3.14, entries 24-26), we found a number of others were transformed less successfully (Table 3.15, entries 6-9). *N*-Heteroaromatic nitriles proved particularly difficult to hydrate, yielding low conversions in every case (Table 3.15, entries 7-9). Similarly, 4-aminobenzonitrile was incompatible with the methodology (Table 3.15, entry 10). We hypothesised that this was likely a result of the substrate's nitrogen competing with the nitrile for coordination to the palladium. This was strengthened by two studies in which the presence of stoichiometric amounts of pyrrole and pyridine in our model reaction was found to completely inhibit formation of primary amide **3.6** (Table 3.16).

Table 3.16. Investigations into competing *N*-coordination.

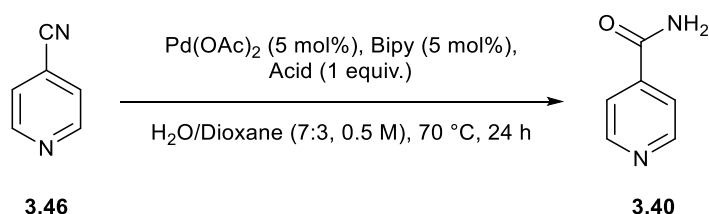


Entry	Additive (1 equiv.)	Conversion into 3.6 (%)
1	-	100
2	Pyridine	0
3	Pyrrole	0

Reactions were performed on a 1 mmol scale. Conversions determined by analysis of the ¹H NMR spectra of the crude reaction mixtures using 1,4-dimethoxybenzene as an internal NMR standard.

Furthermore, attempts to adapt the methodology in order to successfully hydrate these nitrogen-containing substrates were unsuccessful. It was thought that the addition of one equivalent of acid to the reaction would protonate the nitrogen, thus blocking its coordination to the palladium and promoting the hydration of these substrates. Reactions were performed using HCl and AcOH as acids and 4-pyridinecarbonitrile (**3.46**) as the model substrate (Table 3.17). In all cases, however, the introduction of acid was found to inhibit hydration of nitrile **3.46**, compared with the background reaction (Table 3.17, entries 1, 2 and 4). Identical results were also obtained when the catalyst was preformed prior to addition of the acid and nitrile (Table 3.17, entries 3 and 5). However, as previously shown, increased steric bulk around the competing nitrogen allowed efficient hydration of the nitrile (Table 3.14, entry 24).

Table 3.17. Attempts to promote the hydration of **3.46** by employing acid in the reaction.



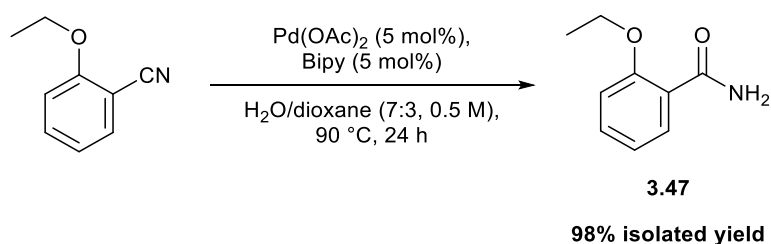
Entry	Acid (1 equiv.)	Catalyst preformed?	Conversion into 3.40 (%)
1	-	No	23
2	AcOH	No	8
3	AcOH	Yes	8
4	HCl ^a	No	0
5	HCl ^a	Yes	0

Reactions were performed on a 1 mmol scale. Conversions determined by analysis of the ¹H NMR spectra of the crude reaction mixtures using 1,4-dimethoxybenzene as an internal NMR standard. ^a 32% w/w HCl employed.

3.6.3. Pharmaceutical Applicability and Large Scale Reaction

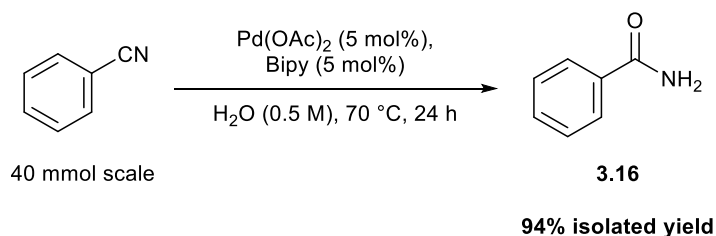
To further increase the impact of the methodology, we wished to illustrate its pharmaceutical applicability. Although electron-donating groups in the *ortho* position hinder the efficiency of the hydration reaction (Table 3.15, entries 1 and 2), we showed that increased temperature (90 °C) could drive the reaction to quantitative conversion using solvent system **B** (Scheme 3.8). This enabled the synthesis of ethenzamide (**3.47**), a common analgesic and anti-

inflammatory drug, in excellent yield (98%). In contrast, 68% conversion into **3.47** was achieved at 70 °C.



Scheme 3.8. Synthesis of ethenzamide, **3.47**.

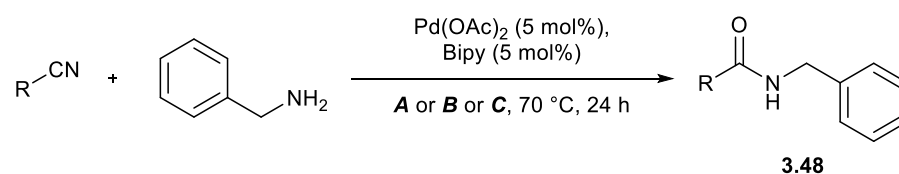
In addition, the scalability of the methodology was also verified by performing the hydration of benzonitrile on a 40 mmol scale. Using solvent system **A**, the reaction mixture was stirred at 70 °C for 24 hours, before purification by silica plug afforded primary amide **3.16** in 94% (4.56 g) isolated yield.



Scheme 3.9. Scaled-up hydration of benzonitrile to afford **3.16**.

3.7. Formation of Secondary Amides

The formation of secondary and tertiary amides through the coupling of nitriles and amines, in the presence of water, was also investigated. The coupling of butyronitrile or benzonitrile with benzylamine was subjected to the previously outlined methodology. The reactions were performed using solvent systems **A** and **B**, whilst a third solvent system, toluene (1 M) with 4 equivalents of water (**C**), was also trialled (Table 3.18). Unfortunately, the crude ^1H NMR spectra revealed limited conversion into secondary amide **3.48** for all reactions. Upon closer inspection of the spectra, we also noticed that no primary amide product had formed from hydration of the nitrile. We postulated that this was, once again, a result of competition between the nitrile and amine for coordination to the palladium catalyst.

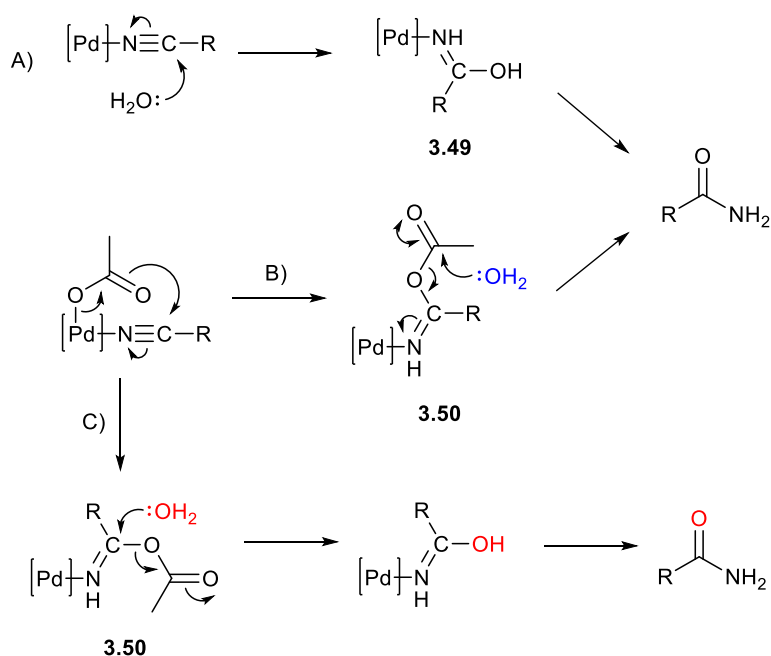
Table 3.18. Attempted formation of secondary amides.

Entry	Nitrile	Solvent system	Conversion into 3.48 (%)
1	Butyronitrile	A	7
2	Butyronitrile	B	6
3	Butyronitrile	C	2
4 ^a	Butyronitrile	C	3
5	Benzonitrile	A	4

Reactions were performed on a 1 mmol scale. Conversions determined by analysis of the ¹H NMR spectra of the crude reaction mixtures using 1,4-dimethoxybenzene as an internal NMR standard. Solvent system **A**: H₂O (0.5 M). Solvent system **B**: H₂O/dioxane (7:3, 0.5 M). Solvent system **C**: Toluene (1 M) with 4 equivalents of H₂O. ^a 2 equivalents of butyronitrile were employed in the reaction.

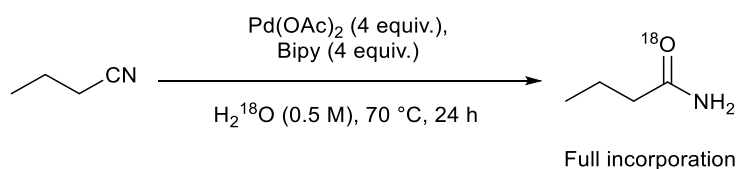
3.8. Mechanistic Investigations

Finally, we hypothesised that the reaction mechanism could proceed through three plausible routes, all of which begin with coordination of the nitrile to the palladium centre, as illustrated in Scheme 3.10. This generally accepted step increases the electrophilicity of the nitrile carbon, thus increasing its susceptibility to nucleophilic attack.⁹² From here, one possible route involves direct attack by water followed by the rearrangement of iminolate species **3.49** to afford the desired amide (pathway A). Alternatively, the reaction may proceed *via* intermediate **3.50**, formed from the internal delivery of oxygen by the acetate ligand of the metal catalyst. Intermediate **3.50** can then undergo nucleophilic attack by water through either pathway B or pathway C *en route* to the primary amide product.



Scheme 3.10. Plausible mechanisms for the Pd(OAc)₂-catalysed hydration of nitriles.

In order to elucidate information on the reaction mechanism, a H₂¹⁸O labelling study was performed (Scheme 3.11). This study enabled us to determine whether the water oxygen is incorporated into the final product and thus rule out some of the potential pathways. Employing H₂¹⁸O and excess Pd(OAc)₂ in the model reaction, full incorporation (97% ¹⁸O) of the ¹⁸O label was observed by mass spectrometry (Figure 3.4). As a result of this, pathway B can be discounted from the plausible mechanisms as a lower percentage incorporation of ¹⁸O would be expected if the reaction proceeded *via* this route.



Scheme 3.11. Hydration of butyronitrile using H₂¹⁸O.

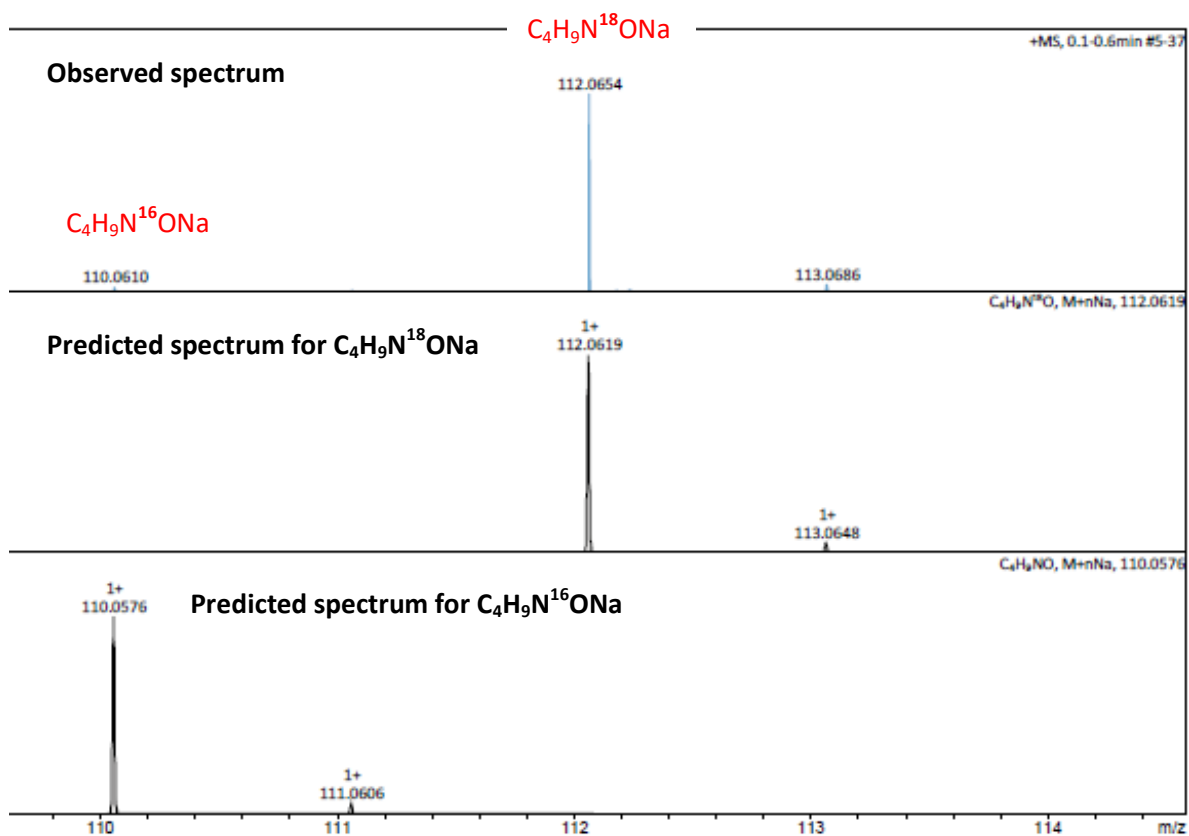


Figure 3.4. Observed and predicted mass spectrometry data from the H_2^{18}O labelling study.

Although this study doesn't distinguish between pathways A or C, the increased efficiency observed when employing $\text{Pd}(\text{OAc})_2$ compared with PdCl_2 (Table 3.5, entries 1 and 2; Table 3.10, entry 3; Table 3.11, entry 5) may suggest that the acetate ligands participate in the reaction mechanism. As a result, this would lead us to believe pathway C is the most likely route, however this theory is unconfirmed. Further studies are to be performed in the future to elucidate the reaction mechanism.

3.9. Conclusions

In conclusion, a selective methodology for the hydration of organonitriles in water has been developed. *In situ* formation of a $\text{Pd}(\text{OAc})_2\text{bipy}$ complex efficiently catalyses the transformation of a wide array of aliphatic and aromatic nitriles into their primary amide products in excellent yields. This methodology has the potential to offer a simple and relatively mild alternative to existing hydration protocols, without the need for hydration-promoting additives such as oximes and hydroxylamines.

The reported methodology has been fully optimised, with two solvent systems (**A** and **B**) developed for nitriles that are soluble and insoluble in water. A broad range of nitriles were compatible with the reaction conditions, including aliphatic substrates and benzonitriles that contained electron-withdrawing groups on the ring. Electron-donating benzonitriles were also well tolerated, with *para*- and *meta*-substituted substrates converted in good to excellent yield. However, a small number of substrates were transformed less efficiently, including *N*-heteroaromatic nitriles and other nitrogen-containing compounds.

The synthesis of ethenzamide demonstrated the pharmaceutical applicability of the methodology, whilst the reaction was also successfully performed on a large scale. Finally, ¹⁸O labelling studies were employed in order to develop a plausible reaction mechanism for the methodology.

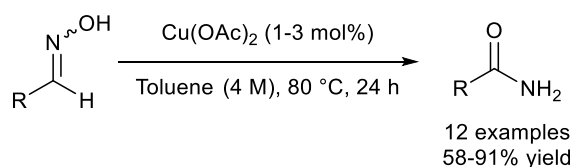
Results and Discussion III

Amides from Aldoximes

4. Results and Discussion III – Amides from Aldoximes

4.1. Previous Work in the Group

Over the last decade the group has conducted extensive research into the rearrangement of aldoximes into primary amides. A range of methods have been developed using a variety of metal catalysts, including indium,¹⁷³ zinc,¹⁷³ ruthenium¹⁴⁵ and iridium¹⁶⁹ complexes. However, one of the most sustainable and inexpensive approaches published by the group involves the use of $\text{Cu}(\text{OAc})_2$ (Scheme 4.1).¹⁷²

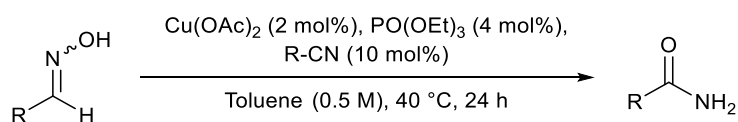


Scheme 4.1. $\text{Cu}(\text{OAc})_2$ -catalysed rearrangement of aldoximes developed by Williams *et al.*

However, although this $\text{Cu}(\text{OAc})_2$ -based approach represented an improvement on previous aldoxime to primary amide methodologies, a relatively high temperature was still required for the rearrangement reaction to proceed. As previously outlined in Section 1.2.3.4, the group investigated the reaction mechanism in the hope that further information on the rearrangement process would allow the temperature of the method to be lowered.⁵¹

The group's results led to the proposal of a second mechanism in which another equivalent of aldoxime attacks the metal-coordinated nitrile (Scheme 1.64). In addition, further studies showed that the addition of a nitrile to the reaction increased the rate of the rearrangement reaction. However, unless the equivalent nitrile was employed, this resulted in the production of an undesired primary amide product derived from the added nitrile.

In order to avoid the formation of a mixture of primary amide products, and therefore a challenging purification procedure, Williams *et al.* employed nitrile additives that corresponded to the starting aldoxime.²⁰⁹ Employing $\text{Cu}(\text{OAc})_2$ (2 mol%), triethyl phosphate (4 mol%) and the corresponding nitrile additive (10 mol%) in toluene, a broad variety of aldoximes were successfully converted into their primary amide products in good to excellent yield at 40 °C in 24 hours (Scheme 4.2).



Scheme 4.2. Aldoxime rearrangement employing a nitrile additive, as developed by Williams *et al.*

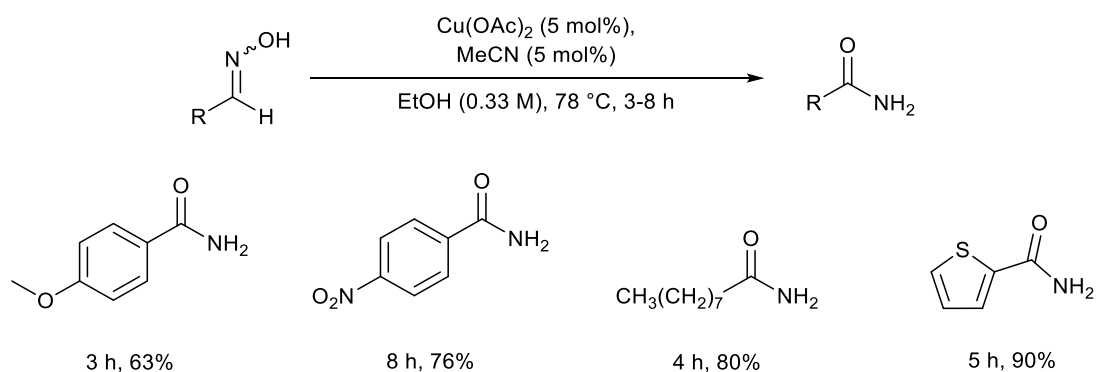
4.2. Aims and Objectives

As previously described, the group demonstrated that addition of a nitrile additive allows the reaction to be performed at a significantly reduced temperature (40 °C). However, the need to purchase or synthesise the corresponding nitrile for each aldoxime rearrangement, which also reduces the maximum possible conversion into the desired amide product, is a significant drawback to the methodology. Instead, we wanted to develop a more convenient and useful approach for the conversion of aldoximes into primary amides at low temperature using the group's existing method as a starting point.

4.3. Optimisation

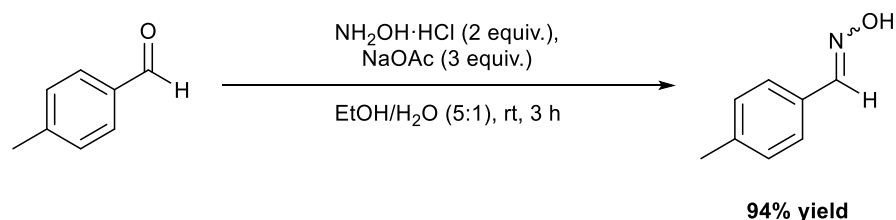
It was initially decided to investigate the use of acetonitrile as the nitrile additive in the rearrangement reaction. Although this would still generate a mixture of amide products, we hypothesised that the acetamide by-product would have a sufficiently different R_f value compared with the majority of the desired amide products, thus making purification by silica column chromatography less challenging.

It was noticed that a similar approach had been published by Ma and Lu in 2016 (Scheme 4.3).²²⁰ The duo employed 5 mol% of both Cu(OAc)_2 and acetonitrile in ethanol to convert a selection of aldoximes into their corresponding primary amide products at 78 °C. The use of ethanol as the solvent was interesting as the Williams group had previously found toluene to be the most suitable solvent for the rearrangement process. As a result, we decided to investigate whether any advantage was gained by using toluene instead of ethanol, both in the presence and absence of acetonitrile, in Ma and Lu's approach.



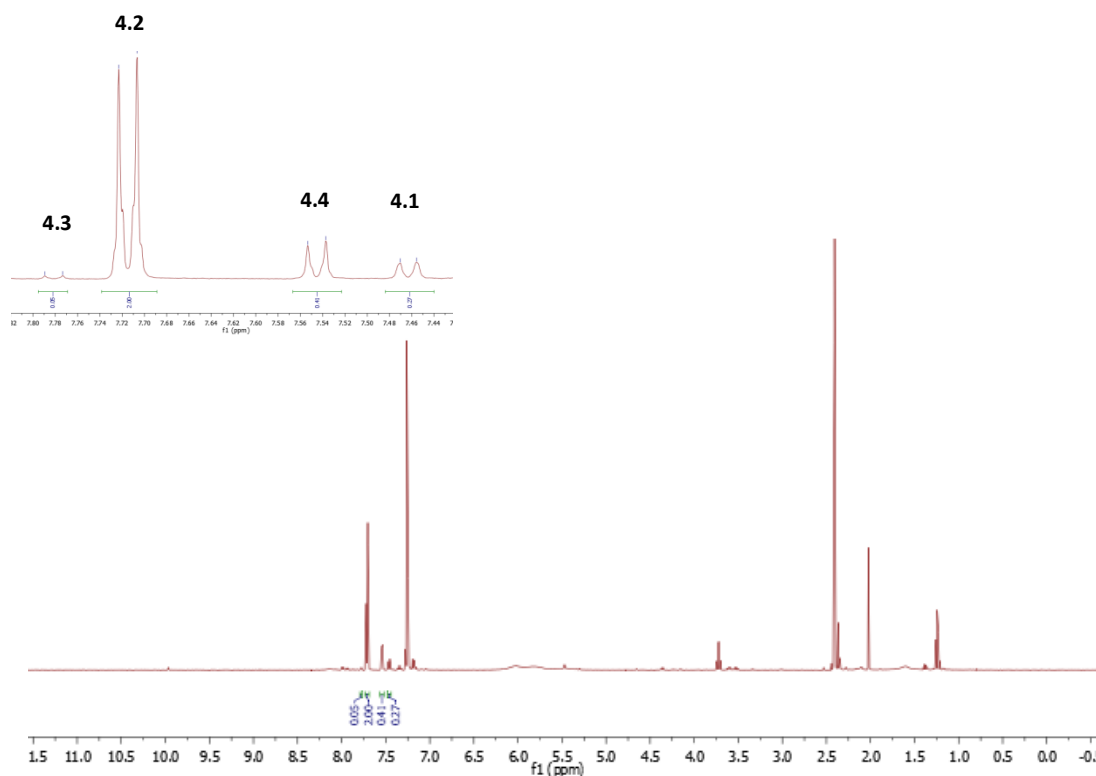
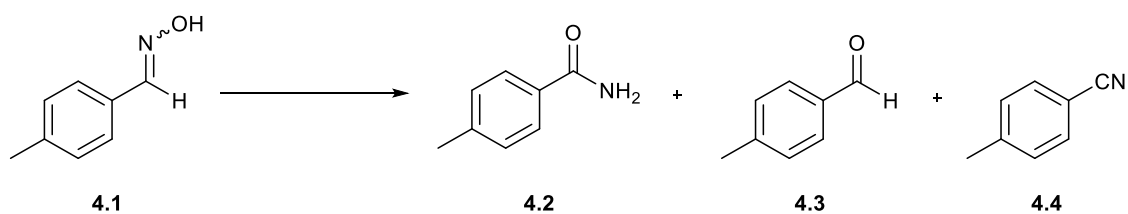
Scheme 4.3. Use of acetonitrile as an additive in the rearrangement reaction, as reported by Ma and Lu, including selected products.

4-Methylbenzaldehyde was chosen as the model substrate for the reaction screening due to ease of spectral determination of conversion into the desired product. The model aldehyde was synthesised using a simple literature method previously employed by the group (Scheme 4.4).⁶



Scheme 4.4. Literature method for the synthesis of 4-methylbenzaldehyde oxime.

Percentage conversion into product **4.2** and by-products **4.3** and **4.4** was determined by analysis of the relative integrals of the doublet peaks corresponding to the aromatic protons in primary amide product **4.2** (7.71 ppm), aldehyde **4.3** (7.78 ppm), nitrile **4.4** (7.55 ppm) and aldoxime starting material **4.1** (7.47 ppm) in the crude ¹H NMR spectra (Scheme 4.5).

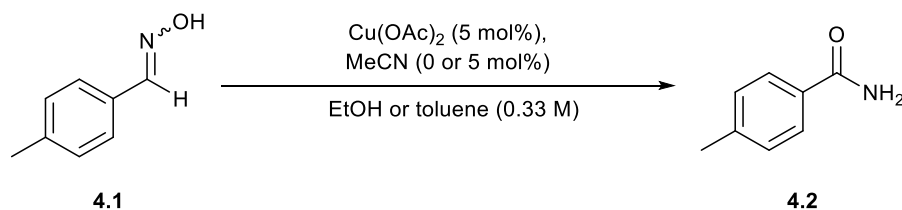


Scheme 4.5. An example of the ¹H NMR spectrum used to determine the relative proportion of **4.1**, **4.2**, **4.3** and **4.4** at the end of the reaction, showing aromatic protons in the starting material (**4.1**), product (**4.2**) and by-products (**4.3** and **4.4**).

Two sets of reactions were performed using Ma and Lu's methodology – one set at 78 °C for 30 minutes and the other at 40 °C for 16 hours (Table 4.1). In both cases toluene was found to promote the aldoxime rearrangement reaction more efficiently than ethanol. For example, when the reaction was performed at 40 °C with just Cu(OAc)₂ present, the use of ethanol as the solvent resulted in 22% conversion into primary amide **4.2** (Table 4.1, entry 5). In comparison, when toluene was employed in the reaction, the conversion increased to 46% (Table 4.1, entry 6). A similar trend was also observed in the reactions employing acetonitrile as an additive – 38% conversion for ethanol and 52% conversion for toluene (Table 4.1, entries 7 and 8). It was also demonstrated that an increase in the reaction concentration from 0.33 M to 1 M afforded higher conversions into primary amide **4.2** (Table 4.1, entries 9 and

10). As a result, we decided to employ a 1 M reaction concentration in subsequent screening reactions.

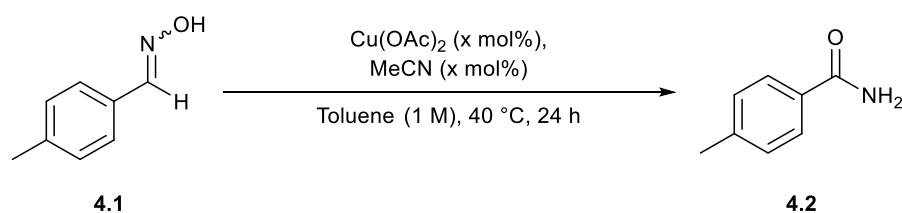
Table 4.1. Comparison between ethanol and toluene as solvents in the aldoxime rearrangement reaction.



Entry	Solvent	MeCN loading (mol%)	Temp. (°C)	Time (h)	Conversion from 4.1 (%)	Conversion into 4.2 (%)
1	Ethanol	-	78	0.5	7	7
2	Toluene	-	78	0.5	57	32
3	Ethanol	5	78	0.5	37	25
4	Toluene	5	78	0.5	62	38
5	Ethanol	-	40	16	28	22
6	Toluene	-	40	16	58	46
7	Ethanol	5	40	16	45	38
8	Toluene	5	40	16	69	52
9 ^a	Ethanol	5	40	16	72	65
10 ^a	Toluene	5	40	16	93	78

Reactions were performed on a 1 mmol scale. Conversions determined by analysis of the ¹H NMR spectra of the crude reaction mixtures. Aldehyde **4.3** and nitrile **4.4** by-products make up the difference between the two tabulated conversions. ^a 1 M concentration employed.

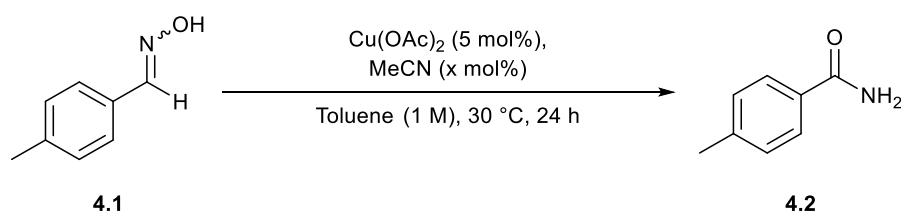
The effect of both Cu(OAc)₂ and MeCN loading on the rearrangement reaction at 40 °C in toluene was then investigated. Employing 2 mol% Cu(OAc)₂, we revealed that increased MeCN loading afforded elevated levels of aldoxime consumption and higher conversions into primary amide **4.2** (Table 4.2, entries 1-4). In addition, ¹H NMR analysis revealed that use of 5 mol% Cu(OAc)₂ in the presence of MeCN resulted in quantitative conversion from aldoxime **4.1**, with 88% conversion into the desired amide product achieved when 5 mol% of the nitrile additive was employed (Table 4.2, entries 5-8). In addition, higher loadings of Cu(OAc)₂ (10 mol%) resulted in an increase in the production of nitrile and aldehyde by-products, leading to reduced conversions into primary amide **4.2** compared with those achieved using 5 mol% Cu(OAc)₂ (Table 4.2, entries 9-12).

Table 4.2. Effect of Cu(OAc)₂ and MeCN loading on the aldoxime rearrangement reaction at 40 °C.

Entry	Cu(OAc) ₂ loading (mol%)	MeCN loading (mol%)	Conversion from 4.1 (%)	Conversion into 4.2 (%)
1	2	-	75	64
2	2	2	82	73
3	2	5	92	82
4	2	10	97	83
5	5	-	94	82
6	5	2	100	87
7	5	5	100	88
8	5	10	100	86
9	10	-	98	74
10	10	2	100	77
11	10	5	100	79
12	10	10	100	75

Reactions were performed on a 1 mmol scale. Conversions determined by analysis of the ¹H NMR spectra of the crude reaction mixtures. Aldehyde **4.3** and nitrile **4.4** by-products make up the difference between the two tabulated conversions.

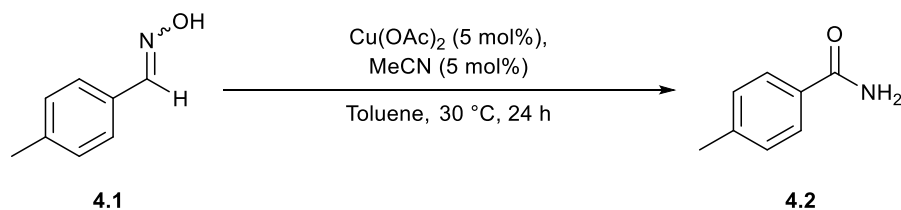
As our aim was to perform the aldoxime rearrangement at low temperature, we decided to explore the reaction at 30 °C (Table 4.3). Employing the optimum Cu(OAc)₂ catalyst loading of 5 mol%, we showed that 71% conversion into primary amide **4.2** could be achieved using an equimolar amount of MeCN (Table 4.3, entry 3).

Table 4.3. MeCN loading screen at 30 °C.

Entry	MeCN loading (mol%)	Conversion from 4.1 (%)	Conversion into 4.2 (%)
1	-	61	50
2	2	63	51
3	5	82	71
4	10	85	68

Reactions were performed on a 1 mmol scale. Conversions determined by analysis of the ^1H NMR spectra of the crude reaction mixtures. Aldehyde **4.3** and nitrile **4.4** by-products make up the difference between the two tabulated conversions.

A concentration screen was subsequently performed using the optimum conditions at 30 °C (Table 4.4). Analysis of the crude ^1H NMR spectra showed that concentrations both above and below 1 M afforded reduced conversion from aldoxime **4.1** into primary amide **4.2**.

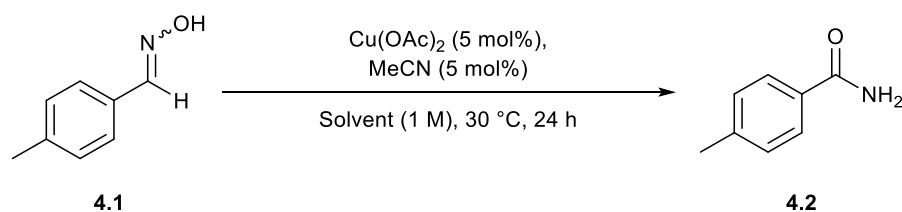
Table 4.4. Concentration screen for the aldoxime rearrangement reaction.

Entry	Concentration (M)	Conversion from 4.1 (%)	Conversion into 4.2 (%)
1	0.25	48	38
2	0.5	71	55
3	0.75	79	66
4	1	82	71
5	1.5	78	63
6	2	76	62
7	4	68	53

Reactions were performed on a 1 mmol scale. Conversions determined by analysis of the ^1H NMR spectra of the crude reaction mixtures. Aldehyde **4.3** and nitrile **4.4** by-products make up the difference between the two tabulated conversions.

Following this, the reaction medium was investigated to confirm that toluene is the superior solvent under these conditions (Table 4.5). A broad spectrum of polar/apolar and protic/aprotic solvents were screened; however, analysis of the crude ^1H NMR spectrum revealed a reduction in conversion for all reactions compared to when the rearrangement was performed in toluene.

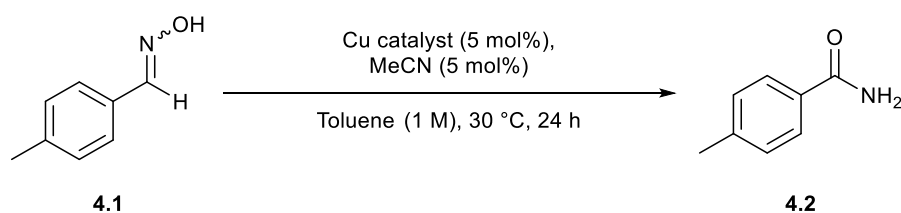
Table 4.5. Solvent screen for the aldoxime rearrangement reaction.



Entry	Solvent	Conversion from 4.1 (%)	Conversion into 4.2 (%)
1	Toluene	82	71
2	Water	7	7
3	Heptane	44	33
4	Methanol	37	28
5	Ethyl acetate	25	20
6	Tetrahydrofuran	15	10
7	1,2-Dichloroethane	62	47
8	Diethyl ether	36	28
9	Acetone	17	13

Reactions were performed on a 1 mmol scale. Conversions determined by analysis of the ^1H NMR spectra of the crude reaction mixtures. Aldehyde **4.3** and nitrile **4.4** by-products make up the difference between the two tabulated conversions.

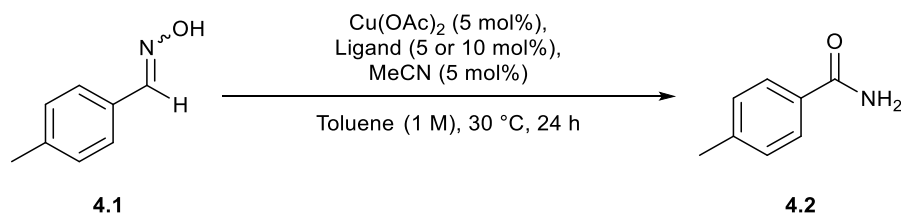
Although the group had previously identified Cu(OAc)_2 as the most suitable catalyst for the aldoxime rearrangement reaction, it was decided to screen a variety of different copper complexes under these new reaction conditions (Table 4.6). However, all of the alternative copper complexes proved extremely inefficient in promoting the rearrangement process, with zero or minimal conversion into primary amide **4.2** observed in each case. Interestingly, use of Cu(OTf)_2 as the catalyst led to high levels of conversion from aldoxime **4.1** into aldehyde **4.3** (52%) and nitrile **4.4** (32%) by-products (Table 4.6, entry 6).

Table 4.6. Copper catalyst screen for the aldoxime rearrangement reaction.

Entry	Cu catalyst	Conversion from 4.1 (%)	Conversion into 4.2 (%)
1	Cu(OAc) ₂	82	71
2	CuCl ₂	0	0
3	CuBr ₂	0	0
4	CuI	0	0
5	CuCO ₃ ·Cu(OH) ₂	0	0
6	Cu(OTf) ₂	93 ^a	9
7	Cu(NO ₃) ₂ ·3H ₂ O	19	3

Reactions were performed on a 1 mmol scale. Conversions determined by analysis of the ¹H NMR spectra of the crude reaction mixtures. Aldehyde **4.3** and nitrile **4.4** by-products make up the difference between the two tabulated conversions. ^a 52% aldehyde **4.3** and 32% nitrile **4.4** were observed in the final reaction mixture.

In order to increase the conversion into the desired primary amide product at 30 °C, the use of ligands in the reaction was explored. It was hoped that the addition of a ligand into the reaction mixture would afford a more active copper catalyst and thus increase the efficiency of the transformation. A selection of typical copper monodentate (10 mol%) and bidentate (5 mol%) ligands was investigated, including nitrogen- (Table 4.7, entries 2-6) and oxygen-based (Table 4.7, entries 6-8) ligands, phosphates (Table 4.7, entry 9) and phosphines (Table 4.7, entries 10 and 11).

Table 4.7. Effect of ligands on the aldoxime rearrangement reaction.

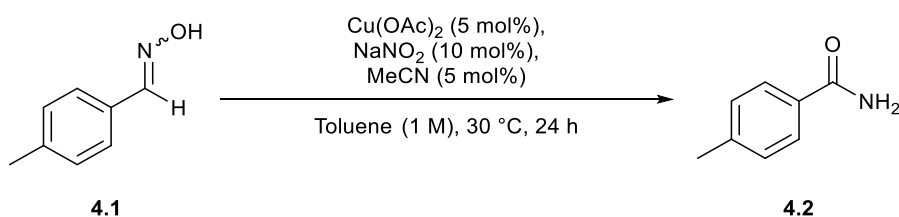
Entry	Ligand (mol%)	Conversion from 4.1 (%)	Conversion into 4.2 (%)
1	-	82	71
2	Pyridine (10)	69	55

3	2,2'-Bipyridine (5)	17	8
4	Ethylenediamine (5)	17	3
5	1,10-Phenanthroline (5)	20	11
6	NaNO ₂ (10)	100	91
7	H ₂ O (10)	82	66
8	1,2-Dihydroxybenzene (5)	25	12
9	P(O)OEt ₃ (10)	79	71
10	1,2-Bis(dicyclohexyl phosphino)ethane (5)	61	48
11	PPh ₃ (10)	29	13

Reactions were performed on a 1 mmol scale. Conversions determined by analysis of the ¹H NMR spectra of the crude reaction mixtures. Aldehyde **4.3** and nitrile **4.4** by-products make up the difference between the two tabulated conversions.

Interestingly, the use of bidentate nitrogen ligands resulted in a significant decrease in the formation of primary amide **4.2** (Table 4.7, entries 3-5), whilst the addition of pyridine to the reaction also inhibited the transformation (Table 4.7, entry 2). This is likely a result of competing nitrogen coordination, between the ligand and the aldoxime/nitrile species in the rearrangement process, to the copper centre. Moreover, the Williams *et al.* had previously employed PO(OEt)₃ as a ligand in their previous aldoxime rearrangement methodology; although analysis of the ¹H NMR spectra revealed that under the new reaction conditions this phosphate had no effect on the conversion observed (Table 4.7, entry 9). However, we were pleased to reveal that addition of NaNO₂ to the reaction mixture afforded quantitative consumption of aldoxime **4.1** and 91% conversion into primary amide **4.2** (Table 4.7, entry 6).

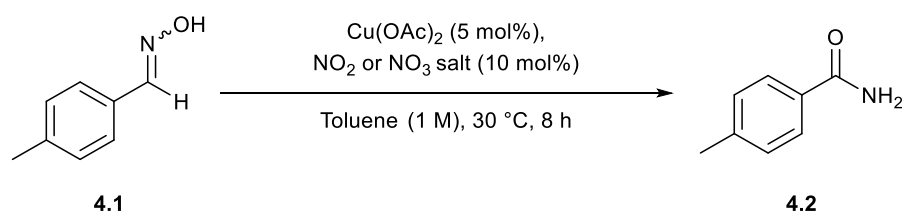
Even more satisfying was the observation that an equally high conversion (92%) into primary amide **4.2** could be achieved upon removing MeCN from the reaction (Table 4.8, entry 2). However, the efficiency of the transformation decreased significantly when the reaction was performed at 20 °C (Table 4.8, entry 3). We also showed that both Cu(OAc)₂ and NaNO₂ are required to achieve high conversion into primary amide **4.2**. Only 50% conversion into the desired primary amide product was observed when NaNO₂ was removed from the reaction (Table 4.8, entry 4), whilst no reaction occurred when the nitrite salt was employed on its own (Table 4.8, entry 5).

Table 4.8. Effect of Cu(OAc)₂, NaNO₂ and MeCN on the rearrangement reaction.

Entry	Cu(OAc) ₂	NaNO ₂	MeCN	Conversion from 4.1 (%)	Conversion into 4.2 (%)
1	✓	✓	✓	100	91
2	✓	✓	-	100	92
3 ^a	✓	✓	-	33	20
4	✓	-	-	61	50
5	-	✓	-	0	0
6	-	-	-	0	0

Reactions were performed on a 1 mmol scale. Conversions determined by analysis of the ¹H NMR spectra of the crude reaction mixtures. Aldehyde **4.3** and nitrile **4.4** by-products make up the difference between the two tabulated conversions. Ticks denote the presence of that reagent in the reaction. ^a Reaction performed at 20 °C.

Due to the success of NaNO₂ in promoting the rearrangement reaction, we subsequently decided to investigate the effect of other nitrite salts on the reaction (Table 4.9, entries 1-4). The reactions were performed for 8 hours to ensure quantitative conversion from aldoxime **4.1** was not achieved. Use of AgNO₂ resulted in comparable conversions to when NaNO₂ was employed in the reaction (76% and 75% into primary amide **4.2** respectively), whereas the addition of KNO₂ afforded decreased conversion (53%). Subsequently, another reaction was also performed employing sodium nitrate (NaNO₃) in order to investigate the importance of the nitrite ligand (Table 4.9, entry 5). Replacing NaNO₂ with NaNO₃ in the reaction led to the conversion into primary amide **4.2** decreasing below that of the background reaction (Table 4.9, entry 1). In addition, as well as the usual nitrile and aldehyde by-products produced by the rearrangement process, significant amounts of the corresponding carboxylic acid (7%) were also observed in this reaction upon ¹H NMR analysis.

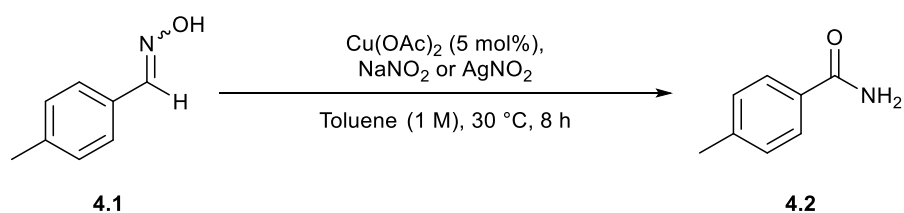
Table 4.9. Effect of nitrite and nitrate salts on the aldoxime rearrangement reaction.

Entry	NO ₂ or NO ₃ salt	Conversion from 4.1 (%)	Conversion into 4.2 (%)
1	-	26	16
2	NaNO ₂	88	75
3	KNO ₂	64	53
4	AgNO ₂	89	76
5	NaNO ₃	18	7 ^a

Reactions were performed on a 1 mmol scale. Conversions determined by analysis of the ¹H NMR spectra of the crude reaction mixtures. Aldehyde **4.3** and nitrile **4.4** by-products make up the difference between the two tabulated conversions. ^a 7% of the corresponding carboxylic acid was formed in addition to the nitrile and aldehyde by-products.

With NaNO₂ and AgNO₂ demonstrating similar activity in the aldoxime rearrangement reaction, a ligand loading screen was conducted using these two nitrite salts (Table 4.10). When an equimolar amount of Cu(OAc)₂ catalyst and NO₂ ligand were employed in the reaction, increased conversion into primary amide **4.2** was observed when using the silver salt (45%) compared with the sodium derivative (22%) (Table 4.10, entries 1 and 5). However, upon employing 10 mol% of NaNO₂/AgNO₂ (2 equivalents versus Cu(OAc)₂), both of the nitrite salts exhibited similar activity, resulting in conversions of 75% and 76% respectively (Table 4.10, entries 2 and 6). Higher additive loadings resulted in no significant increase in conversion into primary amide **4.2** for both NaNO₂ and AgNO₂ (Table 4.10, entries 3, 4, 7 and 8).

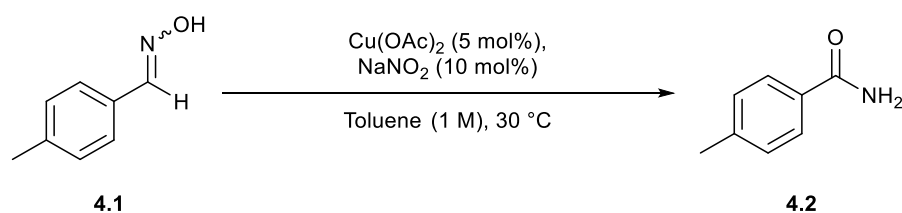
Table 4.10. Nitrite loading screen for the aldoxime rearrangement reaction.



Entry	NO_2 salt	NO_2 salt loading (mol%)	Conversion from 4.1 (%)	Conversion into 4.2 (%)
1	NaNO_2	5	31	22
2	NaNO_2	10	88	75
3	NaNO_2	20	92	77
4	NaNO_2	50	92	78
5	AgNO_2	5	53	45
6	AgNO_2	10	89	76
7	AgNO_2	20	93	78
8	AgNO_2	50	94	78

Reactions were performed on a 1 mmol scale. Conversions determined by analysis of the ^1H NMR spectra of the crude reaction mixtures. Aldehyde **4.3** and nitrile **4.4** by-products make up the difference between the two tabulated conversions.

Although 10 mol% of NaNO_2 and AgNO_2 both afforded similar conversions into primary amide **4.2**, it was decided that NaNO_2 would be used for the rearrangement reaction as it is 7 times cheaper per mole than the silver derivative (based on 25 grams of each reagent from Sigma Aldrich on 09/02/18). A time screen was conducted using our optimised reaction conditions to determine at which point aldoxime **4.1** is fully consumed (Table 4.11).

Table 4.11. Time screen for the aldoxime rearrangement reaction.

Entry	Time (h)	Conversion from 4.1 (%)	Conversion into 4.2 (%)
1	4	26	15
2	8	88	75
3	12	90	77
4	16	93	82
5	20	97	87
6	24	100	92
7 ^a	24	47	35

Reactions were performed on a 1 mmol scale. Conversions determined by analysis of the ^1H NMR spectra of the crude reaction mixtures. Aldehyde **4.3** and nitrile **4.4** by-products make up the difference between the two tabulated conversions. ^a Reaction performed in water (1 M).

^1H NMR analysis revealed that, as expected, a decrease in the percentage of aldoxime **4.1** directly correlates with an increase in the amount of primary amide **4.2** formed, whilst the low levels of nitrile **4.4** and aldehyde **4.3** remain roughly constant over time (Figure 4.1). The time screen clearly illustrated that 24 hours were required for quantitative conversion from aldoxime **4.1** to be achieved under our new reaction conditions. In addition, we also demonstrated at this point that use of water as the solvent afforded significantly reduced conversion into primary amide **4.2** (Table 4.11, entry 7). Meanwhile, the small percentage of nitrile **4.4** observed in the ^1H NMR spectra supports the previously proposed mechanism, in which the starting aldoxime is initially dehydrated to form the corresponding nitrile. Furthermore, reaction between the aldoxime and water released through the dehydration process accounts for the low amounts of aldehyde **4.3** present in the reaction mixture.

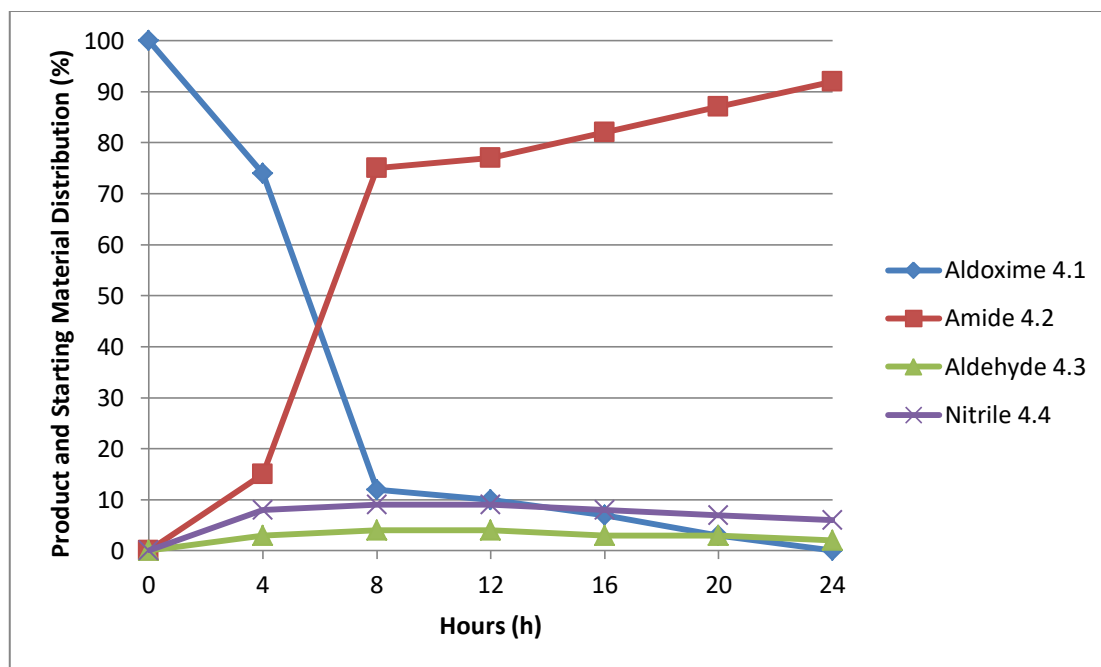
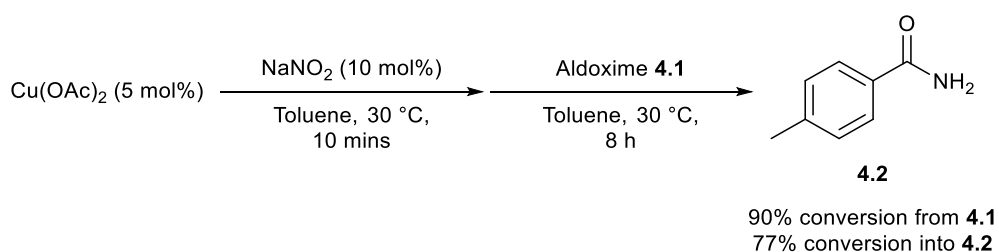


Figure 4.1. Product and starting material distribution as a function of time for the rearrangement of aldoxime **4.1**.

Although quantitative conversion from aldoxime **4.1** had been reached in 24 hours under the current reaction conditions, we decided to investigate the effect of preforming the active catalyst before addition of the oxime substrate. It was hoped that this approach would enable quantitative conversion from aldoxime **4.1** in a shorter reaction time. $\text{Cu}(\text{OAc})_2$, NaNO_2 and half of the toluene were added to the carousel tube and the reaction stirred at 30 °C for 10 minutes to form the active catalyst. Aldoxime **4.1** was then added followed by the other half of the toluene and the reaction mixture left for a further 8 hours at 30 °C (Scheme 4.6).



Scheme 4.6. Preformation of the active catalyst in the aldoxime rearrangement reaction.

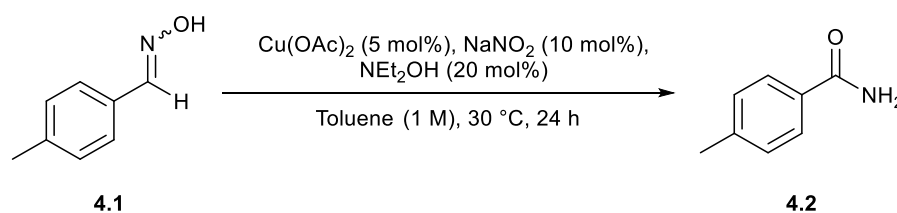
Unfortunately, however, analysis of the crude ^1H NMR spectrum revealed only a very minor improvement in the efficiency of the reaction. Preforming the active catalyst resulted in 90% conversion from aldoxime **4.1** and 77% conversion into primary amide **4.2**, compared with conversions of 88% and 75%, respectively, when the reagents were all added at the start of the reaction (Scheme 4.6; Table 4.11, entry 2). Therefore, taking into account the insignificant

difference in conversions, it was decided that the active catalyst would be formed *in situ*, as before, due to the more convenient nature of this approach.

In addition, as outlined in Section 3.1, the Williams group had previously developed a $\text{Cu}(\text{OAc})_2$ -catalysed protocol for the conversion of nitriles into primary amides at low temperature (Scheme 3.1). It was hoped that this method could be utilised in our aldoxime rearrangement methodology in order to convert the small amount of nitrile **4.4** formed in the reaction into the desired primary amide product. With $\text{Cu}(\text{OAc})_2$ and water already present under our reaction conditions, the only reagent needed to be introduced into the oxime rearrangement was NEt_2OH .

Two separate reactions were performed in which 20 mol% NEt_2OH (approximately 3 equivalents versus the 6% nitrile produced) was added at the start and the end of the reaction (Table 4.12). As expected, addition of the Lewis basic hydroxylamine at the start of the reaction inhibited the aldoxime rearrangement reaction (Table 4.12, entry 1). This is again likely due to coordination of the additive to the copper catalyst. Meanwhile, when NEt_2OH was added after 24 hours nitrile **4.4** remained unconverted after a further 2 hours of reaction time.

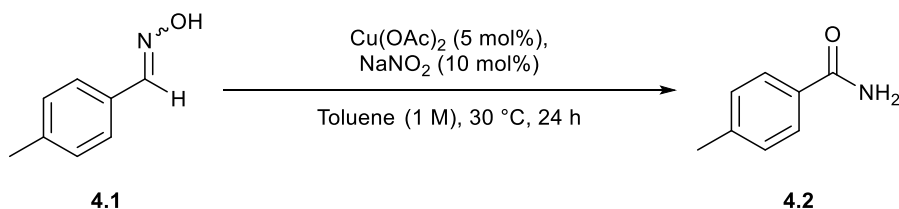
Table 4.12. Addition of NEt_2OH at the start and end of the aldoxime rearrangement reaction.



Entry	Time when NEt_2OH was added (h)	Conversion from 4.1 (%)	Conversion into 4.2 (%)
1	0	23	14
2 ^a	24	100	90

Reactions were performed on a 1 mmol scale. Conversions determined by analysis of the ^1H NMR spectra of the crude reaction mixtures. Aldehyde **4.3** and nitrile **4.4** by-products make up the difference between the two tabulated conversions. ^a Reaction left for a further 2 hours after addition of NEt_2OH .

Scheme 4.7 details the final fully optimised reaction conditions for our model substrate using a combination of $\text{Cu}(\text{OAc})_2$ (5 mol%) and NaNO_2 (10 mol%) in toluene at low temperature.



Scheme 4.7. Fully optimised reaction conditions for the rearrangement of aldoxime **4.1** at low temperature.

4.4. Substrate Scope

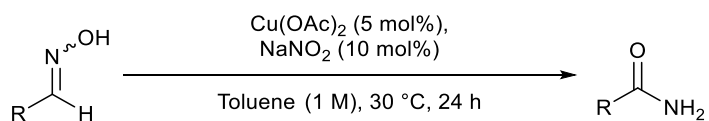
4.4.1. Successful Substrates

A variety of aldoximes were subjected to the fully optimised reaction conditions (Scheme 4.7). Aldoximes which were not available in the lab were synthesised using the method outlined in Scheme 4.4.⁶ QuadrasilTM TA was used to scavenge the copper catalyst and, following filtration, the crude primary amide products were purified by silica column chromatography (eluting with DCM/MeOH).

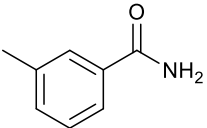
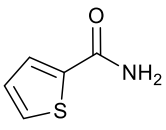
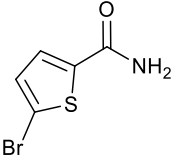
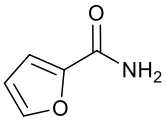
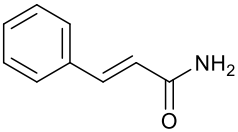
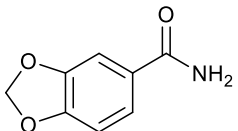
Benzaldoxime and an array of *para*-substituted aromatic aldoximes were successfully converted into their corresponding primary amide products in good to excellent yield (Table 4.13, entries 1-7). Methyl (**4.2**), halogenic (**4.6** and **4.7**), methoxy (**4.8**), amino (**4.9**) and ester (**4.10**) groups were all tolerated by the reaction conditions, although a higher temperature of 50 °C was required to achieve high conversions into primary amides **4.9** and **4.10**. Pleasingly, aromatic substrates containing small groups in the *ortho* position, such as fluorine, were also transformed efficiently (Table 4.13, entry 8), whilst the *meta*-substituted primary amide **4.12** was also afforded in high yield (Table 4.13, entry 9).

In addition, quantitative conversion into the thiophene- and furan-based primary amides **4.13**, **4.14** and **4.15** was also observed (Table 4.13, entries 10-12). Finally, both the vinylic product **4.16** and primary amide **4.17** were afforded in high conversion, although the latter required increased temperature to achieve efficient transformation (Table 4.13, entries 13 and 14).

Table 4.13. Scope of the aldoxime rearrangement reaction.



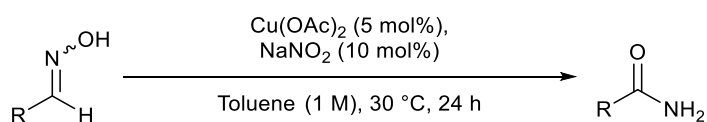
Entry	Product	Conversion from aldoxime (%)	Conversion into primary amide (%)	
1		4.2	100	90 (86)
2		4.5	95	90 (86)
3		4.6	100	84 (80)
4		4.7	100	94 (89)
5		4.8	100	78 (72)
6		4.9	100 100 ^a	53 66 (60) ^a
7		4.10	0 99 ^a	0 87 (80) ^a
8		4.11	89	76 (68)

9		4.12	91	84 (80)
10		4.13	100	100 (97)
11		4.14	100	100 (97)
12		4.15	100	100 (98)
13		4.16	100	76 (71)
14		4.17	41 100 ^a	35 82 (74) ^a

Reactions were performed on a 2 mmol scale. Conversions determined by analysis of the ¹H NMR spectra of the crude reaction mixtures. The corresponding nitrile and aldehyde by-products make up the difference between the two tabulated conversions. ^a Reactions performed at 50 °C.

4.4.2. Less Successful Substrates

However, a number of aldoximes were converted less successfully under the optimised reaction conditions (Table 4.14). Aliphatic substrates proved to be incompatible with the methodology (Table 4.14, entries 1 and 2), whilst the approach is also sensitive to steric effects, with larger groups in the *ortho* aromatic position blocking coordination of the aldoxime/nitrile to the copper centre (Table 4.14, entries 3 and 4).

Table 4.14. Less successful substrates in the aldoxime rearrangement reaction.

Entry	Product	Conversion from aldoxime (%)	Conversion into primary amide (%)
1		4.18	0
2		4.19	0
3		4.20	46
4		4.21	Traces
5		4.22	0
6		4.23	0
7		4.24	0
8		4.25	0

Reactions were performed on a 2 mmol scale. Conversions determined by analysis of the ^1H NMR spectra of the crude reaction mixtures. The corresponding nitrile and aldehyde by-products make up the difference between the two tabulated conversions.

In addition, the unsuccessful synthesis of primary amide **4.22** is likely due to the unreactive nature of the starting aldoxime. The reactivity may have also been further decreased by coordination of the nitro group to the copper centre (Table 4.14, entry 5). Meanwhile, coordination of the oxygen or nitrogen atoms to the copper catalyst inhibited the formation of primary amides **4.23**, **4.24** and **4.25** (Table 4.14, entries 6-8). For example, in the case of **4.25**, the starting aldoxime has a high tendency to form stable six-membered metallacycles with metal ions, which consequently blocks the catalyst (Figure 4.2).

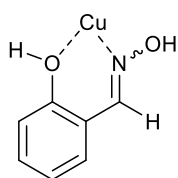


Figure 4.2. Formation of a six-membered metallacycle involving the starting aldoxime and copper centre.

4.5. Reaction Mechanism

It was noticed that during the optimisation process, the combined use of NaNO_2 and $\text{Cu}(\text{OAc})_2$ resulted in a green reaction mixture, in contrast to the blue colour afforded by reactions that only employed $\text{Cu}(\text{OAc})_2$ (Figure 4.3).

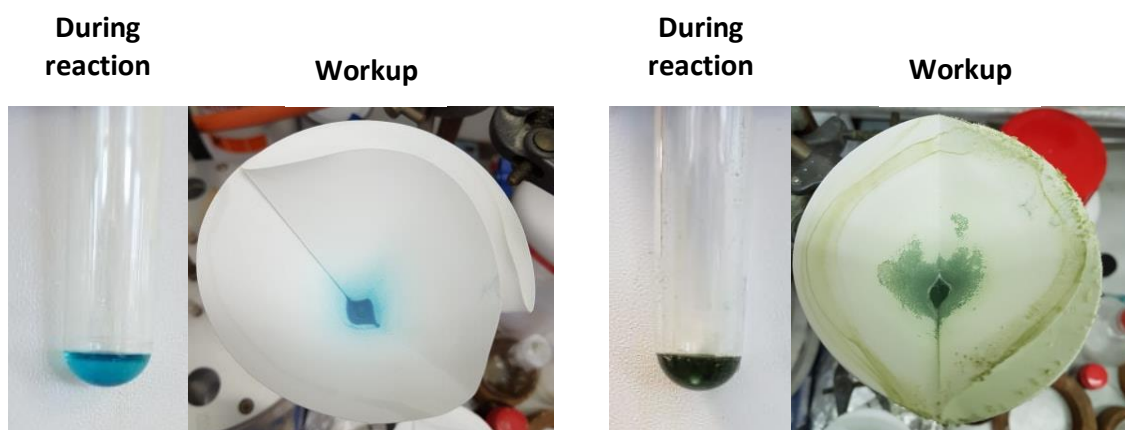
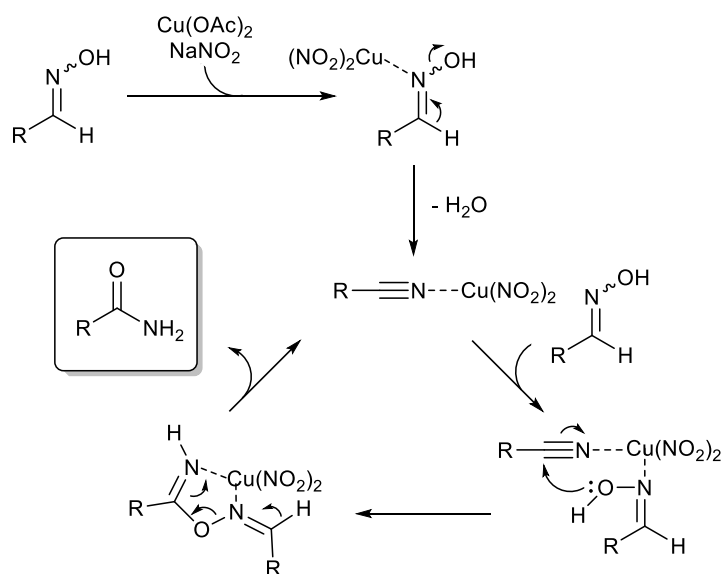


Figure 4.3. Colour difference between reactions employing $\text{Cu}(\text{OAc})_2$ (left) and those containing $\text{Cu}(\text{OAc})_2$ and NaNO_2 (right).

It was hypothesised that this was due to a change in the copper catalyst present in the reaction mixture. The blue colour observed is characteristic of $\text{Cu}(\text{OAc})_2$ whilst the green colour is likely a result of $\text{Cu}(\text{NO}_2)_2$ forming *in situ*. This theory is supported by the literature where nitrite-based copper complexes have been found to be green.²²¹ $\text{Cu}(\text{NO}_2)_2$ then acts as

the active catalytic species in the generally accepted aldoxime rearrangement mechanism (Scheme 4.8).



Scheme 4.8. Plausible mechanism for the aldoxime rearrangement reaction using $\text{Cu}(\text{NO}_2)_2$ as the active catalytic species.

The increased conversions achieved using $\text{Cu}(\text{OAc})_2$ and NaNO_2 suggests that $\text{Cu}(\text{NO}_2)_2$ is a better Lewis acid compared with $\text{Cu}(\text{OAc})_2$. However, further work is required to elucidate whether the nitrite salt simply increases the Lewis acidity of the metal or whether it has a further role in the reaction mechanism. In addition, the configuration of the $\text{Cu}(\text{NO}_2)_2$ complex is also unclear as various modes for the binding of nitrite to transition metal complexes have been observed (Figure 4.4).²²²

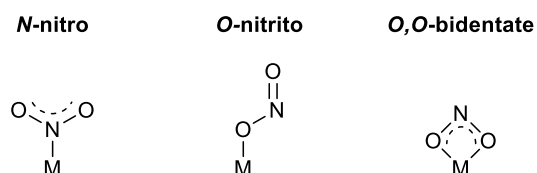


Figure 4.4. Common modes for nitrite-metal binding.²²²

4.6. Conclusions

To the best of our knowledge, this research details the first low temperature (30 °C) protocol for the rearrangement of aldoximes into primary amides using an inexpensive and commercially available copper-based catalytic system. A combination of $\text{Cu}(\text{OAc})_2$ and NaNO_2

furnished a variety of primary amides from aldoximes in toluene in 24 hours. Methyl, halogenic, methoxy, amino and vinylic groups were well tolerated by the methodology, whilst a selection of heterocycles was also successfully converted into primary amides.

Although some substrates, for example aliphatic and sterically hindered aldoximes, proved incompatible with the methodology, a number of the slightly more challenging starting materials could be transformed efficiently by using temperatures of 50 °C. The change in colour observed during the reaction suggests $\text{Cu}(\text{NO}_2)_2$ is formed *in situ* and that this is the active catalytic species responsible for promoting the transformation.

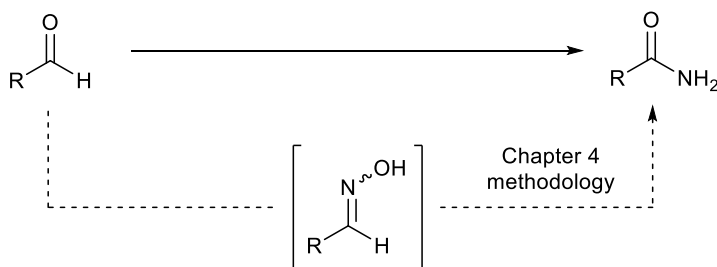
Results and Discussion IV

Amides from Aldehydes

5. Results and Discussion IV – Amides from Aldehydes

5.1. Aims and Objectives

Although the approach outlined in Chapter 4 represents a significant improvement on previous aldoxime rearrangement protocols, we wanted to extend the methodology in order to generate primary amides directly from aldehydes (Scheme 5.1). As detailed earlier, aldoximes are usually synthesised from aldehydes, before a rearrangement reaction affords the desired primary amide product in a second step. However, we theorised that the two steps could potentially be combined to produce a more convenient one-step procedure at low temperature. The aldehyde would firstly be converted into the aldoxime *in situ* and then the methodology detailed in Chapter 4 could be employed to convert the aldoxime into the primary amide product in a one-pot reaction.

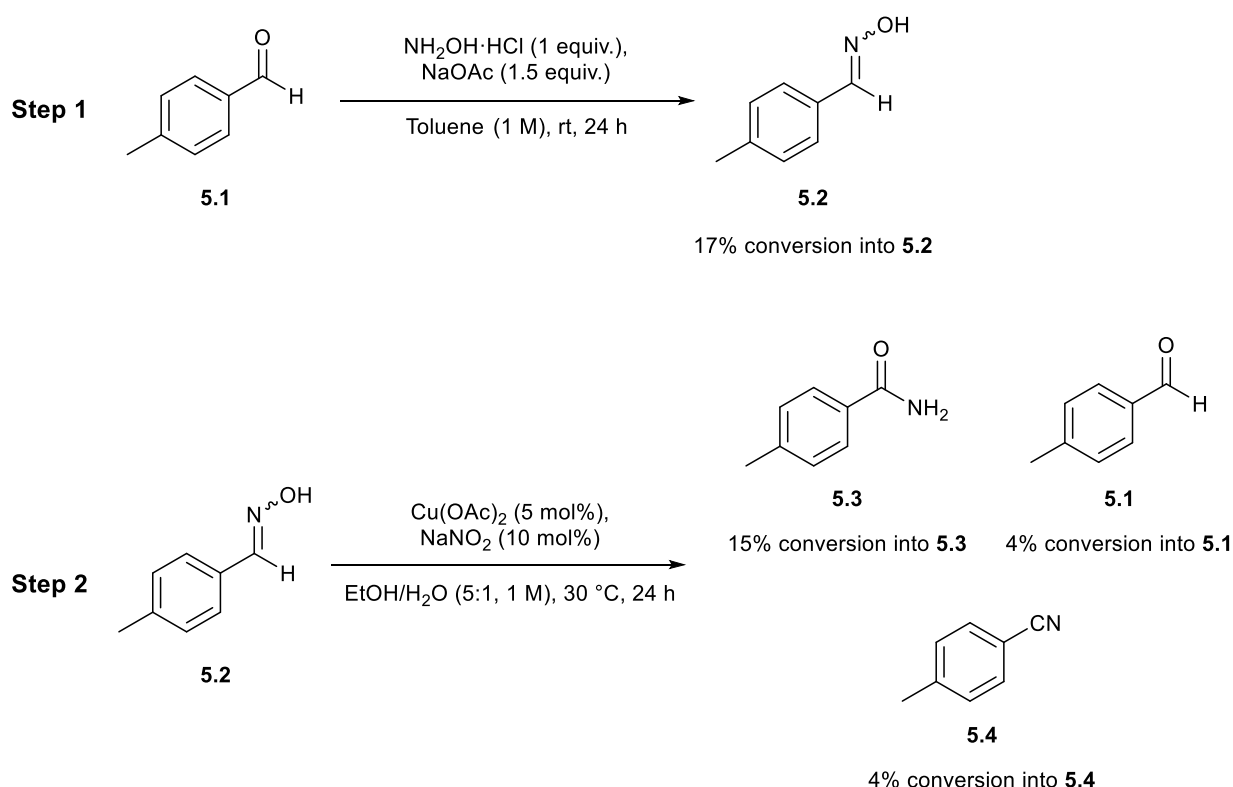


Scheme 5.1. Potential synthesis of primary amides from aldehydes in a one-pot reaction.

5.2. Optimisation

We hypothesised that the hydroxylamine salt used for the formation of the aldoxime (Scheme 4.4) would be incompatible with the copper catalyst employed in the aldoxime rearrangement step. This theory was based on similarly Lewis basic groups (hydroxyl, pyridyl) inhibiting aldoxime rearrangement into the corresponding primary amides in the substrate scope of Chapter 4 (Table 4.14). As a result, the one-pot procedure would need to be performed in a sequential manner, whereby $Cu(OAc)_2$ and $NaNO_2$ are added to the reaction mixture only after quantitative conversion of the aldehyde into the aldoxime. In addition, in contrast to the 2 equivalents of hydroxylamine salt employed in the literature protocol (Scheme 4.4), only stoichiometric amounts would be used in our one-pot approach as any excess hydroxylamine would poison the copper catalyst in the second step.

In order for an efficient one-pot protocol, it was necessary to find a common set of reaction conditions that worked for both the aldehyde to aldoxime transformation and the rearrangement of the aldoxime into the primary amide product. 4-Methylbenzaldehyde (**5.1**) and 4-methylbenzaloxime (**5.2**) were employed as the model aldehyde and aldoxime substrates respectively. We firstly investigated the solvent system for the one-pot procedure. The first and second step reactions were performed in the optimum solvent for the other step, in order to elucidate whether toluene or EtOH/H₂O could be employed as the solvent system (Scheme 5.2). However, toluene proved to be a poor solvent for the first step, with only 17% conversion into aldoxime **5.2**. In addition, use of EtOH/H₂O (5:1) in the aldoxime rearrangement reaction afforded only 15% conversion into primary amide **5.3**. Therefore, these results clearly illustrated that neither toluene nor EtOH/H₂O could be employed as solvents in the one-pot protocol.



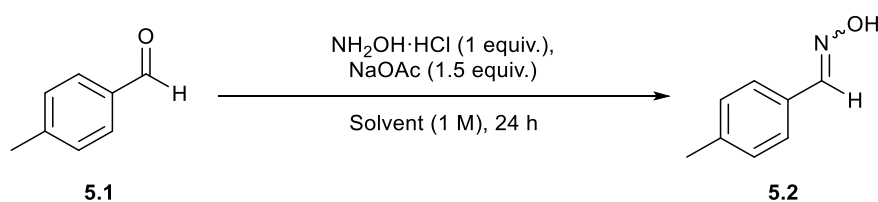
Scheme 5.2. Performing the first and second step reactions in the optimum solvent of the other step.

As a result, we decided to explore the use of other solvents for the conversion of aldehyde **5.1** into primary amide **5.3** *via in situ* formation of the aldoxime. It was noticed that during the solvent screen for the rearrangement of aldoximes in Chapter 4 (Table 4.5), 1,2-dichloroethane (DCE) gave the second highest conversion into the primary amide product

(47%) after toluene (71%). In addition, there was also literature precedence for the use of chlorohydrocarbons as solvents in the conversion of aldehydes into aldoximes; Zhang and Feng employed dry dichloromethane (DCM) to synthesise oximes and hydrazones from the corresponding aldehyde starting materials.²²³ As a result, it was hoped that either DCM or DCE would be an appropriate solvent for the one-pot protocol.

We firstly decided to optimise both of the individual reactions before later combining the two steps to produce our desired one-pot synthesis. The first step was performed in DCE and DCM over a range of reaction temperatures, with all of the reagents added to the reaction at room temperature. Inspection of the crude ¹H NMR spectra for the aldehyde to aldoxime reactions revealed that higher conversions were achieved in DCE compared with DCM (Table 5.1). For example, performing the reaction in DCM at 30 °C afforded 43% conversion into aldoxime **5.2** (Table 5.1, entry 1), whereas quantitative conversion was achieved using DCE in the equivalent reaction (Table 5.1, entry 3). It should also be noted that, unlike the aldoxime rearrangements, no by-products were produced in any of the reactions. In addition, for reactions performed in either solvent, higher temperatures resulted in reduced conversions. When employing DCE as the solvent, conversion into aldoxime **5.2** decreased from quantitative conversion at 30 °C to 57% at 40 °C and then 35% at 50 °C (Table 5.1, entries 3-5).

Table 5.1. Conversion of aldehyde **5.1** into aldoxime **5.2** in DCM/DCE at different temperatures.

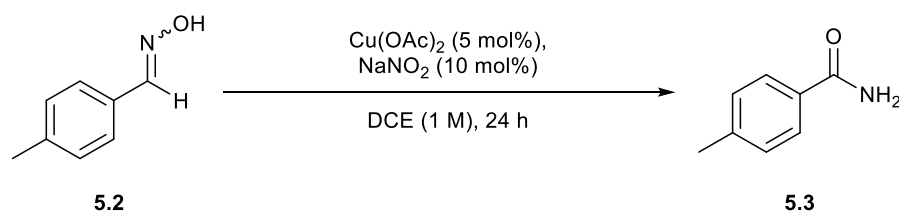


Entry	Solvent	Temperature (°C)	Conversion into 5.2 (%)
1	DCM	30	43
2	DCM	40	28
3	DCE	30	100
4	DCE	40	57
5	DCE	50	35

Reactions were performed on a 1 mmol scale. Conversions determined by analysis of the ¹H NMR spectra of the crude reaction mixtures. No by-products formed.

We subsequently performed the aldoxime rearrangement in DCE, the superior solvent from the first step, at three different temperatures (Table 5.2). Pleasingly, ^1H NMR analysis indicated 75% conversion into primary amide **5.3** at 30 °C (Table 5.2, entry 1), with increased reaction temperatures of 40 °C and 60 °C giving similar conversions. As high conversions were achieved in both steps at 30 °C, it was decided that this reaction temperature would be employed in the subsequent optimisation studies.

Table 5.2. Temperature screen for the oxime rearrangement reaction in DCE.

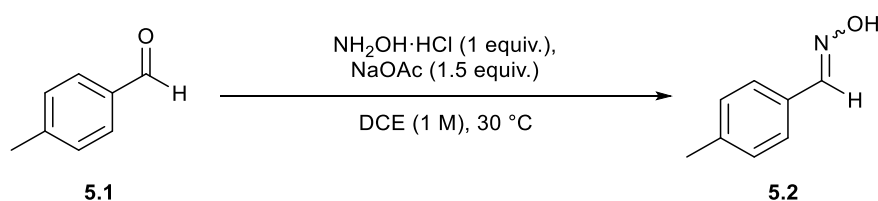


Entry	Temperature (°C)	Conversion from 5.2 (%)	Conversion into 5.3 (%)
1	30	83	75
2	40	86	75
3	60	84	82

Reactions were performed on a 1 mmol scale. Conversions determined by analysis of the ^1H NMR spectra of the crude reaction mixtures. Aldehyde **5.1** and nitrile **5.4** by-products make up the difference between the two tabulated conversions.

A time screen was performed for the aldehyde to aldoxime step to reveal when the reaction had reached completion (Table 5.3). This was important as we reasoned that quantitative conversion into aldoxime **5.2** had to be achieved otherwise the leftover hydroxylamine would inhibit the copper catalyst when it was added to the reaction. Analysis of the crude ^1H NMR spectra showed 24 hours was required for the reaction to reach completion (Table 5.3, entry 5).

Table 5.3. Time screen for the aldehyde to primary amide reaction.

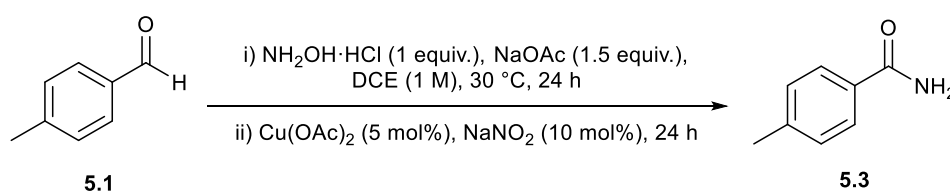


Entry	Time (h)	Conversion into 5.2 (%)
1	4	47
2	8	60
3	16	73
4	20	85
5	24	100

Reactions were performed on a 1 mmol scale. Conversions determined by analysis of the ^1H NMR spectra of the crude reaction mixtures. No by-products formed.

With optimised conditions for the aldehyde to aldoxime and aldoxime to primary amide reactions, it was decided to combine the two steps and perform a one-pot reaction (Table 5.4). Aldehyde **5.1**, $\text{NH}_2\text{OH}\cdot\text{HCl}$ (1 equiv.), NaOAc (1.5 equiv.) and DCE (1 M) were stirred for 24 hours at $30\text{ }^\circ\text{C}$, before $\text{Cu}(\text{OAc})_2$ (5 mol%) and NaNO_2 (10 mol%) were then added to the reaction mixture and the reaction left for a further 24 hours at $30\text{ }^\circ\text{C}$ (Table 5.4, entry 1). However, although a high proportion of aldehyde **5.1** was converted into aldoxime **5.2**, only 2% conversion into primary amide **5.3** was achieved during the reaction. Meanwhile, when a higher temperature of $80\text{ }^\circ\text{C}$ was employed in the second step, 58% conversion into primary amide **5.3** was observed upon analysis of the ^1H NMR spectrum (Table 5.4, entry 2).

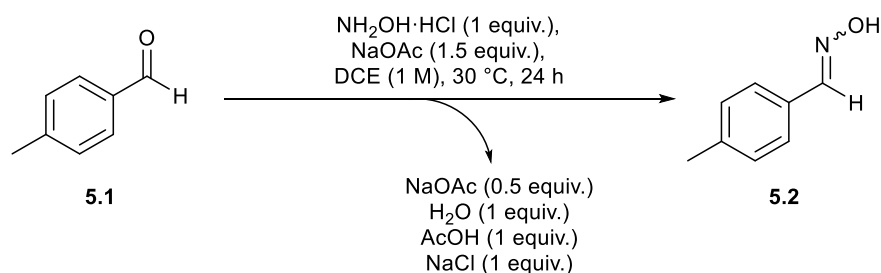
Table 5.4. Initial one-pot protocol for the conversion of aldehyde **5.1** into primary amide **5.3**.



Entry	Temperature of ii) ($^\circ\text{C}$)	Conversion from 5.1 (%)	Conversion into 5.2 (%)	Conversion into 5.3 (%)
1	30	89	77	2
2	80	83	16	58

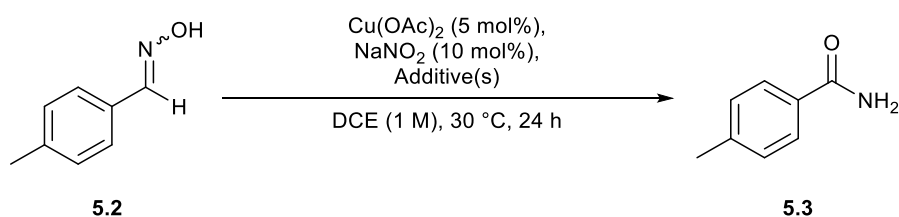
Reactions were performed on a 1 mmol scale. Conversions determined by analysis of the ^1H NMR spectra of the crude reaction mixtures. The remaining percentage conversion from aldehyde **5.1** corresponds to nitrile **5.4**.

It was clear that the poor conversion into primary amide **5.3** achieved at $30\text{ }^\circ\text{C}$ was due to aldoxime **5.2** failing to transform into the final primary amide product. To account for the decreased efficiency of the second step, we theorised that by-products generated from the first step were inhibiting the aldoxime rearrangement reaction (Scheme 5.3).



Scheme 5.3. By-products, including amounts, produced by the aldehyde to aldoxime step.

To further explore this hypothesis we decided to add the by-products generated in the first reaction to the model reaction conditions for the second step (Table 5.5). When NaOAc (0.5 equiv.), H_2O (1 equiv.), AcOH (1 equiv.) and NaCl (1 equiv.) were all added to the reaction together, conversion into primary amide **5.3** decreased to just 6%, compared with 75% for the additive-free reaction (Table 5.5, entries 1 and 2). This therefore confirmed the likelihood that the by-products from the first step were inhibiting the aldoxime rearrangement reaction.

Table 5.5. Addition of first step by-products to the aldoxime rearrangement reaction.

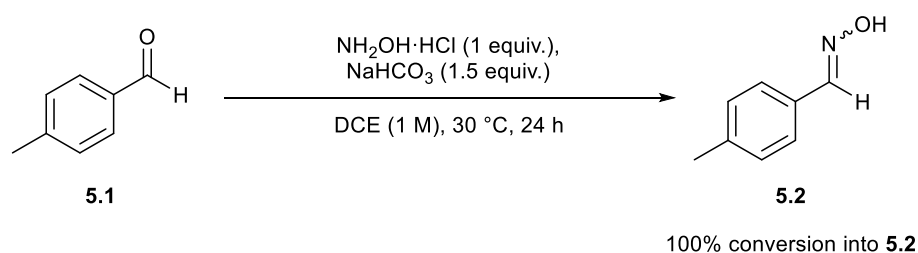
Entry	Additive(s) (equiv.)	Conversion from 5.2 (%)	Conversion into 5.3 (%)
1	-	83	75
2	NaOAc (0.5), H ₂ O (1), NaCl (1), AcOH (1)	31	6 ^a
3	NaOAc (0.5)	85	75
4	NaCl (1)	92	79
5	H ₂ O (1)	100	87
6	AcOH (1)	60	14 ^b

Reactions were performed on a 1 mmol scale. Conversions determined by analysis of the ¹H NMR spectra of the crude reaction mixtures. Aldehyde **5.1** and nitrile **5.4** by-products make up the difference between the two tabulated conversions. ^a 7% of an unidentified by-product also observed. ^b 6% of the corresponding carboxylic acid and 12% of an unidentified by-product also observed.

In order to determine which of the reagents was hindering the second step, we then added the by-products individually. Addition of NaOAc and NaCl to the aldoxime rearrangement reaction had little effect on the conversion into primary amide **5.3**, with 75% and 79% achieved respectively (Table 5.5, entries 3 and 4). Meanwhile, use of H₂O in the reaction surprisingly afforded quantitative conversion from aldoxime **5.2** and 87% conversion into primary amide **5.3**. However, when AcOH was employed in the reaction, inspection of the ¹H NMR spectrum revealed only 14% conversion into primary amide **5.3**. This therefore indicated that AcOH was the by-product responsible for inhibiting the aldoxime rearrangement reaction. We hypothesised that this was likely due to AcOH poisoning the copper catalyst and preventing coordination of both the nitrite ligand and the aldoxime substrate.

These experiments made it clear that NaOAc could not be used as the base in the one-pot protocol. Therefore, we decided to test the performance of NaHCO₃ in the aldehyde to aldoxime reaction. It was thought that this base would be more suitable as the by-products

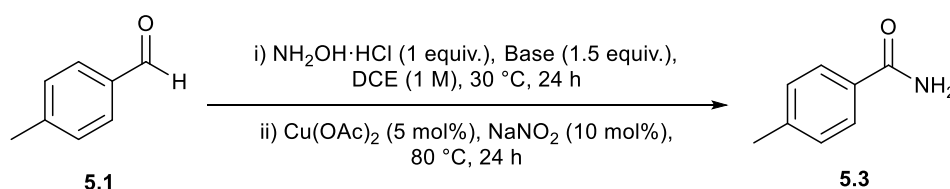
generated (NaCl, H₂O and CO₂) are less likely to inhibit the aldoxime rearrangement step. Pleasingly, quantitative conversion into aldoxime **5.2** was observed upon analysis of the ¹H NMR spectrum when NaHCO₃ was employed as the base (Scheme 5.4).



Scheme 5.4. Use of NaHCO₃ as the base in the aldehyde to aldoxime first step.

It was subsequently decided to investigate whether our one-pot protocol demonstrated increased efficiency when NaHCO₃ was employed as the base (Table 5.6). As predicted, a significant increase in the conversion into primary amide **5.3** was observed using NaHCO₃ (84%) compared with NaOAc (58%). No aldoxime was observed in the NaHCO₃-based reaction, therefore indicating the second step was not inhibited under these reaction conditions and that the copper catalyst was able to transform aldoxime **5.2** into primary amide **5.3** (Table 5.6, entry 2). In addition, at first glance it appears the first step didn't reach quantitative conversion, with 94% conversion from aldehyde **5.1** observed in the one-pot protocol. However, instead of being unreacted starting material, it is likely that this small amount of aldehyde (6%) is formed as a by-product in the second step, as described previously.

Table 5.6. Comparison between the use of NaOAc and NaHCO₃ as the base in the one-pot protocol.

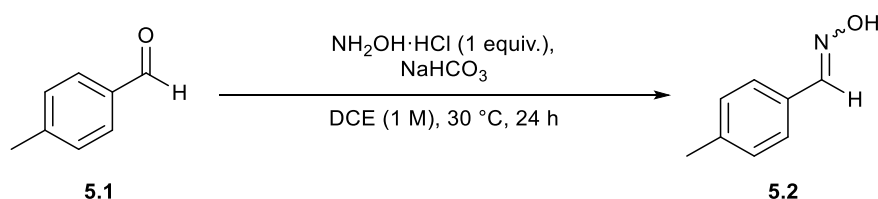


Entry	Base	Conversion from	Conversion into	Conversion into
		5.1 (%)	5.2 (%)	5.3 (%)
1	NaOAc	83	16	58
2	NaHCO ₃	94	0	84

Reactions were performed on a 1 mmol scale. Conversions determined by analysis of the ¹H NMR spectra of the crude reaction mixtures. The remaining percentage conversion from aldehyde **5.1** corresponds to nitrile **5.4**.

After identifying NaHCO_3 as a suitable base for the one-pot procedure, we decided to investigate whether 1.5 equivalents were required to achieve quantitative conversion into aldoxime **5.2** (Table 5.7). A small amount of aldehyde **5.1** was left unreacted when a stoichiometric amount of NaHCO_3 was employed (Table 5.7, entry 1); however, the use of a slight excess (1.1 equivalents) afforded quantitative conversion into aldoxime **5.2** (Table 5.7, entry 2).

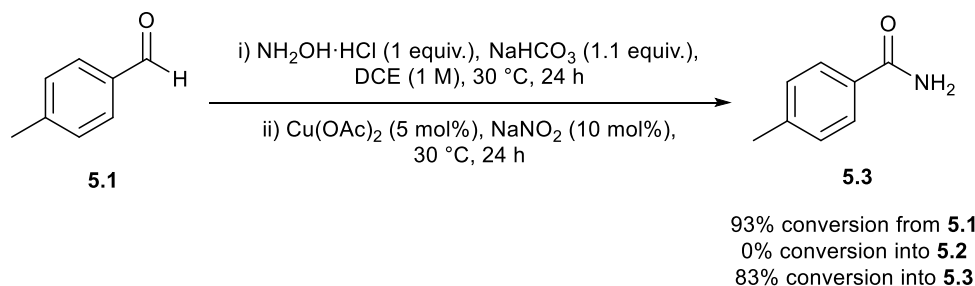
Table 5.7. NaHCO_3 equivalents screen.



Entry	Equivalents of Base	Conversion into 5.2 (%)
1	1	96
2	1.1	100
3	1.5	100

Reactions were performed on a 1 mmol scale. Conversions determined by analysis of the ^1H NMR spectra of the crude reaction mixtures. No by-products formed.

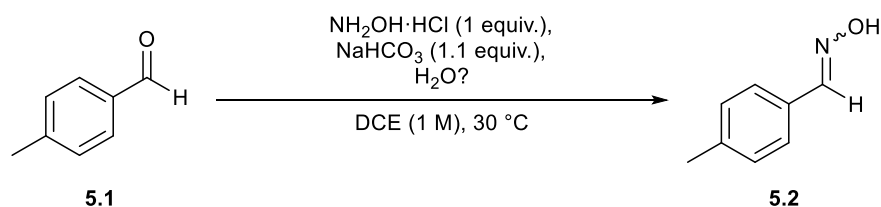
The new reaction conditions for the aldehyde to aldoxime step were then applied to the one-pot reaction. As our aim was to develop a low temperature methodology for the conversion of aldehydes into primary amides, the reaction was performed at 30 °C (Scheme 5.5). Pleasingly, spectroscopic analysis revealed 83% conversion into primary amide **5.3**, with no aldoxime visible in the crude ^1H NMR spectrum.



Scheme 5.5. Conversion of aldehyde **5.1** into primary amide **5.3** using 1.1 equivalents of NaHCO_3 as the base.

After achieving high conversions into primary amide **5.3** using the one-pot protocol, it was decided that we would attempt to further refine the conditions for the aldehyde to aldoxime step. Specifically, we wished to reduce the time required to achieve quantitative conversion from aldehyde **5.1** into aldoxime **5.2**. This would then allow us to perform the overall one-pot reaction in less than the 48 hours it currently required. A time screen was performed and, to our delight, quantitative conversion for the first step was observed after 4 hours upon analysis of the crude ^1H NMR spectra (Table 5.8, entry 6).

Table 5.8. Time screen for the conversion of aldehyde **5.1** into aldoxime **5.2**.

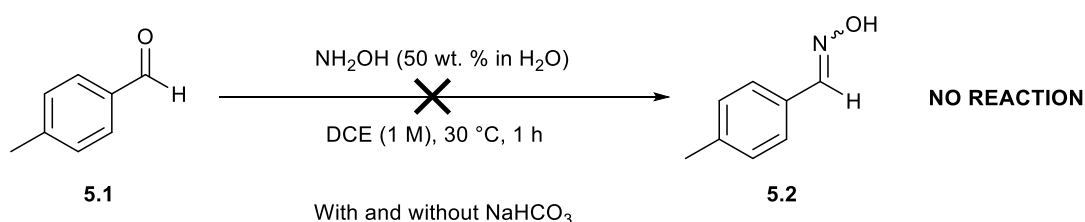


Entry	Time (h)	Water added?	Conversion into 5.2 (%)
1	1	-	18
2	1	✓ (1 equiv.)	93
3	1	✓ (3 equiv.)	100
4	2	-	92
5	3	-	96
6	4	-	100

Reactions were performed on a 1 mmol scale. Conversions determined by analysis of the ^1H NMR spectra of the crude reaction mixtures. No by-products formed.

In addition, we also observed a sharp increase in the conversion from 18% to 92% between one and two hours (Table 5.8, entries 1 and 4). To account for the rapid acceleration in the rate of the reaction after the slow start, we theorised that formation of aldoxime **5.2** was being promoted by a reagent that was generated during the reaction. We revealed that the addition of water to the reaction afforded a significant increase in the conversion into aldoxime **5.2** after one hour (Table 5.8, entries 1-3). Use of 3 equivalents of water resulted in quantitative conversion into aldoxime **5.2** compared with 18% conversion for the water-free reaction. We postulated that the increase in conversion was due to the water improving the solubility of the reaction mixture.

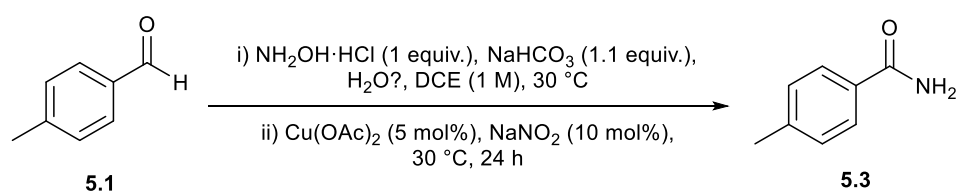
Following this, it was thought that instead of having to add water to the reaction, we could use commercially available NH_2OH in water rather than the hydrochloride salt. However, unfortunately no reaction was observed upon ^1H NMR analysis, both in the presence and absence of NaHCO_3 (Scheme 5.6).



Scheme 5.6. Failed attempt to form aldoxime **5.2** from aldehyde **5.1** using NH_2OH in water.

It was then decided to apply the newly optimised water-based and water-free first step reaction conditions to the one-pot approach. Employing 3 equivalents of water in part i) for 1 hour resulted in a significantly decreased conversion into primary amide **5.3** compared with when the reaction was performed without water for 4 hours (Table 5.9). Specifically, 37% conversion into primary amide **5.3** was achieved when water was added to the reaction (Table 5.9, entry 1) compared with 81% conversion for the water-free approach (Table 5.9, entry 2). This contrasts favourably to the previously performed one-pot reaction in which 83% conversion into primary amide **5.3** was achieved after 48 hours (Scheme 5.5).

Table 5.9. One-pot protocol with and without the addition of water to the first step.



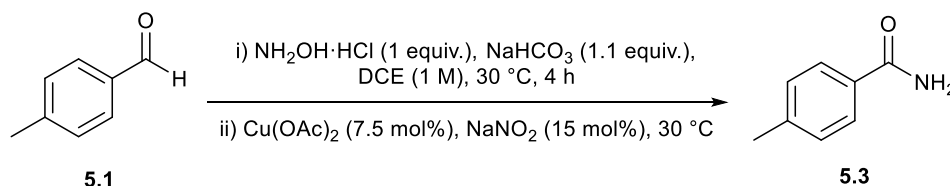
Entry	Part i) conditions	Conversion from	Conversion into	Conversion into
		5.1 (%)	5.2 (%)	5.3 (%)
1	H_2O (3 equiv.), 1 h	96	53	37
2	No H_2O , 4 h	96	7	81

Reactions were performed on a 1 mmol scale. Conversions determined by analysis of the ^1H NMR spectra of the crude reaction mixtures. The remaining percentage conversion from aldehyde **5.1** corresponds to nitrile **5.4**.

However, it was noticed that a small amount (7%) of aldoxime **5.2** was left unreacted when using the water-free reaction conditions (Table 5.9, entry 2). To convert the remaining

aldoxime into primary amide **5.3**, an increased catalyst loading of 7.5 mol% Cu(OAc)₂ and 15 mol% NaNO₂ was employed. Pleasingly, analysis of the crude ¹H NMR spectrum showed quantitative conversion of aldoxime **5.2** into primary amide **5.3** after only 20 hours (Table 5.10, entry 2).

Table 5.10. Final optimisation of one-pot protocol.

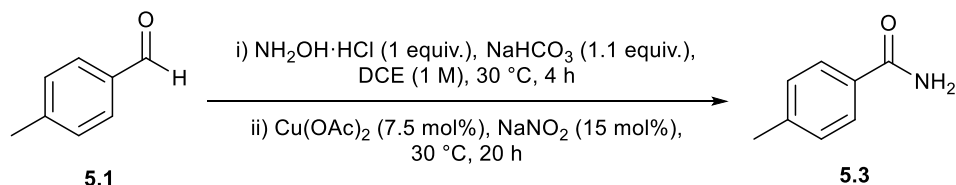


Entry	Part ii) time (h)	Conversion from	Conversion into	Conversion into
		5.1 (%)	5.2 (%)	5.3 (%)
1	24	95	0	85
2	20	95	0	85
3 ^a	20	93	43	44
4 ^b	20	79	24	47
5 ^c	20	91	43	42
6 ^d	20	72	45	22

Reactions were performed on a 1 mmol scale. Conversions determined by analysis of the ¹H NMR spectra of the crude reaction mixtures. The remaining percentage conversion from aldehyde **5.1** corresponds to nitrile **5.4**. ^a Reaction performed in H₂O. ^b Reaction performed in DCM. ^c Reaction performed without NaNO₂. ^d Reagents for both part i) and ii) introduced at the start of the reaction.

Following this, we explored the possibility of replacing DCE with water. However, use of the more environmentally friendly solvent resulted in only 44% conversion into primary amide **5.3** (Table 5.10, entry 3). Meanwhile, a similar conversion (47%) was achieved when DCM, which is cheaper and more readily available than DCE, was employed as the solvent (Table 5.10, entry 4). The impact of NaNO₂ on the efficiency of the reaction was also investigated. Removing the nitrite salt from the optimised reaction conditions yielded 42% conversion into primary amide **5.3**, with a large amount of aldoxime **5.2** left unconverted (Table 5.10, entry 5). This therefore illustrates the importance of NaNO₂ in transforming aldoxime **5.2** into primary amide **5.3** in the one-pot protocol. Finally, as predicted, when all of the reagents from part i) and ii) were introduced at the start of the reaction, formation of primary amide **5.3** was inhibited (Table 5.10, entry 6).

Scheme 5.7 details the final fully optimised reaction conditions for the one-pot protocol which transforms aldehyde **5.1** into primary amide **5.3**, *via in situ* formation of aldoxime **5.2**, in 24 hours at 30 °C.

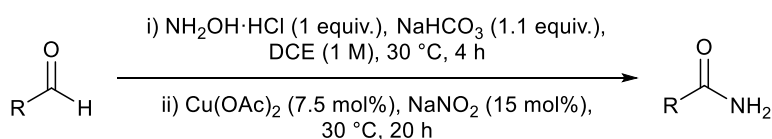


Scheme 5.7. Fully optimised reaction conditions for the conversion of aldehyde **5.1** into primary amide **5.3** in a one-pot protocol at low temperature.

5.3. Substrate Scope

The methodology detailed in Scheme 5.7 was applied to a selection of aldehydes. The aldoxime intermediates formed during the reaction were successfully transformed into primary amides using the copper-catalysed methodology outlined in Chapter 4 (Table 5.11). Quadrasil™ TA was used to scavenge the copper catalyst and, following filtration, the crude primary amide products were purified by silica column chromatography (eluting with DCM/MeOH).

Table 5.11. Scope of the one-pot protocol for the conversion of aldehydes into primary amides.



Entry	Product	Conversion from aldehyde (%)	Conversion into primary amide (%)	
1		5.3	94	84 (80)
2		5.5	96	87 (79)
3		5.6	78	78 (72)

4		5.7	84	65 (62) ^a
5		5.8	70 96 ^a	29 90 (83) ^a
6		5.9	84 97 ^a	35 91 (84) ^a
7		5.10	51 84 ^a	7 50 (41) ^a
8		5.11	25 45 ^a	7 22 ^a
9		5.12	73 93 ^a	0 33 ^a
10		5.13	74 97 ^a	38 88 (80) ^a
11		5.14	68 90 ^a	29 80 (76) ^a

Reactions were performed on a 2 mmol scale. Conversions determined by analysis of the ¹H NMR spectra of the crude reaction mixtures. The corresponding aldoxime and nitrile by-products make up the difference between the two tabulated conversions (nitrile typically < 10%). ^a Part i) and ii) left for 16 hours and 24 hours respectively.

The model primary amide, **5.3**, was isolated in 80% yield (Table 5.11, entry 1), whilst the *para*-chloro derivative was also successfully transformed using the one-pot methodology (Table 5.11, entry 2). In addition, 2-thiophenecarboxaldehyde and 2-furaldehyde underwent efficient

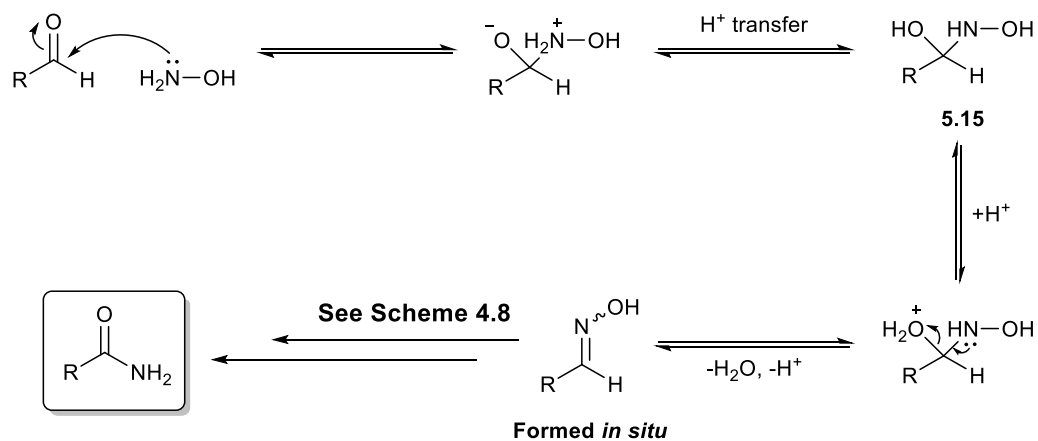
transformation to afford primary amides **5.6** and **5.7** in 72% and 62% yield respectively (Table 5.11, entries 3 and 4).

However, many of the aldehydes were converted less successfully into their corresponding primary amides under the present reaction conditions (Table 5.11, entries 5-11). Importantly, the ^1H NMR spectra revealed a significant percentage of unreacted aldehyde in the crude reaction mixture for many of the reactions. It was thought that failure of the aldehyde to aldoxime step to reach quantitative conversion resulted in the remaining hydroxylamine inhibiting the second step of the one-pot protocol. As a result, it was imperative that part i) was left long enough for quantitative conversion to be reached.

Formation of the aldoxime was left overnight for 16 hours and the copper-catalysed aldoxime rearrangement then stirred for 24 hours overnight. Pleasingly, the new reaction conditions were able to transform benzaldoxime and the *para*-fluoro derivative into their corresponding primary amide products, **5.8** and **5.9**, in 83% and 84% yield respectively (Table 5.11, entries 5 and 6). In addition, the *meta*-substituted primary amide **5.13** was also successfully obtained, whilst cinnamaldehyde was efficiently transformed in primary amide **5.14** in 76% yield (Table 5.11, entries 10 and 11).

5.4. Reaction Mechanism

It is likely the conversion of aldehydes into primary amides under our reaction conditions proceeds *via* the reaction mechanism detailed in Scheme 5.8. Firstly, nucleophilic attack by hydroxylamine on the aldehyde followed by proton transfer yields tetrahedral intermediate **5.15**. This intermediate then collapses, losing water in the process, to form the aldoxime *in situ*. Applying the copper-catalysed methodology developed in Chapter 4 then affords the primary amide *via* the reaction mechanism detailed in Scheme 4.8.



Scheme 5.8. Reaction mechanism for the conversion of an aldehyde into a primary amide using our methodology.

5.5. Conclusions

A one-pot synthesis of primary amides from aldehydes has been developed, *via in situ* formation of the oxime. The protocol is performed at 30 °C, which, to the best of our knowledge, is the lowest temperature published for the transformation. Following *in situ* formation of the aldoxime from the aldehyde, the Cu(OAc)₂/NaNO₂ catalytic system detailed in Chapter 4 efficiently rearranges the aldoxime intermediate into the primary amide product. The protocol was shown to successfully transform aromatic aldehydes in 24 hours, although longer reaction times were required for less reactive substrates.

Experimental

6. Experimental

6.1. Materials and Methods

Unless preparative details are provided, all reagents were purchased from Alfa Aesar, Acros Organics, Aldrich, Fluka or Lancaster and used without further purification. Analytical thin layer chromatography (TLC) was carried out on Merck silica gel 60 F254 aluminium or plastic plates, purchased from Fisher. The organic compounds were visualised under UV (254 nm) irradiation and stained with potassium permanganate dip, followed by gentle heating. Purification of the final products was performed by flash chromatography using the indicated solvent on Aldrich silica gel 60 Å (230-400 mesh).

^1H NMR and ^{13}C NMR spectra were recorded on a Bruker Avance 250 (250 MHz), a Bruker Avance 300 (300 MHz) or an Agilent 500 (500 MHz) in CDCl_3 or DMSO-d^6 as solvents. Chemical shifts (δ) are reported as parts per million (ppm) and are referenced internally to the residual protic solvent signal for CDCl_3 (7.26 ppm) or DMSO-d^6 (2.50 ppm). Coupling constants (J) are reported in Hertz (Hz) and signal multiplicities are reported as singlet (s), doublet (d), triplet (t), quartet (q), quintet (quint), sextet (sext), doublet of doublets (dd), multiplet (m), or broad singlet (br s). HRMS-ESI were run on an Agilent 1200 series LC/MSD coupled to a microTOF electrospray time-of-flight (ESI-TOF) mass spectrometer (Bruker Daltonik).

Infra-red spectra were recorded on a Perkin Elmer Spectrum 100 FT-IR spectrometer, using a Universal ATR accessory for sampling, with relevant absorbances quoted as ν in cm^{-1} . Optical rotation values were measured at room temperature using an Optical Activity AA-10 Automatic Polarimeter ($c = 1, \text{CHCl}_3$). Melting points were determined using Stuart SMP10 melting point equipment using closed end glass capillary tubes and are uncorrected.

6.2. Chapter 2 Experimental Methods and Compound Characterisation

General Procedure I – Sulfuric Acid Catalyst Screen

(Table 2.1, Results and Discussion I)

To an oven dried Radleys carousel tube containing 4-methylbenzylamine (127 μ L, 1 mmol) was added ethyl acetate (1 mL, 1 M) followed by the appropriate amount of H₂SO₄. The carousel tube was then sealed and the reaction mixture heated at 80 °C for 20 hours. After being allowed to cool to room temperature, the solvent was removed *in vacuo* on a rotary evaporator and the resulting crude reaction mixture was analysed by ¹H NMR spectroscopy. Percentage conversion into *N*-(4-methylbenzyl)acetamide was calculated from the crude ¹H NMR spectra by comparison of the peaks at 3.85 ppm (2H, 4-methylbenzylamine) and 4.39 ppm (2H, *N*-(4-methylbenzyl)acetamide).

Optimisation of the Reaction Conditions - Primary Amines

General Procedure II – Acetic Acid Catalyst Loading Screen

(Table 2.2, Results and Discussion I)

To an oven dried Radleys carousel tube containing 4-methylbenzylamine (127 μ L, 1 mmol) was added ethyl acetate (1 mL, 1 M) followed by the appropriate amount of acetic acid. The carousel tube was then sealed and the reaction mixture heated at 80 °C for 20 hours. After being allowed to cool to room temperature, the solvent was removed *in vacuo* on a rotary evaporator and the resulting crude reaction mixture was analysed by ¹H NMR spectroscopy. Percentage conversion into *N*-(4-methylbenzyl)acetamide was calculated from the crude ¹H NMR spectra by comparison of the peaks at 3.85 ppm (2H, 4-methylbenzylamine) and 4.39 ppm (2H, *N*-(4-methylbenzyl)acetamide).

General Procedure III – Reaction Time Screen

(Table 2.3, Results and Discussion I)

To an oven dried Radleys carousel tube containing 4-methylbenzylamine (127 μ L, 1 mmol) was added ethyl acetate (1 mL, 1 M) followed by acetic acid (5.7 μ L, 10 mol%). The carousel tube was then sealed and the reaction mixture heated at 80 °C for the appropriate number of hours. After being allowed to cool to room temperature, the solvent was removed *in vacuo* on a rotary evaporator and the resulting crude reaction mixture was analysed by ¹H NMR spectroscopy. Percentage conversion into *N*-(4-methylbenzyl)acetamide was calculated from

the crude ^1H NMR spectra by comparison of the peaks at 3.85 ppm (2H, 4-methylbenzylamine) and 4.39 ppm (2H, *N*-(4-methylbenzyl)acetamide).

General Procedure IV – Ethyl Acetate Solvent Concentration Screen

(Table 2.4, Results and Discussion I)

To an oven dried Radleys carousel tube containing 4-methylbenzylamine (127 μL , 1 mmol) was added the appropriate amount of ethyl acetate followed by acetic acid (5.7 μL , 10 mol%). The carousel tube was then sealed and the reaction mixture heated at 80 $^\circ\text{C}$ for 20 hours. After being allowed to cool to room temperature, the solvent was removed *in vacuo* on a rotary evaporator and the resulting crude reaction mixture was analysed by ^1H NMR spectroscopy. Percentage conversion into *N*-(4-methylbenzyl)acetamide was calculated from the crude ^1H NMR spectra by comparison of the peaks at 3.85 ppm (2H, 4-methylbenzylamine) and 4.39 ppm (2H, *N*-(4-methylbenzyl)acetamide).

General Procedure V – Reaction Temperature Screen

(Table 2.5, Results and Discussion I)

To an oven dried Radleys carousel tube containing 4-methylbenzylamine (127 μL , 1 mmol) was added ethyl acetate (0.5 mL, 2 M) followed by acetic acid (5.7 μL , 10 mol%). The carousel tube was then sealed and the reaction mixture heated at the appropriate temperature for 20 hours. After being allowed to cool to room temperature, the solvent was removed *in vacuo* on a rotary evaporator and the resulting crude reaction mixture was analysed by ^1H NMR spectroscopy. Percentage conversion into *N*-(4-methylbenzyl)acetamide was calculated from the crude ^1H NMR spectra by comparison of the peaks at 3.85 ppm (2H, 4-methylbenzylamine) and 4.39 ppm (2H, *N*-(4-methylbenzyl)acetamide).

Optimisation of the Reaction Conditions – Secondary Amines

General Procedure VI – Conversion of Secondary Amines into Acetamides under Reaction Conditions A

(Table 2.6, Results and Discussion I)

To an oven dried Radleys carousel tube containing the appropriate secondary amine (1 mmol) was added ethyl acetate (0.5 mL, 2 M) followed by acetic acid (5.7 μL , 10 mol%). The carousel tube was then sealed and the reaction mixture heated at 80 $^\circ\text{C}$ for 20 hours. After being allowed to cool to room temperature, the solvent was removed *in vacuo* on a rotary

evaporator and the resulting crude reaction mixture was analysed by ^1H NMR spectroscopy. Percentage conversion into the acetamide products was calculated from the crude ^1H NMR spectra.

General Procedure VII – Catalyst Loading Screen With Ethyl Acetate

(Table 2.7, Results and Discussion I)

To an oven dried Radleys carousel tube containing *N*-benzylmethylamine (129 μL , 1 mmol) was added ethyl acetate (0.5 mL, 2 M) followed by the appropriate amount of acetic acid. The carousel tube was then sealed and the reaction mixture heated at 80 $^\circ\text{C}$ for 20 hours. After being allowed to cool to room temperature, the solvent was removed *in vacuo* on a rotary evaporator and the resulting crude reaction mixture was analysed by ^1H NMR spectroscopy. Percentage conversion into *N*-benzyl-*N*-methylacetamide was calculated from the crude ^1H NMR spectra by comparison of the peaks at 3.78 ppm (2H, *N*-benzylmethylamine) and 4.46 and 4.53 ppm (2H, *N*-benzyl-*N*-methylacetamide, major and minor rotamers).

General Procedure VIII – Catalyst Loading Screen With Butyl Acetate

(Table 2.8, Results and Discussion I)

To an oven dried Radleys carousel tube containing *N*-benzylmethylamine (129 μL , 1 mmol) was added butyl acetate (0.5 mL, 2 M) followed by the appropriate amount of acetic acid. The carousel tube was then sealed and the reaction mixture heated at 120 $^\circ\text{C}$ for 20 hours. After being allowed to cool to room temperature, the solvent was removed *in vacuo* on a rotary evaporator and the resulting crude reaction mixture was analysed by ^1H NMR spectroscopy. Percentage conversion into *N*-benzyl-*N*-methylacetamide was calculated from the crude ^1H NMR spectra by comparison of the peaks at 3.78 ppm (2H, *N*-benzylmethylamine) and 4.46 and 4.53 ppm (2H, *N*-benzyl-*N*-methylacetamide, major and minor rotamers).

General Procedure IX – Reaction Temperature Screen

(Table 2.9, Results and Discussion I)

To an oven dried Radleys carousel tube containing *N*-benzylmethylamine (129 μL , 1 mmol) was added butyl acetate (0.5 mL, 2 M) followed by acetic acid (28.6 μL , 50 mol%). The carousel tube was then sealed and the reaction mixture heated at the appropriate temperature for 20 hours. After being allowed to cool to room temperature, the solvent was removed *in vacuo* on a rotary evaporator and the resulting crude reaction mixture was

analysed by ^1H NMR spectroscopy. Percentage conversion into *N*-benzyl-*N*-methylacetamide was calculated from the crude ^1H NMR spectra by comparison of the peaks at 3.78 ppm (2H, *N*-benzylmethylamine) and 4.46 and 4.53 ppm (2H, *N*-benzyl-*N*-methylacetamide, major and minor rotamers).

Optimisation of the Reaction Conditions - Anilines

General Procedure X – Catalyst Loading Screen

(Table 2.10, Results and Discussion I)

To an oven dried Radleys carousel tube containing aniline (91 μL , 1 mmol) was added ethyl acetate (0.5 mL, 2 M) followed by the appropriate amount of acetic acid. The carousel tube was then sealed and the reaction mixture heated at 80 $^\circ\text{C}$ for 24 hours. After being allowed to cool to room temperature, the solvent was removed *in vacuo* on a rotary evaporator and the resulting crude reaction mixture was analysed by ^1H NMR spectroscopy. Percentage conversion into *N*-phenylacetamide was calculated from the crude ^1H NMR spectra by comparison of the peaks at 6.50-6.66 ppm (3H, aniline) and 7.28 ppm (2H, *N*-phenylacetamide).

General Procedure XI – Reaction of *para*-Anilinic Substrates with Ethyl Acetate

(Table 2.11, Results and Discussion I)

To an oven dried Radleys carousel tube containing the appropriate *para*-substituted aniline substrate (1 mmol) was added ethyl acetate (0.5 mL, 2 M) followed by acetic acid (143 μL , 2.5 equiv.). The carousel tube was then sealed and the reaction mixture heated at 80 $^\circ\text{C}$ for 24 hours. After being allowed to cool to room temperature, the solvent was removed *in vacuo* on a rotary evaporator and the resulting crude reaction mixture was analysed by ^1H NMR spectroscopy. Percentage conversion was calculated from the crude ^1H NMR spectra.

General Procedure XII – Reaction Temperature Screen

(Table 2.12, Results and Discussion I)

To an oven dried Radleys carousel tube containing aniline (91 μL , 1 mmol) was added butyl acetate (0.5 mL, 2 M) followed by acetic acid (143 μL , 2.5 equiv.). The carousel tube was then sealed and the reaction mixture heated at the appropriate temperature for 24 hours. After being allowed to cool to room temperature, the solvent was removed *in vacuo* on a rotary evaporator and the resulting crude reaction mixture was analysed by ^1H NMR spectroscopy.

Percentage conversion into *N*-phenylacetamide was calculated from the crude ¹H NMR spectra by comparison of the peaks at 6.50-6.66 ppm (3H, aniline) and 7.28 ppm (2H, *N*-phenylacetamide).

Synthesis of Acetamides

General Procedure XIII – Acetylation of Primary Amines

(Table 2.13, Results and Discussion I)

To an oven dried Radleys carousel tube containing the appropriate primary amine (2 mmol) was added ethyl acetate (1 mL, 2 M) followed by acetic acid (11.4 μL, 10 mol%). The carousel tube was then sealed and the reaction mixture heated at 80 °C for 20 hours. After being allowed to cool to room temperature, the solvent was removed *in vacuo* on a rotary evaporator and the resulting crude amide product was purified by silica column chromatography.

General Procedure XIV – Acetylation of Secondary Amines

(Table 2.14, Results and Discussion I)

To an oven dried Radleys carousel tube containing the appropriate secondary amine (2 mmol) was added butyl acetate (1 mL, 2 M) followed by acetic acid (57.2 μL, 50 mol%). The carousel tube was then sealed and the reaction mixture heated at 120 °C for 20 hours. After being allowed to cool to room temperature, the solvent was removed *in vacuo* on a rotary evaporator and the resulting crude amide product was purified by silica column chromatography.

General Procedure XV – Acetylation of Anilines

(Table 2.15, Results and Discussion I)

To an oven dried Radleys carousel tube containing the appropriate aniline (2 mmol) was added butyl acetate (1 mL, 2 M) followed by acetic acid (286 μL, 2.5 equiv.). The carousel tube was then sealed and the reaction mixture heated at 110 °C for 24 hours. After being allowed to cool to room temperature, the solvent was removed *in vacuo* on a rotary evaporator and the resulting crude amide product was purified by silica column chromatography.

General Procedure XVI - Scale-up Example

(Scheme 2.8, Results and Discussion I)

To an oven dried round bottomed flask containing benzylamine (7.3 mL, 67 mmol) was added ethyl acetate (34 mL, 2 M) followed by acetic acid (0.38 mL, 10 mol%). The round bottomed flask was then sealed with a rubber septum and a needle inserted into the top, and the reaction mixture heated at 80 °C for 22 hours. After being allowed to cool to room temperature, the solvent was removed *in vacuo* on a rotary evaporator and the resulting crude amide product was purified by silica column chromatography.

Optimisation of the Reaction Conditions – Ethyl Formate

General Procedure XVII – Catalyst Loading and Reaction Time Screen for the Formylation of Aniline

(Table 2.16, Results and Discussion I)

To an oven dried Radleys carousel tube containing aniline (91 μ L, 1 mmol) was added ethyl formate (0.5 mL, 2 M) followed by the appropriate amount of either formic acid or acetic acid. The carousel tube was then sealed and the reaction mixture heated at 20 °C for the appropriate amount of hours. After being allowed to cool to room temperature, the solvent was removed *in vacuo* on a rotary evaporator and the resulting crude reaction mixture was analysed by ^1H NMR spectroscopy. Percentage conversion into *N*-phenylformamide was calculated from the crude ^1H NMR spectra by comparison of the peaks at 6.50-6.66 ppm (3H, aniline) and 7.26-7.37 ppm (2H, major and minor rotamers, *N*-phenylformamide).

Optimisation of the Reaction Conditions – Methyl Benzoate

General Procedure XVIII – Reaction of Methyl Benzoate with Benzylamine

(Table 2.18, Results and Discussion I)

To an oven dried Radleys carousel tube containing benzylamine (109 μ L, 1 mmol) was added the appropriate amount of methyl benzoate followed by the appropriate amount of acetic acid. The carousel tube was then sealed and the reaction mixture heated at the appropriate temperature for 20 hours. After being allowed to cool to room temperature, the solvent was removed *in vacuo* on a rotary evaporator and the resulting crude reaction mixture was analysed by ^1H NMR spectroscopy. Percentage conversion into *N*-benzylbenzamide was calculated from the crude ^1H NMR spectra by comparison of the peaks at 3.92 ppm (2H, benzylamine) and 4.66 ppm (2H, *N*-benzylbenzamide). Percentage conversion into *N*-

benzylacetamide was calculated from the crude ^1H NMR spectra by comparison of the peaks at 3.92 ppm (2H, benzylamine) and 4.44 ppm (2H, *N*-benzylacetamide). Total conversion was calculated by the addition of the percentage conversions into *N*-benzylbenzamide and *N*-benzylacetamide.

Synthesis of Other Amides

General Procedure XIX – Synthesis of Formamides

(Table 2.17, Results and Discussion I)

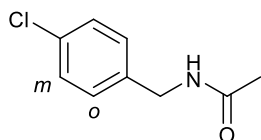
To an oven dried Radleys carousel tube containing the appropriate aniline (2 mmol), was added ethyl formate (1 mL, 2 M) followed by acetic acid (28.6 μL , 50 mol%) or formic acid (23.0 μL , 50 mol%). The carousel tube was then sealed and the reaction mixture heated at 20 $^\circ\text{C}$ for 16 hours. After being allowed to cool to room temperature, the solvent was removed *in vacuo* on a rotary evaporator and the resulting crude amide product was purified by silica column chromatography.

General Procedure XX – Synthesis of Higher Amides

(Table 2.17, Results and Discussion I)

To an oven dried Radleys carousel tube containing the appropriate amine (2 mmol), was added the appropriate ester followed by acetic acid (11.4 μL , 10 mol%), unless otherwise stated. The carousel tube was then sealed and the reaction mixture heated at 110 $^\circ\text{C}$, unless otherwise stated, for 20 hours. After being allowed to cool to room temperature, the solvent was removed *in vacuo* on a rotary evaporator and the resulting crude amide product was purified by silica column chromatography.

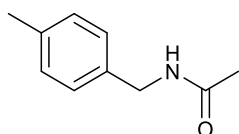
N-(4-Chlorobenzyl)acetamide²²⁴ (2.7)



Following general procedure XIII, 4-chlorobenzylamine (243 μL , 2 mmol) was used as the amine species. The title compound was recovered after purification by column chromatography (94:6, DCM/MeOH, R_f 0.31) as a beige solid (343 mg, 93%).

mp 107-108 °C (lit.²²⁴ 106-108 °C); ¹H NMR (500 MHz, CDCl₃): δ 7.29 (d, *J* = 8.3 Hz, 2H, *o*-CH_{Ar}), 7.21 (d, *J* = 8.3 Hz, 2H, *m*-CH_{Ar}), 5.80 (br s, 1H, NH), 4.39 (d, *J* = 5.9 Hz, 2H, CH₂), 2.02 (s, 3H, CH₃); ¹³C NMR (126 MHz, CDCl₃): δ 170.0, 136.8, 133.3, 129.1, 128.8, 43.0, 23.2; HRMS-ESI calcd for [C₉H₁₀ClNONa]⁺: 206.0349 [M+Na]⁺. Found: 206.0376; FT-IR (neat) ν in cm⁻¹: 1638 (C=O stretch). In agreement with previous literature data.

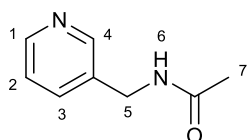
***N*-(4-Methylbenzyl)acetamide²²⁵ (2.2)**



Following general procedure XIII, 4-methylbenzylamine (255 μL, 2 mmol) was used as the amine species. The title compound was recovered after purification by column chromatography (94:6, DCM/MeOH, R_f 0.32) as a beige solid (323 mg, 99%).

mp 112-114 °C (lit.²²⁵ 111 °C); ¹H NMR (500 MHz, CDCl₃): δ 7.18 – 7.12 (m, 4H, CH_{Ar}), 5.76 (br s, 1H, NH), 4.38 (d, *J* = 5.6 Hz, 2H, CH₂), 2.33 (s, 3H, PhCH₃), 2.00 (s, 3H, C(O)CH₃); ¹³C NMR (126 MHz, CDCl₃): δ 169.8, 137.3, 135.2, 129.4, 127.9, 43.5, 23.3, 21.1; HRMS-ESI calcd for [C₁₀H₁₃NONa]⁺: 186.0895 [M+Na]⁺. Found: 186.0910; FT-IR (neat) ν in cm⁻¹: 1633 (C=O stretch). In agreement with previous literature data.

***N*-(Pyridin-3-ylmethyl)acetamide²²⁶ (2.8)**

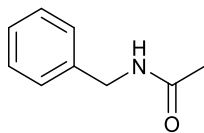


Following general procedure XIII, 3-picolylamine (204 μL, 2 mmol) was used as the amine species. The title compound was recovered after purification by column chromatography (88:12, DCM/MeOH, R_f 0.32) as a yellow oil (271 mg, 90%).

¹H NMR (300 MHz, CDCl₃): δ 8.52 – 8.47 (m, 2H, 1 & 4), 7.63 (d, *J* = 7.8 Hz, 1H, 3), 7.28 – 7.21 (m, 1H, 2), 6.19 (br s, 1H, 6), 4.43 (d, *J* = 5.9 Hz, 2H, 5), 2.02 (s, 3H, 7); ¹³C NMR (126 MHz, CDCl₃): δ 170.4, 149.1, 148.8, 135.8, 134.3, 123.7, 41.1, 23.2; HRMS-ESI calcd for [C₈H₁₁N₂O]⁺:

151.0871 [M+H]⁺. Found: 151.0871; FT-IR (neat) ν in cm⁻¹: 1648 (C=O stretch). In agreement with previous literature data.

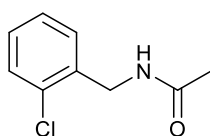
***N*-Benzylacetamide²²⁵ (2.9)**



Following general procedure XIII, benzylamine (218 μ L, 2 mmol) was used as the amine species. The title compound was recovered after purification by column chromatography (95:5, DCM/MeOH, R_f 0.37) as an off-white solid (283 mg, 95%).

mp 61-63 °C (lit.²²⁵ 61 °C); ¹H NMR (500 MHz, CDCl₃): δ 7.34 – 7.22 (m, 5H, *Ph*), 6.14 (br s, 1H, *NH*), 4.39 (d, *J* = 4.4 Hz, 2H, *CH*₂), 1.98 (s, 3H, *CH*₃); ¹³C NMR (126 MHz, CDCl₃): δ 170.0, 138.3, 128.6, 127.8, 127.4, 43.7, 23.2; HRMS-ESI calcd for [C₉H₁₁NONa]⁺: 172.0738 [M+Na]⁺. Found: 172.0758; FT-IR (neat) ν in cm⁻¹: 1640 (C=O stretch). In agreement with previous literature data.

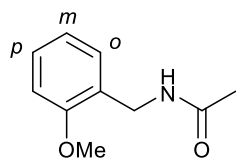
***N*-(2-Chlorobenzyl)acetamide²²⁷ (2.10)**



Following general procedure XIII, 2-chlorobenzylamine (241 μ L, 2 mmol) was used as the amine species. The title compound was recovered after purification by column chromatography (96:4, DCM/MeOH, R_f 0.30) as a white solid (348 mg, 95%).

mp 72-74 °C (lit.²²⁷ 71-73 °C); ¹H NMR (500 MHz, CDCl₃): δ 7.41 – 7.35 (m, 2H, *CH*_{Ar}), 7.25 – 7.22 (m, 2H, *CH*_{Ar}), 5.87 (br s, 1H, *NH*), 4.53 (d, *J* = 6.0 Hz, 2H, *CH*₂), 2.02 (s, 3H, *CH*₃); ¹³C NMR (126 MHz, CDCl₃): δ 170.1, 135.7, 133.5, 130.0, 129.4, 128.8, 127.0, 41.5, 23.1; HRMS-ESI calcd for [C₉H₁₀ClNONa]⁺: 206.0348 [M+Na]⁺. Found: 206.0359; FT-IR (neat) ν in cm⁻¹: 1639 (C=O stretch). In agreement with previous literature data.

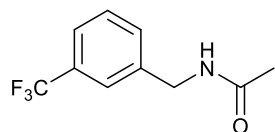
***N*-(2-Methoxybenzyl)acetamide²²⁷ (2.11)**



Following general procedure XIII, 2-methoxybenzylamine (261 μL , 2 mmol) was used as the amine species. The title compound was recovered after purification by column chromatography (95:5, DCM/MeOH, R_f 0.26) as a yellow solid (333 mg, 93%).

mp 93-95 $^{\circ}\text{C}$ (lit.²²⁷ 91-93 $^{\circ}\text{C}$); ^1H NMR (300 MHz, CDCl_3): δ 7.29 – 7.21 (m, 2H, *o*- CH_{Ar} and *p*- CH_{Ar}), 6.94 – 6.83 (m, 2H, *m*- CH_{Ar}), 6.12 (br s, 1H, NH), 4.40 (d, J = 5.8 Hz, 2H, CH_2), 3.84 (s, 3H, OCH_3), 1.95 (s, 3H, $\text{C}(\text{O})\text{CH}_3$); ^{13}C NMR (75 MHz, CDCl_3): δ 169.8, 157.5, 129.8, 128.9, 126.3, 120.7, 110.3, 55.3, 39.4, 23.4; HRMS-ESI calcd for $[\text{C}_{10}\text{H}_{13}\text{NO}_2\text{Na}]^+$: 202.0844 $[\text{M}+\text{Na}]^+$. Found: 202.0851; FT-IR (neat) ν in cm^{-1} : 1646 (C=O stretch). In agreement with previous literature data.

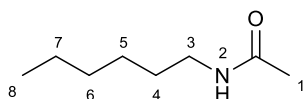
***N*-(3-(Trifluoromethyl)benzyl)acetamide²²⁸ (2.12)**



Following general procedure XIII, 3-(trifluoromethyl)benzylamine (287 μL , 2 mmol) was used as the amine species. The title compound was recovered after purification by column chromatography (93:7, DCM/MeOH, R_f 0.31) as a yellow-white solid (420 mg, 97%).

mp 56-57 $^{\circ}\text{C}$ (lit.²²⁸ 56-57 $^{\circ}\text{C}$); ^1H NMR (500 MHz, CDCl_3): δ 7.51 – 7.35 (m, 4H, CH_{Ar}), 6.67 (br s, 1H, NH), 4.39 (d, J = 6.0 Hz, 2H, CH_2), 1.95 (s, 3H, CH_3); ^{13}C NMR (126 MHz, CDCl_3): δ = 170.5, 139.6, 131.1, 131.0 (q, J = 32.2 Hz), 129.2, 124.3 (q, J = 3.8 Hz), 124.2 (q, J = 3.8 Hz), 124.1 (q, J = 272.2 Hz), 43.1, 23.0; ^{19}F NMR (470 MHz, CDCl_3): δ -62.67 (referenced against 4-fluorotoluene); HRMS-ESI calcd for $[\text{C}_{10}\text{H}_{10}\text{F}_3\text{NONa}]^+$: 240.0612 $[\text{M}+\text{Na}]^+$. Found: 240.0605; FT-IR (neat) ν in cm^{-1} : 1628 (C=O stretch). In agreement with previous literature data.

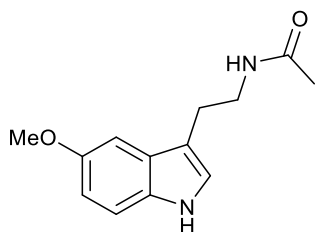
***N*-Hexylacetamide²²⁹ (2.13)**



Following general procedure XIII, hexylamine (264 μ L, 2 mmol) was used as the amine species. The title compound was recovered after purification by column chromatography (96:4, DCM/MeOH, R_f 0.36) as a colourless oil (276 mg, 97%).

^1H NMR (500 MHz, CDCl_3): δ 5.86 (br s, 1H, 2), 3.18 (td, $J = 7.2, 5.9$ Hz, 2H, 3), 1.93 (s, 3H, 1), 1.47 – 1.42 (m, 2H, 4), 1.29 – 1.22 (m, 6H, 5-7), 0.84 (t, $J = 6.7$ Hz, 3H, 8); ^{13}C NMR (126 MHz, CDCl_3): δ 170.2, 39.7, 31.4, 29.5, 26.6, 23.2, 22.5, 13.9; HRMS-ESI calcd for $[\text{C}_8\text{H}_{16}\text{NO}]^+$: 142.1226 $[\text{M}-\text{H}]^-$. Found: 142.1251; FT-IR (neat) ν in cm^{-1} : 1649 (C=O stretch). In agreement with previous literature data.

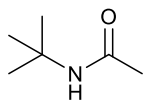
***N*-(2-(5-Methoxy-1*H*-indol-3-yl)ethyl)acetamide²³⁰ (2.14)**



Following general procedure XIII, 5-methoxytryptamine (380 mg, 2 mmol) was used as the amine species. The title compound was recovered after purification by column chromatography (94:6, DCM/MeOH, R_f 0.31) as a dark brown oil (324 mg, 70%).

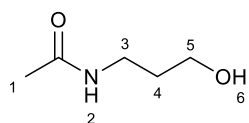
^1H NMR (500 MHz, $\text{DMSO}-d_6$): δ 10.63 (br s, 1H, CHNH), 7.92 (br s, 1H, CH_2NH), 7.22 (d, $J = 8.7$ Hz, 1H, NHCH), 7.09 (s, 1H, CH_{Ar}), 7.01 (s, 1H, CH_{Ar}), 6.74 – 6.68 (m, 1H, CH_{Ar}), 3.78 (s, 3H, OCH_3), 3.30 (q, $J = 7.0$ Hz, 2H, CH_2NH), 2.77 (t, $J = 7.4$ Hz, 2H, CCH_2), 1.81 (s, 3H, $\text{C}(\text{O})\text{CH}_3$); ^{13}C NMR (126 MHz, $\text{DMSO}-d_6$): δ 169.4, 153.4, 131.8, 128.0, 123.7, 112.4, 112.1, 111.5, 100.6, 55.8, 40.2, 25.7, 23.2; HRMS-ESI calcd for $[\text{C}_{13}\text{H}_{16}\text{N}_2\text{O}_2\text{Na}]^+$: 255.1109 $[\text{M}+\text{Na}]^+$. Found: 255.1116; FT-IR (neat) ν in cm^{-1} : 1627 (C=O stretch). In agreement with previous literature data.

***N*-(*tert*-butyl)acetamide (2.15)**



Following general procedure XIII, *tert*-butylamine (210 μ L, 2 mmol) was used as the amine species. Percentage conversion into **2.15** was calculated from the crude ^1H NMR spectra by comparison of the peaks corresponding to the starting material and **2.15**.

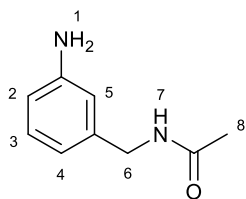
***N*-(3-Hydroxypropyl)acetamide²³¹ (2.16)**



Following general procedure XIII, 3-amino-1-propanol (150 mg, 2 mmol) was used as the amine species. The title compound was recovered after purification by column chromatography (90:10, DCM/MeOH) as a colourless oil (209 mg, 89%).

R_f (80:20, DCM/MeOH) 0.24; ^1H NMR (500 MHz, CDCl_3): δ 6.01 (br s, 1H, 2), 3.64 (t, $J = 5.6$ Hz, 2H, 5), 3.40 (q, $J = 6.1$ Hz, 2H, 3), 3.25 (br s, 1H, 6), 2.00 (s, 3H, 1), 1.71 – 1.65 (m, 2H, 4); ^{13}C NMR (126 MHz, CDCl_3): δ 171.4, 59.3, 36.4, 32.2, 23.1; HRMS-ESI calcd for $[\text{C}_5\text{H}_{12}\text{NO}_2]^+$: 118.0868 $[\text{M}+\text{H}]^+$. Found: 118.0881; FT-IR (neat) ν in cm^{-1} : 1625 (C=O stretch), 3287 (O-H stretch). In agreement with previous literature data.

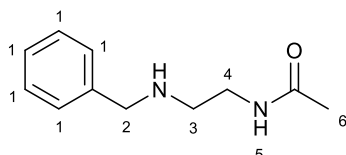
***N*-(3-Aminobenzyl)acetamide²³² (2.17)**



Following general procedure XIII, 3-aminobenzylamine (244 mg, 2 mmol) was used as the amine species. The title compound was recovered after purification by column chromatography (91:9, DCM/MeOH, R_f 0.28) as an orange-brown solid (308 mg, 94%).

mp 97-99 °C; ^1H NMR (500 MHz, CDCl_3): δ 7.11 (t, $J = 7.6$ Hz, 1H, 3), 6.68 – 6.63 (m, 1H, 5), 6.63 – 6.57 (m, 2H, 2 & 4), 5.66 (br s, 1H, 7), 4.34 (d, $J = 5.6$ Hz, 2H, 6), 3.69 (br s, 2H, 1), 2.02 (s, 3H, 8); ^{13}C NMR (126 MHz, CDCl_3): δ 169.8, 146.8, 139.4, 129.6, 117.9, 114.4, 114.2, 43.8, 23.3; HRMS-ESI calcd for $[\text{C}_{18}\text{H}_{24}\text{N}_4\text{O}_2\text{Na}]^+$: 351.1797 $[\text{2M}+\text{Na}]^+$. Found: 351.1747; FT-IR (neat) ν in cm^{-1} : 1617 (C=O stretch).

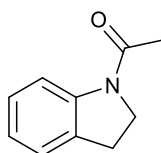
***N*-(2-(Benzylamino)ethyl)acetamide²³³ (2.18)**



Following general procedure XIII, *N*-benzylethylenediamine (300 μL , 2 mmol) was used as the amine species. The title compound was recovered after purification by column chromatography (90:10, DCM/MeOH) as a viscous yellow oil (346 mg, 90%).

R_f (85:15, DCM/MeOH) 0.28; ^1H NMR (500 MHz, CDCl_3): δ 7.36 – 7.24 (m, 5H, 1), 6.05 (br s, 1H, 5), 3.79 (s, 2H, 2), 3.34 (q, $J = 5.5$ Hz, 2H, 4), 2.78 (t, $J = 5.5$ Hz, 2H, 3), 1.97 (s, 3H, 6); ^{13}C NMR (126 MHz, CDCl_3): δ 170.6, 139.7, 128.5, 128.1, 127.1, 53.5, 48.0, 39.1, 23.1; HRMS-ESI calcd for $[\text{C}_{11}\text{H}_{17}\text{N}_2\text{O}]^+$: 193.1341 $[\text{M}+\text{H}]^+$. Found: 193.1324; FT-IR (neat) ν in cm^{-1} : 1638 (C=O stretch).

1-(Indolin-1-yl)ethan-1-one²³⁴ (2.19)

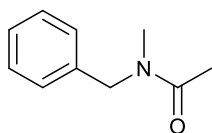


Following general procedure XIV, indoline (224 μL , 2 mmol) was used as the amine species. The title compound was recovered after purification by column chromatography (97:3, DCM/MeOH, R_f 0.31) as a brown solid (251 mg, 78%).

mp 98-100 °C (lit.²³⁴ mp 100-102 °C); ^1H NMR (500 MHz, DMSO-d_6): δ 8.03 (d, $J = 7.6$ Hz, 1H, CH_{Ar}), 7.21 (d, $J = 7.6$ Hz, 1H, CH_{Ar}), 7.13 (t, $J = 7.6$ Hz, 1H, CH_{Ar}), 6.97 (t, $J = 7.6$ Hz, 1H, CH_{Ar}), 4.07 (t, $J = 8.5$ Hz, 2H, NCH_2), 3.12 (t, $J = 8.5$ Hz, 2H, NCH_2CH_2), 2.14 (s, 3H, CH_3); ^{13}C NMR (126

MHz, DMSO-d⁶): δ 168.5, 142.9, 131.7, 126.9, 124.7, 123.0, 115.8, 48.1, 27.3, 24.0; HRMS-ESI calcd for [C₁₀H₁₁NONa]⁺: 184.0738 [M+Na]⁺. Found: 184.0737; FT-IR (neat) ν in cm⁻¹: 1642 (C=O stretch). In agreement with previous literature data.

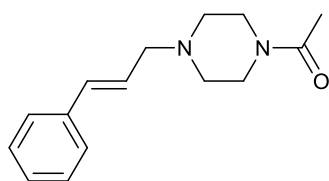
***N*-Benzyl-*N*-methylacetamide²³⁵ (2.4)**



Following general procedure XIV, *N*-benzylmethylamine (258 μ L, 2 mmol) was used as the amine species. The title compound was recovered after purification by column chromatography (96:4, DCM/MeOH, R_f 0.33) as a yellow-brown oil (296 mg, 91%). The product was observed as two rotamers in its ¹H and ¹³C NMR spectra.

¹H NMR (500 MHz, DMSO-d⁶): δ 7.36 – 7.16 (m, 5H, *Ph*), 4.53 (s, 2H, minor rotamer, CH₂), 4.46 (s, 2H, major rotamer, CH₂), 2.88 (s, 3H, major rotamer, NCH₃), 2.77 (s, 3H, minor rotamer, NCH₃), 2.04 (s, 3H, major rotamer, C(O)CH₃), 2.02 (s, 3H, minor rotamer, C(O)CH₃); ¹³C NMR (126 MHz, CDCl₃): δ 170.3 (major rotamer), 170.3 (minor rotamer), 138.3 (major rotamer), 138.0 (minor rotamer), 129.2 (minor rotamer), 128.8 (major rotamer), 127.9 (major rotamer), 127.6 (minor rotamer), 127.4 (minor rotamer), 127.0 (major rotamer), 53.7 (minor rotamer), 50.1 (major rotamer), 35.8 (major rotamer), 33.6 (minor rotamer), 22.0 (major rotamer), 21.7 (minor rotamer); HRMS-ESI calcd for [C₁₀H₁₃NONa]⁺: 186.0895 [M+Na]⁺. Found: 186.0897; FT-IR (neat) ν in cm⁻¹: 1638 (C=O stretch). In agreement with previous literature data.

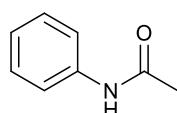
1-(4-Cinnamylpiperazin-1-yl)ethan-1-one²³⁶ (2.20)



Following general procedure XIV, 1-cinnamylpiperazine (405 mg, 2 mmol) was used as the amine species. The title compound was recovered after purification by column chromatography (88:12, DCM/MeOH, R_f 0.31) as a dark brown oil (451 mg, 92%).

^1H NMR (500 MHz, CDCl_3): δ 7.45 – 7.42 (m, 2H, *Ph*), 7.35 – 7.29 (m, 2H, *Ph*), 7.26 – 7.21 (m, 1H, *Ph*), 6.53 (d, $J = 16.0$ Hz, 1H, *PhCH*), 6.30 (dt, $J = 16.0, 6.6$ Hz, 1H, *PhCHCH*), 3.48 – 3.39 (m, 4H, $\text{C}(\text{O})\text{NCH}_2$), 3.11 (d, $J = 6.6$ Hz, 2H, CHCH_2), 2.39 (t, $J = 5.1$ Hz, 2H, CH_2NCH_2), 2.34 (t, $J = 5.1$ Hz, 2H, CH_2NCH_2), 1.98 (s, 3H, CH_3); ^{13}C NMR (126 MHz, CDCl_3): δ 168.1, 136.6, 132.3, 128.5, 127.4, 126.7, 126.2, 60.0, 52.8, 52.3, 45.6, 40.8, 21.2; HRMS-ESI calcd for $[\text{C}_{15}\text{H}_{20}\text{N}_2\text{ONa}]^+$: 267.1473 $[\text{M}+\text{Na}]^+$. Found: 267.1480; FT-IR (neat) ν in cm^{-1} : 1627 (C=O stretch).

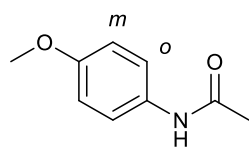
***N*-Phenylacetamide²³⁷ (2.6)**



Following general procedure XV, aniline (182 μL , 2 mmol) was used as the amine species. The title compound was recovered after purification by column chromatography (95:5, DCM/MeOH, R_f 0.30) as a pale brown solid (249 mg, 92%).

mp 114-116 $^\circ\text{C}$ (lit.²³⁷ 114-115 $^\circ\text{C}$); ^1H NMR (500 MHz, DMSO-d_6): δ 9.90 (br s, 1H, *NH*), 7.57 (d, $J = 8.0$ Hz, 2H, *Ph*), 7.28 (t, $J = 7.7$ Hz, 2H, *Ph*), 7.01 (t, $J = 7.4$ Hz, 1H, *Ph*), 2.04 (s, 3H, $\text{C}(\text{O})\text{CH}_3$); ^{13}C NMR (126 MHz, DMSO-d_6): δ 168.2, 139.3, 128.6, 122.9, 118.9, 24.0; HRMS-ESI calcd for $[\text{C}_8\text{H}_{10}\text{NO}]^+$: 136.0762 $[\text{M}+\text{H}]^+$. Found: 136.0773; FT-IR (neat) ν in cm^{-1} : 1662 (C=O stretch). In agreement with previous literature data.

***N*-(4-Methoxyphenyl)acetamide²³⁷ (2.21)**

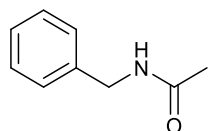


Following general procedure XV, *p*-anisidine (246 mg, 2 mmol) was used as the amine species. The title compound was recovered after purification by column chromatography (95:5, DCM/MeOH, R_f 0.26) as a brown solid (290 mg, 88%).

mp 129-130 $^\circ\text{C}$ (lit.²³⁷ 128-129 $^\circ\text{C}$); ^1H NMR (500 MHz, DMSO-d_6): δ 9.76 (br s, 1H, *NH*), 7.48 (d, $J = 8.9$ Hz, 2H, *o-CH_{Ar}*), 6.86 (d, $J = 8.9$ Hz, 2H, *m-CH_{Ar}*), 3.71 (s, 3H, OCH_3), 2.00 (s, 3H, $\text{C}(\text{O})\text{CH}_3$); ^{13}C NMR (126 MHz, DMSO-d_6): δ 167.7, 155.0, 132.5, 120.5, 113.8, 55.1, 23.8; ESI-

MS of $[C_9H_{11}NO_2]^+$; HRMS-ESI calcd for $[C_9H_{12}NO_2]^+$: 166.0868 $[M+H]^+$. Found: 166.0887; FT-IR (neat) ν in cm^{-1} : 1646 (C=O stretch). In agreement with previous literature data.

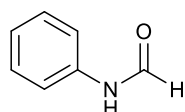
***N*-Benzylacetamide²²⁵ (2.9)**



Following general procedure XVI, benzylamine (7.3 mL, 67 mmol) was used as the amine species. The title compound was recovered after purification by column chromatography (95:5, DCM/MeOH, R_f 0.37) as an off-white solid (9.18 g, 92%).

mp 61-63 °C (lit.²²⁵ 61 °C); 1H NMR (500 MHz, $CDCl_3$): δ 7.34 – 7.21 (m, 5H, *Ph*), 6.18 (br s, 1H, *NH*), 4.37 (d, $J = 4.4$ Hz, 2H, CH_2), 1.97 (s, 3H, CH_3); ^{13}C NMR (126 MHz, $CDCl_3$): δ 170.1, 138.4, 128.7, 127.9, 127.5, 43.8, 23.2; HRMS-ESI calcd for $[C_9H_{11}NONa]^+$: 172.0738 $[M+Na]^+$. Found: 172.0752; FT-IR (neat) ν in cm^{-1} : 1642 (C=O stretch). In agreement with previous literature data.

***N*-Phenylformamide²³⁸ (2.22)**

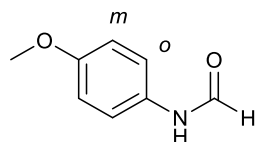


Following general procedure XIX, aniline (182 μ L, 2 mmol) was used as the amine species. The title compound was recovered after purification by column chromatography (95:5, DCM/MeOH, R_f 0.30) as a colourless oil (228 mg, 94%).

1H NMR (300 MHz, $DMSO-d_6$): δ 10.27 – 10.08 (m, 1H, minor and major rotamers, *NH*), 8.79 (d, $J = 11.0$ Hz, 1H, minor rotamer, *CHO*), 8.27 (d, $J = 1.9$ Hz, 1H, major rotamer, *CHO*), 7.59 (d, $J = 7.6$ Hz, 2H, major rotamer, *Ph*), 7.37 – 7.26 (m, 2H, minor and major rotamers, *Ph*), 7.19 (d, $J = 7.5$ Hz, 2H, minor rotamer, *Ph*), 7.11 – 7.02 (m, 1H, minor and major rotamers, *Ph*); ^{13}C NMR (75 MHz, $DMSO-d_6$): δ 162.6 (minor rotamer), 159.6 (major rotamer), 138.4 (minor rotamer), 138.3 (major rotamer), 129.4 (minor rotamer), 128.9 (major rotamer), 123.7 (minor rotamer), 123.6 (major rotamer), 119.1 (major rotamer), 117.5 (minor rotamer); HRMS-ESI

calcd for $[C_7H_7NONa]^+$: 144.0425 $[M+Na]^+$. Found: 144.0481; FT-IR (neat) ν in cm^{-1} : 1670 (C=O stretch). In agreement with previous literature data.

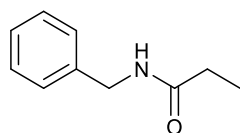
***N*-(4-Methoxyphenyl)formamide²³⁸ (2.23)**



Following general procedure XIX, *p*-anisidine (246 mg, 2 mmol) was used as the amine species. The title compound was recovered after purification by column chromatography (95:5, DCM/MeOH, R_f 0.25) as a white-yellow solid (278 mg, 92%).

mp 79-81 °C (lit.²³⁸ 79-81 °C); 1H NMR (500 MHz, DMSO- d_6): δ 10.05 – 9.90 (m, 1H, minor and major rotamers, NH), 8.59 (d, J = 11.1 Hz, 1H, minor rotamer, CHO), 8.20 (d, J = 1.6 Hz, 1H, major rotamer, CHO), 7.50 (d, J = 9.0 Hz, 2H, major rotamer, o - CH_{Ar}), 7.11 (d, J = 9.0 Hz, 2H, minor rotamer, o - CH_{Ar}), 6.91 – 6.86 (m, 2H, minor and major rotamers, m - CH_{Ar}), 3.72 (s, 3H, OCH_3); ^{13}C NMR (126 MHz, DMSO- d_6): δ 162.5 (minor rotamer), 159.0 (major rotamer), 156.0 (minor rotamer), 155.4 (major rotamer), 131.4 (major rotamer), 131.3 (minor rotamer), 120.6 (major rotamer), 119.7 (minor rotamer), 114.6 (minor rotamer), 114.0 (major rotamer), 55.3 (minor rotamer), 55.2 (major rotamer); HRMS-ESI calcd for $[C_8H_9NO_2Na]^+$: 174.0531 $[M+Na]^+$. Found: 174.0546; FT-IR (neat) ν in cm^{-1} : 1655 (C=O stretch). In agreement with previous literature data.

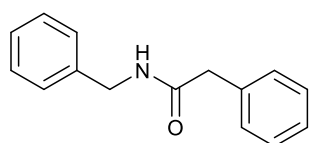
***N*-Benzylpropionamide²³⁹ (2.24)**



Following general procedure XX, benzylamine (218 μ L, 2 mmol) and ethyl propionate (461 μ L, 4 mmol) were used as the amine and ester species, respectively. The title compound was recovered after purification by column chromatography (100% DCM) as a yellow oil (300 mg, 92%).

R_f (96:4, DCM/MeOH) 0.34; ^1H NMR (300 MHz, CDCl_3): δ 7.38 – 7.24 (m, 5H, *Ph*), 5.71 (br s, 1H, *NH*), 4.45 (d, $J = 5.7$ Hz, 2H, PhCH_2), 2.25 (q, $J = 7.6$ Hz, 2H, CH_3CH_2), 1.19 (t, $J = 7.6$ Hz, 3H, CH_3); ^{13}C NMR (75 MHz, CDCl_3): δ 173.6, 138.4, 128.8, 127.9, 127.6, 43.6, 29.8, 9.9; HRMS-ESI calcd for $[\text{C}_{10}\text{H}_{13}\text{NONa}]^+$: 186.0895 $[\text{M}+\text{Na}]^+$. Found: 186.0949; FT-IR (neat) ν in cm^{-1} : 1641 (C=O stretch). In agreement with previous literature data.

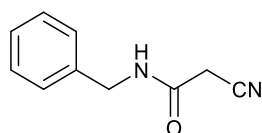
***N*-Benzyl-2-phenylacetamide²⁴⁰ (2.25)**



Following general procedure XX, benzylamine (218 μL , 2 mmol) and ethyl phenylacetate (638 μL , 4 mmol) were used as the amine and ester species, respectively. The title compound was recovered after purification by column chromatography (from 100% DCM to 96:4, DCM/MeOH) as a white solid (419 mg, 93%).

R_f (99:1, DCM/MeOH) 0.34; mp 123-124 $^{\circ}\text{C}$ (lit.²⁴⁰ 121-123 $^{\circ}\text{C}$); ^1H NMR (500 MHz, CDCl_3): δ 7.37 – 7.21 (m, 8H, *Ph*), 7.20 – 7.15 (m, 2H, *Ph*), 6.05 (br s, 1H, *NH*), 4.38 (d, $J = 5.9$ Hz, 2H, NHCH_2), 3.58 (s, 2H, $\text{C}(\text{O})\text{CH}_2$); ^{13}C NMR (126 MHz, CDCl_3): δ 170.9, 138.2, 134.9, 129.4, 129.0, 128.6, 127.5, 127.4, 127.3, 43.8, 43.6; HRMS-ESI calcd for $[\text{C}_{15}\text{H}_{15}\text{NONa}]^+$: 248.1051 $[\text{M}+\text{Na}]^+$. Found: 248.1108; FT-IR (neat) ν in cm^{-1} : 1636 (C=O stretch). In agreement with previous literature data.

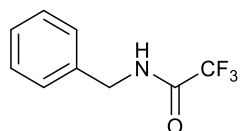
***N*-Benzyl-2-cyanoacetamide²⁴¹ (2.26)**



Following general procedure XX, benzylamine (218 μL , 2 mmol) and ethyl cyanoacetate (426 μL , 4 mmol) were used as the amine and ester species, respectively. The title compound was recovered after purification by column chromatography (from 100% DCM to 96:4, DCM/MeOH) as a white solid (327 mg, 94%).

R_f (96:4, DCM/MeOH) 0.31; mp 124-126 °C (lit.²⁴¹ 124 °C); ¹H NMR (500 MHz, CDCl₃): δ 7.47 – 7.17 (m, 5H, *Ph*), 6.54 (br s, 1H, *NH*), 4.45 (d, *J* = 5.7 Hz, 2H, *PhCH*₂), 3.36 (s, 2H, *CNCH*₂); ¹³C NMR (126 MHz, CDCl₃): δ 160.8, 136.8, 128.9, 128.0, 127.9, 114.6, 44.4, 25.8; HRMS-ESI calcd for [C₁₀H₁₀N₂O₂Na]⁺: 197.0691 [M+Na]⁺. Found: 197.0696; FT-IR (neat) ν in cm⁻¹: 1643 (C=O stretch), 2257 (C≡N stretch). In agreement with previous literature data.

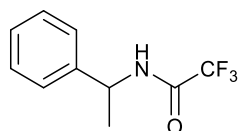
***N*-Benzyl-2,2,2-trifluoroacetamide²⁴² (2.27)**



Following general procedure XX, benzylamine (218 μL, 2 mmol) and ethyl trifluoroacetate (238 μL, 2 mmol) were used as the amine and ester species, respectively, and the reaction was performed at room temperature (25 °C) with no acid catalyst present. The title compound was recovered after purification by column chromatography (100% DCM, R_f 0.36) as a white solid (406 mg, 100%).

mp 74-75 °C (lit.²⁴³ 74-75 °C); ¹H NMR (300 MHz, CDCl₃): δ 7.46 – 7.19 (m, 5H, *Ph*), 6.82 (br s, 1H, *NH*), 4.51 (d, *J* = 5.8 Hz, 2H, *CH*₂); ¹³C NMR (75 MHz, CDCl₃): δ 157.2 (q, *J* = 37.1 Hz), 135.9, 129.1, 128.3, 128.0, 115.9 (q, *J* = 287.7 Hz), 43.9; ¹⁹F NMR (470 MHz, CDCl₃): δ -75.84 (referenced against 4-fluorotoluene); HRMS-ESI calcd for [C₉H₇F₃NO]⁺: 202.0480 [M+H]⁺. Found: 202.0486; FT-IR (neat) ν in cm⁻¹: 1699 (C=O stretch). In agreement with previous literature data.

2,2,2-Trifluoro-*N*-(1-phenylethyl)acetamide²⁴⁴ (2.28)

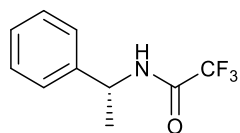


Following general procedure XX, *racemic*-methylbenzylamine (255 μL, 2 mmol) and ethyl trifluoroacetate (238 μL, 2 mmol) were used as the amine and ester species, respectively, and the reaction was performed at room temperature (25 °C) with no acid catalyst present. The

title compound was recovered after purification by column chromatography (100% DCM, R_f 0.30) as a white solid (433 mg, 100%).

mp 89-90 °C (lit.²⁴⁵ 88 °C); ^1H NMR (500 MHz, CDCl_3): δ 7.41 – 7.36 (m, 2H, *Ph*), 7.35 – 7.30 (m, 3H, *Ph*), 6.43 (br s, 1H, *NH*), 5.15 (quint, $J = 7.1$ Hz, 1H, *NHCH*), 1.60 (d, $J = 7.1$ Hz, 3H, CH_3); ^{13}C NMR (126 MHz, CDCl_3): δ 156.3 (q, $J = 37.0$ Hz), 140.9, 129.0, 128.1, 126.1, 115.8 (q, $J = 288.1$ Hz), 49.8, 21.0; ^{19}F NMR (470 MHz, CDCl_3): δ -75.92 (referenced against 4-fluorotoluene); HRMS-ESI calcd for $[\text{C}_{10}\text{H}_{11}\text{F}_3\text{NO}]^+$: 218.0793 $[\text{M}+\text{H}]^+$. Found: 218.0789; FT-IR (neat) ν in cm^{-1} : 1693 (C=O stretch); $[\alpha]_{\text{D}}^{20} + 0$ (c 1.0 in CHCl_3); HPLC: Chiracel OD column (25 cm), 1.0 mL min^{-1} , 98:2 Hexane:IPA, (*S*)-enantiomer retention time 11.20 minutes, (*R*)-enantiomer retention time 19.40 minutes. In agreement with previous literature data.

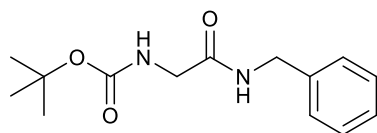
(*R*)-2,2,2-Trifluoro-*N*-(1-phenylethyl)acetamide²⁴⁵ (2.29)



Following general procedure XX, (*R*)-(+)- α -methylbenzylamine (255 μL , 2 mmol) and ethyl trifluoroacetate (238 μL , 2 mmol) were used as the amine and ester species, respectively, and the reaction was performed at room temperature (25 °C) with no acid catalyst present. The title compound was recovered after purification by column chromatography (100% DCM, R_f 0.30) as a white solid (434 mg, 100%).

mp 89 °C (lit.²⁴⁵ 88 °C); ^1H NMR (500 MHz, CDCl_3): δ 7.41 – 7.36 (m, 2H, *Ph*), 7.35 – 7.30 (m, 3H, *Ph*), 6.43 (br s, 1H, *NH*), 5.15 (quint, $J = 7.1$ Hz, 1H, *NHCH*), 1.60 (d, $J = 7.1$ Hz, 3H, CH_3); ^{13}C NMR (126 MHz, CDCl_3): δ 156.3 (q, $J = 37.0$ Hz), 140.9, 129.0, 128.1, 126.1, 115.8 (q, $J = 288.1$ Hz), 49.8, 21.0; ^{19}F NMR (470 MHz, CDCl_3): δ -75.92 (referenced against 4-fluorotoluene); HRMS-ESI calcd for $[\text{C}_{10}\text{H}_{11}\text{F}_3\text{NO}]^+$: 218.0793 $[\text{M}+\text{H}]^+$. Found: 218.0797; FT-IR (neat) ν in cm^{-1} : 1697 (C=O stretch); $[\alpha]_{\text{D}}^{20} + 138$ (c 1.0 in CHCl_3) (lit.²⁰⁶ $[\alpha]_{\text{D}}^{25} + 137$ (c 1.0 in CHCl_3)); HPLC: Chiracel OD column (25 cm), 1.0 mL min^{-1} , 98:2 Hexane:IPA, (*R*)-enantiomer retention time 18.81 minutes, no peak observed for (*S*)-enantiomer at 11.20 minutes, $ee > 99\%$. In agreement with previous literature data.

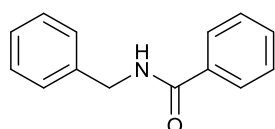
***tert*-Butyl (2-(benzylamino)-2-oxoethyl)carbamate²⁴⁶ (2.30)**



Following general procedure XX, benzylamine (218 μ L, 2 mmol) and *N*-Boc-glycine methyl ester (351 μ L, 2 mmol) were used as the amine and ester species, respectively. The title compound was recovered after purification by column chromatography (94:6, DCM/MeOH, R_f 0.32) as an off-white solid (512 mg, 97%).

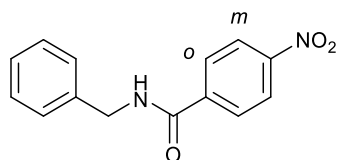
mp 66-68 °C (lit.²⁴⁶ 65 °C); ^1H NMR (300 MHz, CDCl_3): δ 7.34 – 7.16 (m, 5H, *Ph*), 6.93 (br s, 1H, PhCH_2NH), 5.50 (t, $J = 5.1$ Hz, 1H, OC(O)NH), 4.39 (d, $J = 5.8$ Hz, 2H, PhCH_2), 3.79 (d, $J = 5.1$ Hz, 2H, C(O)CH_2), 1.39 (s, 9H, $(\text{CH}_3)_3$); ^{13}C NMR (75 MHz, CDCl_3): δ 169.6, 156.2, 138.0, 128.7, 127.6, 127.5, 80.2, 44.4, 43.3, 28.3; HRMS-ESI calcd for $[\text{C}_{14}\text{H}_{20}\text{N}_2\text{O}_3\text{Na}]^+$: 287.1372 $[\text{M}+\text{Na}]^+$. Found: 287.1346; FT-IR (neat) ν in cm^{-1} : 1655 (amide C=O stretch), 1703 (carbamate C=O stretch). In agreement with previous literature data.

***N*-Benzylbenzamide (2.31)**



Following general procedure XX, benzylamine (218 μ L, 2 mmol) and methyl benzoate (250 μ L, 2 mmol) were used as the amine and ester species, respectively, and the reaction was performed at 150 °C. Percentage conversion into **2.31** was calculated from the crude ^1H NMR spectra by comparison of the peaks corresponding to the starting material and and **2.31**.

***N*-Benzyl-4-nitrobenzamide²⁴⁷ (2.32)**



Following general procedure XX, benzylamine (218 μL , 2 mmol) and methyl 4-nitrobenzoate (362 mg, 2 mmol) were used as the amine and ester species, respectively, and the reaction was performed at 150 $^{\circ}\text{C}$. The title compound was recovered after purification by column chromatography (from 100% DCM to 96:4, DCM/MeOH) as an off-white solid (307 mg, 60%). R_f (98:2, DCM/MeOH) 0.33; mp 140-142 $^{\circ}\text{C}$ (lit.²⁴⁸ 139-140 $^{\circ}\text{C}$); ^1H NMR (500 MHz, CDCl_3): δ 8.26 (d, $J = 8.9$ Hz, 2H, $m\text{-CH}_{Ar}$), 7.94 (d, $J = 8.9$ Hz, 2H, $o\text{-CH}_{Ar}$), 7.40 – 7.29 (m, 5H, *Ph*), 6.59 (br s, 1H, NH), 4.65 (d, $J = 5.7$ Hz, 2H, CH_2); ^{13}C NMR (126 MHz, CDCl_3): δ 165.3, 149.6, 139.9, 137.4, 128.9, 128.2, 128.0, 127.9, 123.8, 44.5; HRMS-ESI calcd for $[\text{C}_{14}\text{H}_{12}\text{N}_2\text{O}_3\text{Na}]^+$: 279.0746 $[\text{M}+\text{Na}]^+$. Found: 279.0726; FT-IR (neat) ν in cm^{-1} : 1629 (C=O stretch). In agreement with previous literature data.

Investigations into the Reaction Mechanism

General Procedure XXI – $\text{PhCH}_2\text{CH}_2\text{CO}_2\text{H}$ Catalyst Screen

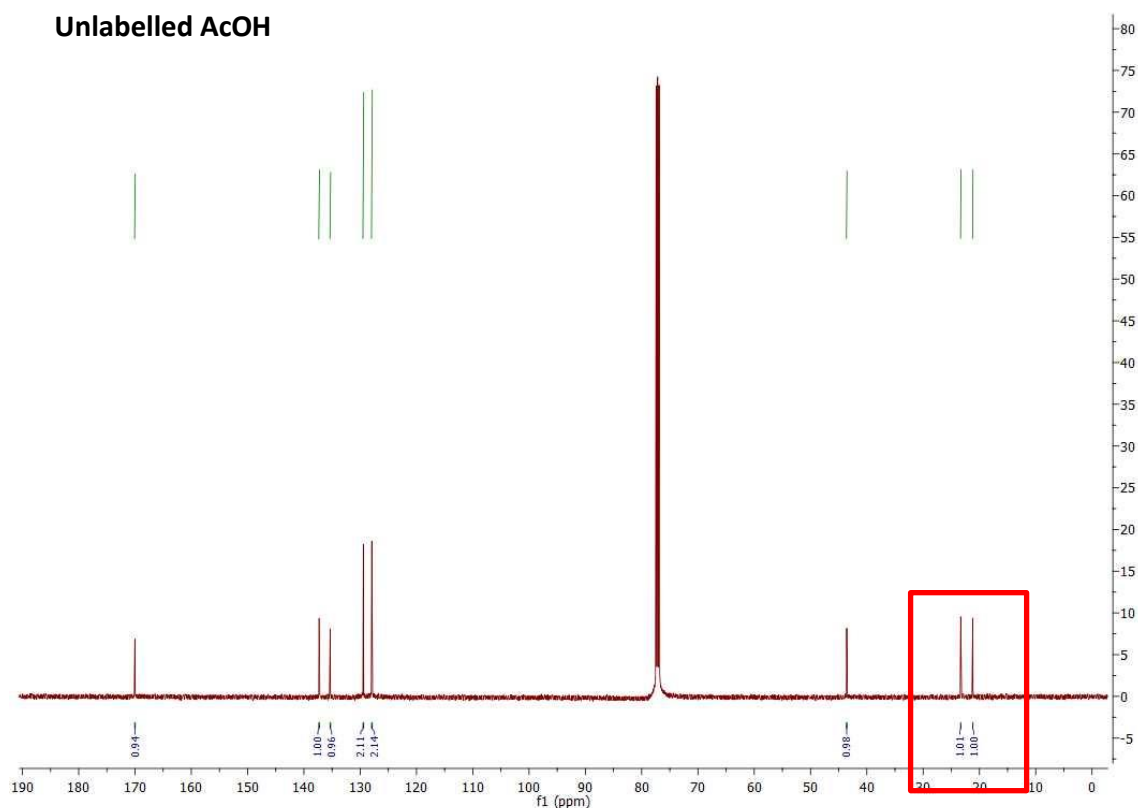
(Table 2.19, Results and Discussion I)

To an oven dried Radleys carousel tube containing 4-methylbenzylamine (127 μL , 1 mmol) was added the appropriate amount of ethyl acetate, followed by the appropriate amount of 3-phenylpropionic acid. The carousel tube was then sealed and the reaction mixture heated at 80 $^{\circ}\text{C}$ for 20 hours. After being allowed to cool to room temperature, the reaction mixture was diluted with ethyl acetate (20 mL) and washed with NaHCO_3 (3 x 20 mL). The organics were dried with MgSO_4 , filtered and concentrated *in vacuo* on a rotary evaporator. The resulting crude reaction mixture was analysed by ^1H NMR spectroscopy. Percentage conversion into *N*-(4-methylbenzyl)acetamide and *N*-(4-methylbenzyl)-3-phenylpropanamide was calculated from the crude ^1H NMR spectra by comparison of the peaks at 3.85 ppm (2H, 4-methylbenzylamine), 4.39 ppm (2H, *N*-(4-methylbenzyl)acetamide and *N*-(4-methylbenzyl)-3-phenylpropanamide). Product ratios were also calculated from the crude ^1H NMR spectra by comparison of the peaks at 3.00 ppm (2H, *N*-(4-methylbenzyl)-3-phenylpropanamide) and 2.02 ppm (3H, *N*-(4-methylbenzyl)acetamide).

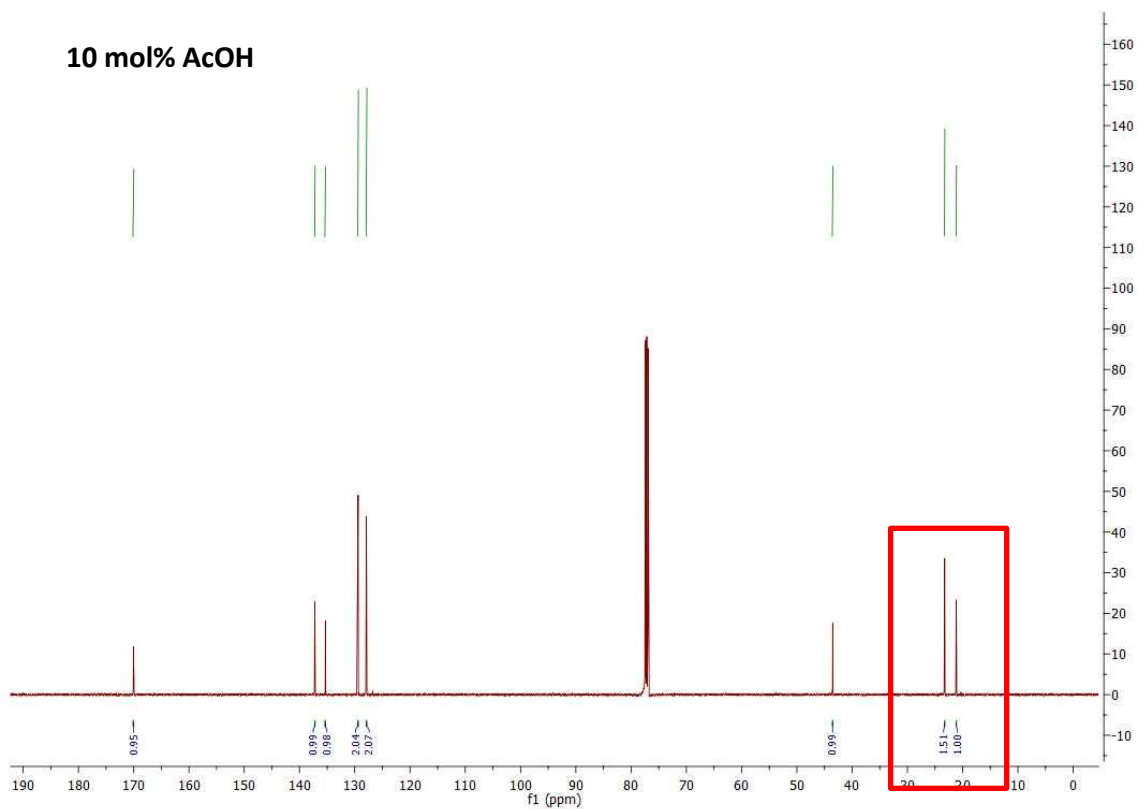
General Procedure XXII – ^{13}C -Labelled Acetic Acid Screen

(Table 2.20, Results and Discussion I)

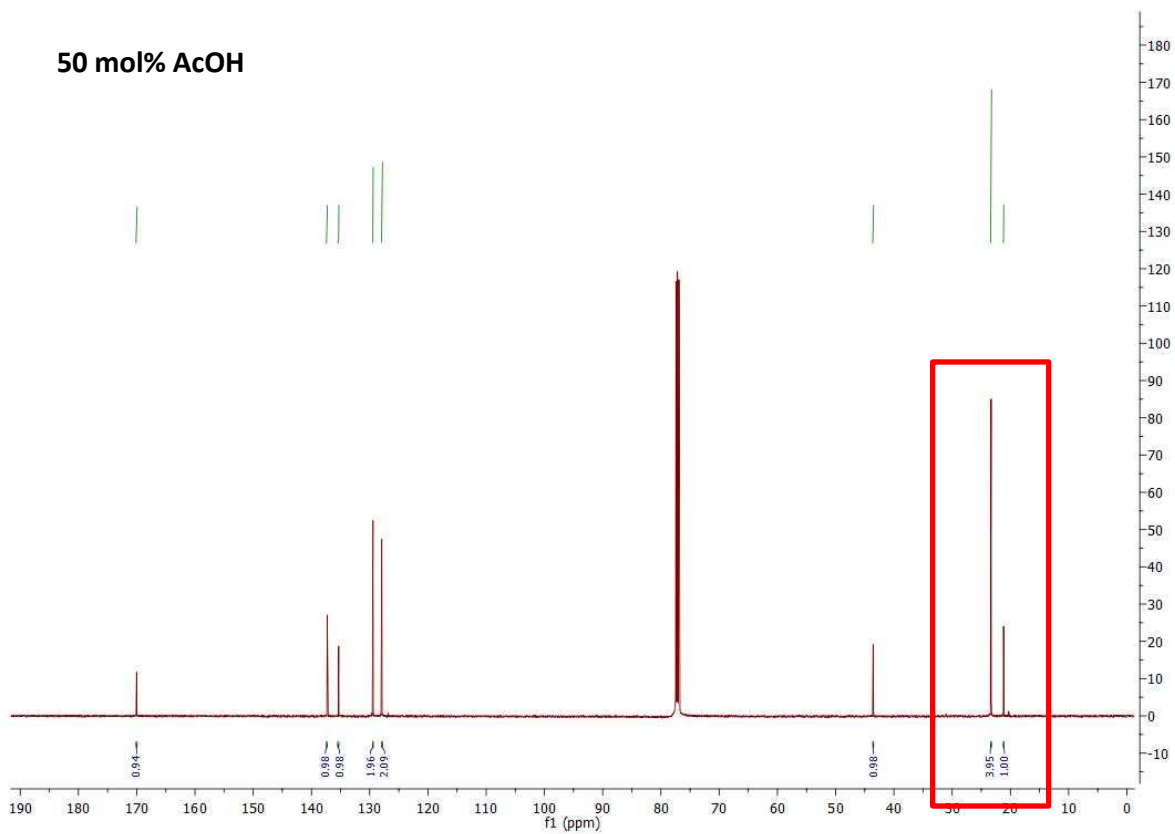
To an oven dried Radleys carousel tube containing 4-methylbenzylamine (127 μL , 1 mmol) was added ethyl acetate (0.5 mL, 2 M) followed by the appropriate amount of acetic acid-2- ^{13}C . The carousel tube was then sealed and the reaction mixture heated at 80 $^{\circ}\text{C}$ for 20 hours. After being allowed to cool to room temperature, the reaction mixture was diluted with ethyl acetate (20 mL) and washed with NaHCO_3 (3 x 20 mL). The organics were dried with MgSO_4 , filtered and concentrated *in vacuo* on a rotary evaporator. The resulting crude reaction mixture was analysed by ^1H and ^{13}C NMR spectroscopy. Percentage incorporation of labelled acetic acid was calculated using (i) the integrals of the two acetyl methyl peaks in each of the quantitative ^{13}C NMR spectra; (ii) the integrals of the arene methyl satellite peaks and the acetyl methyl satellite peaks in each of the ^1H NMR spectra.



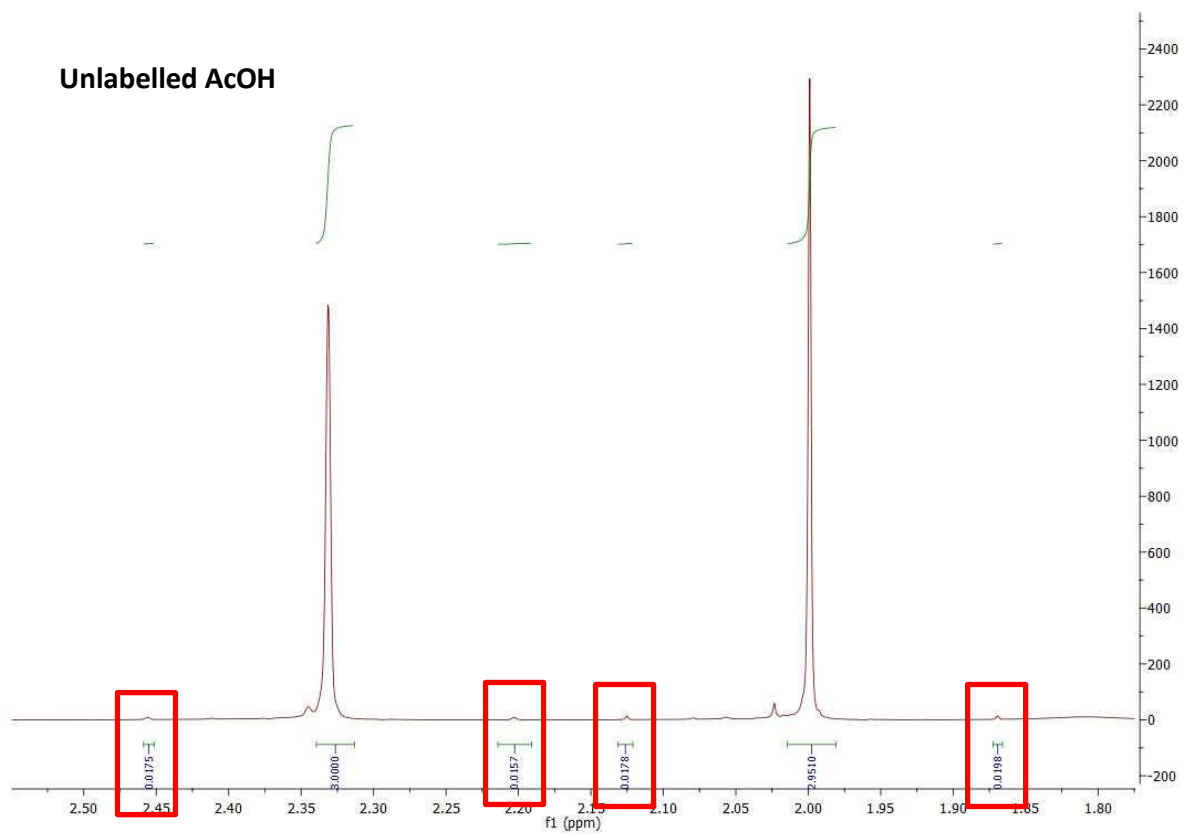
10 mol% AcOH



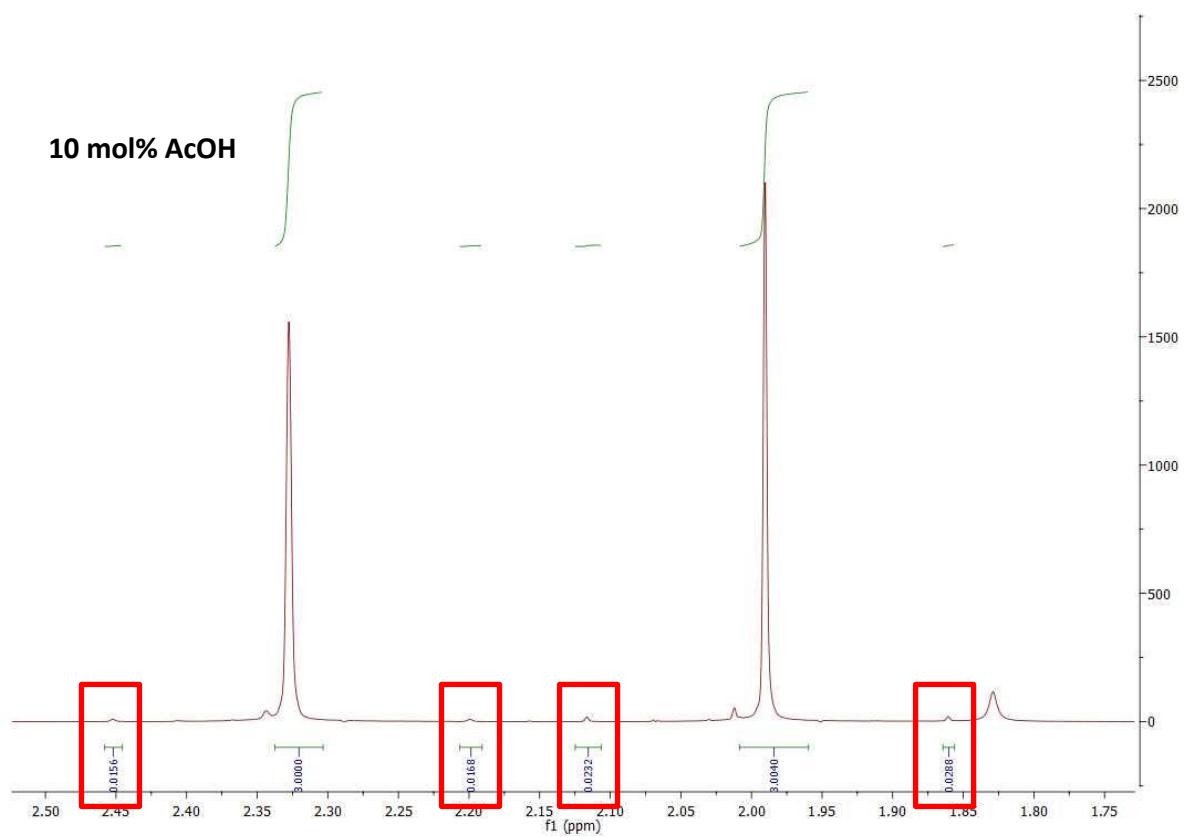
50 mol% AcOH

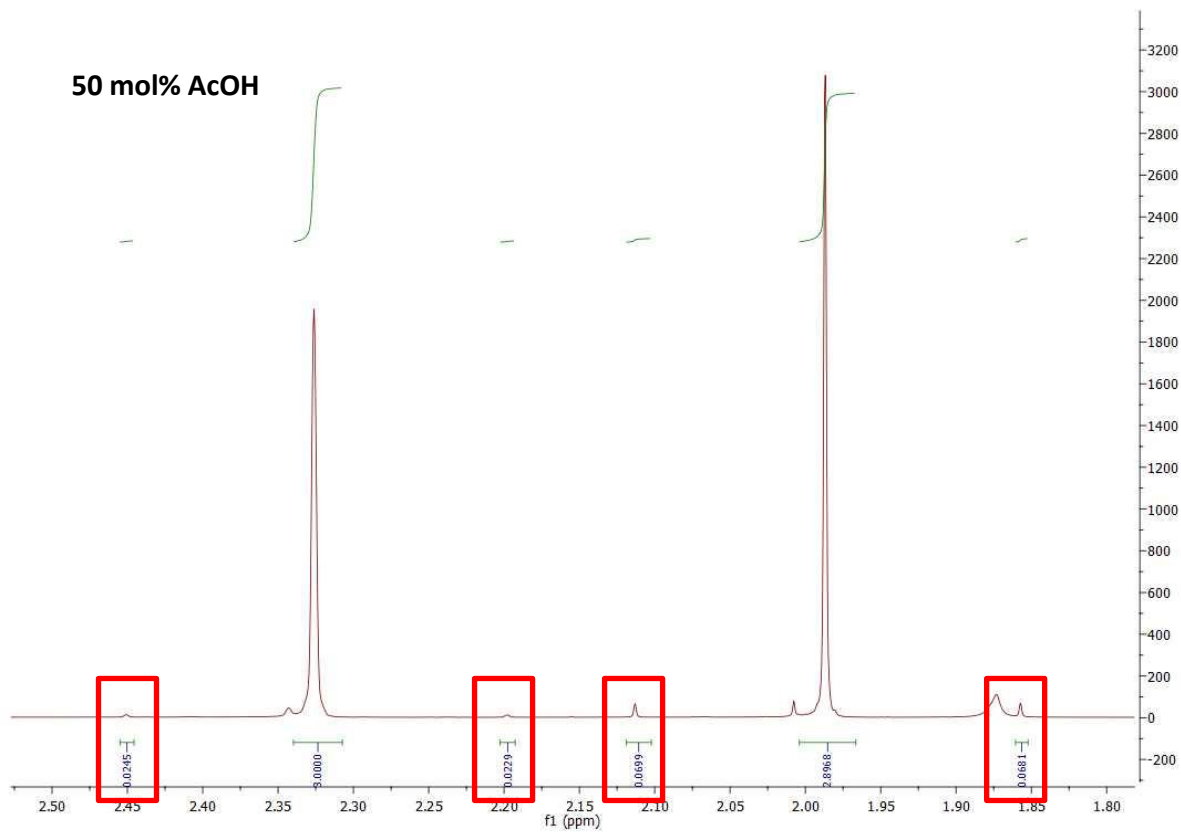


Unlabelled AcOH



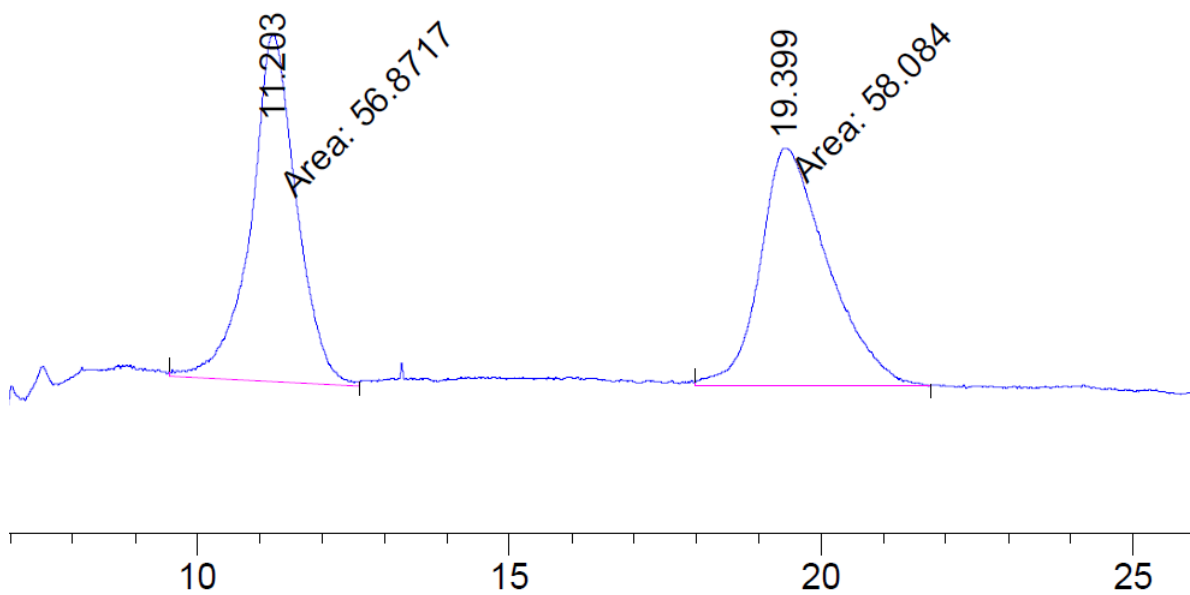
10 mol% AcOH



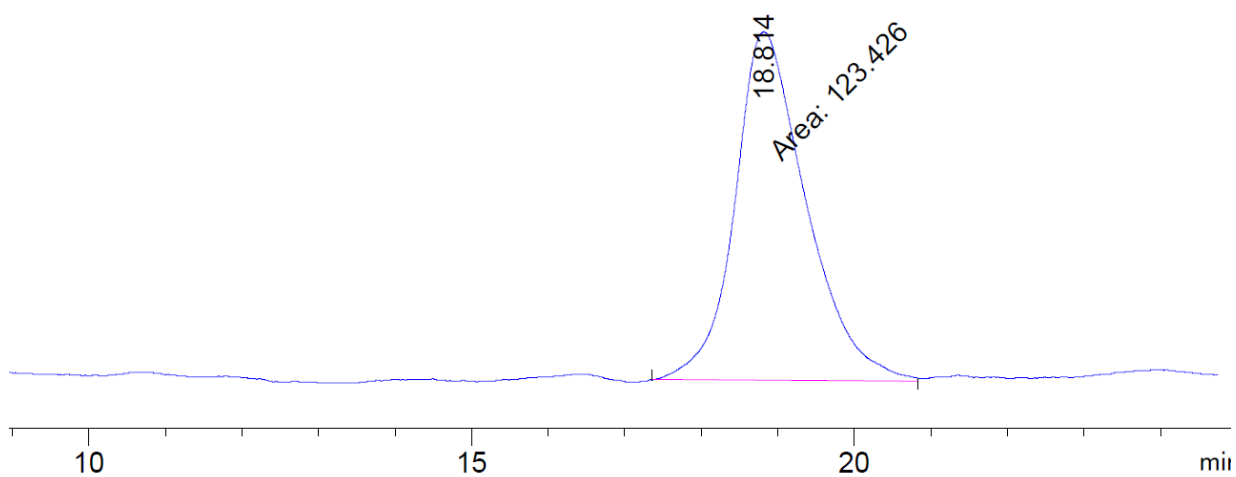


HPLC Traces

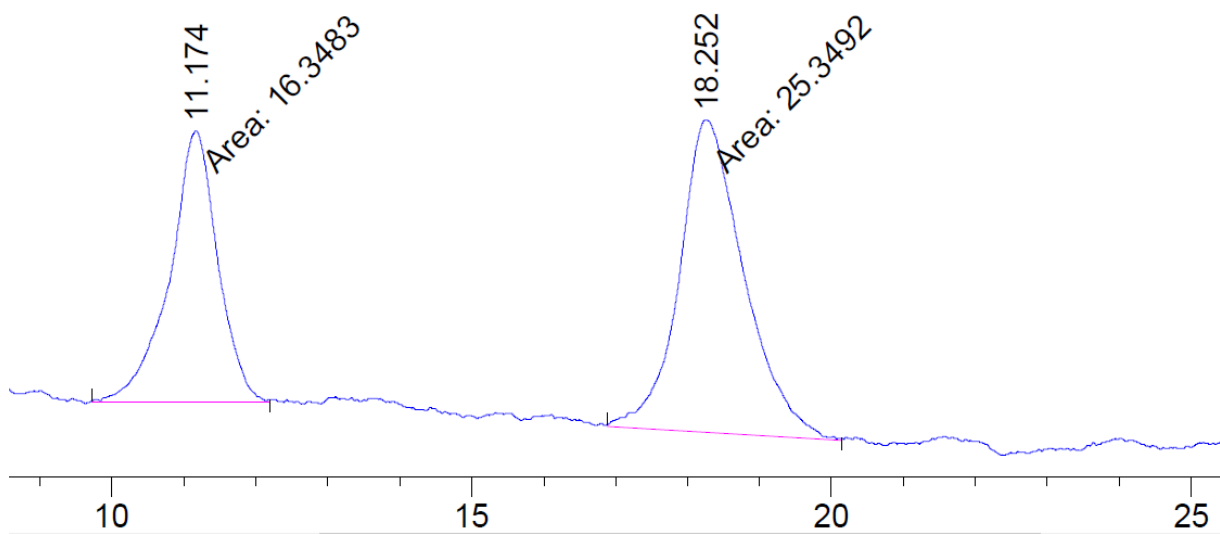
racemic-2,2,2-Trifluoro-N-(1-phenylethyl)acetamide



(R)-2,2,2-Trifluoro-N-(1-phenylethyl)acetamide



(R)-2,2,2-Trifluoro-N-(1-phenylethyl)acetamide + 2,2,2-Trifluoro-N-(1-phenylethyl)acetamide



6.3. Chapter 3 Experimental Methods and Compound Characterisation

General Procedure XXIII – Additive Screen under Reaction Conditions A

(Table 3.1, Results and Discussion II)

To an oven dried Schlenk carousel tube containing 4-methoxybenzotrile (133 mg, 1 mmol) was added $\text{Cu}(\text{OAc})_2$ (18 mg, 10 mol%), the appropriate additive (1 equivalent, unless stated otherwise), water (72 μL , 4 mmol) and toluene (1 mL, 1 M). The tube was then sealed and the reaction mixture heated at 110 °C for 24 hours. After being allowed to cool to room temperature, the crude reaction mixture was diluted with methanol (5 mL) and the solvent removed *in vacuo* on a rotary evaporator. Percentage conversion into 4-methoxybenzamide was calculated from the crude ^1H NMR spectra by comparison of the peaks at 6.95 ppm (2H, 4-methoxybenzamide) and 7.06 ppm (2H, 4-methoxybenzotrile).

General Procedure XXIV – Additive Screen under Reaction Conditions B

(Table 3.1, Results and Discussion II)

To an oven dried Schlenk carousel tube containing 4-methoxybenzotrile (133 mg, 1 mmol) was added $\text{Cu}(\text{OAc})_2$ (18 mg, 10 mol%), the appropriate additive (1 equivalent), water (0.5 mL, 2 M) and toluene (0.5 mL, 2 M). The tube was then sealed and the reaction mixture heated at 100 °C for 24 hours. After being allowed to cool to room temperature, the crude reaction mixture was diluted with methanol (5 mL) and the solvent removed *in vacuo* on a rotary evaporator. Percentage conversion into 4-methoxybenzamide was calculated from the crude ^1H NMR spectra by comparison of the peaks at 6.95 ppm (2H, 4-methoxybenzamide) and 7.06 ppm (2H, 4-methoxybenzotrile).

General Procedure XXV – Metal Oxalate and Metal Acetate Catalyst Screen

(Table 3.2, Results and Discussion II)

To an oven dried Schlenk carousel tube containing 4-methoxybenzotrile (133 mg, 1 mmol) was added the appropriate catalyst (10 mol%, unless otherwise stated), water (72 μL , 4 mmol) and toluene (1 mL, 1 M). The tube was then sealed and the reaction mixture heated at 110 °C for 24 hours. After being allowed to cool to room temperature, the crude reaction mixture was diluted with methanol (5 mL) and the solvent removed *in vacuo* on a rotary evaporator. Percentage conversion into 4-methoxybenzamide was calculated from the crude

¹H NMR spectra by comparison of the peaks at 6.95 ppm (2H, 4-methoxybenzamide) and 7.06 ppm (2H, 4-methoxybenzotrile).

General Procedure XXVI – Copper(II) Hydroxide and Copper(II) Carbonate Hydroxide as Catalysts in the Hydration Reaction

(Table 3.3, Results and Discussion II)

To an oven dried Schlenk carousel tube containing 4-methoxybenzotrile (133 mg, 1 mmol) was added the appropriate copper complex (20 mol%) and the appropriate solvent system (1 mL, 1 M). The tube was then sealed and the reaction mixture heated at the appropriate temperature for 24 hours. After being allowed to cool to room temperature, the crude reaction mixture was diluted with methanol (5 mL) and the solvent removed *in vacuo* on a rotary evaporator. Percentage conversion into 4-methoxybenzamide was calculated from the crude ¹H NMR spectra by comparison of the peaks at 6.95 ppm (2H, 4-methoxybenzamide) and 7.06 ppm (2H, 4-methoxybenzotrile).

General Procedure XXVII – Initial Metal Catalyst Screen

(Table 3.4, Results and Discussion II)

To an oven dried Schlenk carousel tube containing butyronitrile (87 μL, 1 mmol) was added the appropriate catalyst (10 mol%, unless otherwise stated) and water (72 μL, 4 mmol). The tube was then sealed and the reaction mixture heated at 110 °C for 24 hours. After being allowed to cool to room temperature, the crude reaction mixture was diluted with methanol (5 mL) and the solvent removed *in vacuo* on a rotary evaporator. 1,4-Dimethoxybenzene (46 mg, 1/3 mmol) was used as an NMR standard and the crude reaction mixture was analysed by ¹H NMR spectroscopy in DMSO-d⁶. Percentage conversion into butyramide was calculated from the crude ¹H NMR spectra by comparison of the peaks at 2.02 ppm (2H, butyramide) and 6.84 ppm (4/3H, NMR standard).

General Procedure XXVIII – Palladium Catalyst Screen

(Table 3.5, Results and Discussion II)

To an oven dried Schlenk carousel tube containing butyronitrile (87 μL, 1 mmol) was added the appropriate palladium catalyst (10 mol%) and water (72 μL, 4 mmol). The tube was then sealed and the reaction mixture heated at 110 °C for 24 hours. After being allowed to cool to room temperature, the crude reaction mixture was diluted with methanol (5 mL) and the

solvent removed *in vacuo* on a rotary evaporator. 1,4-Dimethoxybenzene (46 mg, 1/3 mmol) was used as an NMR standard and the crude reaction mixture was analysed by ^1H NMR spectroscopy in DMSO-d^6 . Percentage conversion into butyramide was calculated from the crude ^1H NMR spectra by comparison of the peaks at 2.02 ppm (2H, butyramide) and 6.84 ppm (4/3H, NMR standard).

General Procedure XXIX – Solvent Screen

(Table 3.6, Results and Discussion II)

To an oven dried Schlenk carousel tube containing butyronitrile (87 μL , 1 mmol) was added $\text{Pd}(\text{OAc})_2$ (22 mg, 10 mol%), water (72 μL , 4 mmol) and the appropriate solvent (1 mL, 1 M). The tube was then sealed and the reaction mixture heated at 110 $^\circ\text{C}$ for 24 hours. After being allowed to cool to room temperature, the crude reaction mixture was diluted with methanol (5 mL) and the solvent removed *in vacuo* on a rotary evaporator. 1,4-Dimethoxybenzene (46 mg, 1/3 mmol) was used as an NMR standard and the crude reaction mixture was analysed by ^1H NMR spectroscopy in DMSO-d^6 . Percentage conversion into butyramide was calculated from the crude ^1H NMR spectra by comparison of the peaks at 2.02 ppm (2H, butyramide) and 6.84 ppm (4/3H, NMR standard).

General Procedure XXX – Palladium(II) Acetate Catalyst Loading Screen at 110 $^\circ\text{C}$

(Table 3.7, Results and Discussion II)

To an oven dried Schlenk carousel tube containing butyronitrile (87 μL , 1 mmol) was added the appropriate amount of palladium acetate and water (1 mL, 1 M). The tube was then sealed and the reaction mixture heated at 110 $^\circ\text{C}$, unless otherwise stated, for 24 hours. After being allowed to cool to room temperature, the crude reaction mixture was diluted with methanol (5 mL) and the solvent removed *in vacuo* on a rotary evaporator. 1,4-Dimethoxybenzene (46 mg, 1/3 mmol) was used as an NMR standard and the crude reaction mixture was analysed by ^1H NMR spectroscopy in DMSO-d^6 . Percentage conversion into butyramide was calculated from the crude ^1H NMR spectra by comparison of the peaks at 2.02 ppm (2H, butyramide) and 6.84 ppm (4/3H, NMR standard).

General Procedure XXXI – Palladium(II) Acetate:Bipy Ratio Screen

(Table 3.8, Results and Discussion II)

To an oven dried Schlenk carousel tube containing butyronitrile (87 μ L, 1 mmol) was added the appropriate amount of palladium acetate, the appropriate amount of 2,2'-bipyridine and water (1 mL, 1 M). The tube was then sealed and the reaction mixture heated at 80 °C, unless otherwise stated, for 24 hours. After being allowed to cool to room temperature, the crude reaction mixture was diluted with methanol (5 mL) and the solvent removed *in vacuo* on a rotary evaporator. 1,4-Dimethoxybenzene (46 mg, 1/3 mmol) was used as an NMR standard and the crude reaction mixture was analysed by ^1H NMR spectroscopy in DMSO- d^6 . Percentage conversion into butyramide was calculated from the crude ^1H NMR spectra by comparison of the peaks at 2.02 ppm (2H, butyramide) and 6.84 ppm (4/3H, NMR standard).

General Procedure XXXII – Ligand Screen

(Table 3.9, Results and Discussion II)

No preforming of catalyst: To an oven dried Schlenk carousel tube containing butyronitrile (87 μ L, 1 mmol) was added palladium acetate (11 mg, 5 mol%), water (1 mL, 1 M) and the appropriate ligand (5 mol%).

Preforming of catalyst: To an oven dried Schlenk carousel tube containing palladium acetate (11 mg, 5 mol%) was added 2,2'-bipyridine (7.8 mg, 5 mol%) and water (0.5 mL). The reaction mixture was stirred for 5 minutes until the palladium species solubilised and a light yellow solution was observed. Butyronitrile (87 μ L, 1 mmol) and water (0.5 mL) were then added.

The tube was then sealed and the reaction mixture heated at 60 °C for 24 hours. After being allowed to cool to room temperature, the crude reaction mixture was diluted with methanol (5 mL) and the solvent removed *in vacuo* on a rotary evaporator. 1,4-Dimethoxybenzene (46 mg, 1/3 mmol) was used as an NMR standard and the crude reaction mixture was analysed by ^1H NMR spectroscopy in DMSO- d^6 . Percentage conversion into butyramide was calculated from the crude ^1H NMR spectra by comparison of the peaks at 2.02 ppm (2H, butyramide) and 6.84 ppm (4/3H, NMR standard).

General Procedure XXXIII – Water Concentration, Temperature, Catalyst Loading and Catalyst Formation Screen

(Table 3.10, Results and Discussion II)

No preforming of catalyst: To an oven dried Schlenk carousel tube containing butyronitrile (87 μ L, 1 mmol) was added the appropriate amount of palladium acetate, the appropriate amount of 2,2'-bipyridine and the appropriate amount of water.

Preforming of catalyst: To an oven dried Schlenk carousel tube containing the appropriate amount of palladium acetate was added the appropriate amount of 2,2'-bipyridine and half of the appropriate amount of water. The reaction mixture was stirred for 5 minutes until the palladium species solubilised and a light yellow solution was observed. Butyronitrile (87 μ L, 1 mmol) and the other half of the water were then added.

The tube was then sealed and the reaction mixture heated at the appropriate temperature for 24 hours. After being allowed to cool to room temperature, the crude reaction mixture was diluted with methanol (5 mL) and the solvent removed *in vacuo* on a rotary evaporator. 1,4-Dimethoxybenzene (46 mg, 1/3 mmol) was used as an NMR standard and the crude reaction mixture was analysed by ^1H NMR spectroscopy in DMSO-d^6 . Percentage conversion into butyramide was calculated from the crude ^1H NMR spectra by comparison of the peaks at 2.02 ppm (2H, butyramide) and 6.84 ppm (4/3H, NMR standard).

General Procedure XXXIV – Metal Acetate and Palladium(II) Chloride Screen at 70 °C

(Table 3.11, Results and Discussion II)

To an oven dried Schlenk carousel tube containing butyronitrile (87 μ L, 1 mmol) was added the appropriate catalyst (5 mol%), 2,2'-bipyridine, (7.8 mg, 5 mol%) if appropriate, and water (2 mL, 0.5 M). The tube was then sealed and the reaction mixture heated at 70 °C for 24 hours. After being allowed to cool to room temperature, the crude reaction mixture was diluted with methanol (5 mL) and the solvent removed *in vacuo* on a rotary evaporator. 1,4-Dimethoxybenzene (46 mg, 1/3 mmol) was used as an NMR standard and the crude reaction mixture was analysed by ^1H NMR spectroscopy in DMSO-d^6 . Percentage conversion into butyramide was calculated from the crude ^1H NMR spectra by comparison of the peaks at 2.02 ppm (2H, butyramide) and 6.84 ppm (4/3H, NMR standard).

General Procedure XXXV – Silver Salt Screen with Palladium(II) Chloride

(Table 3.12, Results and Discussion II)

To an oven dried Schlenk carousel tube containing butyronitrile (87 μ L, 1 mmol) was added PdCl₂ (8.9 mg, 5 mol%), the appropriate silver salt (10 mol%) and water (2 mL, 0.5 M). The tube was then sealed and the reaction mixture heated at 70 °C for 24 hours. After being allowed to cool to room temperature, the crude reaction mixture was diluted with methanol (5 mL) and the solvent removed *in vacuo* on a rotary evaporator. 1,4-Dimethoxybenzene (46 mg, 1/3 mmol) was used as an NMR standard and the crude reaction mixture was analysed by ¹H NMR spectroscopy in DMSO-d⁶. Percentage conversion into butyramide was calculated from the crude ¹H NMR spectra by comparison of the peaks at 2.02 ppm (2H, butyramide) and 6.84 ppm (4/3H, NMR standard).

General Procedure XXXVI – Dioxane Co-Solvent Screen

(Table 3.13, Results and Discussion II)

To an oven dried Schlenk carousel tube containing 4-chlorobenzonitrile (138 mg, 1 mmol) was added palladium acetate (11 mg, 5 mol%), 2,2'-bipyridine, (7.8 mg, 5 mol%, unless stated otherwise), and the appropriate water to organic solvent ratio (total 2 mL, 0.5 M). The tube was then sealed and the reaction mixture heated at the appropriate temperature for 24 hours. After being allowed to cool to room temperature, the crude reaction mixture was diluted with methanol (5 mL) and the solvent removed *in vacuo* on a rotary evaporator. 1,4-Dimethoxybenzene (46 mg, 1/3 mmol) was used as an NMR standard and the crude reaction mixture was analysed by ¹H NMR spectroscopy in DMSO-d⁶. Percentage conversion into 4-chlorobenzamide was calculated from the crude ¹H NMR spectra by comparison of the peaks at 7.93 ppm (2H, 4-chlorobenzamide) and 6.81 ppm (4/3H, NMR standard).

General Procedure XXXVII – Additive Inhibition Investigations

(Table 3.16, Results and Discussion II)

To an oven dried Schlenk carousel tube containing butyronitrile (87 μ L, 1 mmol) was added palladium acetate (11 mg, 5 mol%), 2,2'-bipyridine, (7.8 mg, 5 mol%), the appropriate additive (1 equiv.) and water (2 mL, 0.5 M). The tube was then sealed and the reaction mixture heated at 70 °C for 24 hours. After being allowed to cool to room temperature, the crude reaction mixture was diluted with methanol (5 mL) and the solvent removed *in vacuo* on a rotary evaporator. 1,4-Dimethoxybenzene (46 mg, 1/3 mmol) was used as an NMR standard and the

crude reaction mixture was analysed by ^1H NMR spectroscopy in DMSO-d^6 . Percentage conversion into butyramide was calculated from the crude ^1H NMR spectra by comparison of the peaks at 2.02 ppm (2H, butyramide) and 6.84 ppm (4/3H, NMR standard).

General Procedure XXXVIII – Addition of Acid to the Hydration of 4-Pyridinecarbonitrile Reaction

(Table 3.17, Results and Discussion II)

No preforming of catalyst: To an oven dried Schlenk carousel tube containing 4-pyridinecarbonitrile (104 mg, 1 mmol) was added palladium acetate (11 mg, 5 mol%), 2,2'-bipyridine, (7.8 mg, 5 mol%), the appropriate acid (1 equiv.), dioxane (0.6 mL) and water (1.4 mL).

Preforming of catalyst: To an oven dried Schlenk carousel tube containing palladium acetate (11 mg, 5 mol%) was added 2,2'-bipyridine, (7.8 mg, 5 mol%), dioxane (0.3 mL) and water (0.7 mL). The reaction mixture was stirred for 5 minutes until the palladium species solubilised and a light yellow solution was observed. 4-Pyridinecarbonitrile (104 mg, 1 mmol), the appropriate acid (1 equiv), dioxane (0.3 mL) and water (0.7 mL) were then added.

The tube was then sealed and the reaction mixture heated at 70 °C for 24 hours. After being allowed to cool to room temperature, the crude reaction mixture was diluted with methanol (5 mL) and the solvent removed *in vacuo* on a rotary evaporator. 1,4-Dimethoxybenzene (46 mg, 1/3 mmol) was used as an NMR standard and the crude reaction mixture was analysed by ^1H NMR spectroscopy in DMSO-d^6 . Percentage conversion into isonicotinamide was calculated from the crude ^1H NMR spectra by comparison of the peaks at 8.71 ppm (2H, isonicotinamide) and 6.84 ppm (4/3H, NMR standard).

Synthesis of Primary Amides

General Procedure XXXIX – Synthesis of Primary Amide Products in Water (Solvent System A)

(Table 3.14, Results and Discussion II)

To an oven dried Schlenk carousel tube containing the appropriate nitrile (1 mmol) was added palladium acetate (11 mg, 5 mol%), 2,2'-bipyridine, (7.8 mg, 5 mol%) and water (2 mL, 0.5 M). The tube was then sealed and the reaction mixture heated at 70 °C for 24 hours. After being allowed to cool to room temperature, the reaction mixture was diluted with methanol (5 mL)

and the solvent removed *in vacuo* on a rotary evaporator whilst azeotroping with toluene. Where the reaction had gone to quantitative conversion or the starting nitrile was volatile, the crude reaction mixture was passed through a short plug of silica to remove the catalyst (eluting with DCM/MeOH, 95:5). Otherwise, the primary amide products were purified by column chromatography (eluting with DCM/MeOH, 95:5, unless otherwise stated).

General Procedure XL – Synthesis of Primary Amide Products in Water/Dioxane (Solvent System B)

(Table 3.14, Results and Discussion II)

To an oven dried Schlenk carousel tube containing the appropriate nitrile (1 mmol) was added palladium acetate (11 mg, 5 mol%), 2,2'-bipyridine, (7.8 mg, 5 mol%), dioxane (0.6 mL) and water (1.4 mL). The tube was then sealed and the reaction mixture heated at 70 °C for 24 hours. After being allowed to cool to room temperature, the reaction mixture was diluted with methanol (5 mL) and the solvent removed *in vacuo* on a rotary evaporator whilst azeotroping with toluene. Where the reaction had gone to quantitative conversion or the starting nitrile was volatile, the crude reaction mixture was passed through a short plug of silica to remove the catalyst (eluting with DCM/MeOH, 95:5). Otherwise, the primary amide products were purified by column chromatography (eluting with DCM/MeOH, 95:5, unless otherwise stated).

General Procedure XLI – Notable Substrate Exceptions

(Table 3.15, Results and Discussion II)

To an oven dried Schlenk carousel tube containing the appropriate nitrile (1 mmol) was added palladium acetate (11 mg, 5 mol%), 2,2'-bipyridine, (7.8 mg, 5 mol%) and either water (2 mL, 0.5 M, solvent system **A**) or water/dioxane (1.4 mL/0.6 mL, solvent system **B**) as stated. The tube was then sealed and the reaction mixture heated at 70 °C for 24 hours. After being allowed to cool to room temperature, the reaction mixture was diluted with methanol (5 mL) and the solvent removed *in vacuo* on a rotary evaporator. 1,4-Dimethoxybenzene (46 mg, 1/3 mmol) was used as an NMR standard and the crude reaction mixture was analysed by ¹H NMR spectroscopy.

General Procedure XLII – Synthesis of Ethenzamide

(Scheme 3.8, Results and Discussion II)

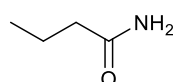
To an oven dried Schlenk carousel tube containing 2-ethoxybenzotrile (147 mg, 1 mmol) was added palladium acetate (11 mg, 5 mol%), 2,2'-bipyridine, (7.8 mg, 5 mol%), dioxane (0.6 mL) and water (1.4 mL). The tube was then sealed and the reaction mixture heated at 90 °C for 24 hours. After being allowed to cool to room temperature, the reaction mixture was diluted with methanol (5 mL) and the solvent removed *in vacuo* on a rotary evaporator whilst azeotroping with toluene. The crude reaction mixture was passed through a short plug of silica to remove the catalyst (eluting with DCM/MeOH, 95:5).

General Procedure XLIII - Scale-up Example

(Scheme 3.9, Results and Discussion II)

To an oven dried round bottomed flask containing benzonitrile (4.12 mL, 40 mmol) was added palladium acetate (0.45 g, 5 mol%), 2,2'-bipyridine, (0.31 g, 5 mol%) and water (80 mL, 0.5 M). The round bottomed flask was then sealed with a rubber septum and a needle inserted into the top, and the reaction mixture heated at 70 °C for 24 hours. After being allowed to cool to room temperature, the reaction mixture was diluted with methanol (100 mL) and the solvent removed *in vacuo* on a rotary evaporator whilst azeotroping with toluene. The crude reaction mixture was passed through a short plug of silica to remove the catalyst (eluting with DCM/MeOH, 95:5).

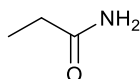
Butyramide⁹² (3.6)



Following general procedure XXXIX, butyronitrile (87 μ L, 1 mmol) was used as the nitrile species. The title compound was recovered as a white solid (84 mg, 97%) after being passed through a silica plug and the solvent evaporated.

mp 115-117 °C (lit.⁹² 115-117 °C); ¹H NMR (500 MHz, DMSO-d⁶): δ 7.23 (br s, 1H, NH), 6.71 (br s, 1H, NH), 2.01 (t, J = 7.4 Hz, 2H, C(O)CH₂), 1.55 – 1.41 (sext, J = 7.4 Hz, 2H, CH₃CH₂), 0.84 (t, J = 7.4 Hz, 3H, CH₃); ¹³C NMR (126 MHz, DMSO-d⁶): δ 174.4, 37.2, 18.6, 13.7; HRMS-ESI calcd for [C₄H₉NONa]⁺: 110.0576 [M+Na]⁺. Found: 110.0558; FT-IR (neat) ν in cm⁻¹: 3360, 3173, 1655, 1630. In agreement with previous literature data.

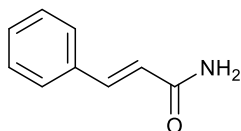
Propionamide⁹² (3.11)



Following general procedure XXXIX, propionitrile (72 μ L, 1 mmol) was used as the nitrile species. The title compound was recovered as a white solid (64 mg, 88%) after being passed through a silica plug and the solvent evaporated.

mp 78-80 $^{\circ}$ C (lit.²⁴⁹ 79 $^{\circ}$ C); 1 H NMR (500 MHz, CDCl_3): δ 5.36 (br s, 2H, NH_2), 2.27 (q, $J = 7.6$ Hz, 2H, CH_2), 1.17 (t, $J = 7.6$ Hz, 3H, CH_3); 13 C NMR (126 MHz, CDCl_3): δ 176.2, 29.1, 9.8; HRMS-ESI calcd for $[\text{C}_3\text{H}_7\text{NONa}]^+$: 96.0420 $[\text{M}+\text{Na}]^+$. Found: 96.0420; FT-IR (neat) ν in cm^{-1} : 3351, 3176, 1627, 1605. In agreement with previous literature data.

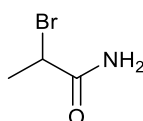
Cinnamamide⁹² (3.12)



Following general procedure XL, cinnamitrile (129 mg, 1 mmol) was used as the nitrile species. The title compound was recovered after purification by column chromatography (R_f 0.16) as an off-white solid (136 mg, 93%).

mp 149-151 $^{\circ}$ C (lit.⁹² 149-151 $^{\circ}$ C); 1 H NMR (500 MHz, CDCl_3): δ 7.65 (d, $J = 15.7$ Hz, 1H, PhCH), 7.54 – 7.48 (m, 2H, Ph), 7.41 – 7.33 (m, 3H, Ph), 6.47 (d, $J = 15.7$ Hz, 1H, PhCHCH), 5.78 (br s, 2H, NH_2); 13 C NMR (126 MHz, CDCl_3): δ 168.0, 142.6, 134.7, 130.1, 129.0, 128.1, 119.7; HRMS-ESI calcd for $[\text{C}_9\text{H}_9\text{NONa}]^+$ and $[\text{C}_9\text{H}_{10}\text{NO}]^+$: 170.0576 $[\text{M}+\text{Na}]^+$ and 148.0757 $[\text{M}+\text{H}]^+$. Found: 170.0580 and 148.0760; FT-IR (neat) ν in cm^{-1} : 3382, 3161, 1655, 1607. In agreement with previous literature data.

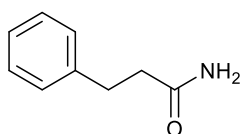
2-Bromopropanamide²⁵⁰ (3.13)



Following general procedure XXXIX, 2-bromopropionitrile (87 μ L, 1 mmol) was used as the nitrile species. The title compound was recovered as an orange/brown solid (129 mg, 85%) after being passed through a silica plug and the solvent evaporated.

mp 119-121 °C (lit.²⁵¹ 122-123 °C); ¹H NMR (500 MHz, DMSO-d⁶): δ 7.61 (br s, 1H, NH), 7.19 (br s, 1H, NH), 4.43 (q, *J* = 6.8 Hz, 1H, CHBr), 1.62 (d, *J* = 6.8 Hz, 3H, CH₃); ¹³C NMR (126 MHz, CDCl₃): δ 170.7, 44.1, 21.7; HRMS-ESI calcd for [C₃H₆BrNONa]⁺ and [C₃H₇BrNO]⁺: 173.9525 [M+Na]⁺ and 151.9706 [M+H]⁺. Found: 173.9524 and 151.9702; FT-IR (neat) ν in cm⁻¹: 3326, 3164, 1661, 1628. In agreement with previous literature data.

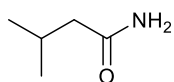
3-Phenylpropanamide⁹² (3.14)



Following general procedure XXXIX, 3-phenylpropionitrile (131 μL, 1 mmol) was used as the nitrile species. The title compound was recovered as a white solid (136 mg, 91%) after being passed through a silica plug and the solvent evaporated.

mp 97-99 °C (lit.⁹² 96-98 °C); ¹H NMR (300 MHz, CDCl₃): δ 7.33 – 7.26 (m, 2H, *Ph*), 7.25 – 7.17 (m, 3H, *Ph*), 5.40 (br s, 2H, NH), 2.98 (t, *J* = 7.7 Hz, 2H, PhCH₂CH₂), 2.54 (t, *J* = 7.7 Hz, 2H, PhCH₂); ¹³C NMR (126 MHz, CDCl₃): δ 174.6, 140.8, 128.7, 128.5, 126.5, 37.7, 31.5; HRMS-ESI calcd for [C₉H₁₁NONa]⁺: 172.0733 [M+Na]⁺. Found: 172.0730; FT-IR (neat) ν in cm⁻¹: 3388, 3185, 1646, 1627. In agreement with previous literature data.

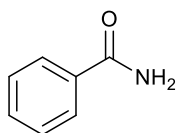
3-Methylbutanamide²⁵² (3.15)



Following general procedure XXXIX, isovaleronitrile (105 μL, 1 mmol) was used as the nitrile species. The title compound was recovered as a white solid (76 mg, 75%) after being passed through a silica plug and the solvent evaporated.

mp 134-136 °C (lit.²⁵² 134-135 °C); ¹H NMR (500 MHz, DMSO-d⁶): δ 7.20 (br s, 1H, NH), 6.67 (br s, 1H, NH), 1.99 – 1.87 (m, 3H, CH and CH₂), 0.87 (d, *J* = 6.4 Hz, 6H, CH(CH₃)₂); ¹³C NMR (126 MHz, DMSO-d⁶): δ 173.6, 44.5, 25.3, 22.3; HRMS-ESI calcd for [C₅H₁₁NONa]⁺ and [C₅H₁₂NO]⁺: 124.0733 [M+Na]⁺ and 102.0913 [M+H]⁺. Found: 124.0733 and 102.0916; FT-IR (neat) ν in cm⁻¹: 3346, 3175, 1661, 1627. In agreement with previous literature data.

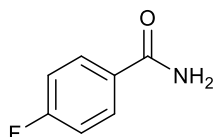
Benzamide⁹² (3.16)



Following general procedure XXXIX, benzonitrile (103 μ L, 1 mmol) was used as the nitrile species. The title compound was recovered as a white solid (117 mg, 97%) after being passed through a silica plug and the solvent evaporated.

mp 127-128 °C (lit.⁹² 129-130 °C); ¹H NMR (500 MHz, DMSO-d⁶): δ 7.96 (br s, 1H, NH), 7.87 (d, J = 7.3 Hz, 2H, Ph), 7.52 (t, J = 7.3 Hz, 1H, Ph), 7.44 (t, J = 7.4 Hz, 2H, Ph), 7.35 (br s, 1H, NH); ¹³C NMR (126 MHz, DMSO-d⁶): δ 167.8, 134.2, 131.2, 128.2, 127.4; HRMS-ESI calcd for [C₇H₈NO]⁺: 122.0600 [M+H]⁺. Found: 122.0601; FT-IR (neat) ν in cm⁻¹: 3361, 3165, 1655, 1619. In agreement with previous literature data.

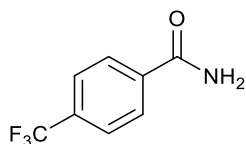
4-Fluorobenzamide⁹² (3.17)



Following general procedure XXXIX, 4-fluorobenzonitrile (121 mg, 1 mmol) was used as the nitrile species. The title compound was recovered as a white solid (125 mg, 90%) after being passed through a silica plug and the solvent evaporated.

mp 152-154 °C (lit.⁹² 153-155 °C); ¹H NMR (500 MHz, DMSO-d⁶): δ 7.98 (br s, 1H, NH), 7.94 (dd, J = 8.8, 5.6 Hz, 2H, CH_{Ar}), 7.38 (br s, 1H, NH), 7.27 (t, J = 8.8 Hz, 2H, CH_{Ar}); ¹³C NMR (126 MHz, DMSO-d⁶): δ 166.8, 163.9 (d, J = 248.3 Hz), 130.7 (d, J = 2.9 Hz), 130.1 (d, J = 9.0 Hz), 115.1 (d, J = 21.6 Hz); ¹⁹F NMR (470 MHz, DMSO-d⁶): δ -111.07 (referenced against trifluoroacetic acid); HRMS-ESI calcd for [C₇H₆FNONa]⁺: 162.0326 [M+Na]⁺. Found: 162.0324; FT-IR (neat) ν in cm⁻¹: 3322, 3146, 1670, 1622. In agreement with previous literature data.

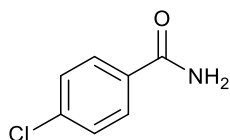
4-(Trifluoromethyl)benzamide⁹² (3.18)



Following general procedure XXXIX, 4-(trifluoromethyl)benzotrile (171 mg, 1 mmol) was used as the nitrile species. The title compound was recovered as a white solid (180 mg, 95%) after being passed through a silica plug and the solvent evaporated.

mp 183-184 °C (lit.⁹² 183-185 °C); ¹H NMR (500 MHz, DMSO-d⁶): δ 8.18 (br s, 1H, NH), 8.06 (d, *J* = 8.1 Hz, 2H, CH_{Ar}), 7.84 (d, *J* = 8.1 Hz, 2H, CH_{Ar}), 7.61 (br s, 1H, NH); ¹³C NMR (126 MHz, DMSO-d⁶): δ 166.6, 138.1, 131.1 (q, *J* = 31.8 Hz), 128.3, 125.2 (q, *J* = 3.8 Hz), 123.9 (q, *J* = 272.4 Hz); ¹⁹F NMR (470 MHz, DMSO-d⁶): δ -62.72 (referenced against trifluoroacetic acid); HRMS-ESI calcd for [C₈H₇F₃NO]⁺: 190.0474 [M+H]⁺. Found: 190.0486; FT-IR (neat) *v* in cm⁻¹: 3368, 3167, 1652, 1620. In agreement with previous literature data.

4-Chlorobenzamide⁹² (3.10)

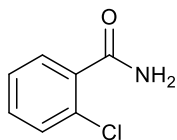


Following general procedure XXXIX, 4-chlorobenzotrile (138 mg, 1 mmol) was used as the nitrile species. The title compound was recovered after purification by column chromatography (R_f 0.20) as a white solid (111 mg, 71%).

Following general procedure XL, 4-chlorobenzotrile (138 mg, 1 mmol) was used as the nitrile species. The title compound was recovered as a white solid (153 mg, 98%) after being passed through a silica plug and the solvent evaporated.

mp 178-180 °C (lit.⁹² 178-181 °C); ¹H NMR (500 MHz, DMSO-d⁶): δ 8.03 (br s, 1H, NH), 7.88 (d, *J* = 8.6 Hz, 2H, CH_{Ar}), 7.52 (d, *J* = 8.6 Hz, 2H, CH_{Ar}), 7.45 (br s, 1H, NH); ¹³C NMR (126 MHz, DMSO-d⁶): δ 166.8, 136.0, 133.0, 130.0, 128.3; HRMS-ESI calcd for [C₇H₆ClNONa]⁺ and [C₇H₇ClNO]⁺: 178.0030 [M+Na]⁺ and 156.0211 [M+H]⁺. Found: 178.0034 and 156.0215; FT-IR (neat) *v* in cm⁻¹: 3364, 3171, 1651, 1618. In agreement with previous literature data.

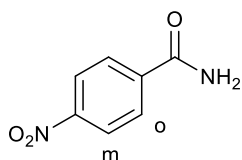
2-Chlorobenzamide⁹² (3.19)



Following general procedure XL, 2-chlorobenzonitrile (138 mg, 1 mmol) was used as the nitrile species. The title compound was recovered after purification by column chromatography (R_f 0.21) as a white solid (111 mg, 71%).

mp 138-139 °C (lit.⁹² 139-140 °C); ^1H NMR (500 MHz, DMSO- d_6): δ 7.86 (br s, 1H, NH), 7.57 (br s, 1H, NH), 7.50 – 7.34 (m, 4H, CH_{Ar}); ^{13}C NMR (126 MHz, DMSO- d_6): δ 168.1, 137.1, 130.5, 129.6, 129.6, 128.6, 127.0; HRMS-ESI calcd for $[\text{C}_7\text{H}_6\text{ClN}_2\text{O}]^+$ and $[\text{C}_7\text{H}_7\text{ClNO}]^+$: 178.0030 $[\text{M}+\text{Na}]^+$ and 156.0211 $[\text{M}+\text{H}]^+$. Found: 178.0034 and 156.0213; FT-IR (neat) ν in cm^{-1} : 3355, 3156, 1649, 1625. In agreement with previous literature data.

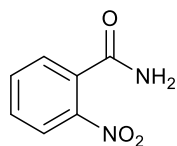
4-Nitrobenzamide⁹² (3.20)



Following general procedure XL, 4-nitrobenzonitrile (148 mg, 1 mmol) was used as the nitrile species. The title compound was recovered as a white solid (163 mg, 98%) after being passed through a silica plug and the solvent evaporated.

mp 196-198 °C (lit.⁹² 197-199 °C); ^1H NMR (500 MHz, DMSO- d_6): δ 8.32 – 8.23 (m, 3H, NH and $m\text{-CH}_{Ar}$), 8.09 (d, J = 8.7 Hz, 2H, $o\text{-CH}_{Ar}$), 7.72 (br s, 1H, NH); ^{13}C NMR (126 MHz, DMSO- d_6): δ 166.2, 149.0, 140.0, 128.9, 123.4; HRMS-ESI calcd for $[\text{C}_7\text{H}_7\text{N}_2\text{O}_3]^+$: 167.0451 $[\text{M}+\text{H}]^+$. Found: 167.0453; FT-IR (neat) ν in cm^{-1} : 3475, 3162, 1672, 1594. In agreement with previous literature data.

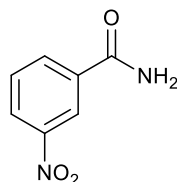
2-Nitrobenzamide¹⁴⁵ (3.21)



Following general procedure XL, 2-nitrobenzotrile (148 mg, 1 mmol) was used as the nitrile species. The title compound was recovered as a white solid (163 mg, 98%) after being passed through a silica plug and the solvent evaporated.

mp 174-175 °C (lit.¹⁴⁵ 174-176 °C); ¹H NMR (500 MHz, DMSO-d⁶): δ 8.13 (br s, 1H, NH), 7.99 (d, *J* = 8.1 Hz, 1H, CH_{Ar}), 7.76 (t, *J* = 7.5 Hz, 1H, CH_{Ar}), 7.70 – 7.61 (m, 3H, NH and CH_{Ar}); ¹³C NMR (126 MHz, DMSO-d⁶): δ 167.1, 147.2, 133.3, 132.6, 130.6, 128.8, 123.9; HRMS-ESI calcd for [C₇H₆N₂O₃Na]⁺ and [C₇H₇N₂O₃]⁺: 189.0271 [M+Na]⁺ and 167.0451 [M+H]⁺. Found: 189.0274 and 167.0452; FT-IR (neat) *v* in cm⁻¹: 3351, 3165, 1652, 1623. In agreement with previous literature data.

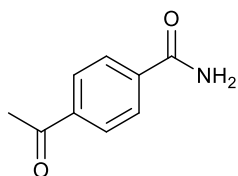
3-Nitrobenzamide⁵³ (3.22)



Following general procedure XL, 3-nitrobenzotrile (148 mg, 1 mmol) was used as the nitrile species. The title compound was recovered as a white solid (163 mg, 98%) after being passed through a silica plug and the solvent evaporated.

mp 141-142 °C (lit.⁵³ 141 °C); ¹H NMR (500 MHz, DMSO-d⁶): δ 8.75 – 8.64 (m, 1H, CH_{Ar}), 8.40 – 8.28 (m, 3H, NH and CH_{Ar}), 7.70 – 7.61 (m, 1H, CH_{Ar}), 7.71 (br s, 1H, NH); ¹³C NMR (126 MHz, DMSO-d⁶): δ 165.7, 147.8, 135.8, 133.8, 130.0, 125.9, 122.2; HRMS-ESI calcd for [C₇H₆N₂O₃Na]⁺ and [C₇H₇N₂O₃]⁺: 189.0271 [M+Na]⁺ and 167.0451 [M+H]⁺. Found: 189.0273 and 167.0451; FT-IR (neat) *v* in cm⁻¹: 3379, 3164, 1662, 1610. In agreement with previous literature data.

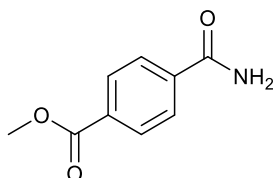
4-Acetylbenzamide²⁵³ (3.23)



Following general procedure XXXIX, 4-acetylbenzamide (145 mg, 1 mmol) was used as the nitrile species. The title compound was recovered as a white solid (159 mg, 98%) after being passed through a silica plug and the solvent evaporated.

mp 191-193 °C (lit.¹¹⁹ 190 °C); ¹H NMR (500 MHz, DMSO-d⁶): δ 8.13 (br s, 1H, NH), 8.00 (q, *J* = 8.6 Hz, 4H, CH_{Ar}), 7.55 (br s, 1H, NH), 2.61 (s, 3H, CH₃); ¹³C NMR (126 MHz, DMSO-d⁶): δ 197.7, 167.1, 138.6, 138.1, 128.1, 127.7, 26.9; HRMS-ESI calcd for [C₉H₉NO₂Na]⁺ and [C₉H₁₀NO₂]⁺: 186.0525 [M+Na]⁺ and 164.0706 [M+H]⁺. Found: 186.0532 and 164.0712; FT-IR (neat) ν in cm⁻¹: 3399, 3177, 1678, 1652. In agreement with previous literature data.

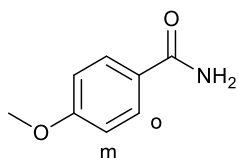
Methyl 4-carbamoylbenzoate²⁵⁴ (3.24)



Following general procedure XL, methyl 4-cyanobenzoate (161 mg, 1 mmol) was used as the nitrile species. The title compound was recovered as a white solid (170 mg, 95%) after being passed through a silica plug and the solvent evaporated.

mp 208-209 °C (lit.²⁵⁵ 206-209 °C); ¹H NMR (500 MHz, DMSO-d⁶): δ 8.14 (br s, 1H, NH), 8.00 (q, *J* = 8.5 Hz, 4H, CH_{Ar}), 7.56 (br s, 1H, NH), 3.87 (s, 3H, CH₃); ¹³C NMR (126 MHz, DMSO-d⁶): δ 167.0, 165.7, 138.4, 131.8, 129.0, 127.8, 52.3; HRMS-ESI calcd for [C₉H₉NO₃Na]⁺ and [C₉H₁₀NO₃]⁺: 202.0475 [M+Na]⁺ and 180.0655 [M+H]⁺. Found: 202.0479 and 180.0659; FT-IR (neat) ν in cm⁻¹: 3359, 3158, 1655, 1625. In agreement with previous literature data.

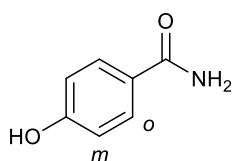
4-Methoxybenzamide¹⁴⁵ (3.4)



Following general procedure XXXIX, anisonitrile (133 mg, 1 mmol) was used as the nitrile species. The title compound was recovered after purification by column chromatography (R_f 0.28) as a white solid (115 mg, 76%).

mp 167-168 °C (lit.¹⁴⁵ 166-168 °C); ^1H NMR (500 MHz, DMSO- d_6): δ 7.87 – 7.77 (m, 3H, NH and $o\text{-CH}_{Ar}$), 7.16 (br s, 1H, NH), 6.97 (d, J = 8.8 Hz, 2H, $m\text{-CH}_{Ar}$), 3.80 (s, 3H, CH_3); ^{13}C NMR (126 MHz, DMSO- d_6): δ 167.4, 161.5, 129.3, 126.5, 113.4, 55.3; HRMS-ESI calcd for $[\text{C}_8\text{H}_9\text{NO}_2\text{Na}]^+$ and $[\text{C}_8\text{H}_{10}\text{NO}_2]^+$: 174.0525 $[\text{M}+\text{Na}]^+$ and 152.0706 $[\text{M}+\text{H}]^+$. Found: 174.0528 and 152.0707; FT-IR (neat) ν in cm^{-1} : 3389, 3162, 1643, 1615. In agreement with previous literature data.

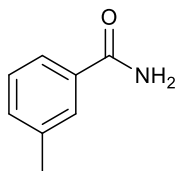
4-Hydroxybenzamide¹⁸² (3.25)



Following general procedure XXXIX, 4-cyanophenol (119 mg, 1 mmol) was used as the nitrile species. The title compound was recovered after purification by column chromatography (90:10, DCM/MeOH, R_f 0.14) as an off-white solid (116 mg, 85%).

mp 159-160 °C (lit.²⁵⁶ 161-162 °C); ^1H NMR (500 MHz, DMSO- d_6): δ 9.93 (br s, 1H, OH), 7.76 – 7.66 (m, 3H, NH and $o\text{-CH}_{Ar}$), 7.05 (br s, 1H, NH), 6.77 (d, J = 8.7 Hz, 2H, $m\text{-CH}_{Ar}$); ^{13}C NMR (126 MHz, DMSO- d_6): δ 167.6, 160.1, 129.4, 125.0, 114.6; HRMS-ESI calcd for $[\text{C}_7\text{H}_7\text{NO}_2\text{Na}]^+$ and $[\text{C}_7\text{H}_8\text{NO}_2]^+$: 160.0369 $[\text{M}+\text{Na}]^+$ and 138.0550 $[\text{M}+\text{H}]^+$. Found: 160.0375 and 138.0553; FT-IR (neat) ν in cm^{-1} : 3333, 3111, 1643, 1616. In agreement with previous literature data.

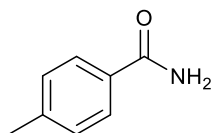
3-Methylbenzamide⁹² (3.26)



Following general procedure XXXIX, *m*-tolunitrile (120 μ L, 1 mmol) was used as the nitrile species. The title compound was recovered as an off-white solid (104 mg, 77%) after being passed through a silica plug and the solvent evaporated.

mp 93-94 °C (lit.⁹² 92-93 °C); ¹H NMR (500 MHz, CDCl₃): δ 7.65 (s, 1H, CH_{Ar}), 7.60 – 7.56 (m, 1H, CH_{Ar}), 7.36 – 7.30 (m, 2H, CH_{Ar}), 6.08 (br s, 1H, NH), 5.82 (br s, 1H, NH), 2.41 (s, 3H, CH₃); ¹³C NMR (126 MHz, CDCl₃): δ 169.6, 138.7, 133.4, 132.9, 128.6, 128.3, 124.4, 21.5; HRMS-ESI calcd for [C₈H₉NONa]⁺: 158.0576 [M+Na]⁺. Found: 158.0576; FT-IR (neat) ν in cm⁻¹: 3372, 3190, 1647, 1614. In agreement with previous literature data.

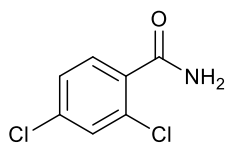
4-Methylbenzamide⁵³ (3.27)



Following general procedure XL, *p*-tolunitrile (117 mg, 1 mmol) was used as the nitrile species. The title compound was recovered as a white solid (128 mg, 95%) after being passed through a silica plug and the solvent evaporated.

mp 160-162 °C (lit.⁵³ 161-162 °C); ¹H NMR (500 MHz, DMSO-d⁶): δ 7.87 (br s, 1H, NH), 7.77 (d, *J* = 8.2 Hz, 2H, CH_{Ar}), 7.28 – 7.21 (m, 3H, NH and CH_{Ar}), 2.34 (s, 3H, CH₃); ¹³C NMR (126 MHz, DMSO-d⁶): δ 167.7, 141.0, 131.5, 128.7, 127.5, 20.9; HRMS-ESI calcd for [C₈H₉NONa]⁺ and [C₈H₁₀NO]⁺: 158.0576 [M+Na]⁺ and 136.0757 [M+H]⁺. Found: 158.0583 and 136.0762; FT-IR (neat) ν in cm⁻¹: 3342, 3160, 1668, 1615. In agreement with previous literature data.

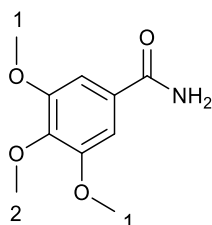
2,4-Dichlorobenzamide⁹² (3.28)



Following general procedure XL, 2,4-dichlorobenzonitrile (172 mg, 1 mmol) was used as the nitrile species. The title compound was recovered after purification by column chromatography (R_f 0.24) as a white solid (160 mg, 84%).

mp 192-194 °C (lit.⁹² 193-195 °C); ¹H NMR (500 MHz, DMSO-d⁶): δ 7.92 (br s, 1H, NH), 7.69 – 7.62 (m, 2H, NH and CH_{Ar}), 7.47 (d, J = 0.9 Hz, 2H, CH_{Ar}); ¹³C NMR (126 MHz, DMSO-d⁶): δ 167.2, 136.0, 134.2, 130.9, 130.0, 129.1, 127.2; HRMS-ESI calcd for [C₇H₅Cl₂NONa]⁺ and [C₇H₆Cl₂NO]⁺: 211.9640 [M+Na]⁺ and 189.9821 [M+H]⁺. Found: 211.9648 and 189.9827; FT-IR (neat) ν in cm⁻¹: 3372, 3175, 1647, 1619. In agreement with previous literature data.

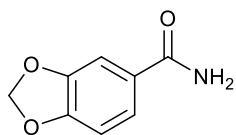
3,4,5-Trimethoxybenzamide²⁵⁷ (3.29)



Following general procedure XL, 3,4,5-trimethoxybenzonitrile (193 mg, 1 mmol) was used as the nitrile species. The title compound was recovered as a white solid (202 mg, 96%) after being passed through a silica plug and the solvent evaporated.

mp 175-176 °C (lit.²⁵⁷ 174-176 °C); ¹H NMR (500 MHz, DMSO-d⁶): δ 7.94 (br s, 1H, NH), 7.32 (br s, 1H, NH), 7.21 (s, 2H, CH_{Ar}), 3.81 (s, 6H, 1), 3.69 (s, 3H, 2); ¹³C NMR (126 MHz, DMSO-d⁶): δ 167.3, 152.5, 139.9, 129.4, 105.1, 60.0, 56.0; HRMS-ESI calcd for [C₁₀H₁₃NO₄Na]⁺ and [C₁₀H₁₄NO₄]⁺: 234.0737 [M+Na]⁺ and 212.0917 [M+H]⁺. Found: 234.0745 and 212.0924; FT-IR (neat) ν in cm⁻¹: 3357, 3174, 1660, 1616. In agreement with previous literature data.

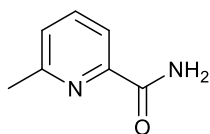
Benzo[d][1,3]dioxole-5-carboxamide²⁵⁸ (3.30)



Following general procedure XXXIX, piperonylnitrile (147 mg, 1 mmol) was used as the nitrile species. The title compound was recovered after purification by column chromatography (R_f 0.21) as a white solid (155 mg, 93%).

mp 165-167 °C (lit.²⁵⁸ 164-166 °C); ^1H NMR (500 MHz, DMSO- d_6): δ 7.80 (br s, 1H, NH), 7.46 (dd, $J = 8.1, 1.7$ Hz, 1H, CH_{Ar}), 7.40 (d, $J = 1.7$ Hz, 1H, CH_{Ar}), 7.22 (br s, 1H, NH), 6.96 (d, $J = 8.1$ Hz, 1H, CH_{Ar}), 6.08 (br s, 2H, CH_2); ^{13}C NMR (126 MHz, DMSO- d_6): δ 166.9, 149.6, 147.2, 128.3, 122.5, 107.7, 107.5, 101.6; HRMS-ESI calcd for $[\text{C}_9\text{H}_9\text{NO}_2\text{Na}]^+$: 186.0531 $[\text{M}+\text{Na}]^+$. Found: 186.0533; FT-IR (neat) ν in cm^{-1} : 3352, 3158, 1654, 1626. In agreement with previous literature data.

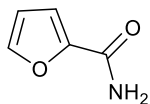
6-Methylpicolinamide²⁵⁹ (3.31)



Following general procedure XL, 2-cyano-6-methylpyridine (118 mg, 1 mmol) was used as the nitrile species. The title compound was recovered after purification by column chromatography (R_f 0.26) as a white solid (114 mg, 84%).

mp 113-115 °C (lit.²⁵⁹ 116 °C); ^1H NMR (300 MHz, DMSO- d_6): δ 8.00 (br s, 1H, NH), 7.89 – 7.80 (m, 2H, CH_{Ar}), 7.63 (br s, 1H, NH), 7.48 – 7.41 (m, 1H, CH_{Ar}), 2.54 (s, 3H, CH_3); ^{13}C NMR (75 MHz, DMSO- d_6): δ 166.1, 157.1, 149.7, 137.8, 126.0, 119.0, 23.9; HRMS-ESI calcd for $[\text{C}_7\text{H}_8\text{N}_2\text{ONa}]^+$ and $[\text{C}_7\text{H}_9\text{N}_2\text{O}]^+$: 159.0529 $[\text{M}+\text{Na}]^+$ and 137.0709 $[\text{M}+\text{H}]^+$. Found: 159.0535 and 137.0711; FT-IR (neat) ν in cm^{-1} : 3436, 3142, 1685, 1588. In agreement with previous literature data.

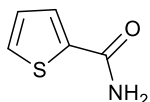
Furan-2-carboxamide⁹² (3.32)



Following general procedure XXXIX, 2-furonitrile (88 μL , 1 mmol) was used as the nitrile species. The title compound was recovered as a light brown solid (107 mg, 96%) after being passed through a silica plug and the solvent evaporated.

mp 141-142 $^{\circ}\text{C}$ (lit.⁹² 141-142 $^{\circ}\text{C}$); ^1H NMR (500 MHz, CDCl_3): δ 7.47 (dd, $J = 1.7, 0.7$ Hz, 1H, CH_{Ar}), 7.17 (dd, $J = 3.5, 0.7$ Hz, 1H, CH_{Ar}), 6.52 (dd, $J = 3.5, 1.7$ Hz, 1H, CH_{Ar}), 6.25 (br s, 1H, NH), 5.61 (br s, 1H, NH); ^{13}C NMR (126 MHz, CDCl_3): δ 160.2, 147.6, 144.5, 115.3, 112.5; HRMS-ESI calcd for $[\text{C}_5\text{H}_5\text{NO}_2\text{Na}]^+$ and $[\text{C}_5\text{H}_6\text{NO}_2]^+$: 134.0212 $[\text{M}+\text{Na}]^+$ and 112.0393 $[\text{M}+\text{H}]^+$. Found: 134.0213 and 112.0395; FT-IR (neat) ν in cm^{-1} : 3340, 3159, 1661, 1621. In agreement with previous literature data.

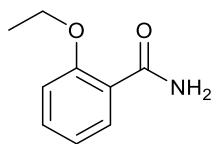
Thiophene-2-carboxamide⁹² (3.33)



Following general procedure XXXIX, 2-thiophenecarbonitrile (93 μL , 1 mmol) was used as the nitrile species. The title compound was recovered as a white solid (125 mg, 98%) after being passed through a silica plug and the solvent evaporated.

mp 177-178 $^{\circ}\text{C}$ (lit.⁹² 177-179 $^{\circ}\text{C}$); ^1H NMR (300 MHz, DMSO-d_6): δ 7.97 (br s, 1H, NH), 7.76 – 7.71 (m, 2H, CH_{Ar}), 7.40 (br s, 1H, NH), 7.15 – 7.09 (m, 1H, CH_{Ar}); ^{13}C NMR (126 MHz, DMSO-d_6): δ 162.8, 140.3, 130.9, 128.6, 127.8; HRMS-ESI calcd for $[\text{C}_5\text{H}_5\text{NOSNa}]^+$: 149.9984 $[\text{M}+\text{Na}]^+$. Found: 149.9993; FT-IR (neat) ν in cm^{-1} : 3359, 3167, 1651, 1602. In agreement with previous literature data.

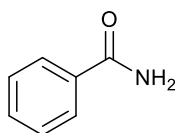
2-Ethoxybenzamide⁵³ (3.47)



Following general procedure XLII, 2-ethoxybenzotrile (140 μL , 1 mmol) was used as the nitrile species. The title compound was recovered as a white solid (162 mg, 98%) after being passed through a silica plug and the solvent evaporated.

mp 129-131 $^{\circ}\text{C}$ (lit.⁵³ 131-132 $^{\circ}\text{C}$); ^1H NMR (300 MHz, DMSO-d^6): δ 7.85 – 7.77 (m, 1H, CH_{Ar}), 7.58 (br s, 2H, NH), 7.50 – 7.41 (m, 1H, CH_{Ar}), 7.16 – 7.08 (m, 1H, CH_{Ar}), 7.05 – 6.97 (m, 1H, CH_{Ar}), 4.16 (q, $J = 7.0$ Hz, 2H, CH_2), 1.39 (t, $J = 7.0$ Hz, 3H, CH_3); ^{13}C NMR (75 MHz, DMSO-d^6): δ 166.4, 156.5, 132.5, 130.8, 122.7, 120.4, 112.9, 64.2, 14.5; HRMS-ESI calcd for $[\text{C}_9\text{H}_{11}\text{NO}_2\text{Na}]^+$: 188.0682 $[\text{M}+\text{Na}]^+$. Found: 188.0688; FT-IR (neat) ν in cm^{-1} : 3368, 3170, 1640, 1626. In agreement with previous literature data.

Benzonitrile⁹² (3.16)



Following general procedure XLIII, benzonitrile (4.12 mL, 40 mmol) was used as the nitrile species. The title compound was recovered as a white solid (4.56 g, 94%) after being passed through a silica plug and the solvent evaporated.

mp 127-128 $^{\circ}\text{C}$ (lit.⁹² 129-130 $^{\circ}\text{C}$); ^1H NMR (500 MHz, DMSO-d^6): δ 8.01 (br s, 1H, NH), 7.90 (d, $J = 7.7$ Hz, 2H, Ph), 7.50 (t, $J = 7.3$ Hz, 1H, Ph), 7.47 – 7.36 (m, 3H, NH and Ph); ^{13}C NMR (126 MHz, DMSO-d^6): δ 168.0, 134.3, 131.2, 128.2, 127.5; HRMS-ESI calcd for $[\text{C}_7\text{H}_7\text{NONa}]^+$ and $[\text{C}_7\text{H}_8\text{NO}]^+$: 144.0420 $[\text{M}+\text{Na}]^+$ and 122.0600 $[\text{M}+\text{H}]^+$. Found: 144.0426 and 122.0606; FT-IR (neat) ν in cm^{-1} : 3360, 3166, 1652, 1623. In agreement with previous literature data.

Secondary Amide Formation

General Procedure XLIV – Coupling of Nitriles with Benzylamine

(Table 3.18, Results and Discussion II)

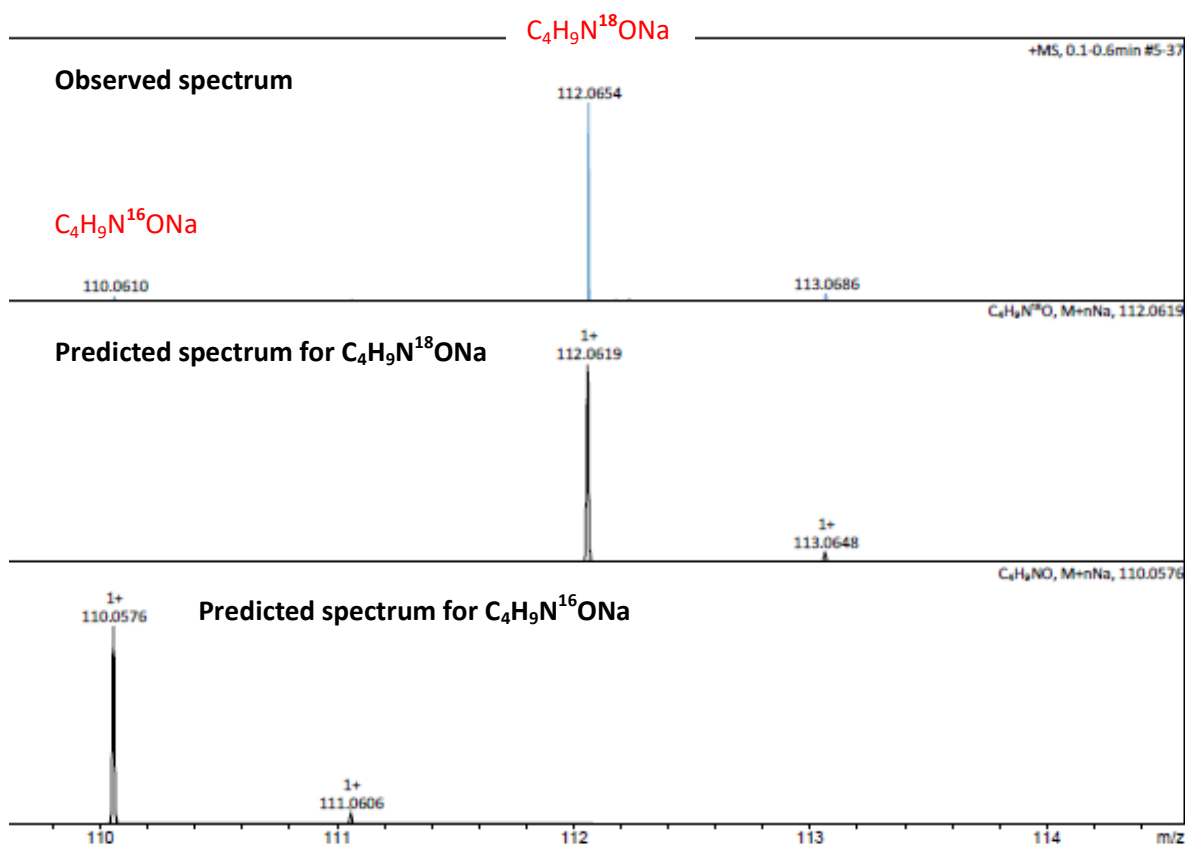
To an oven dried Schlenk carousel tube containing the appropriate nitrile (1 mmol) was added palladium acetate (11 mg, 5 mol%), 2,2'-bipyridine, (7.8 mg, 5 mol%), and the appropriate solvent system (**A-C**). The tube was then sealed and the reaction mixture heated at 70 °C for 24 hours. After being allowed to cool to room temperature, the crude reaction mixture was diluted with methanol (5 mL) and the solvent removed *in vacuo* on a rotary evaporator. 1,4-Dimethoxybenzene (46 mg, 1/3 mmol) was used as an NMR standard and the crude reaction mixture was analysed by ¹H NMR spectroscopy in DMSO-d⁶.

Investigations into the Reaction Mechanism

General Procedure XLV – H₂¹⁸O-Labeling Study

(Scheme 3.11, Results and Discussion II)

To an oven dried Schlenk carousel tube containing butyronitrile (22 μL, 0.25 mmol) was added palladium acetate (225 mg, 1 mmol), 2,2'-bipyridine (156 mg, 1 mmol) and H₂¹⁸O (0.5 mL, 0.5 M, 97% atom ¹⁸O). The tube was then sealed and the reaction mixture heated at 70 °C for 24 hours. After being allowed to cool to room temperature, the reaction mixture was diluted with methanol (5 mL) and the solvent removed *in vacuo* on a rotary evaporator whilst azeotroping with toluene. The crude reaction mixture was passed through a short plug of silica to remove the catalyst (eluting with DCM/MeOH, 95:5), the solvent evaporated and the resulting product analysed by mass spectrometry for incorporation of the ¹⁸O label. Full incorporation (97%) was observed.



6.4. Chapter 4 Experimental Methods and Compound Characterisation

General Procedure XLVI – Bulk Synthesis of 4-Methylbenzaldehyde oxime Model Substrate

(Scheme 4.4, Results and Discussion III)

To a stirred solution of hydroxylamine hydrochloride (2.78 g, 40 mmol) in ethanol (50 mL) and water (10 mL) was added *p*-tolualdehyde (2.36 mL, 20 mmol) at 0 °C. Sodium acetate (4.92 g, 60 mmol) was added slowly and the reaction mixture was allowed to warm to room temperature and left stirring for 3 hours. Ethanol was removed from the solution, then water (40 mL) was added and the product was extracted into DCM (2 x 60 mL). The combined organic extracts were dried over MgSO₄ and the solvent removed *in vacuo*. The resulting aldoxime was analysed by its ¹H and ¹³C NMR spectra and mass spectrometry data and used without further purification.

General Procedure XLVII – Comparison between Toluene and Ethanol as Solvents

(Table 4.1, Results and Discussion III)

To an oven dried Radleys carousel tube containing 4-methylbenzaldehyde oxime (135 mg, 1 mmol) was added Cu(OAc)₂ (9.1 mg, 5 mol%), acetonitrile (2.6 μL, 5 mol%) if appropriate and either ethanol or toluene (0.33 mL, 0.33 M, unless stated otherwise). The tube was then sealed and the reaction mixture heated at the appropriate temperature for the appropriate amount of time. After being allowed to cool, QuadraSil™ TA was added and the reaction left to stir at room temperature for 5 minutes. The crude reaction mixture was diluted with DCM (5 mL), filtered and the solvent removed *in vacuo* on a rotary evaporator. Percentage conversion into 4-methylbenzamide and the by-products was calculated from the crude ¹H NMR spectra by comparison of the peaks at 7.47 ppm (2H, 4-methylbenzaldehyde oxime), 7.55 ppm (2H, 4-methylbenzonitrile), 7.71 ppm (2H, 4-methylbenzamide) and 7.78 ppm (2H, 4-methylbenzaldehyde).

General Procedure XLVIII – Copper(II) Acetate and Acetonitrile Loading Screen at 40 °C

(Table 4.2, Results and Discussion III)

To an oven dried Radleys carousel tube containing 4-methylbenzaldehyde oxime (135 mg, 1 mmol) was added the appropriate amount of Cu(OAc)₂ and acetonitrile, followed by toluene (1 mL, 1 M). The tube was then sealed and the reaction mixture heated at 40 °C for 24 hours.

After being allowed to cool, QuadraSil™ TA was added and the reaction left to stir at room temperature for 5 minutes. The crude reaction mixture was diluted with DCM (5 mL), filtered and the solvent removed *in vacuo* on a rotary evaporator. Percentage conversion into 4-methylbenzamide and the by-products was calculated from the crude ¹H NMR spectra by comparison of the peaks at 7.47 ppm (2H, 4-methylbenzaldehyde oxime), 7.55 ppm (2H, 4-methylbenzoxime), 7.71 ppm (2H, 4-methylbenzamide) and 7.78 ppm (2H, 4-methylbenzaldehyde).

General Procedure XLIX – Acetonitrile Loading Screen at 30 °C

(Table 4.3, Results and Discussion III)

To an oven dried Radleys carousel tube containing 4-methylbenzaldehyde oxime (135 mg, 1 mmol) was added Cu(OAc)₂ (9.1 mg, 5 mol%), the appropriate amount of acetonitrile and toluene (1 mL, 1 M). The tube was then sealed and the reaction mixture heated at 30 °C for 24 hours. After being allowed to cool, QuadraSil™ TA was added and the reaction left to stir at room temperature for 5 minutes. The crude reaction mixture was diluted with DCM (5 mL), filtered and the solvent removed *in vacuo* on a rotary evaporator. Percentage conversion into 4-methylbenzamide and the by-products was calculated from the crude ¹H NMR spectra by comparison of the peaks at 7.47 ppm (2H, 4-methylbenzaldehyde oxime), 7.55 ppm (2H, 4-methylbenzoxime), 7.71 ppm (2H, 4-methylbenzamide) and 7.78 ppm (2H, 4-methylbenzaldehyde).

General Procedure L – Concentration Screen at 30 °C

(Table 4.4, Results and Discussion III)

To an oven dried Radleys carousel tube containing 4-methylbenzaldehyde oxime (135 mg, 1 mmol) was added Cu(OAc)₂ (9.1 mg, 5 mol%), acetonitrile (2.6 μL, 5 mol%) and the appropriate amount of toluene. The tube was then sealed and the reaction mixture heated at 30 °C for 24 hours. After being allowed to cool, QuadraSil™ TA was added and the reaction left to stir at room temperature for 5 minutes. The crude reaction mixture was diluted with DCM (5 mL), filtered and the solvent removed *in vacuo* on a rotary evaporator. Percentage conversion into 4-methylbenzamide and the by-products was calculated from the crude ¹H NMR spectra by comparison of the peaks at 7.47 ppm (2H, 4-methylbenzaldehyde oxime), 7.55 ppm (2H, 4-methylbenzoxime), 7.71 ppm (2H, 4-methylbenzamide) and 7.78 ppm (2H, 4-methylbenzaldehyde).

General Procedure LI – Solvent Screen

(Table 4.5, Results and Discussion III)

To an oven dried Radleys carousel tube containing 4-methylbenzaldehyde oxime (135 mg, 1 mmol) was added $\text{Cu}(\text{OAc})_2$ (9.1 mg, 5 mol%), acetonitrile (2.6 μL , 5 mol%) and the appropriate solvent (1 mL, 1 M). The tube was then sealed and the reaction mixture heated at 30 °C for 24 hours. After being allowed to cool, QuadraSil™ TA was added and the reaction left to stir at room temperature for 5 minutes. The crude reaction mixture was diluted with DCM (5 mL), filtered and the solvent removed *in vacuo* on a rotary evaporator. Percentage conversion into 4-methylbenzamide and the by-products was calculated from the crude ^1H NMR spectra by comparison of the peaks at 7.47 ppm (2H, 4-methylbenzaldehyde oxime), 7.55 ppm (2H, 4-methylbenzonitrile), 7.71 ppm (2H, 4-methylbenzamide) and 7.78 ppm (2H, 4-methylbenzaldehyde).

General Procedure LII – Copper Catalyst Screen

(Table 4.6, Results and Discussion III)

To an oven dried Radleys carousel tube containing 4-methylbenzaldehyde oxime (135 mg, 1 mmol) was added the appropriate copper catalyst (5 mol%), acetonitrile (2.6 μL , 5 mol%) and toluene (1 mL, 1 M). The tube was then sealed and the reaction mixture heated at 30 °C for 24 hours. After being allowed to cool, QuadraSil™ TA was added and the reaction left to stir at room temperature for 5 minutes. The crude reaction mixture was diluted with DCM (5 mL), filtered and the solvent removed *in vacuo* on a rotary evaporator. Percentage conversion into 4-methylbenzamide and the by-products was calculated from the crude ^1H NMR spectra by comparison of the peaks at 7.47 ppm (2H, 4-methylbenzaldehyde oxime), 7.55 ppm (2H, 4-methylbenzonitrile), 7.71 ppm (2H, 4-methylbenzamide) and 7.78 ppm (2H, 4-methylbenzaldehyde).

General Procedure LIII – Ligand Screen

(Table 4.7, Results and Discussion III)

To an oven dried Radleys carousel tube containing 4-methylbenzaldehyde oxime (135 mg, 1 mmol) was added $\text{Cu}(\text{OAc})_2$ (9.1 mg, 5 mol%), acetonitrile (2.6 μL , 5 mol%), the appropriate ligand (5 or 10 mol%) and toluene (1 mL, 1 M). The tube was then sealed and the reaction mixture heated at 30 °C for 24 hours, unless otherwise stated. After being allowed to cool, QuadraSil™ TA was added and the reaction left to stir at room temperature for 5 minutes.

The crude reaction mixture was diluted with DCM (5 mL), filtered and the solvent removed *in vacuo* on a rotary evaporator. Percentage conversion into 4-methylbenzamide and the by-products was calculated from the crude ¹H NMR spectra by comparison of the peaks at 7.47 ppm (2H, 4-methylbenzaldehyde oxime), 7.55 ppm (2H, 4-methylbenzoxime), 7.71 ppm (2H, 4-methylbenzamide) and 7.78 ppm (2H, 4-methylbenzaldehyde).

General Procedure LIV – Effect of Copper(II) Acetate, Sodium Nitrite and Acetonitrile on the Rearrangement Reaction

(Table 4.8, Results and Discussion III)

To an oven dried Radleys carousel tube containing 4-methylbenzaldehyde oxime (135 mg, 1 mmol) was added Cu(OAc)₂ (9.1 mg, 5 mol%), sodium nitrite (6.9 mg, 10 mol%), acetonitrile (2.6 μL, 5 mol%) and toluene (1 mL, 1 M), unless stated otherwise. The tube was then sealed and the reaction mixture heated at 30 °C unless stated otherwise for 24 hours. After being allowed to cool, QuadraSil™ TA was added and the reaction left to stir at room temperature for 5 minutes. The crude reaction mixture was diluted with DCM (5 mL), filtered and the solvent removed *in vacuo* on a rotary evaporator. Percentage conversion into 4-methylbenzamide and the by-products was calculated from the crude ¹H NMR spectra by comparison of the peaks at 7.47 ppm (2H, 4-methylbenzaldehyde oxime), 7.55 ppm (2H, 4-methylbenzoxime), 7.71 ppm (2H, 4-methylbenzamide) and 7.78 ppm (2H, 4-methylbenzaldehyde).

General Procedure LV – Nitrite/Nitrate Screen

(Table 4.9, Results and Discussion III)

To an oven dried Radleys carousel tube containing 4-methylbenzaldehyde oxime (135 mg, 1 mmol) was added Cu(OAc)₂ (9.1 mg, 5 mol%), the appropriate nitrite or nitrate (10 mol%) and toluene (1 mL, 1 M). The tube was then sealed and the reaction mixture heated at 30 °C for 8 hours. After being allowed to cool, QuadraSil™ TA was added and the reaction left to stir at room temperature for 5 minutes. The crude reaction mixture was diluted with DCM (5 mL), filtered and the solvent removed *in vacuo* on a rotary evaporator. Percentage conversion into 4-methylbenzamide and the by-products was calculated from the crude ¹H NMR spectra by comparison of the peaks at 7.47 ppm (2H, 4-methylbenzaldehyde oxime), 7.55 ppm (2H, 4-methylbenzoxime), 7.71 ppm (2H, 4-methylbenzamide) and 7.78 ppm (2H, 4-methylbenzaldehyde).

General Procedure LVI – Silver Nitrite/Sodium Nitrite Loading Screen

(Table 4.10, Results and Discussion III)

To an oven dried Radleys carousel tube containing 4-methylbenzaldehyde oxime (135 mg, 1 mmol) was added $\text{Cu}(\text{OAc})_2$ (9.1 mg, 5 mol%), the appropriate amount of NaNO_2 or AgNO_2 and toluene (1 mL, 1 M). The tube was then sealed and the reaction mixture heated at 30 °C for 8 hours. After being allowed to cool, QuadraSil™ TA was added and the reaction left to stir at room temperature for 5 minutes. The crude reaction mixture was diluted with DCM (5 mL), filtered and the solvent removed *in vacuo* on a rotary evaporator. Percentage conversion into 4-methylbenzamide and the by-products was calculated from the crude ^1H NMR spectra by comparison of the peaks at 7.47 ppm (2H, 4-methylbenzaldehyde oxime), 7.55 ppm (2H, 4-methylbenzoxime), 7.71 ppm (2H, 4-methylbenzamide) and 7.78 ppm (2H, 4-methylbenzaldehyde).

General Procedure LVII – Time Screen

(Table 4.11, Results and Discussion III)

To an oven dried Radleys carousel tube containing 4-methylbenzaldehyde oxime (135 mg, 1 mmol) was added $\text{Cu}(\text{OAc})_2$ (9.1 mg, 5 mol%), NaNO_2 (6.9 mg, 10 mol%) and toluene (1 mL, 1 M), unless stated otherwise. The tube was then sealed and the reaction mixture heated at 30 °C for the appropriate amount of time. After being allowed to cool, QuadraSil™ TA was added and the reaction left to stir at room temperature for 5 minutes. The crude reaction mixture was diluted with DCM (5 mL), filtered and the solvent removed *in vacuo* on a rotary evaporator. Percentage conversion into 4-methylbenzamide and the by-products was calculated from the crude ^1H NMR spectra by comparison of the peaks at 7.47 ppm (2H, 4-methylbenzaldehyde oxime), 7.55 ppm (2H, 4-methylbenzoxime), 7.71 ppm (2H, 4-methylbenzamide) and 7.78 ppm (2H, 4-methylbenzaldehyde).

General Procedure LVIII – Preformation of the Catalyst

(Scheme 4.6, Results and Discussion III)

To an oven dried Radleys carousel tube was added $\text{Cu}(\text{OAc})_2$ (9.1 mg, 5 mol%), NaNO_2 (6.9 mg, 10 mol%) and toluene (0.5 mL). The tube was then sealed and the reaction mixture heated at 30 °C for 10 minutes. 4-Methylbenzaldehyde oxime (135 mg, 1 mmol) and toluene (0.5 mL) were then added and the reaction mixture heated at 30 °C for 8 hours. After being allowed to cool, QuadraSil™ TA was added and the reaction left to stir at room temperature

for 5 minutes. The crude reaction mixture was diluted with DCM (5 mL), filtered and the solvent removed *in vacuo* on a rotary evaporator. Percentage conversion into 4-methylbenzamide and the by-products was calculated from the crude ^1H NMR spectra by comparison of the peaks at 7.47 ppm (2H, 4-methylbenzaldehyde oxime), 7.55 ppm (2H, 4-methylbenzoxime), 7.71 ppm (2H, 4-methylbenzamide) and 7.78 ppm (2H, 4-methylbenzaldehyde).

General Procedure LIX – Addition of Diethylhydroxylamine at the Start of the Reaction

(Table 4.12, Results and Discussion III)

To an oven dried Radleys carousel tube containing 4-methylbenzaldehyde oxime (135 mg, 1 mmol) was added $\text{Cu}(\text{OAc})_2$ (9.1 mg, 5 mol%), NaNO_2 (6.9 mg, 10 mol%), NEt_2OH (21 μL , 20 mol%) and toluene (1 mL, 1 M). The tube was then sealed and the reaction mixture heated at 30 °C for 24 hours. After being allowed to cool, QuadraSilTM TA was added and the reaction left to stir at room temperature for 5 minutes. The crude reaction mixture was diluted with DCM (5 mL), filtered and the solvent removed *in vacuo* on a rotary evaporator. Percentage conversion into 4-methylbenzamide and the by-products was calculated from the crude ^1H NMR spectra by comparison of the peaks at 7.47 ppm (2H, 4-methylbenzaldehyde oxime), 7.55 ppm (2H, 4-methylbenzoxime), 7.71 ppm (2H, 4-methylbenzamide) and 7.78 ppm (2H, 4-methylbenzaldehyde).

General Procedure LX – Addition of Diethylhydroxylamine at the End of the Reaction

(Table 4.12, Results and Discussion III)

To an oven dried Radleys carousel tube containing 4-methylbenzaldehyde oxime (135 mg, 1 mmol) was added $\text{Cu}(\text{OAc})_2$ (9.1 mg, 5 mol%), NaNO_2 (6.9 mg, 10 mol%) and toluene (1 M). The tube was then sealed and the reaction mixture heated at 30 °C for 24 hours. NEt_2OH (21 μL , 20 mol%) was added to the reaction and the reaction mixture heated at 30 °C for a further 2 hours. After being allowed to cool, QuadraSilTM TA was added and the reaction left to stir at room temperature for 5 minutes. The crude reaction mixture was diluted with DCM (5 mL), filtered and the solvent removed *in vacuo* on a rotary evaporator. Percentage conversion into 4-methylbenzamide and the by-products was calculated from the crude ^1H NMR spectra by comparison of the peaks at 7.47 ppm (2H, 4-methylbenzaldehyde oxime), 7.55 ppm (2H, 4-methylbenzoxime), 7.71 ppm (2H, 4-methylbenzamide) and 7.78 ppm (2H, 4-methylbenzaldehyde).

General Procedure LXI – Synthesis of Aldoximes

To a stirred solution of hydroxylamine hydrochloride (1.38 g, 20 mmol) in ethanol/water (5:1, 30 mL) was added the appropriate aldehyde (10 mmol) at 0 °C. Sodium acetate (2.46 g, 30 mmol) was added slowly and the reaction mixture was allowed to warm to room temperature and left stirring for 3 hours. Ethanol was removed *in vacuo*, water (20 mL) added to the residue and the product extracted into dichloromethane (2 x 30 mL). The combined organic extracts were then dried over magnesium sulphate and the solvent removed *in vacuo*. The resulting aldoximes were analysed by their ^1H and ^{13}C NMR spectra and mass spectrometry data and used without further purification.

General Procedure LXII – Synthesis of Primary Amides

(Table 4.13, Results and Discussion III)

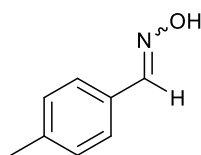
To an oven dried Radleys carousel tube containing the appropriate aldoxime (2 mmol) was added $\text{Cu}(\text{OAc})_2$ (18 mg, 5 mol%), NaNO_2 (14 mg, 10 mol%) and toluene (2 mL, 1 M). The tube was then sealed and the reaction mixture heated at 30 °C, unless otherwise stated, for 24 hours. After being allowed to cool, QuadraSilTM TA was added and the reaction left to stir at room temperature for 5 minutes. The crude reaction mixture was diluted with DCM (5 mL), filtered, washed and the solvent removed *in vacuo* on a rotary evaporator. Percentage conversion was calculated from the crude ^1H NMR spectra and the crude amide products were purified by silica column chromatography (eluting with a 100% DCM to 95:5 DCM/MeOH gradient).

General Procedure LXIII – Unsuccessful Substrates

(Table 4.14, Results and Discussion III)

To an oven dried Radleys carousel tube containing the appropriate aldoxime (2 mmol) was added $\text{Cu}(\text{OAc})_2$ (18 mg, 5 mol%), NaNO_2 (14 mg, 10 mol%) and toluene (2 mL, 1 M). The tube was then sealed and the reaction mixture heated at 30 °C for 24 hours. After being allowed to cool, QuadraSilTM TA was added and the reaction left to stir at room temperature for 5 minutes. The crude reaction mixture was diluted with DCM (5 mL), filtered, washed and the solvent removed *in vacuo* on a rotary evaporator. Percentage conversion was calculated from the crude ^1H NMR spectra by comparison of the peaks of the starting aldoxime, amide product and by-products.

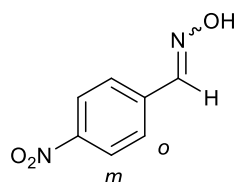
4-Methylbenzaldehyde oxime²⁶⁰



Following general procedure LXI, 4-methylbenzaldehyde (1.18 mL, 10 mmol) was used as the aldehyde species. The title compound was recovered after aqueous work-up as a white solid (1.27 g, 94%).

mp 72-74 °C (lit.²⁶¹ 76-78 °C); ¹H NMR (300 MHz, CDCl₃): δ 8.12 (s, 1H, C(=NOH)H), 7.47 (d, *J* = 8.2 Hz, 2H, CH_{Ar}), 7.20 (d, *J* = 8.2 Hz, 2H, CH_{Ar}), 2.37 (s, 3H, CH₃); ¹³C NMR (126 MHz, CDCl₃): δ 150.2, 140.4, 129.5, 129.1, 127.0, 21.5; HRMS-ESI calcd for [C₈H₁₀NO]⁺: 136.0757 [M+H]⁺. Found: 136.0793. In agreement with previous literature data.

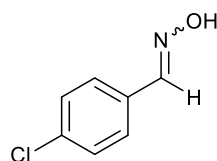
4-Nitrobenzaldehyde oxime²⁶²



Following general procedure LXI, 4-nitrobenzaldehyde (1.51 g, 10 mmol) was used as the aldehyde species. The title compound was recovered after aqueous work-up as an off-white solid (1.10 g, 66%).

mp 135-136 °C (lit.²⁶² 132-133 °C); ¹H NMR (500 MHz, CDCl₃): δ 8.25 (d, *J* = 8.8 Hz, 2H, *m*-CH_{Ar}), 8.20 (s, 1H, C(=NOH)H), 7.75 (d, *J* = 8.8 Hz, 2H, *o*-CH_{Ar}), 7.66 (br s, 1H, OH); ¹³C NMR (126 MHz, DMSO-d₆): δ 147.9, 147.2, 139.9, 127.7, 124.3; HRMS-ESI calcd for [C₇H₆N₂O₃Na]⁺: 189.0271 [M+Na]⁺. Found: 189.0279. In agreement with previous literature data.

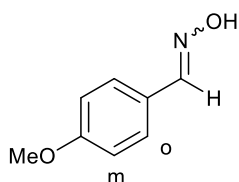
4-Chlorobenzaldehyde oxime²⁶³



Following general procedure LXI, 4-chlorobenzaldehyde (1.41 g, 10 mmol) was used as the aldehyde species. The title compound was recovered after aqueous work-up as a white solid (1.37 g, 89%).

mp 111-112 °C (lit.²⁶³ 110 °C); ¹H NMR (500 MHz, CDCl₃): δ 8.10 (s, 1H, C(=NOH)H), 7.58 (br s, 1H, OH), 7.51 (d, *J* = 8.5 Hz, 2H, CH_{Ar}), 7.36 (d, *J* = 8.5 Hz, 2H, CH_{Ar}); ¹³C NMR (126 MHz, DMSO-d⁶): δ 147.5, 134.2, 132.4, 129.1, 128.4; HRMS-ESI calcd for [C₇H₆ClNONa]⁺: 178.0030 [M+Na]⁺. Found: 178.0049. In agreement with previous literature data.

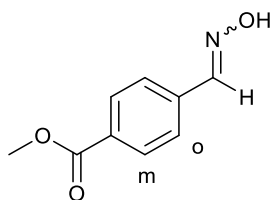
4-Methoxybenzaldehyde oxime²⁶⁴



Following general procedure LXI, 4-methoxybenzaldehyde (1.22 mL, 10 mmol) was used as the aldehyde species. The title compound was recovered after aqueous work-up as a white solid (1.49 g, 99%).

mp 72-75 °C (lit.²⁶⁴ 73-74 °C); ¹H NMR (500 MHz, CDCl₃): δ 8.10 (s, 1H, C(=NOH)H), 7.90 (br s, 1H, OH), 7.52 (d, *J* = 8.7 Hz, 2H, *o*-CH_{Ar}), 6.92 (d, *J* = 8.7 Hz, 2H, *m*-CH_{Ar}), 3.84 (s, 3H, OCH₃); ¹³C NMR (126 MHz, DMSO-d⁶): δ 160.6, 148.1, 128.3, 126.1, 114.5, 55.5; HRMS-ESI calcd for [C₈H₁₀NO₂]⁺: 152.0706 [M+H]⁺. Found: 152.0722. In agreement with previous literature data.

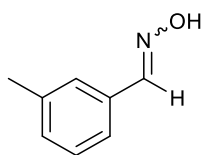
Methyl 4-((hydroxyimino)methyl)benzoate²⁶⁵



Following general procedure LXI, methyl 4-formylbenzoate (1.64 g, 10 mmol) was used as the aldehyde species. The title compound was recovered after aqueous work-up as a white solid (1.46 g, 82%).

mp 122-125 °C (lit.²⁶⁵ 119-122 °C); ¹H NMR (500 MHz, CDCl₃): δ 8.18 (s, 1H, C(=NOH)H), 8.06 (d, *J* = 8.4 Hz, 2H, *m*-CH_{Ar}), 7.79 (br s, 1H, OH), 7.65 (d, *J* = 8.4 Hz, 2H, *o*-CH_{Ar}), 3.94 (s, 3H, CH₃); ¹³C NMR (126 MHz, DMSO-d⁶): δ 166.3, 147.9, 138.0, 130.3, 130.0, 127.0, 52.6; HRMS-ESI calcd for [C₉H₁₀NO₃]⁺: 180.0655 [M+H]⁺. Found: 180.0661. In agreement with previous literature data.

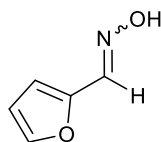
3-Methylbenzaldehyde oxime²⁶⁶



Following general procedure LXI, 3-methylbenzaldehyde (1.18 mL, 10 mmol) was used as the aldehyde species. The title compound was recovered after aqueous work-up as a yellow oil (1.32 g, 98%).

¹H NMR (500 MHz, CDCl₃): δ 8.13 (s, 1H, C(=NOH)H), 7.40 (s, 1H, CH_{Ar}), 7.37 (d, *J* = 7.6 Hz, 1H, CH_{Ar}), 7.28 (t, *J* = 7.6 Hz, 1H, CH_{Ar}), 7.21 (t, *J* = 7.6 Hz, 1H, CH_{Ar}), 2.38 (s, 3H, CH₃); ¹³C NMR (126 MHz, CDCl₃): δ 150.8, 138.5, 132.0, 131.1, 128.8, 127.8, 124.5, 21.3; HRMS-ESI calcd for [C₈H₁₀NO]⁺: 136.0757 [M+H]⁺. Found: 136.0772. In agreement with previous literature data.

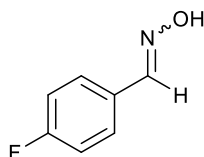
Furan-2-carbaldehyde oxime²⁶⁷



Following general procedure LXI, furfural (0.83 mL, 10 mmol) was used as the aldehyde species. The title compound was recovered after aqueous work-up as a white solid (1.10 g, 99%).

mp 91-93 °C (lit.²⁶⁷ 90 °C); ¹H NMR (300 MHz, CDCl₃): δ 8.39 (br s, 1H, OH), 7.51 (s, 1H, C(=NOH)H), 7.51 – 7.44 (m, 1H, CH_{Ar}), 7.35 – 7.27 (m, 1H, CH_{Ar}), 6.59 – 6.51 (m, 1H, CH_{Ar}); ¹³C NMR (126 MHz, CDCl₃): δ 145.1, 143.4, 137.2, 118.2, 112.3; HRMS-ESI calcd for [C₅H₅NO₂Na]⁺: 134.0212 [M+Na]⁺. Found: 134.0215. In agreement with previous literature data.

4-Fluorobenzaldehyde oxime⁵⁴

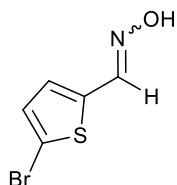


Following general procedure LXI, 4-fluorobenzaldehyde (1.07 mL, 10 mmol) was used as the aldehyde species. The title compound was recovered after aqueous work-up as a white solid (1.35 g, 97%).

mp 86-87 °C (lit.⁵⁴ 84 °C); ¹H NMR (500 MHz, CDCl₃): δ 8.12 (s, 1H, C(=NOH)H), 7.71 (br s, 1H, OH), 7.61 – 7.53 (m, 2H, CH_{Ar}), 7.13 – 7.04 (m, 2H, CH_{Ar}); ¹³C NMR (126 MHz, DMSO-d₆): δ

163.0, 147.5 (d, $J = 248.3$ Hz), 130.0 (d, $J = 2.9$ Hz), 128.8 (d, $J = 8.2$ Hz), 116.0 (d, $J = 21.9$ Hz); ^{19}F NMR (470 MHz, CDCl_3): δ -110.27 (referenced against 4-fluorotoluene); HRMS-ESI calcd for $[\text{C}_7\text{H}_7\text{FNO}]^+$: 140.0506 $[\text{M}+\text{H}]^+$. Found: 140.0513. In agreement with previous literature data.

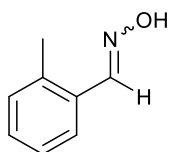
5-Bromothiophene-2-carbaldehyde oxime²⁶⁵



Following general procedure LXI, 5-bromothiophene-2-carboxaldehyde (1.19 mL, 10 mmol) was used as the aldehyde species. The title compound was recovered after aqueous work-up as a brown solid (1.92 g, 93%).

mp 149-151 °C (lit.²⁶⁵ 149 °C); ^1H NMR (300 MHz, CDCl_3): δ 8.92 (br s, 1H, OH), 7.63 (s, 1H, C(=NOH)H), 7.12 (d, $J = 4.2$ Hz, 1H, CH_{Ar}), 7.08 (d, $J = 4.2$ Hz, 1H, CH_{Ar}); ^{13}C NMR (126 MHz, DMSO-d_6): δ 140.1, 132.9, 131.6, 129.8, 117.9; HRMS-ESI calcd for $[\text{C}_5\text{H}_4\text{BrNOSNa}]^+$: 227.9089 $[\text{M}+\text{Na}]^+$. Found: 227.9094. In agreement with previous literature data.

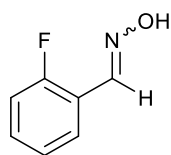
2-Methylbenzaldehyde oxime²⁶⁸



Following general procedure LXI, 2-methylbenzaldehyde (1.16 mL, 10 mmol) was used as the aldehyde species. The title compound was recovered after aqueous work-up as a yellow oil (1.34 g, 99%).

^1H NMR (500 MHz, CDCl_3): δ 8.45 (s, 1H, C(=NOH)H), 7.70 – 7.63 (m, 1H, CH_{Ar}), 7.34 – 7.26 (m, 1H, CH_{Ar}), 7.26 – 7.18 (m, 2H, CH_{Ar}), 2.44 (s, 3H, CH_3); ^{13}C NMR (126 MHz, CDCl_3): δ 147.7, 136.4, 131.5, 131.0, 129.3, 126.6, 126.2, 19.7; HRMS-ESI calcd for $[\text{C}_8\text{H}_{10}\text{NO}]^+$: 136.0757 $[\text{M}+\text{H}]^+$. Found: 136.0771. In agreement with previous literature data.

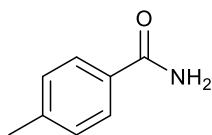
2-Fluorobenzaldehyde oxime²⁶⁹



Following general procedure LXI, 2-fluorobenzaldehyde (1.05 mL, 10 mmol) was used as the aldehyde species. The title compound was recovered after aqueous work-up as a clear oil (1.38 g, 99%).

¹H NMR (500 MHz, CDCl₃): δ 8.38 (s, 1H, C(=NOH)H), 7.76 – 7.68 (m, 1H, CH_{Ar}), 7.41 – 7.32 (m, 1H, CH_{Ar}), 7.19 – 7.12 (m, 1H, CH_{Ar}), 7.12 – 7.05 (m, 1H, CH_{Ar}); ¹³C NMR (126 MHz, DMSO-d⁶): δ 160.3 (d, *J* = 250.1 Hz), 142.1 (d, *J* = 3.7 Hz), 131.0 (d, *J* = 8.2 Hz), 126.8 (d, *J* = 3.1 Hz), 124.6 (d, *J* = 3.3 Hz), 120.9 (d, *J* = 10.8 Hz), 115.9 (d, *J* = 21.0 Hz); ¹⁹F NMR (470 MHz, CDCl₃): δ -121.40 (referenced against 4-fluorotoluene); HRMS-ESI calcd for [C₇H₇FNO]⁺: 140.0506 [M+H]⁺. Found: 140.0522. In agreement with previous literature data.

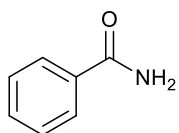
4-Methylbenzamide⁵³ (4.2)



Following general procedure LXII, 4-methylbenzaldehyde oxime (270 mg, 2 mmol) was used as the aldoxime species. The title compound was recovered after purification by silica column chromatography as a white solid (229 mg, 85%).

mp 161-163 °C (lit.⁵³ 161-162 °C); ¹H NMR (500 MHz, DMSO-d⁶): δ 7.90 (br s, 1H, NH), 7.79 (d, *J* = 8.2 Hz, 2H, CH_{Ar}), 7.31 – 7.21 (m, 3H, NH and CH_{Ar}), 2.33 (s, 3H, CH₃); ¹³C NMR (126 MHz, DMSO-d⁶): δ 167.8, 141.0, 131.5, 128.7, 127.5, 20.9; HRMS-ESI calcd for [C₈H₁₀NO]⁺: 136.0757 [M+H]⁺. Found: 136.0775; FT-IR (neat) ν in cm⁻¹: 3340, 3163, 1672, 1620. In agreement with previous literature data.

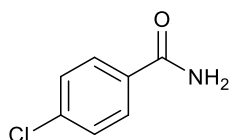
Benzamide⁹² (4.5)



Following general procedure LXII, benzaldehyde oxime (242 mg, 2 mmol) was used as the aldoxime species. The title compound was recovered after purification by silica column chromatography as a white solid (208 mg, 86%).

mp 128-129 °C (lit.⁹² 129-130 °C); ¹H NMR (500 MHz, DMSO-d⁶): δ 8.02 (br s, 1H, NH), 7.93 – 7.88 (m, 2H, Ph), 7.53 – 7.48 (m, 1H, Ph), 7.47 – 7.41 (m, 2H, Ph), 7.40 (br s, 1H, NH); ¹³C NMR (126 MHz, DMSO-d⁶): δ 168.0, 134.3, 131.2, 128.2, 127.5; HRMS-ESI calcd for [C₇H₈NO]⁺: 122.0600 [M+H]⁺. Found: 122.0626; FT-IR (neat) ν in cm⁻¹: 3365, 3167, 1655, 1621. In agreement with previous literature data.

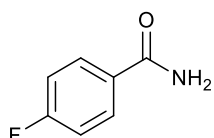
4-Chlorobenzamide⁹² (4.6)



Following general procedure LXII, 4-chlorobenzaldehyde oxime (311 mg, 2 mmol) was used as the aldoxime species. The title compound was recovered after purification by silica column chromatography as a white solid (248 mg, 80%).

mp 178-180 °C (lit.⁹² 178-181 °C); ¹H NMR (500 MHz, DMSO-d⁶): δ 8.06 (br s, 1H, NH), 7.90 (d, *J* = 8.7 Hz, 2H, CH_{Ar}), 7.50 (d, *J* = 8.7 Hz, 2H, CH_{Ar}), 7.47 (br s, 1H, NH); ¹³C NMR (126 MHz, DMSO-d⁶): δ 166.9, 136.1, 133.0, 129.4, 128.3; HRMS-ESI calcd for [C₇H₆ClN₂O]⁺: 178.0030 [M+Na]⁺. Found: 178.0039; FT-IR (neat) ν in cm⁻¹: 3367, 3172, 1653, 1619. In agreement with previous literature data.

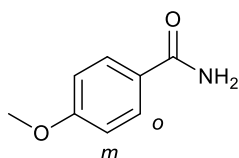
4-Fluorobenzamide⁹² (4.7)



Following general procedure LXII, 4-fluorobenzaldehyde oxime (278 mg, 2 mmol) was used as the aldoxime species. The title compound was recovered after purification by silica column chromatography as a white solid (247 mg, 89%).

mp 153-155 °C (lit.⁹² 153-155 °C); ¹H NMR (500 MHz, CDCl₃): δ 7.83 (dd, *J* = 8.9, 5.3 Hz, 2H, *CH*_{Ar}), 7.13 (t, *J* = 8.9 Hz, 2H, *CH*_{Ar}), 5.83 (br s, 2H, NH₂); ¹³C NMR (126 MHz, DMSO-d₆): δ 166.8, 163.9 (d, *J* = 248.3 Hz), 130.7 (d, *J* = 2.9 Hz), 130.1 (d, *J* = 9.0 Hz), 115.1 (d, *J* = 21.6 Hz); ¹⁹F NMR (470 MHz, CDCl₃): δ -109.39 (referenced against 4-fluorotoluene); HRMS-ESI calcd for [C₇H₆FNONa]⁺: 162.0326 [M+Na]⁺. Found: 162.0348; FT-IR (neat) ν in cm⁻¹: 3329, 3150, 1671, 1624. In agreement with previous literature data.

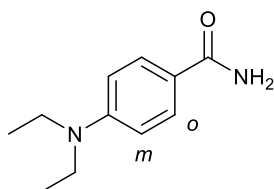
4-Methoxybenzamide¹⁴⁵ (4.8)



Following general procedure LXII, 4-methoxybenzaldehyde oxime (302 mg, 2 mmol) was used as the aldoxime species. The title compound was recovered after purification by silica column chromatography as a white solid (217 mg, 72%).

mp 167-169 °C (lit.¹⁴⁵ 166-168 °C); ¹H NMR (500 MHz, CDCl₃): δ 7.78 (d, *J* = 8.9 Hz, 2H, *o*-CH_{Ar}), 6.94 (d, *J* = 8.9 Hz, 2H, *m*-CH_{Ar}), 5.72 (br s, 2H, NH₂), 3.86 (s, 3H, CH₃); ¹³C NMR (126 MHz, CDCl₃): δ 169.0, 162.7, 129.4, 125.7, 114.0, 55.6; HRMS-ESI calcd for [C₈H₁₀NO₂]⁺: 152.0706 [M+H]⁺. Found: 152.0718; FT-IR (neat) ν in cm⁻¹: 3390, 3166, 1646, 1616. In agreement with previous literature data.

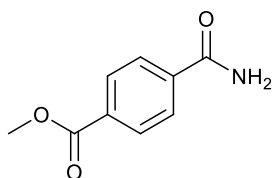
4-(Diethylamino)benzamide¹⁷³ (4.9)



Following general procedure LXII, 4-diethylaminobenzaldehyde oxime (384 mg, 2 mmol) was used as the aldoxime species. The title compound was recovered after purification by silica column chromatography as a white solid (230 mg, 60%).

mp 147-149 °C (lit.¹⁷³ 144-147 °C); ¹H NMR (500 MHz, CDCl₃): δ 7.68 (d, *J* = 9.1 Hz, 2H, *o*-CH_{Ar}), 6.63 (d, *J* = 9.1 Hz, 2H, *m*-CH_{Ar}), 5.59 (br s, 2H, NH₂), 3.41 (q, *J* = 7.1 Hz, 2H, CH₂), 1.19 (t, *J* = 7.1 Hz, 3H, CH₃); ¹³C NMR (126 MHz, CDCl₃): δ 169.4, 150.5, 129.5, 119.1, 110.5, 44.6, 12.6; HRMS-ESI calcd for [C₁₁H₁₆N₂ONa]⁺: 215.1155 [M+Na]⁺. Found: 215.1192; FT-IR (neat) ν in cm⁻¹: 3382, 3197, 1652, 1620. In agreement with previous literature data.

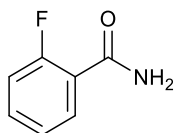
Methyl 4-carbamoylbenzoate²⁵⁴ (4.10)



Following general procedure LXII, methyl 4-((hydroxyimino)methyl)benzoate (358 mg, 2 mmol) was used as the aldoxime species. The title compound was recovered after purification by silica column chromatography as a white solid (286 mg, 80%).

mp 209-210 °C (lit.²⁵⁵ 206-209 °C); ¹H NMR (500 MHz, DMSO-d⁶): δ 8.14 (br s, 1H, NH), 8.00 (q, *J* = 8.6 Hz, 4H, CH_{Ar}), 7.55 (br s, 1H, NH), 3.88 (s, 3H, CH₃); ¹³C NMR (126 MHz, DMSO-d⁶): δ 167.0, 165.7, 138.4, 131.8, 129.0, 127.8, 52.3; HRMS-ESI calcd for [C₉H₉NO₃Na]⁺: 202.0475 [M+Na]⁺. Found: 202.0492; FT-IR (neat) ν in cm⁻¹: 3360, 3160, 1661, 1624. In agreement with previous literature data.

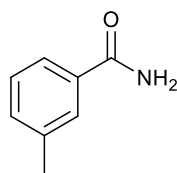
2-Fluorobenzamide²⁷⁰ (4.11)



Following general procedure LXII, 2-fluorobenzaldehyde oxime (278 mg, 2 mmol) was used as the aldoxime species. The title compound was recovered after purification by silica column chromatography as an off-white solid (189 mg, 68%).

mp 117-119 °C (lit.²⁷⁰ 118 °C); ¹H NMR (500 MHz, CDCl₃): δ 8.07 (td, *J* = 7.9, 1.9 Hz, 1H, CH_{Ar}), 7.49 – 7.43 (m, 1H, CH_{Ar}), 7.23 (td, *J* = 7.6, 1.1 Hz, 1H, CH_{Ar}), 7.10 (ddd, *J* = 12.0, 8.3, 1.1 Hz, 1H, CH_{Ar}), 6.91 (br s, 1H, NH), 6.73 (br s, 1H, NH); ¹³C NMR (126 MHz, CDCl₃): δ 165.4 (d, *J* = 2.6 Hz), 161.0 (d, *J* = 248.5 Hz), 133.9 (d, *J* = 9.4 Hz), 132.2 (d, *J* = 2.0 Hz), 124.8 (d, *J* = 3.4 Hz), 120.4 (d, *J* = 11.5 Hz), 116.1 (d, *J* = 24.8 Hz); ¹⁹F NMR (470 MHz, CDCl₃): δ -114.91 (referenced against 4-fluorotoluene); HRMS-ESI calcd for [C₇H₆FNONa]⁺: 162.0326 [M+Na]⁺. Found: 162.0337; FT-IR (neat) ν in cm⁻¹: 3384, 3180, 1652, 1624. In agreement with previous literature data.

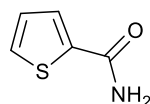
3-Methylbenzamide⁹² (4.12)



Following general procedure LXII, 3-methylbenzaldehyde oxime (270 mg, 2 mmol) was used as the aldoxime species. The title compound was recovered after purification by silica column chromatography as a white solid (216 mg, 80%).

mp 93-94 °C (lit.⁹² 92-93 °C); ¹H NMR (500 MHz, CDCl₃): δ 7.66 – 7.64 (m, 1H, CH_{Ar}), 7.60 – 7.57 (m, 1H, CH_{Ar}), 7.36 – 7.31 (m, 2H, CH_{Ar}), 6.09 (br s, 1H, NH), 5.87 (br s, 1H, NH), 2.40 (s, 3H, CH₃); ¹³C NMR (126 MHz, CDCl₃): δ 169.7, 138.7, 133.4, 132.9, 128.6, 128.3, 124.4, 21.5; HRMS-ESI calcd for [C₈H₁₀NO]⁺: 136.0757 [M+H]⁺. Found: 136.0790; FT-IR (neat) ν in cm⁻¹: 3370, 3191, 1650, 1610. In agreement with previous literature data.

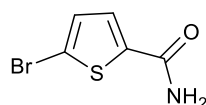
Thiophene-2-carboxamide⁹² (4.13)



Following general procedure LXII, thiophene-2-carboxaldehyde oxime (254 mg, 2 mmol) was used as the aldoxime species. The title compound was recovered after purification by silica column chromatography as a white solid (246 mg, 97%).

mp 178-179 °C (lit.⁹² 177-179 °C); ¹H NMR (500 MHz, DMSO-d⁶): δ 7.95 (br s, 1H, NH), 7.75 – 7.71 (m, 2H, CH_{Ar}), 7.36 (br s, 1H, NH), 7.14 – 7.11 (m, 1H, CH_{Ar}); ¹³C NMR (126 MHz, DMSO-d⁶): δ 162.8, 140.3, 130.9, 128.6, 127.9; HRMS-ESI calcd for [C₅H₅NOSNa]⁺: 149.9984 [M+Na]⁺. Found: 149.9999; FT-IR (neat) ν in cm⁻¹: 3367, 3171, 1653, 1612. In agreement with previous literature data.

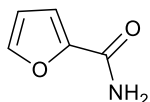
5-Bromothiophene-2-carboxamide²⁷¹ (4.14)



Following general procedure LXII, 5-bromothiophene-2-carbaldehyde oxime (412 mg, 2 mmol) was used as the aldoxime species. The title compound was recovered after purification by silica column chromatography as a white solid (399 mg, 97%).

mp 166-167 °C (lit.²⁷¹ 164-166 °C); ¹H NMR (500 MHz, DMSO-d⁶): δ 8.03 (br s, 1H, NH), 7.57 (d, *J* = 4.0 Hz, 1H, CH_{Ar}), 7.51 (br s, 1H, NH), 7.27 (d, *J* = 4.0 Hz, 1H, CH_{Ar}); ¹³C NMR (126 MHz, DMSO-d⁶): δ 161.8, 142.2, 131.5, 129.3, 116.8; HRMS-ESI calcd for [C₅H₅BrNOS]⁺: 205.9270 [M+H]⁺. Found: 205.9280; FT-IR (neat) ν in cm⁻¹: 3370, 3173, 1660, 1619. In agreement with previous literature data.

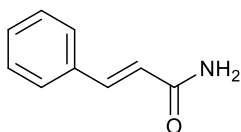
Furan-2-carboxamide⁹² (4.15)



Following general procedure LXII, furan-2-carbaldehyde oxime (222 mg, 2 mmol) was used as the aldoxime species. The title compound was recovered after purification by silica column chromatography as a white solid (217 mg, 98%).

mp 143-144 °C (lit.⁹² 141-142 °C); ¹H NMR (500 MHz, CDCl₃): δ 7.47 (dd, *J* = 1.7, 0.7 Hz, 1H, CH_{Ar}), 7.17 (dd, *J* = 3.5, 0.7 Hz, 1H, CH_{Ar}), 6.52 (dd, *J* = 3.5, 1.7 Hz, 1H, CH_{Ar}), 6.25 (br s, 1H, NH), 5.61 (br s, 1H, NH); ¹³C NMR (126 MHz, CDCl₃): δ 160.2, 147.6, 144.5, 115.3, 112.5; HRMS-ESI calcd for [C₅H₆NO₂]⁺: 112.0393 [M+H]⁺. Found: 112.0409; FT-IR (neat) ν in cm⁻¹: 3343, 3156, 1660, 1618. In agreement with previous literature data.

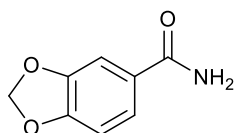
Cinnamamide⁹² (4.16)



Following general procedure LXII, cinnamaldehyde oxime (294 mg, 2 mmol) was used as the aldoxime species. The title compound was recovered after purification by silica column chromatography as an off-white solid (209 mg, 71%).

mp 150-152 °C (lit.⁹² 149-151 °C); ¹H NMR (500 MHz, CDCl₃): δ 7.65 (d, *J* = 15.7 Hz, 1H, PhCH), 7.54 – 7.50 (m, 2H, Ph), 7.41 – 7.35 (m, 3H, Ph), 6.46 (d, *J* = 15.7 Hz, 1H, PhCHCH), 5.57 (br s, 2H, NH₂); ¹³C NMR (126 MHz, CDCl₃): δ 167.8, 142.8, 134.7, 130.2, 129.0, 128.1, 119.5; HRMS-ESI calcd for [C₉H₁₀NO]⁺: 148.0757 [M+H]⁺. Found: 148.0781; FT-IR (neat) ν in cm⁻¹: 3380, 3165, 1656, 1609. In agreement with previous literature data.

Benzo[d][1,3]dioxole-5-carboxamide²⁵⁸ (4.17)



Following general procedure LXII, piperonaldoxime (330 mg, 2 mmol) was used as the aldoxime species. The title compound was recovered after purification by silica column chromatography as an off-white solid (244 mg, 74%).

mp 166-167 °C (lit.²⁵⁸ 164-166 °C); ¹H NMR (500 MHz, DMSO-d⁶): δ 7.80 (br s, 1H, NH), 7.46 (dd, *J* = 8.2, 1.8 Hz, 1H, CH_{Ar}), 7.40 (d, *J* = 1.8 Hz, 1H, CH_{Ar}), 7.22 (br s, 1H, NH), 6.96 (d, *J* = 8.2 Hz, 1H, CH_{Ar}), 6.08 (br s, 2H, CH₂); ¹³C NMR (126 MHz, DMSO-d⁶): δ 166.9, 149.6, 147.2, 128.3, 122.5, 107.7, 107.5, 101.6; HRMS-ESI calcd for [C₈H₇NO₃Na]⁺: 188.0318 [M+Na]⁺. Found: 188.0326; FT-IR (neat) ν in cm⁻¹: 3350, 3162, 1653, 1627. In agreement with previous literature data.

6.5. Chapter 5 Experimental Methods and Compound Characterisation

General Procedure LXIV – Conversion of Aldehydes into Aldoximes in Toluene

(Scheme 5.2, Results and Discussion IV)

To a stirred solution of hydroxylamine hydrochloride (69 mg, 1 mmol) in toluene (1 mL, 1 M) was added 4-methylbenzaldehyde (118 μ L, 1 mmol) at 0 °C. Sodium acetate (123 mg, 1.5 mmol) was added slowly and the reaction mixture was allowed to warm to room temperature and left stirring for 24 hours. The crude reaction mixture was diluted with DCM (5 mL) and the solvent removed *in vacuo* on a rotary evaporator. Percentage conversion into 4-methylbenzaldehyde oxime was calculated from the crude ^1H NMR spectra by comparison of the peaks at 7.78 ppm (2H, 4-methylbenzaldehyde) and 7.47 ppm (2H, 4-methylbenzaldehyde oxime).

General Procedure LXV – Conversion of Aldoximes into Amides in EtOH/H₂O

(Scheme 5.2, Results and Discussion IV)

To an oven dried Radleys carousel tube containing 4-methylbenzaldehyde oxime (135 mg, 1 mmol) was added $\text{Cu}(\text{OAc})_2$ (9.1 mg, 5 mol%), NaNO_2 (6.9 mg, 10 mol%) and EtOH/H₂O (5:1, 1 M). The tube was then sealed and the reaction mixture heated at 30 °C for 24 hours. After being allowed to cool, QuadraSilTM TA was added and the reaction left to stir at room temperature for 5 minutes. The crude reaction mixture was diluted with DCM (5 mL), filtered, washed and the solvent removed *in vacuo* on a rotary evaporator. Percentage conversion into 4-methylbenzamide was calculated from the crude ^1H NMR spectra by comparison of the peaks at 7.47 ppm (2H, 4-methylbenzaldehyde oxime), 7.55 ppm (2H, 4-methylbenzamide), 7.71 ppm (2H, 4-methylbenzamide) and 7.78 ppm (2H, 4-methylbenzaldehyde).

General Procedure LXVI – Conversion of Aldehydes into Aldoximes in DCM/DCE

(Table 5.1, Results and Discussion IV)

To an oven dried Radleys carousel tube containing 4-methylbenzaldehyde (118 μ L, 1 mmol) was added hydroxylamine hydrochloride (69 mg, 1 mmol), sodium acetate (123 mg, 1.5 mmol) and the appropriate solvent (1 mL, 1 M). The tube was then sealed and the reaction mixture heated at the appropriate temperature for 24 hours. The crude reaction mixture was diluted with DCM (5 mL) and the solvent removed *in vacuo* on a rotary evaporator. Percentage conversion into 4-methylbenzaldehyde oxime was calculated from the crude ^1H

NMR spectra by comparison of the peaks at 7.78 ppm (2H, 4-methylbenzaldehyde) and 7.47 ppm (2H, 4-methylbenzaldehyde oxime).

General Procedure LXVII – Temperature Screen for the Rearrangement of 4-methylbenzaldehyde oxime in DCE

(Table 5.2, Results and Discussion IV)

To an oven dried Radleys carousel tube containing 4-methylbenzaldehyde oxime (135 mg, 1 mmol) was added Cu(OAc)₂ (9.1 mg, 5 mol%), NaNO₂ (6.9 mg, 10 mol%) and DCE (1 mL, 1 M). The tube was then sealed and the reaction mixture heated at the appropriate temperature for 24 hours. After being allowed to cool, QuadraSil™ TA was added and the reaction left to stir at room temperature for 5 minutes. The crude reaction mixture was diluted with DCM (5 mL), filtered, washed and the solvent removed *in vacuo* on a rotary evaporator. Percentage conversion into 4-methylbenzamide was calculated from the crude ¹H NMR spectra by comparison of the peaks at 7.47 ppm (2H, 4-methylbenzaldehyde oxime), 7.55 ppm (2H, 4-methylbenzamide), 7.71 ppm (2H, 4-methylbenzamide) and 7.78 ppm (2H, 4-methylbenzaldehyde).

General Procedure LXVIII – Time Screen for the Conversion of Aldehydes into Amides

(Table 5.3, Results and Discussion IV)

To an oven dried Radleys carousel tube containing 4-methylbenzaldehyde (118 μL, 1 mmol) was added hydroxylamine hydrochloride (69 mg, 1 mmol), sodium acetate (123 mg, 1.5 mmol) and DCE (1 mL, 1 M). The tube was then sealed and the reaction mixture heated at 30 °C for the appropriate amount of time. The crude reaction mixture was diluted with DCM (5 mL) and the solvent removed *in vacuo* on a rotary evaporator. Percentage conversion into 4-methylbenzaldehyde oxime was calculated from the crude ¹H NMR spectra by comparison of the peaks at 7.78 ppm (2H, 4-methylbenzaldehyde) and 7.47 ppm (2H, 4-methylbenzaldehyde oxime).

General Procedure LXIX – Initial One-Pot Protocol for the Conversion of Aldehydes into Amides

(Table 5.4, Results and Discussion IV)

To an oven dried Radleys carousel tube containing 4-methylbenzaldehyde (118 μL, 1 mmol) was added hydroxylamine hydrochloride (69 mg, 1 mmol), sodium acetate (123 mg, 1.5

mmol) and DCE (1 mL, 1 M). The tube was then sealed and the reaction mixture heated at 30 °C. After 24 hours $\text{Cu}(\text{OAc})_2$ (9.1 mg, 5 mol%) and NaNO_2 (6.9 mg, 10 mol%) were added and the reaction was left for a further 24 hours at the appropriate temperature. After being allowed to cool, QuadraSil™ TA was added and the reaction left to stir at room temperature for 5 minutes. The crude reaction mixture was diluted with DCM (5 mL), filtered, washed and the solvent removed *in vacuo* on a rotary evaporator. Percentage conversion into 4-methylbenzamide was calculated from the crude ^1H NMR spectra by comparison of the peaks at 7.47 ppm (2H, 4-methylbenzaldehyde oxime), 7.55 ppm (2H, 4-methylbenzoxime), 7.71 ppm (2H, 4-methylbenzamide) and 7.78 ppm (2H, 4-methylbenzaldehyde).

General Procedure LXX – Addition of First Step By-Products to the Reaction

(Table 5.5, Results and Discussion IV)

To an oven dried Radleys carousel tube containing 4-methylbenzaldehyde oxime (135 mg, 1 mmol) was added $\text{Cu}(\text{OAc})_2$ (9.1 mg, 5 mol%), NaNO_2 (6.9 mg, 10 mol%), the appropriate additive(s) and DCE (1 mL, 1 M). The tube was then sealed and the reaction mixture heated at 30 °C for 24 hours. After being allowed to cool, QuadraSil™ TA was added and the reaction left to stir at room temperature for 5 minutes. The crude reaction mixture was diluted with DCM (5 mL), filtered, washed and the solvent removed *in vacuo* on a rotary evaporator. Percentage conversion into 4-methylbenzamide was calculated from the crude ^1H NMR spectra by comparison of the peaks at 7.47 ppm (2H, 4-methylbenzaldehyde oxime), 7.55 ppm (2H, 4-methylbenzoxime), 7.71 ppm (2H, 4-methylbenzamide), 7.78 ppm (2H, 4-methylbenzaldehyde), 8.03 ppm (2H, 4-methylbenzoic acid) and any peaks corresponding to unidentified by-products.

General Procedure LXXI – Use of Sodium Bicarbonate as the Base

(Scheme 5.4, Results and Discussion IV)

To an oven dried Radleys carousel tube containing 4-methylbenzaldehyde (118 μL , 1 mmol) was added hydroxylamine hydrochloride (69 mg, 1 mmol), sodium acetate (123 mg, 1.5 mmol) and DCE (1 mL, 1 M). The tube was then sealed and the reaction mixture heated at 30 °C for 24 hours. The crude reaction mixture was diluted with DCM (5 mL) and the solvent removed *in vacuo* on a rotary evaporator. Percentage conversion into 4-methylbenzaldehyde oxime was calculated from the crude ^1H NMR spectra by comparison of the peaks at 7.78 ppm (2H, 4-methylbenzaldehyde) and 7.47 ppm (2H, 4-methylbenzaldehyde oxime).

General Procedure LXXII – Comparison Between Sodium Acetate and Sodium Bicarbonate in the One-Pot Protocol

(Table 5.6, Results and Discussion IV)

To an oven dried Radleys carousel tube containing 4-methylbenzaldehyde (118 μ L, 1 mmol) was added hydroxylamine hydrochloride (69 mg, 1 mmol), the appropriate base (1.5 mmol) and DCE (1 mL, 1 M). The tube was then sealed and the reaction mixture heated at 30 °C. After 24 hours $\text{Cu}(\text{OAc})_2$ (9.1 mg, 5 mol%) and NaNO_2 (6.9 mg, 10 mol%) were added and the reaction was left for a further 24 hours at 80 °C. After being allowed to cool, QuadraSil™ TA was added and the reaction left to stir at room temperature for 5 minutes. The crude reaction mixture was diluted with DCM (5 mL), filtered, washed and the solvent removed *in vacuo* on a rotary evaporator. Percentage conversion into 4-methylbenzamide was calculated from the crude ^1H NMR spectra by comparison of the peaks at 7.47 ppm (2H, 4-methylbenzaldehyde oxime), 7.55 ppm (2H, 4-methylbenzonitrile), 7.71 ppm (2H, 4-methylbenzamide) and 7.78 ppm (2H, 4-methylbenzaldehyde).

General Procedure LXXIII – Sodium Bicarbonate Equivalents Screen

(Table 5.7, Results and Discussion IV)

To an oven dried Radleys carousel tube containing 4-methylbenzaldehyde (118 μ L, 1 mmol) was added hydroxylamine hydrochloride (69 mg, 1 mmol), the appropriate amount of sodium bicarbonate and DCE (1 mL, 1 M). The tube was then sealed and the reaction mixture heated at 30 °C for 24 hours. The crude reaction mixture was diluted with DCM (5 mL) and the solvent removed *in vacuo* on a rotary evaporator. Percentage conversion into 4-methylbenzaldehyde oxime was calculated from the crude ^1H NMR spectra by comparison of the peaks at 7.78 ppm (2H, 4-methylbenzaldehyde) and 7.47 ppm (2H, 4-methylbenzaldehyde oxime).

General Procedure LXXIV – One-Pot Protocol using 1.1 Equivalents of Sodium Bicarbonate

(Scheme 5.5, Results and Discussion IV)

To an oven dried Radleys carousel tube containing 4-methylbenzaldehyde (118 μ L, 1 mmol) was added hydroxylamine hydrochloride (69 mg, 1 mmol), sodium bicarbonate (92 mg, 1.1 mmol) and DCE (1 mL, 1 M). The tube was then sealed and the reaction mixture heated at 30 °C. After 24 hours $\text{Cu}(\text{OAc})_2$ (9.1 mg, 5 mol%) and NaNO_2 (6.9 mg, 10 mol%) were added and the reaction was left for a further 24 hours at 30 °C. After being allowed to cool, QuadraSil™

TA was added and the reaction left to stir at room temperature for 5 minutes. The crude reaction mixture was diluted with DCM (5 mL), filtered, washed and the solvent removed *in vacuo* on a rotary evaporator. Percentage conversion into 4-methylbenzamide was calculated from the crude ¹H NMR spectra by comparison of the peaks at 7.47 ppm (2H, 4-methylbenzaldehyde oxime), 7.55 ppm (2H, 4-methylbenzoxime), 7.71 ppm (2H, 4-methylbenzamide) and 7.78 ppm (2H, 4-methylbenzaldehyde).

General Procedure LXXV – Time Screen for the Conversion of Aldehydes into Amides With and Without Water

(Table 5.8, Results and Discussion IV)

To an oven dried Radleys carousel tube containing 4-methylbenzaldehyde (118 μ L, 1 mmol) was added hydroxylamine hydrochloride (69 mg, 1 mmol), sodium bicarbonate (92 mg, 1.1 mmol), water (1-3 mmol) if appropriate and DCE (1 mL, 1 M). The tube was then sealed and the reaction mixture heated at 30 °C for the appropriate amount of time. The crude reaction mixture was diluted with DCM (5 mL) and the solvent removed *in vacuo* on a rotary evaporator. Percentage conversion into 4-methylbenzaldehyde oxime was calculated from the crude ¹H NMR spectra by comparison of the peaks at 7.78 ppm (2H, 4-methylbenzaldehyde) and 7.47 ppm (2H, 4-methylbenzaldehyde oxime).

General Procedure LXXVI –Conversion of Aldehydes into Amides Using Aqueous Hydroxylamine

(Scheme 5.6, Results and Discussion IV)

To an oven dried Radleys carousel tube containing 4-methylbenzaldehyde (118 μ L, 1 mmol) was added hydroxylamine in H₂O (61 μ L, 1 mmol, 50% wt in H₂O), sodium bicarbonate (92 mg, 1.1 mmol) if appropriate, and DCE (1 mL, 1 M). The tube was then sealed and the reaction mixture heated at 30 °C for 1 hour. The crude reaction mixture was diluted with DCM (5 mL) and the solvent removed *in vacuo* on a rotary evaporator. Percentage conversion into 4-methylbenzaldehyde oxime was calculated from the crude ¹H NMR spectra by comparison of the peaks at 7.78 ppm (2H, 4-methylbenzaldehyde) and 7.47 ppm (2H, 4-methylbenzaldehyde oxime).

General Procedure LXXVII – One-Pot Protocol With and Without Water in the First Step

(Table 5.9, Results and Discussion IV)

To an oven dried Radleys carousel tube containing 4-methylbenzaldehyde (118 μ L, 1 mmol) was added hydroxylamine hydrochloride (69 mg, 1 mmol), sodium bicarbonate (92 mg, 1.1 mmol), water if appropriate and DCE (1 mL, 1 M). The tube was then sealed and the reaction mixture heated at 30 $^{\circ}$ C. After the appropriate amount of time $\text{Cu}(\text{OAc})_2$ (9.1 mg, 5 mol%) and NaNO_2 (6.9 mg, 10 mol%) were added and the reaction was left for a further 24 hours at 30 $^{\circ}$ C. After being allowed to cool, QuadraSilTM TA was added and the reaction left to stir at room temperature for 5 minutes. The crude reaction mixture was diluted with DCM (5 mL), filtered, washed and the solvent removed *in vacuo* on a rotary evaporator. Percentage conversion into 4-methylbenzamide was calculated from the crude ^1H NMR spectra by comparison of the peaks at 7.47 ppm (2H, 4-methylbenzaldehyde oxime), 7.55 ppm (2H, 4-methylbenzoxime), 7.71 ppm (2H, 4-methylbenzamide) and 7.78 ppm (2H, 4-methylbenzaldehyde).

General Procedure LXXVIII – Final Optimisation of One-Pot Protocol

(Table 5.10, Results and Discussion IV)

To an oven dried Radleys carousel tube containing 4-methylbenzaldehyde (118 μ L, 1 mmol) was added hydroxylamine hydrochloride (69 mg, 1 mmol), sodium bicarbonate (92 mg, 1.1 mmol) and DCE (1 mL, 1 M), unless otherwise stated. The tube was then sealed and the reaction mixture heated at 30 $^{\circ}$ C. After 4 hours $\text{Cu}(\text{OAc})_2$ (14 mg, 7.5 mol%) and NaNO_2 (10 mg, 15 mol%) were added and the reaction was left for the appropriate amount of time at 30 $^{\circ}$ C, unless otherwise stated. After being allowed to cool, QuadraSilTM TA was added and the reaction left to stir at room temperature for 5 minutes. The crude reaction mixture was diluted with DCM (5 mL), filtered, washed and the solvent removed *in vacuo* on a rotary evaporator. Percentage conversion into 4-methylbenzamide was calculated from the crude ^1H NMR spectra by comparison of the peaks at 7.47 ppm (2H, 4-methylbenzaldehyde oxime), 7.55 ppm (2H, 4-methylbenzoxime), 7.71 ppm (2H, 4-methylbenzamide) and 7.78 ppm (2H, 4-methylbenzaldehyde).

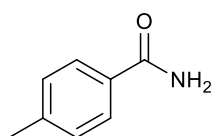
General Procedure LXXIX – Substrate Scope for the One-Pot Protocol

(Table 5.11, Results and Discussion IV)

To an oven dried Radleys carousel tube containing the appropriate aldehyde (2 mmol) was added hydroxylamine hydrochloride (139 mg, 1 mmol), sodium bicarbonate (184 mg, 1.1

mmol) and DCE (2 mL, 1 M). The tube was then sealed and the reaction mixture heated at 30 °C. After 4 hours Cu(OAc)₂ (27 mg, 7.5 mol%) and NaNO₂ (21 mg, 15 mol%) were added and the reaction was left for 20 hours at 30 °C, unless otherwise stated. After being allowed to cool, QuadraSil™ TA was added and the reaction left to stir at room temperature for 5 minutes. The crude reaction mixture was diluted with DCM (5 mL), filtered, washed and the solvent removed *in vacuo* on a rotary evaporator. Percentage conversion was calculated from the crude ¹H NMR spectra and the crude amide products were purified by silica column chromatography (eluting with a 100% DCM to 95:5 DCM/MeOH gradient).

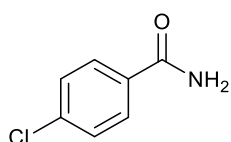
4-Methylbenzamide⁵³ (5.3)



Following general procedure LXXIX, 4-methylbenzaldehyde (236 μL, 2 mmol) was used as the aldehyde species. The title compound was recovered after purification by silica column chromatography as a white solid (216 mg, 80%).

mp 161-163 °C (lit.⁵³ 161-162 °C); ¹H NMR (500 MHz, CDCl₃): δ 7.71 (d, *J* = 8.2 Hz, 2H, CH_{Ar}), 7.24 (d, *J* = 8.2 Hz, 2H, CH_{Ar}), 5.99 (br s, 2H, NH₂), 2.40 (s, 3H, CH₃); ¹³C NMR (126 MHz, CDCl₃): δ 169.5, 142.7, 130.6, 129.4, 127.5, 21.6; HRMS-ESI calcd for [C₈H₁₀NO]⁺: 136.0757 [M+H]⁺. Found: 136.0759; FT-IR (neat) ν in cm⁻¹: 3343, 3158, 1667, 1613. In agreement with previous literature data.

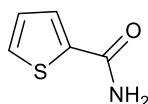
4-Chlorobenzamide⁹² (5.5)



Following general procedure LXXIX, 4-chlorobenzaldehyde (281 mg, 2 mmol) was used as the aldehyde species. The title compound was recovered after purification by silica column chromatography as a white solid (246 mg, 79%).

mp 179-181 °C (lit.⁹² 178-181 °C); ¹H NMR (500 MHz, DMSO-d⁶): δ 8.12 (br s, 1H, NH), 7.93 (d, *J* = 8.6 Hz, 2H, CH_{Ar}), 7.55 (br s, 1H, NH), 7.45 (d, *J* = 8.6 Hz, 2H, CH_{Ar}); ¹³C NMR (126 MHz, DMSO-d⁶): δ 167.3, 136.4, 133.1, 129.4, 128.4; HRMS-ESI calcd for [C₇H₆ClNONa]⁺: 178.0030 [M+Na]⁺. Found: 178.0031; FT-IR (neat) ν in cm⁻¹: 3369, 3173, 1653, 1618. In agreement with previous literature data.

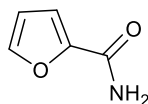
Thiophene-2-carboxamide⁹² (5.6)



Following general procedure LXXIX, 2-thiophenecarboxaldehyde (187 μL, 2 mmol) was used as the aldehyde species. Cu(OAc)₂ and NaNO₂ were added after 16 hours and the reaction was then left for a further 24 hours. The title compound was recovered after purification by silica column chromatography as a white solid (183 mg, 72%).

mp 177-179 °C (lit.⁹² 177-179 °C); ¹H NMR (500 MHz, CDCl₃): δ 7.55 – 7.51 (m, 2H, CH_{Ar}), 7.10 (dd, *J* = 5.0, 3.7 Hz, 1H, CH_{Ar}), 5.75 (br s, 2H, NH₂); ¹³C NMR (126 MHz, CDCl₃): δ 163.6, 137.9, 131.1, 129.4, 127.9; HRMS-ESI calcd for [C₅H₅NOSNa]⁺: 149.9984 [M+Na]⁺. Found: 149.9986; FT-IR (neat) ν in cm⁻¹: 3367, 3169, 1649, 1610. In agreement with previous literature data.

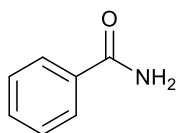
Furan-2-carboxamide⁹² (5.7)



Following general procedure LXXIX, 2-furaldehyde (166 μL, 2 mmol) was used as the aldehyde species. Cu(OAc)₂ and NaNO₂ were added after 16 hours and the reaction was then left for a further 24 hours. The title compound was recovered after purification by silica column chromatography as a light brown solid (138 mg, 62%).

mp 141-142 °C (lit.⁹² 141-142 °C); ¹H NMR (500 MHz, CDCl₃): δ 7.47 (dd, *J* = 1.7, 0.7 Hz, 1H, CH_{Ar}), 7.17 (dd, *J* = 3.5, 0.7 Hz, 1H, CH_{Ar}), 6.52 (dd, *J* = 3.5, 1.7 Hz, 1H, CH_{Ar}), 6.25 (br s, 1H, NH), 5.61 (br s, 1H, NH); ¹³C NMR (126 MHz, CDCl₃): δ 160.3, 147.7, 144.6, 115.4, 112.6; HRMS-ESI calcd for [C₅H₅NO₂Na]⁺: 134.0212 [M+Na]⁺. Found: 134.0214; FT-IR (neat) ν in cm⁻¹: 3345, 3158, 1666, 1623. In agreement with previous literature data.

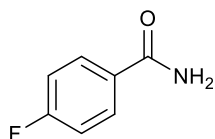
Benzamide⁹² (5.8)



Following general procedure LXXIX, benzaldehyde (203 μL , 2 mmol) was used as the aldehyde species. $\text{Cu}(\text{OAc})_2$ and NaNO_2 were added after 16 hours and the reaction was then left for a further 24 hours. The title compound was recovered after purification by silica column chromatography as a white solid (201 mg, 83%).

mp 127-19 $^{\circ}\text{C}$ (lit.⁹² 129-130 $^{\circ}\text{C}$); ^1H NMR (500 MHz, DMSO-d_6): δ 8.00 (br s, 1H, NH), 7.91 – 7.87 (m, 2H, Ph), 7.53 – 7.48 (m, 1H, Ph), 7.47 – 7.41 (m, 2H, Ph), 7.38 (br s, 1H, NH); ^{13}C NMR (126 MHz, DMSO-d_6): δ 168.0, 134.3, 131.2, 128.2, 127.5; HRMS-ESI calcd for $[\text{C}_7\text{H}_8\text{NO}]^+$: 122.0600 $[\text{M}+\text{H}]^+$. Found: 122.0605; FT-IR (neat) ν in cm^{-1} : 3366, 3163, 1658, 1620. In agreement with previous literature data.

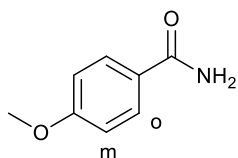
4-Fluorobenzamide⁹² (5.9)



Following general procedure LXXIX, 4-fluorobenzaldehyde (215 μL , 2 mmol) was used as the aldehyde species. $\text{Cu}(\text{OAc})_2$ and NaNO_2 were added after 16 hours and the reaction was then left for a further 24 hours. The title compound was recovered after purification by silica column chromatography as a white solid (234 mg, 84%).

mp 152-154 $^{\circ}\text{C}$ (lit.⁹² 153-155 $^{\circ}\text{C}$); ^1H NMR (500 MHz, CDCl_3): δ 7.83 (dd, $J = 8.9, 5.3$ Hz, 2H, CH_{Ar}), 7.13 (t, $J = 8.9$ Hz, 2H, CH_{Ar}), 5.83 (br s, 2H, NH_2); ^{13}C NMR (126 MHz, DMSO-d_6): δ 166.8, 163.8 (d, $J = 248.3$ Hz), 130.7 (d, $J = 2.9$ Hz), 130.1 (d, $J = 9.0$ Hz), 115.1 (d, $J = 21.6$ Hz); ^{19}F NMR (470 MHz, CDCl_3): δ -109.49 (referenced against 4-fluorotoluene); HRMS-ESI calcd for $[\text{C}_7\text{H}_6\text{FNONa}]^+$: 162.0326 $[\text{M}+\text{Na}]^+$. Found: 162.0325; FT-IR (neat) ν in cm^{-1} : 3328, 3150, 1672, 1624. In agreement with previous literature data.

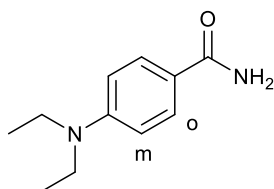
4-Methoxybenzamide¹⁴⁵ (5.10)



Following general procedure LXXIX, *p*-anisaldehyde (243 μ L, 2 mmol) was used as the aldehyde species. $\text{Cu}(\text{OAc})_2$ and NaNO_2 were added after 16 hours and the reaction was then left for a further 24 hours. The title compound was recovered after purification by silica column chromatography as a white solid (124 mg, 41%).

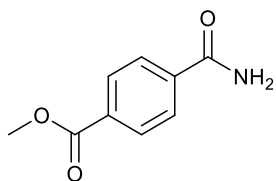
mp 166-168 $^{\circ}\text{C}$ (lit.¹⁴⁵ 166-168 $^{\circ}\text{C}$); ^1H NMR (500 MHz, CDCl_3): δ 7.79 (d, $J = 8.9$ Hz, 2H, *o*- CH_{Ar}), 6.95 (d, $J = 8.9$ Hz, 2H, *m*- CH_{Ar}), 5.73 (br s, 2H, NH_2), 3.87 (s, 3H, CH_3); ^{13}C NMR (126 MHz, DMSO-d_6): δ 169.0, 162.8, 129.4, 125.7, 114.0, 55.6; HRMS-ESI calcd for $[\text{C}_8\text{H}_{10}\text{NO}_2]^+$: 152.0706 $[\text{M}+\text{H}]^+$. Found: 152.0709; FT-IR (neat) ν in cm^{-1} : 3391, 3166, 1644, 1612. In agreement with previous literature data.

4-(Diethylamino)benzamide (5.11)



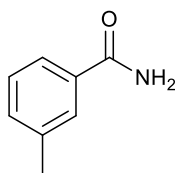
Following general procedure LXXIX, 4-diethylaminobenzaldehyde (354 mg, 2 mmol) was used as the aldehyde species. $\text{Cu}(\text{OAc})_2$ and NaNO_2 were added after 16 hours and the reaction was then left for a further 24 hours. Percentage conversion into **5.11** was calculated from the crude ^1H NMR spectra by comparison of the peaks corresponding to the starting aldehyde, aldoxime, nitrile and **5.11**.

Methyl 4-carbamoylbenzoate (5.12)



Following general procedure LXXIX, methyl 4-formylbenzoate (328 mg, 2 mmol) was used as the aldehyde species. $\text{Cu}(\text{OAc})_2$ and NaNO_2 were added after 16 hours and the reaction was then left for a further 24 hours. Percentage conversion into **5.12** was calculated from the crude ^1H NMR spectra by comparison of the peaks corresponding to the starting aldehyde, aldoxime, nitrile and **5.12**.

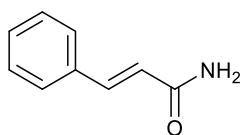
3-Methylbenzamide⁹² (5.13)



Following general procedure LXXIX, 3-methylbenzaldehyde (236 μL , 2 mmol) was used as the aldehyde species. $\text{Cu}(\text{OAc})_2$ and NaNO_2 were added after 16 hours and the reaction was then left for a further 24 hours. The title compound was recovered after purification by silica column chromatography as a white solid (216 mg, 80%).

mp 92-94 °C (lit.⁹² 92-93 °C); ^1H NMR (500 MHz, CDCl_3): δ 7.67 – 7.65 (m, 1H, CH_{Ar}), 7.61 – 7.57 (m, 1H, CH_{Ar}), 7.37 – 7.33 (m, 2H, CH_{Ar}), 6.10 (br s, 1H, NH), 5.88 (br s, 1H, NH), 2.41 (s, 3H, CH_3); ^{13}C NMR (126 MHz, CDCl_3): δ 169.8, 138.8, 133.5, 133.0, 128.7, 128.4, 124.5, 21.6; HRMS-ESI calcd for $[\text{C}_8\text{H}_9\text{NONa}]^+$: 158.0576 $[\text{M}+\text{Na}]^+$. Found: 158.0579; FT-IR (neat) ν in cm^{-1} : 3375, 3197, 1650, 1615. In agreement with previous literature data.

Cinnamide⁹² (5.14)



Following general procedure LXXIX, *trans*-cinnamaldehyde (252 μL , 2 mmol) was used as the aldehyde species. $\text{Cu}(\text{OAc})_2$ and NaNO_2 were added after 16 hours and the reaction was then

left for a further 24 hours. The title compound was recovered after purification by silica column chromatography as an off-white solid (223 mg, 76%).

mp 150-151 °C (lit.⁹² 149-151 °C); ¹H NMR (500 MHz, DMSO-d⁶): δ 7.62 (br s, 1H, NH), 7.58 – 7.53 (m, 2H, Ph), 7.47 (d, *J* = 15.9 Hz, 1H, PhCH), 7.42 – 7.32 (m, 3H, Ph), 7.20 (br s, 1H, NH), 6.66 (d, *J* = 15.9 Hz, 1H, PhCHCH); ¹³C NMR (126 MHz, DMSO-d⁶): δ 166.9, 139.3, 134.9, 129.5, 128.9, 127.6, 122.3; HRMS-ESI calcd for [C₉H₉NONa]⁺: 148.0757 [M+H]⁺. Found: 148.0761; FT-IR (neat) ν in cm⁻¹: 3389, 3167, 1656, 1611. In agreement with previous literature data.

References

1. H. Lundberg, F. Tinnis, N. Selander and H. Adolfsson, *Chem. Soc. Rev.*, 2014, **43**, 2714.
2. A. Johansson, P. Kollman, S. Rothenberg and J. McKelvey, *J. Am. Chem. Soc.*, 1974, **96**, 3794.
3. R. E. Hubbard and M. K Haider, *Encyclopaedia of Life Sciences: Hydrogen Bonds in Proteins: Role and Strength*, York, 2010.
4. D. Chen, N. Oezguen, P. Urvil, C. Ferguson, S. M. Dann and T. C. Savidge, *Sci. Adv.*, 2016, **2**, 1.
5. J. M. Berg, J. L. Tymoczko and L. Stryer, *Biochemistry*, W. H. Freeman, New York, 5th edn., 2002.
6. C. L. Allen, PhD Thesis, University of Bath, 2012.
7. C. L. Allen and J. M. J. Williams, *Chem. Soc. Rev.*, 2011, **40**, 3405.
8. B. S. Jursic and Z. Zdravkovski, *Synth. Commun.*, 1993, **23**, 2761.
9. H. Lundberg, F. Tinnis and H. Adolfsson, *Chem. Eur. J.*, 2012, **18**, 3822.
10. H. Charville, D. A. Jackson, G. Hodges, A. Whiting and M. R Wilson, *Eur. J. Chem.*, 2011, **30**, 5981.
11. C. Schotten, *Ber.*, 1884, **17**, 2544.
12. E. Baumann, *Ber.*, 1886, **19**, 3218.
13. E. Fischer, *Ber.*, 1903, **36**, 2982.
14. E. Valeur and M. Bradley, *Chem. Soc. Rev.*, 2009, **38**, 606.
15. A. El-Faham and F. Albericio, *Chem. Rev.*, 2011, **111**, 6557.
16. J. C. Sheehan and G. P. Hess, *J. Am. Chem. Soc.*, 1955, **77**, 1067.
17. G. W. Anderson and F. M. Callahan, *J. Am. Chem. Soc.*, 1958, **80**, 2902.
18. W. Koenig and R. Geiger, *Chem. Ber.*, 1970, **103**, 788.
19. C. A. G. N. Montalbetti and V. Falque, *Tetrahedron*, 2005, **61**, 10827.
20. L. A. Carpino, *J. Am. Chem. Soc.*, 1993, **115**, 4397.
21. L. A. Carpino, H. Imazumi, B. M. Foxman, M. J. Vela, P. Henklein, A. El-Faham, J. Klose and M. Bienert, *Org. Lett.*, 2000, **2**, 2253.
22. W. Van den Nest, S. Yuval and F. Albericio, *J. Pept. Sci.*, 2001, **7**, 115.
23. M. Malow, K. D. Wehrstedt and S. Neuenfeld, *Tetrahedron Lett.*, 2007, **48**, 1233.
24. A. Williams and I. T. Ibrahim, *Chem. Rev.*, 1981, **81**, 589.
25. A. El-Faham, R. S. Funosas, R. Prohens and F. Albericio, *Chem. Eur. J.*, 2009, **15**, 9404.
26. C. Najera, *Synlett*, 2002, **9**, 1388.

27. B. Castro, J. R. Dormoy, G. Evin and C. Selve, *Tetrahedron Lett.*, 1975, **14**, 1219.
28. J. Coste, D. Lenguyen and B. Castro, *Tetrahedron Lett.*, 1990, **31**, 205.
29. E. Fischer and E. Fourneau, *Ber. Dtsch. Chem. Ges.*, 1901, **34**, 2688.
30. L. A. Carpino, M. Beyermann, H. Wenschuh and M. Bienert, *Acc. Chem. Res.*, 1996, **29**, 268.
31. D. J. C. Constable, P. J. Dunn, J. D. Hayler, G. R. Humphrey, J. L. Leazer, R. J. Linderman, K. Lorenz, J. Manley, B. A. Pearlman, A. Wells, A. Zaks and T. Y. Zhang, *Green Chem.*, 2007, **9**, 411.
32. P. Nelson and A. Pelter, *J. Chem. Soc.*, 1965, **9**, 5142.
33. K. Ishihara, S. Ohara and H. Yamamoto, *J. Org. Chem.*, 1996, **61**, 4196.
34. R. M. Al-Zoubi, O. Marion and D. G. Hall, *Angew. Chem., Int. Ed.*, 2008, **47**, 2876.
35. N. Gernigon, R. M. Al-Zoubi and D. G. Hall, *J. Org. Chem.*, 2012, **77**, 8386.
36. K. Arnold, B. Davies, D. Herault and A. Whiting, *Angew. Chem., Int. Ed.*, 2008, **47**, 2673.
37. M. T. Sabatini, L. T. Boulton and T. D. Sheppard, *Sci. Adv.*, 2017, **3**, 1.
38. A. Werdehausen and H. Weiss, *Ger. Pat.*, DE2110060, 1972.
39. M. Mader and P. Helquist, *Tetrahedron Lett.*, 1988, **29**, 3049.
40. L. Y. Shteinberg, S. A. Kondratov and S. M. Shein, *Zh. Org. Khim.*, 1988, **24**, 1968.
41. L. Y. Shteinberg, S. M. Shein and S. E. Mishchenko, *Zh. Org. Khim.*, 1995, **31**, 233.
42. L. Y. Shteinberg, S. A. Kondratov and S. M. Shein, *Russ. J. Org. Chem.*, 2005, **41**, 304.
43. L. Y. Shteinberg, S. A. Kondratov and S. M. Shein, *Zh. Org. Khim.*, 1989, **25**, 1945.
44. C. L. Allen, A. R. Chhatwal and J. M. J. Williams, *Chem. Commun.*, 2012, **48**, 666.
45. T. Krause, S. Baader, B. Erb and L. J. Gooßen, *Nat. Commun.*, 2016, **7**, 1.
46. Y. Suto, N. Yamagiwa and Y. Torisawa, *Tetrahedron Lett.*, 2008, **49**, 5732.
47. C. W. Qian, X. M. Zhang, Y. Zhang and Q. Shen, *J. Organomet. Chem.*, 2010, **695**, 747.
48. S. I. Murahashi, T. Naota and E. Saito, *J. Am. Chem. Soc.*, 1986, **108**, 7846.
49. C. J. Copley, M. van den Heuvel, A. Abbadi and J. G. de Vries, *Tetrahedron Lett.*, 2000, **41**, 2467.
50. R. S. Ramon, N. Marion and S. P. Nolan, *Chem. Eur. J.*, 2009, **15**, 8695.
51. C. L. Allen, R. Lawrence, L. Emmett and J. M. J. Williams, *Adv. Synth. Catal.*, 2011, **353**, 3262.
52. D. Gananangari and R. H. Crabtree, *Organometallics*, 2009, **28**, 922.
53. M. A. Ali and T. Punniyamurthy, *Adv. Synth. Catal.*, 2010, **352**, 288.

54. R. N. S. Ramón, J. Bosson, S. Diez-González, N. Marion and S. P. Nolan, *J. Org. Chem.*, 2010, **75**, 1197.
55. C. Gunanathan, Y. Ben-David and D. Milstein, *Science*, 2007, **317**, 790.
56. L. U. Nordstrom, H. Vogt and R. Madsen, *J. Am. Chem. Soc.*, 2008, **130**, 17672.
57. T. Zweifel, J. V. Naubron and H. Grützmacher, *Angew. Chem., Int. Ed.*, 2009, **48**, 559.
58. A. J. A. Watson, A. C. Maxwell and J. M. J. Williams, *Org. Lett.*, 2009, **11**, 2667.
59. M. R. Suchy, A. A. H. Elmehriki and R. H. E. Hudson, *Org. Lett.*, 2011, **13**, 3952.
60. C. L. Allen, B. N. Atkinson and J. M. J. Williams, *Angew. Chem., Int. Ed.*, 2012, **51**, 1383.
61. T. B. Nguyen, J. Sorres, M. Q. Tran, L. Ermolenko and A. Al-Mourabit, *Org. Lett.*, 2012, **14**, 3202.
62. P. Starkov and T. D. Sheppard, *Org. Biomol. Chem.*, 2011, **9**, 1320.
63. S. Calimsiz and M. A. Lipton, *J. Org. Chem.*, 2005, **70**, 6218.
64. A. Klapars, S. Parris, K. W. Anderson and S. L. Buchwald, *J. Am. Chem. Soc.*, 2004, **126**, 3529.
65. A. Vasudevan, C. I. Villamil and S. W. Djuric, *Org. Lett.*, 2004, **6**, 3361.
66. J. Lasri, M. E. Gonzalez-Rosende and J. Sepulveda-Arques, *Org. Lett.*, 2003, **5**, 3851.
67. N. A. Stephenson, J. Zhu, S. H. Gellman and S. S. Stahl, *J. Am. Chem. Soc.*, 2009, **131**, 10003.
68. J. M. Hoerter, K. M. Cui, S. H. Gellman, Q. Cui and S. S. Stahl, *J. Am. Chem. Soc.*, 2007, **130**, 647.
69. J. M. Hoerter, K. M. Otte, S. H. Gellman and S. S. Stahl, *J. Am. Chem. Soc.*, 2006, **128**, 5177.
70. M. Tamura, T. Tonomura, K.-I. Shimizu and A. Satsuma, *Green Chem.*, 2012, **14**, 717.
71. M. Zhang, S. Imm, S. Bahn, L. Neubert, H. Neumann and M. Beller, *Angew. Chem., Int. Ed.*, 2012, **51**, 3905.
72. B. C. Ranu and P. Dutta, *Synth. Commun.*, 2003, **33**, 297.
73. R. Arora, S. Paul and R. Gupta, *Can. J. Chem.*, 2005, **83**, 1137.
74. C. Han, J. P. Lee, E. Lobkovsky and J. A. Porco, *J. Am. Chem. Soc.*, 2005, **127**, 10039.
75. A. Basha, M. Lipton and S. M. Weinreb, *Tetrahedron Lett.*, 1977, **48**, 4171.
76. K. Ishihara, Y. Kuroki, N. Hanaki, S. Ohara and H. Yamamoto, *J. Am. Chem. Soc.*, 1996, **118**, 1569.

77. Y. Kuroki, K. Ishihara, N. Hanaki, S. Ohara and H. Yamamoto, *Bull. Chem. Soc. Jpn.*, 1998, **71**, 1221.
78. M. Movassaghi and M. Schmidt, *Org. Lett.*, 2005, **7**, 2453.
79. C. Sabot, K. A. Kumar, S. Meunier and C. Mioskowski, *Tetrahedron Lett.*, 2007, **48**, 3863.
80. K. E. Price, C. Larrivee-Aboussafy, B. M. Lillie, R. W. McLaughlin, J. Mustakis, K. W. Hettenbach, J. M. Hawkins and R. Vaidyanathan, *Org. Lett.*, 2009, **11**, 2003.
81. X. Yang and V. B. Birman, *Org. Lett.*, 2009, **11**, 1499.
82. T. Ohshima, Y. Hayashi, K. Agura, Y. Fujii, A. Yoshiyama and K. Mashima, *Chem Commun.*, 2012, **48**, 5434.
83. D. T. Nguyen, D. C. Lenstra and J. Mecinovic, *RSC Adv.*, 2015, **5**, 77658.
84. B. N. Atkinson, A. R. Chhatwal, H. V. Lomax, J. W. Walton and J. M. Williams, *Chem. Commun.*, 2012, **48**, 11626.
85. D. C. Lenstra, D. T. Nguyen and J. Mecinovic, *Tetrahedron*, 2015, **71**, 5547.
86. H. Morimoto, R. Fujiwara, Y. Shimizu, K. Morisaki, and T. Ohshima, *Org. Lett.*, 2014, **16**, 2018.
87. Y. Shimizu, H. Morimoto, M. Zhang and T. Ohshima, *Angew. Chem., Int. Ed.* 2012, **51**, 8564.
88. N. Caldwell, C. Jamieson, I. Simpson and T. Tuttle, *Org. Lett.*, 2013, **15**, 2506.
89. N. Caldwell, C. Jamieson, I. Simpson and A. J. B. Watson, *ACS Sustain. Chem. Eng.*, 2013, **1**, 1339.
90. N. Caldwell, P. S. Campbell, C. Jamieson, F. Potjewyd, I. Simpson and A. J. B. Watson, *J. Org. Chem.*, 2014, **79**, 9347.
91. N. Caldwell, C. Jamieson, I. Simpson and A. J. B. Watson, *Chem. Commun.*, 2015, **51**, 9495.
92. P. Marcé, J. Lynch, A. J. Blacker and J. M. J. Williams, *Chem. Commun.*, 2016, **52**, 1436.
93. C. E. Mabermann, *Encyclopedia of Chemical Technology*, Wiley, New York, vol. 1, 1991.
94. R. Opsahl, *Encyclopedia of Chemical Technology*, Wiley, New York, vol. 1, 1991.
95. D. Lipp, *Encyclopedia of Chemical Technology*, Wiley, New York, vol. 1, 1991.
96. T. E. Schmid, A. Gómez-Herrera, O. Songis, D. Sneddon, A. Révolte, F. Nahra and C. S. Cazin, *J. Catal. Sci. Technol.*, 2015, **5**, 2865.

97. G. C. Midya, A. Kapat, S. Maiti and J. Dash, *J. Org. Chem.*, 2015, **80**, 4148.
98. V. Y. Kukushkin and A. J. L. Pombeiro, *Inorg. Chim. Acta*, 2005, **358**, 1.
99. R. W. Dugger, J. A. Ragan and D. H. B. Ripin, *Org. Process Res. Dev.*, 2005, **9**, 253.
100. A. R. Katritzky, B. Pilarski and L. Urogdi, *Synthesis*, 1989, 949.
101. A. Goto, K. Endo and S. Saito, *Angew. Chem. Int. Ed.*, 2008, **47**, 3607.
102. M. C. K. B. Djoman and A. N. Ajjou, *Tetrahedron Lett.*, 2000, **41**, 4845.
103. C. M. Jensen and W. C. Trogler, *J. Am. Chem. Soc.*, 1986, **108**, 723.
104. V. Cadierno, J. Francos and J. Gimeno, *Chem. Eur. J.*, 2008, **14**, 6601.
105. V. Cadierno, J. Díez, J. Francos and J. Gimeno, *Chem. Eur. J.*, 2010, **16**, 9808.
106. R. García-Álvarez, J. Díez, P. Crochet and V. Cadierno, *Organometallics*, 2010, **29**, 3955.
107. S. E. García-Garrido, J. Francos, V. Cadierno, J.-M. Basset and V. Polshettiwar, *ChemSusChem*, 2011, **4**, 104.
108. R. García-Álvarez, J. Francos, P. Crochet and V. Cadierno, *Tetrahedron Lett.*, 2011, **52**, 4218.
109. R. García-Álvarez, J. Díez, P. Crochet and V. Cadierno, *Organometallics*, 2011, **30**, 5442.
110. R. García-Álvarez, M. Zablocka, P. Crochet, C. Duhayon, J.-P. Majoral and V. Cadierno, *Green Chem.*, 2013, **15**, 2447.
111. E. Tomás-Mendivil, F. J. Suárez, J. Díez and V. Cadierno, *Chem. Commun.*, 2014, **50**, 9661.
112. T. Oshiki, H. Yamashita, K. Sawada, M. Utsunomiya, K. Takahashi and K. Takai, *Organometallics*, 2005, **24**, 6287.
113. T. Šmejkal and B. Breit, *Organometallics*, 2007, **26**, 2461.
114. T. Oshiki, I. Hyodo and A. Ishizuka, *J. Synth. Org. Chem., Jpn.*, 2010, **68**, 41.
115. M. Muranaka, I. Hyodo, W. Okumura and T. Oshiki, *Catal. Today*, 2011, **164**, 552.
116. D. B. Grotjahn, *Chem. Eur. J.*, 2005, **11**, 7146.
117. A. S. Borovik, *Acc. Chem. Res.*, 2005, **38**, 54.
118. X. Ma, Y. He, P. Wang and M. Lu, *Appl. Organometal. Chem.*, 2012, **26**, 377.
119. J. Lee, M. Kim, S. Chang and H.-Y. Lee, *Org. Lett.*, 2009, **11**, 5598.
120. E. S. Kim, H. S. Kim and J. N. Kim, *Tetrahedron Lett.*, 2009, **50**, 2973.
121. E. S. Kim, H. S. Lee, S. H. Kim and J. N. Kim, *Tetrahedron Lett.*, 2010, **51**, 1589.
122. R. W. Goetz and I. L. Mador, *US Pat.*, 3670021, 1972.

123. G. Villain, G. Constant, A. Gaset and P. Kalck, *J. Mol. Catal.*, 1980, **7**, 355.
124. N. V. Kaminskaia and N. M. Kostic, *J. Chem. Soc. Dalton Trans.*, 1996, **0**, 3677.
125. N. V. Kaminskaia, I. A. Guzei and N. M. Kostic, *J. Chem. Soc. Dalton Trans.*, 1998, **0**, 3879.
126. W. Oberhauser, M. Bartoli, G. Petrucci, D. Bandelli, M. Frediani, L. Capozzoli, C. Cepek, S. Bhardwaj and L. Rosi, *J. Mol. Catal. A: Chem.*, 2015, **410**, 26.
127. A. Ishizuka, Y. Nakazaki and T. Oshiki, *Chem. Lett.*, 2009, **38**, 360.
128. K. Shimizu, T. Kubo, A. Satsuma, T. Kamachi and K. Yoshizawa, *ACS Catal.*, 2012, **2**, 2467.
129. T. Subramanian and K. Pitchumani, *Catal. Commun.*, 2012, **29**, 109.
130. Y.-M. Liu, L. He, M.-M. Wang, Y. Cao, H.-Y. He and K.-N. Fan, *ChemSusChem*, 2012, **5**, 1392.
131. R. B. N. Baig and R. S. Varma, *Chem. Commun.*, 2012, **48**, 6220.
132. S. Kumar and P. Das, *New J. Chem.*, 2013, **37**, 2987.
133. M. B. Gawande, P. S. Branco, I. D. Nogueira, C. A. A. Ghumman, N. Bundaleski, A. Santos, O. M. N. D. Teodoro and R. Luque, *Green Chem.*, 2013, **15**, 682.
134. A. Y. Kim, H. S. Bae, S. Park, S. Park and K. H. Park, *Catal. Lett.*, 2011, **141**, 685.
135. K. Shimizu, N. Imaiida, K. Sawabe and A. Satsuma, *Appl. Catal. A*, 2012, **421**, 114.
136. H. Woo, K. Lee, S. Park and K. H. Park, *Molecules*, 2014, **19**, 699.
137. K. Yamaguchi, M. Matsushita and N. Mizuno, *Angew. Chem., Int. Ed.*, 2004, **116**, 1602.
138. Á. Kiss and Z. Hell, *Tetrahedron Lett.*, 2011, **52**, 6021.
139. C. Battilocchio, J. M. Hawkins and S. V. Ley, *Org. Lett.*, 2014, **16**, 1060.
140. A. Matsuoka, T. Isogawa, Y. Morioka, B. R. Knappett, A. E. H. Wheatley, S. Saito and H. Naka, *RSC Adv.*, 2015, **5**, 12152.
141. H. Sharghi and M. Hosseini, *Synthesis*, 2002, **8**, 1057.
142. H. Sharghi and M. H. Sarvari, *J. Chem. Res. (S)*, 2001, 446.
143. H. Sharghi and M. Hosseini, *Tetrahedron*, 2002, **58**, 10323.
144. S. Park, Y.-A. Choi, H. Han, S. H. Yang and S. Chang, *Chem. Commun.*, 2003, 1936.
145. N. A. Owston, A. J. Parker and J. M. J. Williams, *Org. Lett.*, 2007, **9**, 3599.
146. D. Gnanamgari and R. H. Crabtree, *Organometallics*, 2009, **28**, 922.
147. P. Kumar, A. K. Singh, R. Pandey and D. S. Pandey, *J. Organomet. Chem.*, 2011, **696**, 3454.

148. M. Nirmala, R. Manikandan, G. Prakash and P. Viswanathamurthi, *Appl. Organomet. Chem.*, 2014, **28**, 18.
149. N. Raja, M. U. Raja and R. Ramesh, *Inorg. Chem. Commun.*, 2012, **19**, 51.
150. G. Prakash and P. Viswanathamurthi, *Spectrochim. Acta, Part A*, 2014, **129**, 352.
151. R. N. Prabhu and R. Ramesh, *RSC Adv.*, 2012, **2**, 4515.
152. R. Manikandan, G. Prakash, R. Kathirvel and P. Viswanathamurthi, *Spectrochim. Acta, Part A*, 2013, **116**, 501.
153. R. García-Álvarez, A. E. Díaz-Álvarez, J. Borge, P. Crochet and V. Cadierno, *Organometallics*, 2012, **31**, 6482.
154. R. García-Álvarez, A. E. Díaz-Álvarez, P. Crochet and V. Cadierno, *RSC Adv.*, 2013, **3**, 5889.
155. D. Tyagi, R. K. Rai, A. D. Dwivedi, S. M. Mobin and S. K. Singh, *Inorg. Chem. Front.*, 2015, **2**, 116.
156. P. J. González-Liste, V. Cadierno and S. E. García-Garrido, *ACS Sustain. Chem. Eng.* 2015, **3**, 3004.
157. J. Francos, L. Menéndez-Rodríguez, E. Tomás-Mendivil, P. Crochet and V. Cadierno, *RSC Adv.*, 2016, **6**, 39044.
158. L. Menéndez-Rodríguez, E. Tomás-Mendivil, J. Francos, C. Nájera, P. Crochet and V. Cadierno, *Catal. Sci. Technol.*, 2015, **5**, 3754.
159. K. Tambara and G. D. Pantos, *Org. Biomol. Chem.*, 2013, **11**, 2466.
160. F. Xu, Y.-Y. Song, Y.-J. Li, E.-L. Li, X.-R. Wang, W.-Y. Li and C.-S. Liu, *ChemistrySelect*, 2018, **3**, 3474.
161. L. Xu, N. Li, H.-G. Peng and P. Wu, *ChemCatChem*, 2013, **5**, 2462.
162. H.-G. Peng, L. Xu, H. Wu, K. Zhang and P. Wu, *Chem. Commun.*, 2013, **49**, 2709.
163. S. Zhao, J. Xu, M. Wei and Y.-F. Song, *Green Chem.*, 2011, **13**, 384.
164. S. Zhao, L. Liu and Y.-F. Song, *Dalton Trans.*, 2012, **41**, 9855.
165. H. Fujiwara, Y. Ogasawara, K. Yamaguchi and N. Mizuno, *Angew. Chem., Int. Ed.*, 2007, **46**, 5202.
166. H. Fujiwara, Y. Ogasawara, M. Kotani, K. Yamaguchi and N. Mizuno, *Chem. -Asian J.*, 2008, **3**, 1715.
167. R. R. Gowda and D. Chakraborty, *Eur. J. Org. Chem.*, 2011, **2011**, 2226.
168. R. Das and D. Chakraborty, *Catal. Commun.*, 2012, **26**, 48.
169. N. A. Owston, A. J. Parker and J. M. J. Williams, *Org. Lett.*, 2007, **9**, 73.

170. N. C. Ganguly, S. Roy and P. Mondal, *Tetrahedron Lett.*, 2012, **53**, 1413.
171. A. Martínez-Asencio, M. Yus and D. J. Ramón, *Tetrahedron*, 2012, **68**, 3948.
172. S. K. Sharma, S. D. Bishopp, C. L. Allen, R. Lawrence, M. J. Bamford, A. A. Lapkin, P. Plucinski, R. J. Watson and J. M. J. Williams, *Tetrahedron Lett.*, 2011, **52**, 4252.
173. C. L. Allen, C. Burel and J. M. J. Williams, *Tetrahedron Lett.*, 2010, **51**, 2724.
174. A. J. Leusink, T. G. Meerbeek and J. G. Noltes, *Recl. Trav. Chim. Pays-Bas*, 1976, **95**, 123.
175. S. H. Yang and S. Chang, *Org. Lett.*, 2001, **3**, 4209.
176. H. S. Kim, S. H. Kim and J. M. Kim, *Tetrahedron Lett.*, 2009, **50**, 1717.
177. N. Jiang and A. J. Ragauskas, *Tetrahedron Lett.*, 2010, **51**, 4479.
178. Y.-T. Li, B.-S. Liao, H.-P. Chen and S.-T. Liu, *Synthesis*, 2011, 2639.
179. T. J. Ahmed, S. M. M. Knapp and D. R. Tyler, *Coord. Chem. Rev.*, 2011, **255**, 949.
180. E. L. Downs and D. R. Tyler, *Coord. Chem. Rev.*, 2014, **280**, 28.
181. A. J. Leusink, T. G. Meerbeek and J. G. Noltes, *Recl. Trav. Chim. Pays-Bas*, 1977, **96**, 142.
182. M. Kim, J. Lee, H.-Y. Lee and S. Chang, *Adv. Synth. Catal.*, 2009, **351**, 1807.
183. S. Paul, P. Nanda, R. Gupta and A. Laupy, *Tetrahedron Lett.*, 2002, **43**, 4261.
184. C. T. Chen, J. H. Kuo, C. H. Li, N. B. Barhate, S. W. Hon, T. W. Li, S. D. Chao, C. C. Liu, Y. C. Li, I. H. Chang, J. S. Lin, C. J. Liu and Y. C. Chou, *Org. Lett.*, 2001, **3**, 3729.
185. S. P. Chavan, R. Anand, K. Pasupathy and B. S. Rao, *Green Chem.*, 2001, **3**, 320.
186. G. Sabitha, B. V. S. Reddy, R. Srividya and J. S. Yadav, *Synth. Commun.*, 1999, **29**, 2311.
187. R. K. Sodhi, V. Kumar and S. Paul, *Open Catal. J.*, 2013, **6**, 1.
188. P. Saravanan and V.K. Singh, *Tetrahedron Lett.*, 1999, **40**, 2611.
189. K. Phukan, M. Ganguly and N. Devi, *Synth. Commun.*, 2009, **39**, 2694.
190. G. Hofle, V. Steglich and H. Vorbruggen, *Angew. Chem., Int. Ed. Engl.*, 1978, **17**, 569.
191. V. K. Yadav, K. G. Babu and M. Mittal, *Tetrahedron*, 2001, **57**, 7047.
192. K. Ishihara, M. Kubota, H. Kurihara and H. Yamamoto, *J. Am. Chem. Soc.*, 1995, **117**, 4413.
193. H. Zhao, A. Pendri and R. B. Greenwald, *J. Org. Chem.*, 1998, **63**, 7559.
194. K. Ishihara, M. Kubota and H. Yamamoto, *Synlett*, 1996, 265.
195. J. Izumi, I. Shiina and T. Mukaiyama, *Chem. Lett.*, 1995, 141.
196. T. Mukaiyama, I. Shiina and M. Miyashita, *Chem. Lett.*, 1992, 625.

197. E. W. P. Damen, L. Braamer and H. W. Scheeren, *Tetrahedron Lett.*, 1998, **39**, 6081.
198. S. Chandrasekhar, T. Ramchander and M. Takhi, *Tetrahedron Lett.*, 1998, **39**, 3263.
199. P. R. Likhar, *J. Mol. Catal. A: Chem.*, 2009, **302**, 142.
200. A. C. Shekhar, A. R. Kumar, G. Sathaiah, V. L. Paul, M. Sridhar and P. S. Rao, *Tetrahedron Lett.*, 2009, **50**, 7099.
201. G. Brahmachari, S. Laskar and S. Sarkar, *Indian J. Chem.*, 2010, **49**, 1274.
202. F. G. Bordwell and D. Algrim, *J. Org. Chem.*, 1976, **41**, 2507.
203. J. H. Shah, S. Izenwasser, B. Geter-Douglass, J. M. Witkin and A. H. Newman, *J. Med. Chem.*, 1995, **38**, 4284.
204. T. M. Raynham, T. R. Hammonds, J. H. Gilliatt, M. D. Charles, G. A. Pave, C. H. Foxton, J. L. Carr and N. S. Mistry, *US Pat.*, US2009/247519A1, 2009.
205. X. Han, H. Javanbakht, M. Jiang, C. Liang, J. Wang, Y. Wang, Z. Wang, R. J. Weikert, S. Yang and C. Zhou, *US Pat.*, US2015/210682A1, 2015
206. J-G. Kim and D. O. Jang, *Tetrahedron Lett.*, 2010, **51**, 683.
207. M. R. Crampton and I. A. Robotham, *J. Chem. Res. (S)*, 1997, **0**, 22.
208. X.-Y. Ma and M. Lu, *J. Chem. Res.*, 2011, 480.
209. J. Lynch, PhD Thesis, University of Bath, 2013.
210. A. Hassine, S. Sebti, A. Solhy, N. Thiebault, E. Bilal, C. Len and A. Fihri, *Curr. Org. Chem.*, 2016, **20**, 2022.
211. B. S. Rao, A. Srivani, D. D. Lakshmi and N. Lingaiah, *Catal. Lett.*, 2016, **146**, 2025.
212. T. Mizuno, *JP Pat.*, JP2005170821, 2005.
213. G. Sánchez, J. L. Serrano, M. C. Ramírez de Arellano, J. Pérez and G. López, *Polyhedron*, 2000, **19**, 1395.
214. C. J. McKenzie, and R. Robson, *J. Chem. Soc., Chem. Commun.*, 1988, **2**, 112.
215. G. Villain and A. Gaset, *J. Mol. Catal.*, 1981, **12**, 103.
216. S. Zhang, H. Xu, C. Lou, A. M. Senan, Z. Chen and G. Yin, *Eur. J. Org. Chem.*, 2017, **14**, 1870.
217. E. S. Kim, H. S. Lee and J. N. Kim, *Tetrahedron Lett.*, 2009, **50**, 6286.
218. B. N. Atkinson, PhD Thesis, University of Bath, 2014.
219. T. A. Stephenson, S. M. Morehouse, A. R. Powell, J. P. Heffer and G. Wilkinson, *J. Chem. Soc.*, 1965, **0**, 3632.
220. X. Ma and M. Lu, *J. Chem. Res.*, 2016, **40**, 594.

221. H. Golchoubian, Z. Khazaei, E. Rezaei, G. Moayyedi and D. Farmanzadeh, *Polyhedron*, 2015, **90**, 108.
222. A. J. Timmons and M. D. Symes, *Chem. Soc. Rev.*, 2015, **44**, 6708.
223. Z. Tan, S. Zhang, Y. Zhang, Y. Li, M. Ni and B. Feng, *J. Org. Chem.*, 2017, **82**, 9384.
224. R. W. Darbeau, E. H. White, F. Song, N. R. Darbeau and J. Chou, *J. Org. Chem.*, 1999, **64**, 5966.
225. M. Barbero, S. Bazzi, S. Cadamuro and S. Dughera, *Eur. J. Org. Chem.*, 2009, **2009**, 311.
226. M. P. Trova, A. Wissner, M. L. Carroll, S. S. Kerwar, W. C. Pickett, R. E. Schaub, L. W. Torley and C. A. Kohler, *J. Med. Chem.*, 1993, **36**, 580.
227. J. T. Li, X. Meng and X. Zhai, *Ultrason. Sonochem.*, 2009, **16**, 590.
228. I. Pravst and S. Stavber, *J. Fluorine Chem.*, 2013, **156**, 276.
229. B. Nammalwar, N. P. Muddala, F. M. Watts and R. A. Bunce, *Tetrahedron*, 2015, **71**, 9101.
230. D. W. Thomson, A. G. J. Commeureuc, S. Berlin and J. A. Murphy, *Synth. Commun.*, 2003, **33**, 3631.
231. R. Pelagalli, I. Chiarotto, M. Feroci and S. Vecchio, *Green Chem.*, 2012, **14**, 2251.
232. Y. Lee, P. Martasek, L. J. Roman and R. B. Silverman, *Bioorg. Med. Chem. Lett.*, 2000, **10**, 2771.
233. K. Kondo, E. Sekimoto, J. Nakao and Y. Murakami, *Tetrahedron*, 2000, **56**, 5843.
234. M. D. Ganton and M. A. Kerr, *Org. Lett.*, 2005, **7**, 4777.
235. K. Nishiwakia, T. Ogawaa, K. Shigetaa, K. Takahashib and K. Matsuo, *Tetrahedron*, 2006, **62**, 7034.
236. K. Seijakn, *JP Pat.*, JP30314, 1968.
237. L. Liu, H. Liu, H. Pi, S. Yang, M. Yao, W. Du and W. Deng, *Synth. Commun.*, 2011, **41**, 553.
238. K. Bao, W. Zhang, X. Bu, Z. Song, L. Zhang and M. Cheng, *Chem. Commun.*, 2008, **42**, 5429.
239. D. C. Johnson and T. S. Widlanski, *Tetrahedron Lett.*, 2004, **45**, 8483.
240. V. A. Ignatenko, N. Deligonul and R. Viswanathan, *Org. Lett.*, 2010, **12**, 3594.
241. K. M. Al-Zaydi, *Ultrason. Sonochem.*, 2009, **16**, 805.
242. A. Ojeda-Porras, A. Hernández-Santana and D. Gamba-Sánchez, *Green Chem.*, 2015, **17**, 3157.

243. E. J. Bourne, C. E. Tatlow and J. C. Tatlow, *J. Chem. Soc.*, 1952, 4014.
244. K. W. Fiori and J. D. Bois, *J. Am. Chem. Soc.*, 2007 **129**, 562.
245. S. Pache, C. Botuha, R. Franz and E. P. Kündig, *Helv. Chim. Acta*, 2000, **83**, 2436.
246. K. C. Nadimpally, K. Thalluri, N. B. Palakurthy, A. Saha and B. Mandal, *Tetrahedron Lett.*, 2011, **52**, 2579.
247. A. R. Katritzky, C. Cai and S. K. Singh, *J. Org. Chem.*, 2006, **71**, 3375.
248. H. Suzuki, J. Tsuji, Y. Hiroi, N. Sato and A. Osuka, *Chem. Lett.*, 1983, **12**, 449.
249. P. C. Kuzma, L. E. Brown and T. M. Harris, *J. Org. Chem.*, 1984, **49**, 2015.
250. F. T. Oakes and N. J. Leonard, *J. Org. Chem.*, 1985, **50**, 4986.
251. C. L. Stevens, T. K. Mukherjee and V. J. Traynelis, *J. Am. Chem. Soc.*, 1956, **78**, 2264.
252. K. Takaki, A. Okamura, Y. Ohshiro and T. Agawa, *J. Org. Chem.*, 1978, **43**, 402.
253. D. U. Nielsen, R. H. Taaning, A. T. Lindhardt, T. M. Gogsig and T. Skrydstrup, *Org. Lett.*, 2011, **13**, 4454.
254. N. Lakshminarayana, Y. R. Prasad, L. Gharat, A. Thomas, S. Narayanan, A. Raghuram, C. V. Srinivasan and B. Gopalan, *Eur. J. Med. Chem.*, 2010, **45**, 3709.
255. I. I. Dozorova, L. I. Koloskova, V. K. Ermakova, M. G. Pleshakov, V. I. Snegotskii, T. K. Filatova and N. V. Falina, *Khim. Farm. Zh.*, 1990, **24**, 73.
256. S. Ghosh, P. P. Bag and C. M. Reddy, *Cryst. Growth Des.*, 2011, **11**, 3489.
257. J. D. Hall, N. W. Duncan-Gould, N. A. Siddiqi, J. N. Kelly, L. A. Hoeflerlin, S. J. Morrison and J. K. Wyatt, *Bioorg. Med. Chem.*, 2005, **13**, 1409.
258. J. W. Jaroszewski, D. Staerk, S. B. Holm-Moller, T. H. Jensen, H. Franzyk and B. Somanadhan, *Nat. Prod. Res.*, 2005, **19**, 291.
259. T. Koyama, T. Nanba, T. Hirota, S. Ohmori and M. Yamato, *Chem. Pharm. Bull.*, 1977, **25**, 964.
260. C. L. Allen, S. Davulcu and J. M. J. Williams, *Org. Lett.*, 2010, **12**, 5096.
261. R. H. Wiley and B. J. Wakefield, *J. Org. Chem.*, 1960, **25**, 546.
262. G. D. Vilela, R. R. da Rosa, P. H. Schneider, I. H. Bechtold, J. Eccher and A. A. Merlo, *Tetrahedron Lett.*, 2011, **52**, 6569.
263. B. C. Sanders, F. Friscourt, P. A. Ledin, N. E. Mbua, S. Arumugam, J. Guo, T. J. Boltje, V. V. Popik and G.-J. Boons, *J. Am. Chem. Soc.*, 2011, **133**, 949.
264. N. Kapuriya, K. Kapuriya, N. M. Dodia, Y. W. Lin, R. Kakadiya, C. T. Wu, C. H. Chen, Y. Naliapara and T. L. Su, *Tetrahedron Lett.*, 2008, **49**, 2886.

265. J. K. Augustine, R. Kumar, A. Bombrun and A. B. Mandal, *Tetrahedron Lett.*, 2011, **52**, 1074.
266. S. R. Neufeldt and M. S. Sanford, *Org. Lett.*, 2010, **12**, 532.
267. N. Jain, A. Kumar and S. M. S. Chauhan, *Tetrahedron Lett.*, 2005, **46**, 2599.
268. L. Di Nunno, P. Vitale and A. Scilimati, *Tetrahedron*, 2008, **64**, 11198.
269. K. S. Kadam, T. Gandhi, A. Gupte, A. K. Gangopadhyay and R. Sharma, *Synthesis*, 2016, **48**, 3996.
270. M. Belaud-Rotureau, T. L. Tin, H. T. P. Thi, H. N. Thi, R. Aissaoui, F. Gohier, A. Derdour, A. Nourry, A. S. Castanet, P. P. N. Kim and J. Mortier, *Org. Lett.*, 2010, **12**, 2406.
271. S. Shimokawa, Y. Kawagoe, K. Moriyama and H. Togo, *Org. Lett.*, 2016, **18**, 784.